論文 / 著書情報
Article / Book Information

題目(和文)	
Title(English)	Quark condensate and pion properties in isospin-asymmetric nuclear matter
著者(和文)	HUEBSCHStephan
Author(English)	Stephan Huebsch
出典(和文)	学位:博士(理学), 学位授与機関:東京工業大学, 報告番号:甲第12054号, 授与年月日:2021年9月24日, 学位の種別:課程博士, 審査員:慈道 大介,山口 昌英,今村 洋介,関澤 一之,藤岡 宏之
Citation(English)	Degree:Doctor (Science), Conferring organization: Tokyo Institute of Technology, Report number:甲第12054号, Conferred date:2021/9/24, Degree Type:Course doctor, Examiner:,,,,
学位種別(和文)	博士論文
Type(English)	Doctoral Thesis

Tokyo Institute of Technology
School of Science
Department of Physics

Quark condensate and pion properties in isospin-asymmetric nuclear matter

Stephan Hübsch

August 2021

Supervised by Prof. Daisuke Jido

I hereby declare that this thesis is my original work and it has been written by me in its entirety. I have acknowledged all sources of information which have been used in this work. The results in this thesis have been published in Ref. [1, 2].

PhD Thesis (2021)
Tokyo Institute of Technology

Abstract

Dynamical symmetry breaking of QCD's chiral symmetry is the mechanism responsible for the bulk of all hadron mass in the universe. One of the order parameters of chiral symmetry breaking is the chiral quark condensate. Theoretical model-independent calculations have shown that the absolute value of this quark condensate is reduced in nuclear matter. This might be an indication of (at least partial) restoration of the chiral symmetry compared to the unbroken phase in the vacuum. The linear-order density dependence of this symmetry breaking process is well known. If we knew higher orders of this density dependence, we might be able to extrapolate to even higher densities. This could for instance lead to a better understanding of neutron stars.

The goal of this work is to investigate the density dependence of the chiral quark condensate as well as certain pion properties in isospin-asymmetric nuclear matter using in-medium chiral perturbation theory up to the next-to-leading order of the density expansion. The isospin asymmetry of the nuclear matter ground state is realized via different proton and neutron densities, expressed via the ratio $r = \rho_n/\rho_p$. Hence a ratio of $r = 1.5$ corresponds to a neutron-to-proton ratio commonly found in heavy nuclei and $r \approx 10$ represents the situation in neutron stars.

For our calculations, we use an SU(2) in-medium chiral perturbation theory, initially formulated by Oller and further developed by Meißner, Oller and Wirzba. The partition function is defined in terms of the ground state, which we assume to be described by Fermi seas of non-interacting protons and neutrons. These states can be written as excitations of the vacuum, where we include all momenta up to the Fermi momentum, which depends on the nucleon density. Since this approach allows us to calculate general Green's functions, we can apply it to both the quark condensate as well as the pion properties. Our expansion scheme allows us to consider diagrams with one or two in-medium nucleon propagators and pion-nucleon interactions up to second order in the chiral counting. In total, we restrict our calculations to the order of the Fermi momentum to the fifth power. Higher contributions, i.e. proportional to the square of the nucleon density can be considered by including nucleon-nucleon correlation effects.

In order to compute the density dependence of the chiral quark condensate in nuclear matter, we investigate the two-point pseudoscalar correlation function by means of the chiral Ward identity. We find that at normal nuclear density, the absolute value of the quark condensate is

reduced by around 35% compared to its vacuum value. This is in good agreement with earlier model-independent calculations. Although the effect of isospin-asymmetric nuclear matter is small, it is non-zero and leads to slight changes for large asymmetry of protons and neutrons. At fixed density, the reduction of the quark condensate is unchanged under the inversion of the neutron-to-proton ratio, i.e. a certain ratio r and the inverse ratio $1/r$ lead to the same result.

By extending this method using the chiral Ward identity to an SU(3) Lagrangian, we can also investigate the density dependence of the difference of the up- and down quark condensates in nuclear matter. The density dependence of this difference is smaller than for the sum of up- and down quark condensates, but the effect of isospin-asymmetric nuclear matter is more pronounced. Depending on whether the nuclear matter ground state exhibits more protons or more neutrons, the sign of this difference changes. Furthermore, we also present results of the density dependence of the strange quark condensate, although this result is largely dependent on the choice of the SU(3) low-energy constants.

For the in-medium pion properties, we first calculate the in-medium pion self-energy, which lets us compute the in-medium pion mass and wave function renormalization. The isospin asymmetry in the nuclear matter leads to a splitting of the pion triplet quantities, since the self-energy now has three independent components corresponding to the three states in the pion triplet. It is interesting that under the inversion of the neutron-to-proton ratio, the neutral pion's properties are unchanged, whereas the charged pions' properties are exchanged. We find that for normal nuclear density and a neutron-to-proton ratio of $r = 1.5$, the negative pion's mass is increased by around 10%. This agrees with an extrapolation of experimental data of the pion-nucleon optical potential, obtained from pionic atoms. Furthermore, we also investigate the in-medium pion decay constant via a different set of Feynman diagrams. We find that the negative pion's decay constant is reduced by around 10% at normal nuclear density and a neutron-to-proton ratio of $r = 1.5$. Our results for the pion properties are in good agreement with experimental findings.

Acknowledgements

First and foremost, I would like to thank my supervisor Prof. Daisuke Jido for guiding me in my research during the three years of my PhD. I have learned a lot about theoretical nuclear physics, but also about Japanese culture. I am grateful for the friendly work environment you provided, where I enjoyed pursuing my research. Thank you for introducing me to many opportunities to present my work at conferences and workshops, and to discuss with the nuclear hadron physics community.

Next, I want to thank Associate Prof. Yosuke Imamura, who was co-supervising my PhD, Prof. Masahide Yamaguchi, Associate Prof. Kazuyuki Sekizawa and Associate Prof. Hiroyuki Fujioka for being in the committee evaluating this thesis. Before starting my PhD, I was very fortunate to spend my first four months in Japan in Prof. Katsushi Ito's and Associate Prof. Yosuke Imamura's particle physics group, while I was still doing my Master's degree in Austria. Thank you for your hospitality and enabling me to do a project work in your group. During this time, Prof. Makoto Oka was the head of the nuclear physics group, who kindly invited me to join seminars in his group at any occasion. Also thank you Associate Prof. Todd Tilma, Associate Prof. Hideto Kanamori and Dr. Kenta Itahashi, for giving me the opportunity to work as a teaching assistant in your lectures, an activity I thoroughly enjoyed. I would further like to thank Prof. Atsushi Hosaka for his suggestion to calculate the in-medium density dependence of $\langle \bar{u}u - \bar{d}d \rangle^*$ during the JPS autumn meeting of 2019.

I would also like to thank the students in the nuclear hadron physics group, especially the ones with whom I have shared my office at the Tokyo Institute of Technology: Kenji Aoki, Taiju Amano, Masanari Jimbo, and Zanpeng Yin, thank you for the enjoyable time at Tokyo Tech. And thank you Emanuele Bugliarello, for joining me at the Japanese language classes at Tokyo Tech, as well as after hours in the gym. 東工大の皆様、誠にありがとうございました。

さらに、歴史や美術、日本料理など、日本文化の様々な側面を紹介して下さった小室至様にも感謝しております。お陰様で、私は日本でとても歓迎されていると感じました。

Finally, I would like to express my gratitude to my family in Austria and especially my wife Marie-Therese, who joined me in going to Japan, and who, despite doing a physics PhD of her own, supported me on every step along the way.

Tokyo, July 2021
Stephan Hübsch

Contents

1. Introduction

Quantum chromodynamics (QCD) is the currently accepted mathematical description of the strong force. It is an SU(3) gauge-field theory, formulated in terms of quarks and gluons. As such it is also the theoretical basis for hadron physics, concerning particles which are held together by the strong force. One peculiar feature of QCD is asymptotic freedom [3, 4], which means that the strong coupling constant, governing the strength of quark-gluon and gluon-gluon interactions, changes its value as follows: At high energies, the coupling constant is small. This is called the perturbative regime, since perturbation theory can be applied for small couplings. At low energies, the coupling constant gets large, and perturbation theory breaks down. This is the non-perturbative regime, in which confinement plays an essential role: There are no free quarks or gluons, only hadronic bound states. The low-energy regime can be explored e.g., via numerical methods (lattice QCD) or effective field theories. One particularly successful effective field theory of QCD is chiral perturbation theory (ChPT) [5–10]. Instead of quarks and gluons, the effective degrees of freedom are their bound states, i.e., hadrons.

ChPT has a long history of continuous development and theoretical advances. Over 60 years ago, Goldberger and Treiman discovered the Goldberger–Treiman relation [11], which connected quantities from the weak interactions (the nucleon axial coupling g_A and the pion decay constant f_π) with those of the strong interactions (the pion-nucleon coupling $g_{\pi N}$ and the nucleon mass m_N). This was in surprisingly good agreement with experimental data [12] and led to the discovery of QCD's spontaneous chiral symmetry breaking by Nambu [13–15]. Based on that, the Goldberger–Treiman relation appeared again naturally in linear sigma models [16]. The newly developed current algebra and partially conserved axial current (PCAC) relation were used to calculate pion-scattering quantities (e.g. the pion-pion scattering length [17]), but it was later concluded that effective Lagrangians are a more convenient starting point in order to arrive at the same results [18, 19]. In particular, Ref. [19] presents an effective pion Lagrangian, which is capable of reproducing pion-scattering amplitudes at tree-level, which had earlier been obtained via the current algebra and the PCAC relation. Effective Lagrangians based on $\mathrm{SU}(2) \times \mathrm{SU}(2)$ and $\mathrm{SU}(3) \times \mathrm{SU}(3)$ chiral symmetries are discussed by Coleman and Callan in Refs. [20, 21]. Beyond the tree-level, pion-loop amplitudes were found to be divergent, owing to characteristic $x \log(x)$-terms, that are today known as "chiral logarithms". Here, x parametrizes the chiral symmetry breaking [22–24]. Various methods have been proposed to deal with these divergences [25] and several calculations of pion scattering processes followed [26–29].

In 1984, Gasser and Leutwyler introduced chiral perturbation theory [30, 31] by introducing scalar, pseudoscalar, vector and axial-vector external fields in the Lagrangian and constructing an effective theory based on SU(2) chiral transformations. This effective Lagrangian produced an expansion in powers of quark masses and pion momenta. In the following year, higher-order terms were introduced to the effective Lagrangian (see e.g. Ref. [32]). The next important step with respect to in-medium properties was the formulation of in-medium chiral perturbation theory by Oller in 2002 [33], which has since been further developed by Meißner, Oller and Wirzba [34]. The ground state of the partition function was assumed to be a non-interacting Fermi sea of nucleons, having momenta up to the Fermi momentum. Since the Fermi momentum depends on the nucleon density, this allowed the evaluation of in-medium Green's functions and the investigation of their density dependence.

The main motivation of this work is to investigate QCD's chiral symmetry, or more precisely, the dynamical breaking of chiral symmetry. It is believed that this dynamical breaking process is responsible for generating the large hadron masses from small quark masses. The symmetry breaking can be described by order parameters, which are usually correlation functions of parity partners. One such order parameter is the chiral quark condensate $\langle \bar{q}q \rangle$. In the symmetric phase, it is exactly zero, but after the symmetry breaking, it acquires a finite, non-zero value. However, recently it was found [35] that this value gets reduced in nuclear matter: Jido, Hatsuda and Kunihiro used experimental data from deeply bound pionic atoms [36, 37] to determine that the parameter b_1^*, which appears in the s-wave optical potential for the negative pion, $2m_\pi U_{s\text{-wave}} = -4\pi\,[1 + m_\pi/m_N]\,[b_0^*\rho - b_1^*(\rho_p - \rho_n)]$, increases at high densities: $b_1/b_1^*|_{\rho=\rho_0} \approx 0.79 \pm 0.05$. Furthermore, using data from pion-nucleon scattering [38, 39], the coefficient β in the isospin singlet πN-scattering amplitude $\mathcal{T}^{(+)}(\omega, m_\pi)|_{\boldsymbol{q}=\mathbf{0}} \approx \alpha + \beta\omega^2$ was found to be $\beta \approx (2.17 \pm 0.04)\ \mathrm{fm}^3$. A further extrapolation led to the conclusion that the quark condensate gets reduced by 37% at normal nuclear density: $\langle \bar{q}q \rangle^*/\langle \bar{q}q \rangle \approx 1 - 0.37\,\rho/\rho_0$. This affects the reduction of the mass difference between chiral parity partners, such as ρ and a_1 [18, 40] or N and $N(1535)$ [41–44], or it can lead to an attractive enhancement of scalar-isoscalar $\pi\pi$ correlations in nuclei [45–47], amongst others.

In this thesis, we want to focus on three questions:

1. The absolute value of the quark condensate gets reduced in nuclear matter. The linear-order density dependence of this process is well-known. If we knew higher-order terms, we might be able to extrapolate to even higher densities, e.g., as they appear in neutron stars. What are these higher-order terms?

2. The reduction of the quark condensate in nuclear matter suggests a partial restoration of chiral symmetry. Since the breaking of chiral symmetry is the origin of hadron masses, this restoration of chiral symmetry should have an effect on hadron properties. How do hadron properties change in nuclear matter?

3. The number of protons and neutrons in a system is rarely equal. For instance, in heavy nuclei, the neutron-to-proton ratio is around 1.5. In neutron stars, the same ratio is assumed to be around 10. If the number of protons and neutrons is not equal, we speak of isospin-asymmetric nuclear matter. What is the effect of isospin-asymmetric nuclear matter on the quark condensate and hadron properties?

To examine the first two questions, we investigate the density dependence of the quark condensate, as well as the density dependence of pion properties in nuclear matter. In particular, we will investigate the pions' mass, wave function renormalization and decay constant in nuclear matter. In order to answer the third question, we will perform our calculations using in-medium chiral perturbation theory in isospin-asymmetric nuclear matter. This introduces a parameter corresponding to the ratio of neutron and proton densities, which can be adjusted freely.

A common approach to calculate the quark condensate is using the Hellmann–Feynman theorem [48, 49] to first calculate the energy density and then take a derivative with respect to the quark mass [50–52]. This requires the knowledge of how certain hadron quantities depend on the quark mass, which is subject to debate. While it is possible to introduce several assumptions how specific hadron quantities depend on the quark mass, we use a different approach in this thesis as a method for bypassing this difficulty concerning the quark mass dependence: we make use of the chiral Ward identity. This allows us to connect the quark condensate to two-point correlation functions of pseudoscalar currents, which can be computed via chiral perturbation theory. For the pion properties, we precisely define the in-medium pion state and how to connect the in-vacuum to the in-medium properties. Thus, by calculating the pions' self-energy, we can compute the in-medium mass, wave function renormalization and decay constant.

The structure of this thesis is as follows. In Chapter 2, we introduce the theoretical foundation of our calculations: We will discuss QCD, its symmetries, and in-vacuum chiral perturbation theory. In Chapter 3, we discuss the main topic of this work: in-medium chiral perturbation theory. Following the literature, we derive the density expansion of the effective Lagrangian and present the Feynman rules for our calculations. In Chapter 4, we first show how to calculate the quark condensate in the framework of chiral perturbation theory and then compute the relevant Feynman diagrams. We also perform a simple extension to an SU(3) Lagrangian in order to examine the difference of up and down quark condensates, as well as the strange quark condensate. In Chapter 5, we discuss in-medium pion properties. We first define the in-medium pion state and related quantities and then calculate the pion self-energy and decay constant using two sets of Feynman diagrams. Finally, we summarize this thesis in Chapter 6.

2. Quantum Chromodynamics and Chiral Perturbation Theory

Quantum chromodynamics (QCD), the current theory of the strong interaction between quarks, describes the force responsible for hadron interactions. As such, it is the fundamental theory to discuss the in-medium properties of hadronic quantities. In this chapter, we will give a brief overview of QCD, present the symmetries of the theory and explain why there is a need for effective field theories. In Section 2.1, we briefly discuss the QCD Lagrangian and in Section 2.2, we list its symmetries and how those symmetries are broken. In Section 2.3, we discuss spontaneous symmetry breaking in general, in order to discuss the Nambu–Goldstone theorem, since the pions are the Nambu–Goldstone bosons of an SU(2) chiral symmetry. In Section 2.4, we motivate the introduction of effective theories and in Section 2.5, we state how the Nambu–Goldstone bosons transform under the chiral symmetry, to finally arrive at in-vacuum chiral perturbation theory.

2.1. The QCD Lagrangian

Quantum Chromodynamics is a gauge field theory based on the Lie group SU(3), which describes strong interactions. The Lagrangian density in its compact form reads

$$\mathcal{L}_{\mathrm{QCD}} = \bar{q}\Big[\mathrm{i}\not{D} - \mathsf{M}\Big]q - \frac{1}{4}G^{a}_{\mu\nu}G^{\mu\nu,a}, \tag{2.1}$$

or explicitly,

$$\mathcal{L}_{\mathrm{QCD}} = \bar{q}^{\alpha}_{f,i}\Big[\mathrm{i}\gamma^{\mu}_{\alpha\beta}\partial_\mu\delta_{ff'}\delta_{ij} - g\gamma^{\mu}_{\alpha\beta}\mathrm{t}^{a}_{ij}A^{a}_{\mu}\delta_{ff'} - \mathsf{M}_{ff'}\delta_{ij}\delta_{\alpha\beta}\Big]q^{\beta}_{f',j} - \frac{1}{4}G^{a}_{\mu\nu}G^{\mu\nu,a}, \tag{2.2}$$

where repeated indices are summed over. The $q^{\alpha}_{f,i}$ are quark spinor fields of flavor f, mass matrix $\mathsf{M} = \mathrm{diag}(m_1, \ldots, m_{N_f})$ and color i, with i taking values from 1 to $N_c = 3$. The γ^μ are the Dirac γ-matrices, satisfying the Clifford algebra,

$$\{\gamma^\mu, \gamma^\nu\}_{\alpha\beta} = 2\eta^{\mu\nu}\delta_{\alpha\beta}, \tag{2.3}$$

with spinor indices α, β, ranging from 1 to 4. The A^{a}_{μ} are the $N_c^2 - 1 = 8$ gauge fields, ensuring local SU(N_c) invariance of Eq. (2.2) with a taking values from 1 to $N_c^2 - 1$. The matrices

$\mathsf{t}^a_{ij} = \frac{1}{2}\lambda^a_{ij}$ are the generators of SU(3) and λ^a the Gell-Mann-matrices. The parameter g is the coupling between quarks and gluons. In analogy to QED, the gluon field strength tensors are defined as:

$$\begin{aligned} G^a_{\mu\nu}\mathsf{t}^a = \mathbb{G}_{\mu\nu} = D_\mu\mathcal{A}_\nu - D_\nu\mathcal{A}_\mu &= D_\mu A^a_\nu\mathsf{t}^a - D_\nu A^a_\mu\mathsf{t}^a \\ &= \partial_\mu A^a_\nu\mathsf{t}^a - \partial_\nu A^a_\mu\mathsf{t}^a + \mathrm{i}gA^a_\mu A^b_\nu[\mathsf{t}^a,\mathsf{t}^b] \\ &= \partial_\mu A^a_\nu\mathsf{t}^a - \partial_\nu A^a_\mu\mathsf{t}^a - g\, f^{abc}A^a_\mu A^b_\nu\mathsf{t}^c, \end{aligned} \tag{2.4}$$

where f^{abc} denotes the completely antisymmetric structure constants of the $\mathfrak{su}(3)$ Lie algebra, satisfying:

$$[\mathsf{t}^a,\mathsf{t}^b]_{ij} = \mathrm{i}f^{abc}[\mathsf{t}^c]_{ij}, \tag{2.5}$$

and D_μ is the covariant derivative, that has to be introduced in order to ensure local gauge invariance:

$$\partial_\mu\delta_{ij} \to D_{\mu,ij} = \partial_\mu\delta_{ij} + \mathrm{i}g\mathcal{A}_{\mu,ij} = \partial_\mu\delta_{ij} + \mathrm{i}gA^a_\mu[\mathsf{t}^a]_{ij}. \tag{2.6}$$

This Lagrangian exhibits several symmetries, which are the topic of the following section.

2.2. Symmetries in QCD

Quantum chromodynamics exhibits many symmetries, which will be discussed in the following paragraphs.

Color symmetry. This is the exact SU(3) symmetry, the theory was based on. It is a local symmetry and gives rise to $N_c^2 - 1 = 8$ gluon fields, which act as gauge fields.

Flavor symmetry. A quark's flavor determines its charge, hypercharge and possible interactions. The different flavors and their masses are arranged in Table 2.1, in order of ascending mass. At the typical low-energy scale of QCD, set by the nucleon mass $m_N = 939$ MeV, one can consider up and down quarks degenerate. This gives rise to a global SU(2) symmetry, also known as isospin symmetry. For all other flavors the effects of explicit symmetry breaking are noticeable and it is necessary to consider them in the construction of QCD models.

CPT symmetry. Quantum chromodynamics is CPT invariant, as well as C, P and T invariant separately.

Flavor	**Mass**	**Renormalization Scale**
up	$m_u = 2.16^{+0.49}_{-0.26}$ MeV	$\mu = 2$ GeV
down	$m_d = 4.67^{+0.48}_{-0.17}$ MeV	$\mu = 2$ GeV
strange	$m_s = 93^{+11}_{-5}$ MeV	$\mu = 2$ GeV
charm	$m_c = 1.27 \pm 0.02$ GeV	$\mu = m_c$
bottom	$m_b = 4.18^{+0.04}_{-0.03}$ GeV	$\mu = m_b$
top	$m_t = 172.76 \pm 0.30$ GeV	obtained via $\bar{t}t$ cross sections

Table 2.1.: Quark flavors and their $\overline{\text{MS}}$ masses [53].

Chiral symmetry. Since quarks are fermions, they can be represented by spinors that transform in the $(\frac{1}{2}, 0) \oplus (0, \frac{1}{2})$ representation of the Lorentz group, hence they exhibit chirality. Chiral symmetry is a flavor symmetry, that is, it acts on the flavor index of quarks[1]. Using chiral projection operators ($\chi = R, L$),

$$P_{\substack{R\\L}} = \tfrac{1}{2}(\mathbb{1} \pm \gamma^5), \quad q_\chi = P_\chi q, \quad \bar{q}_\chi = \bar{q} P_{-\chi}, \tag{2.7}$$

the quark sector of the QCD Lagrangian can be written like:

$$\mathcal{L} = \bar{q}(\mathrm{i}\not{D} - \mathsf{M})q \quad \rightarrow \quad \mathcal{L} = \sum_\chi \bar{q}_\chi \mathrm{i}\not{D} q_\chi - \bar{q}_\chi \mathsf{M} q_{-\chi}, \tag{2.8}$$

using $\bar{q}_\chi \gamma^\mu q_{-\chi} = 0$ and $\bar{q}_\chi q_\chi = 0$. We consider transformations under $\mathrm{U}(N_f)_R \times \mathrm{U}(N_f)_L$:

$$\mathrm{U}(N_f)_R : \begin{cases} q_R \rightarrow \mathrm{e}^{-\mathrm{i}\vartheta_R^a \mathsf{t}^a} q_R \\ q_L \rightarrow q_L \end{cases}, \quad \mathrm{U}(N_f)_L : \begin{cases} q_R \rightarrow q_R \\ q_L \rightarrow \mathrm{e}^{-\mathrm{i}\vartheta_L^a \mathsf{t}^a} q_L \end{cases}. \tag{2.9}$$

Since we are considering global symmetries, we can define $2N_f^2$ currents due to Noether's theorem and calculate their divergence:

$$j_\chi^{\mu a} = \bar{q}_\chi \gamma^\mu \mathsf{t}^a q_\chi = \bar{q} \gamma^\mu P_\chi \mathsf{t}^a q, \qquad \partial_\mu j_\chi^{\mu a} = \mathrm{i}\left(\bar{q}_{-\chi} \mathsf{M} \mathsf{t}^a q_\chi - \bar{q}_\chi \mathsf{t}^a \mathsf{M} q_{-\chi}\right). \tag{2.10}$$

The charges Q fulfill the same algebra as the generators of $\mathrm{SU}(N_f)_R \times \mathrm{SU}(N_f)_L$:

$$[Q_R^a, Q_R^b] = \mathrm{i} f^{abc} Q_R^c, \quad [Q_R^a, Q_L^b] = 0, \quad [Q_L^a, Q_L^b] = \mathrm{i} f^{abc} Q_L^c. \tag{2.11}$$

It is now possible to take a linear combination of the right- and left-chiral currents to define vector- and axial-vector currents:

$$j_V^{\mu a} = j_R^{\mu a} + j_L^{\mu a}, \quad j_A^{\mu a} = j_R^{\mu a} - j_L^{\mu a} \tag{2.12}$$

[1]Therefore it is important to keep track of the ordering of generators and the mass matrix.

This is equivalent to defining a vector transformation by $\vartheta_R = \vartheta_L$ and an axial-vector transformation by $\vartheta_R = -\vartheta_L$. The algebra of the new charges reads:

$$[Q^a_{_V}, Q^b_{_V}] = \mathrm{i} f^{abc} Q^c_{_V}, \quad [Q^a_{_V}, Q^b_{_A}] = \mathrm{i} f^{abc} Q^c_{_A}, \quad [Q^a_{_A}, Q^b_{_A}] = \mathrm{i} f^{abc} Q^c_{_V}, \tag{2.13}$$

which shows that the vector-currents are closed and can be interpreted as coming from a group $\mathrm{SU}(N_f)_V$. The same reasoning leads to a $\mathrm{U}(1)_V$ and a $\mathrm{U}(1)_A$. However, the 8 generators $Q^a_{_A}$ ($a \neq 0$) do not close into a subalgebra of our original one. So there is no group generated by them, instead we have a coset space:

$$Q^a_{_A} \in \Big(\mathrm{SU}(N_f)_R \times \mathrm{SU}(N_f)_L\Big) \Big/ \mathrm{SU}(N_f)_V, \quad a = 1, \ldots, N_f^2 - 1. \tag{2.14}$$

We conclude that the original $\mathrm{U}(N_f)_R \times \mathrm{U}(N_f)_L$ symmetry group gets spontaneously broken to $\mathrm{U}(1)_V \times \mathrm{SU}(N_f)_V \times \mathrm{U}(1)_A$ and those generators that are not part of the diagonal subgroup[2] of $\mathrm{SU}(N_f)_R \times \mathrm{SU}(N_f)_L$.

For completeness, we list the currents' equal-time commutation relations[3]. Integration over d^3x leads back to the relations for the charges:

$$L,\, R \text{ basis} \quad [j^{0a}_\chi(t,\boldsymbol{x}), j^{0b}_{\chi'}(t,\boldsymbol{y})] = \mathrm{i} f^{abc} j^{0c}_\chi(t,\boldsymbol{x}) \delta^{(3)}(\boldsymbol{x}-\boldsymbol{y}) \delta_{\chi\chi'}, \tag{2.15a}$$

$$V,\, A \text{ basis} \quad [j^{0a}_V(t,\boldsymbol{x}), j^{0b}_V(t,\boldsymbol{y})] = \mathrm{i} f^{abc} j^{0c}_V(t,\boldsymbol{x}) \delta^{(3)}(\boldsymbol{x}-\boldsymbol{y}), \tag{2.15b}$$

$$[j^{0a}_V(t,\boldsymbol{x}), j^{0b}_A(t,\boldsymbol{y})] = \mathrm{i} f^{abc} j^{0c}_A(t,\boldsymbol{x}) \delta^{(3)}(\boldsymbol{x}-\boldsymbol{y}), \tag{2.15c}$$

$$[j^{0a}_A(t,\boldsymbol{x}), j^{0b}_A(t,\boldsymbol{y})] = \mathrm{i} f^{abc} j^{0c}_V(t,\boldsymbol{x}) \delta^{(3)}(\boldsymbol{x}-\boldsymbol{y}). \tag{2.15d}$$

Chiral symmetry is broken in many different ways (see Table 2.2):

- Explicit breaking: the non-degenerate or non-vanishing quark masses break chiral symmetry explicitly. In case of equal, but non-zero quark masses, $\mathrm{U}(N_f)_R \times \mathrm{U}(N_f)_L$ gets broken down to $\mathrm{U}(N_f)_V$. And if the quark masses are not even equal, then $\mathrm{U}(N_f)_V$ gets broken down to $\mathrm{U}(1)_V$.

- Anomaly: the anomalous term can be calculated using the Fujikawa method [54] or by calculating one-loop Feynman diagrams, e.g. the triangle diagram. It is proportional to a surface term $\sim \tilde{G}G$.

- Spontaneous breaking: this affects the $N_f^2 - 1$ non-diagonal part of the original chiral group $\mathrm{SU}(N_f)_R \times \mathrm{SU}(N_f)_L$. It would lead to $N_f^2 - 1$ massless Nambu–Goldstone bosons. However, since those generators are also broken explicitly, they do have a small mass.

[2] $\mathrm{SU}(N_f)_V$ is the diagonal subgroup of $\mathrm{SU}(N_f)_R \times \mathrm{SU}(N_f)_L$. Using the notation $(g_1, g_2) \in G_1 \times G_2$, it contains the elements (g, g), since $\vartheta_R = \vartheta_L$.

[3] Only the $\mathrm{SU}(N)$-part, which means $a \neq 0$.

Transformation	**Current**	$\partial_\mu j^{\mu a}_{\sim}$	**EB**	**A**	**SSB**
$\mathrm{e}^{-\mathrm{i}\epsilon_V^0 \mathsf{t}^0} \in \mathrm{U}(1)_V$	$j_V^{\mu 0} = \bar{q}\gamma^\mu q$	$0^{\,(1)}$			
$\mathrm{e}^{-\mathrm{i}\epsilon_V^a \mathsf{t}^a} \in \mathrm{SU}(N_f)_V$	$j_V^{\mu a} = \bar{q}\gamma^\mu \mathsf{t}^a q$	$\mathrm{i}\bar{q}[\mathsf{M}, \mathsf{t}^a]q^{\,(2)}$	•		
$\mathrm{e}^{-\mathrm{i}\epsilon_A^0 \gamma^5 \mathsf{t}^0} \in \mathrm{U}(1)_A$	$j_A^{\mu 0} = \bar{q}\gamma^\mu\gamma^5 q$	$\mathrm{i}\bar{q}\mathsf{M}\gamma^5 q^{\,(3)} + \frac{g^2 N_f}{32\pi^2}\widetilde{G}^a_{\mu\nu}G^{\mu\nu a\,(4)}$	•	•	
$\mathrm{e}^{-\mathrm{i}\epsilon_A^a \gamma^5 \mathsf{t}^a}$	$j_A^{\mu a} = \bar{q}\gamma^\mu\gamma^5 \mathsf{t}^a q$	$\mathrm{i}\bar{q}\{\mathsf{M}, \mathsf{t}^a\}\gamma^5 q^{\,(5)}$	•		•

Table 2.2.: Summary of QCD's chiral symmetry and its breaking. "EB", "A", and "SSB" stand for "explicit breaking", "anomaly", and "spontaneous symmetry breaking", respectively. $^{(1)}$This conserved current leads to the conservation of baryon number. $^{(2)}$Since t^3 and t^8 are diagonal, they commute with M, which leads to conserved isospin and hypercharge currents. $^{(3)}$For equal quark masses $\mathsf{M} = m\mathbb{1}$, this term can be written as a pseudoscalar current, mj_P. $^{(4)}$This term is the $\mathrm{U}(1)_A$ anomaly. $^{(5)}$For equal quark masses $\mathsf{M} = m\mathbb{1}$, this term can be written as a pseudoscalar current, mj_P^a, which is known as the PCAC relation.

Consider the isovector axial-vector currents $j_A^{\mu a}$ and their role in the definition of the decay constant of a certain Nambu–Goldstone boson (NG):

$$\langle 0|j_A^{\mu a}(x)|\mathrm{NG}^b(p)\rangle \sim \mathrm{i}f_{\mathrm{NG}}\, p^\mu \mathrm{e}^{\mathrm{i}p\cdot x}\delta^{ab}.$$

Since this current is not conserved due to explicit symmetry breaking, we can write:

$$\langle 0|\underbrace{\partial_\mu j_A^{\mu a}(x)}_{\neq 0}|\mathrm{NG}^b(p)\rangle \sim \mathrm{i}f_{\mathrm{GB}}\, p^2 \mathsf{t}^a \mathrm{e}^{\mathrm{i}p\cdot x}\delta^{ab} \propto m_{\mathrm{NG}}^2 \neq 0,$$

and the particles are called Pseudo-Nambu–Goldstone bosons. Actually, we should speak of **dynamical symmetry breaking** here, since the field operators that acquire a vacuum expectation value, $\bar{q}q$ are not an elementary field of the theory, but a composite field. Dynamical symmetry breaking generates the constituent quark masses and is responsible for 98% of mass in the universe.

The spontaneous breaking of chiral symmetry will be the main focus of the next section.

Further symmetries. For completeness, QCD also exhibits the following symmetries: Z-symmetry (spontaneously broken in the gauge sector of QCD at finite temperatures; many confinement studies are based on this theory) and conformal symmetry (broken by the so-called trace anomaly).

2.3. Spontaneous chiral symmetry breaking and the Nambu–Goldstone theorem

In this section, we will discuss spontaneous symmetry breaking and the Nambu–Goldstone theorem, which states that spontaneous symmetry breaking leads to massless particles, as discussed in various textbooks [9, 10, 55–57]. Let us consider a theory with quantum fields $\varphi_i(x^\mu)$ and that the action is invariant under a continuous symmetry transformation. This leads to conserved currents via Noether's theorem [58, 59]:

$$j^\mu(x) = j^\mu_a(x)\epsilon^a, \qquad\qquad j^\mu_a(x) = \frac{\partial\mathcal{L}}{\partial(\partial_\mu\varphi_i(x))}\frac{\delta\varphi_i(x)}{\delta\epsilon^a}, \tag{2.16}$$

such that $\partial_\mu j^\mu_a = 0$. We can then define the following conserved charges Q^a by integrating the 0-components of the currents j^μ_a: $Q^a = \int \mathrm{d}^3\boldsymbol{x}\, j^0_a(x)$, which can be used to generate the symmetry transformation of the fields, since they form a representation of the symmetry algebra on the Hilbert space[4]:

$$\varphi_i(x) \to \varphi'_i(x) = \mathrm{e}^{\mathrm{i}\epsilon^a Q^a}\varphi_i(x)\mathrm{e}^{-\mathrm{i}\epsilon^a Q^a} = \varphi_i(x) + \delta\varphi_i(x) \quad \to \delta\varphi_i(x) \approx \mathrm{i}\epsilon^a[Q^a, \varphi_i(x)]. \tag{2.17}$$

where the approximation denotes omitting terms of order ϵ^2. The fields $\varphi_i(x)$ belong to a certain representation of the symmetry group. If we denote the generators in that representation with $[\mathsf{t}^a]_{ij}$, we can write their transformation behavior also like this:

$$\varphi_i(x) \to \varphi'_i(x) = \left[\mathrm{e}^{\mathrm{i}\epsilon^a\mathsf{t}^a}\right]_{ij}\varphi_j(x) = \varphi_i(x) + \delta\varphi_i(x) \quad \to \delta\varphi_i(x) \approx \mathrm{i}\epsilon^a[\mathsf{t}^a]_{ij}\varphi_j(x). \tag{2.18}$$

where again the approximation denotes omitting terms of order ϵ^2. By comparing the two expressions for $\delta\varphi_i(x)$, we get: $[Q^a, \varphi_i(x)] = [\mathsf{t}^a]_{ij}\varphi_j(x)$.

A state $|\psi\rangle$ breaks this symmetry if there exists any operator A such that:

$$\langle\psi|\,[Q^a, A]\,|\psi\rangle \neq 0. \tag{2.19}$$

If such an operator A does not exist, the state $|\psi\rangle$ is symmetric under $U = \exp(\mathrm{i}\epsilon^a Q^a)$. This is consistent with the statement that a state is symmetric under the transformation U if $U|\psi\rangle = |\psi\rangle$, because then the left-hand side of Eq. (2.19) would vanish. We now define *spontaneous* symmetry breaking (SSB) in the case that $|\psi\rangle \to |0\rangle$, i.e. a symmetry transformation leaves the equations of motion invariant, but not the vacuum ground state of the theory: $\exists\, A$: $\langle 0|\,[Q^a, A]\,|0\rangle \neq 0$. We thus distinguish two cases:

1. **No SSB:** If the unitary transformation operators leave the vacuum invariant, then there is no spontaneous breaking of the symmetry:

$$\mathrm{e}^{\mathrm{i}\epsilon^a Q^a}\,|0\rangle = |0\rangle\,. \tag{2.20}$$

[4] This means: $[\mathsf{t}^a, \mathsf{t}^b] = \mathrm{i}f^{abc}\,\mathsf{t}^c$ and $[Q^a, Q^b] = \mathrm{i}f^{abc}Q^c$.

Expanding this in a Taylor series reveals that all charge operators must annihilate the vacuum: $Q^a |0\rangle = 0 \; \forall \, a$. Thus, for any operator A, the symmetry is not broken in the ground state:

$$\langle 0| [Q^a, A] |0\rangle = \underbrace{\langle 0| Q^a}_{0} A |0\rangle - \langle 0| A \underbrace{Q^a |0\rangle}_{0} = 0. \tag{2.21}$$

This is also known as the "Wigner–Weyl realization" of a symmetry.

2. SSB: If the transformation operators do not leave the vacuum invariant, then the symmetry has been spontaneously broken:

$$\mathrm{e}^{\mathrm{i}\epsilon^a Q^a} |0\rangle \neq |0\rangle \,. \tag{2.22}$$

This means, there must be at least one charge operator which does not annihilate the vacuum: $\exists \, a : Q^a |0\rangle \neq 0$. Consequently, there must exist an operator that acquires a non-zero vacuum expectation value:

$$\langle 0| [Q^a, A] |0\rangle \neq 0. \tag{2.23}$$

The quantity in Eq. (2.23) takes on the role as an order parameter: "*An order parameter is a non-vanishing vacuum expectation value of some local field, which transforms non-trivially under the symmetry group.*" [60]. And if this "local field" $[Q^a, A]$ is not an elementary field, but instead a composite field[5], we speak of *dynamical* symmetry breaking. This is known as the "Nambu–Goldstone realization" of a symmetry.

A naive way to arrive at massless particle states in the spectrum is to claim that since one charge operator does not annihilate the vacuum, it should be another state which we could denote with λ: $Q^a |0\rangle = |\lambda\rangle$. Since the Q^a are symmetry generators of the theory, they commute with the Hamiltonian, which implies $H |\lambda\rangle = HQ^a |0\rangle = Q^a H |0\rangle = 0$, i.e. the state $|\lambda\rangle$ is an eigenstate of the Hamiltonian with zero eigenvalue. However, the action of Q^a on the ground state $|0\rangle$ leads to a non-normalizable in the case of spontaneous symmetry breaking, as stated by the Fabri–Picasso theorem [61]:

$$\begin{aligned} \| Q |0\rangle \| = \langle 0| QQ |0\rangle &= \int \mathrm{d}^3\boldsymbol{x} \, \langle 0| j_0(x) Q |0\rangle & \text{(2.24a)} \\ &= \int \mathrm{d}^3\boldsymbol{x} \, \langle 0| e^{\mathrm{i}Px} j_0(0) e^{-\mathrm{i}Px} Q e^{\mathrm{i}Px} e^{-\mathrm{i}Px} |0\rangle & \text{(2.24b)} \\ &= \int \mathrm{d}^3\boldsymbol{x} \, \langle 0| j_0(0) Q |0\rangle \,. & \text{(2.24c)} \end{aligned}$$

Here we assumed that both the vacuum state $|0\rangle$ as well as the charge operator Q are translationally invariant. If $Q|0\rangle = 0$, then the norm is zero. If not, the integral on the right-hand side diverges (because nothing depends on x anymore) and the norm of the state $Q|0\rangle$ gets infinitely large. Therefore, $Q|0\rangle$ can only be part of the Hilbert space if $Q|0\rangle = 0$. So instead, let us discuss a more rigorous proof of the Nambu–Goldstone theorem.

[5]e.g. the quark condensate $\bar{q}q$, whereas only $q(x)$ would be an elementary field.

Nambu–Goldstone theorem. The Nambu–Goldstone theorem [62–64] states that for every spontaneously broken generator, there will be a massless, spin-0 particle (a so-called Nambu–Goldstone boson) in the theory: *"Consider a Poincaré invariant theory that is invariant under a group G and has conserved currents j^μ_a. Let Q^a be a generator of G that breaks the symmetry spontaneously. Then there are massless spin-0 particles (Nambu–Goldstone bosons) which couple to the currents j^μ_a and thus have the same quantum numbers."*

To start the proof, let us remind ourselves that spontaneous symmetry breaking takes place, if there exists an order parameter operator $[Q^a, A]$, which yields a non-zero vacuum expectation value: $\langle 0| [Q^a, A] |0\rangle \neq 0$. In order to avoid any subtlety with the ill-defined charge Q in the case of SSB, we use the commutator of the current j^0:

$$\langle 0| [Q^a, A] |0\rangle = \int \mathrm{d}^3\boldsymbol{x}\, \langle 0| [j^0_a(x), A] |0\rangle \neq 0. \tag{2.25}$$

We insert a completeness relation of one-particle states $\mathbb{1} = \sum_n \int \mathrm{d}^3\boldsymbol{k}\,(2\pi)^{-3}\, |n,\boldsymbol{k}\rangle\langle n,\boldsymbol{k}|$ between the current $j^0_a(x)$ and the operator A, where the states $|n,\boldsymbol{k}\rangle$ have momentum $\boldsymbol{k}$ and n represents all other quantum numbers. These states are normalized[6] by $\langle n',\boldsymbol{k}'|n,\boldsymbol{k}\rangle = (2\pi)^3\delta_{nn'}\delta^{(3)}(\boldsymbol{k}-\boldsymbol{k}')$. This yields:

$$\langle 0| [Q^a, A] |0\rangle = \sum_n \int \frac{\mathrm{d}^3\boldsymbol{k}}{(2\pi)^3}\, \mathrm{d}^3\boldsymbol{x} \left[\langle 0| j^0_a(x) |n,\boldsymbol{k}\rangle\langle n,\boldsymbol{k}| A |0\rangle - c.c. \right] \neq 0, \tag{2.26}$$

where *c.c.* denotes complex conjugation. We use $T(a)\varphi(x)T^{-1}(a) = \varphi(x{+}a)$ with the translation operator $T(a) = \mathrm{e}^{\mathrm{i}P^\mu a_\mu}$ in order to remove the position dependence on the current $j^0_a(x)$. Here $P^\mu |n,\boldsymbol{k}\rangle = k^\mu |n,\boldsymbol{k}\rangle$ and $P^\mu |0\rangle = 0$ denote the momentum operator acting on a state with momentum k^μ and the vacuum, respectively:

$$\langle 0| [Q^a, A] |0\rangle = \sum_n \int \frac{\mathrm{d}^3\boldsymbol{k}}{(2\pi)^3}\, \mathrm{d}^3\boldsymbol{x} \left[\langle 0| j^0_a(0) |n,\boldsymbol{k}\rangle\langle n,\boldsymbol{k}| A |0\rangle\, \mathrm{e}^{-\mathrm{i}k\cdot x} - c.c. \right] \neq 0. \tag{2.27}$$

We evaluate the $\mathrm{d}^3\boldsymbol{x}$ integration, which yields a Dirac delta function:

$$\langle 0| [Q^a, A] |0\rangle = \sum_n \int \mathrm{d}^3\boldsymbol{k} \left[\langle 0| j^0_a(0) |n,\boldsymbol{k}\rangle\langle n,\boldsymbol{k}| A |0\rangle\, \mathrm{e}^{-\mathrm{i}E(\boldsymbol{k})t} - c.c. \right] \delta^{(3)}(\boldsymbol{k}) \neq 0. \tag{2.28a}$$

We can conclude two things:

1. Since the right-hand side has to be non-zero for spontaneous symmetry breaking, the two matrix elements $\langle 0| j^0_a(0) |n,\boldsymbol{k}\rangle$ and $\langle n,\boldsymbol{k}| A |0\rangle$ must be non-zero as well. This implies that there be a one-particle state $|n,\boldsymbol{k}\rangle$ with the same parity and internal quantum numbers as j^0_a and the operator A. In particular, this means that the state is a spin-0 state.

[6] We temporarily choose this normalization instead of the covariant normalization where states are normalized according to: $\langle n',\boldsymbol{k}'|n,\boldsymbol{k}\rangle = (2\pi)^3 2E(\boldsymbol{k})\delta_{nn'}\delta^{(3)}(\boldsymbol{k}-\boldsymbol{k}')$, in order to avoid dividing by zero, since massless states would be normalized to 0 using this normalization where the completeness relation reads: $\mathbb{1} = \sum_n \int \mathrm{d}^3\boldsymbol{k}\,(2\pi)^{-3}(2E(\boldsymbol{k}))^{-1}\, |n,\boldsymbol{k}\rangle\langle n,\boldsymbol{k}|$.

2. Since the right-hand side must be time-independent, we require that $E(\boldsymbol{k}) = 0$. Since we also have a delta function $\delta^{(3)}(\boldsymbol{k})$, the energy at zero momentum must vanish, which is only possible for massless states. This massless particle state is called a Nambu–Goldstone boson. Note that the covariant state normalization does not work here, because the $\mathrm{d}^3\boldsymbol{k}$ would be divided by the energy, and if the energy and the state norm are zero, we would divide zero by zero[7].

Furthermore, for every symmetry transformation generator Q^a that does not annihilate the vacuum, there is one such massless state.

QCD and chiral symmetry. In the case of QCD's chiral symmetry, the generators that spontaneously break chiral symmetry are the ones belonging to the non-diagonal subgroup of $\mathrm{SU}(N)_L \times \mathrm{SU}(N)_R$ (see Table 2.2) and the operator A is a pseudoscalar current:

$$Q^a = \int \mathrm{d}^3\boldsymbol{x}\, \bar{q}\gamma^\mu\gamma^5\frac{\tau^a}{2}q, \qquad\qquad A^b = P^b = \bar{q}\mathrm{i}\gamma^5\tau^b q. \tag{2.29}$$

The order parameter operator is thus given by:

$$[Q^a, A^b] = \int \mathrm{d}^3\boldsymbol{x}\, [\bar{q}\gamma^0\gamma^5\frac{\tau^a}{2}q(x), \bar{q}\mathrm{i}\gamma^5\tau^b q(y)]. \tag{2.30}$$

We can simplify this commutator with the help of the following identity:

$$[q^\dagger(x)\Gamma^A\Lambda^a q(x), q^\dagger(y)\Gamma^B\Lambda^b q(y)]_{x^0=y^0} = \delta^{(3)}(\boldsymbol{x}-\boldsymbol{y})q^\dagger(x)[\Gamma^A\Lambda^a, \Gamma^B\Lambda^b]q(x), \tag{2.31}$$

where Γ^A and Λ^a are generic gamma matrices and Pauli matrices, respectively. In our case, $\Gamma^A = \gamma^0\gamma^0\gamma^5$, $\Gamma^B = \gamma^0\gamma^5$, $\Lambda^a = \frac{\tau^a}{2}$, $\Lambda^b = \tau^b$, such that we can simplify the commutator as follows:

$$[\Gamma^A\Lambda^a, \Gamma^B\Lambda^b] = \underbrace{[\Gamma^A, \Gamma^B]}_{-2\gamma^0}\Lambda^a\Lambda^b + \Gamma^B\Gamma^A\underbrace{[\Lambda^a, \Lambda^b]}_{\mathrm{i}\epsilon^{abc}\tau^c}. \tag{2.32}$$

This means, the order parameter operator is given by:

$$[Q^a, A^b] = -\delta^{ab}\bar{q}(x)q(x), \tag{2.33}$$

and the order parameter is the quark condensate: $\langle 0|[Q^a, A^b]|0\rangle = -\delta^{ab}\langle 0|\bar{q}q|0\rangle$. If we consider Eq. (2.28a) with the covariant normalization (i.e. divide by $2k_0$) and define the following matrix elements with the pions as the Nambu–Goldstone bosons,

$$\langle 0|j_a^\mu(x)|\pi^b(\boldsymbol{k})\rangle = \mathrm{i}\delta^{ab}k^\mu f_\pi \mathrm{e}^{-\mathrm{i}\boldsymbol{k}\cdot x}, \qquad\qquad \langle 0|P^a(x)|\pi^b(\boldsymbol{k})\rangle = \delta^{ab}G_\pi \mathrm{e}^{-\mathrm{i}\boldsymbol{k}\cdot x}, \tag{2.34}$$

then Eq. (2.28a) directly yields the Glashow–Weinberg relation: $f_\pi G_\pi = -\langle 0|\bar{q}q|0\rangle$.

[7]Strictly speaking, none of the states $|n, \boldsymbol{k}\rangle$ are normalizable because of the delta function. A more rigorous proof assumes a finite volume V to discretize the momenta and takes the limit $V \to \infty$, as done e.g. in Ref. [55].

2.4. Effective field theories

An effective field theory is generally a low-energy approximation to a more fundamental underlying theory. Considering some energy scale Λ of the fundamental theory, we are only interested in energies below that scale. In fact, it is not even necessary to know the details of the underlying theory at energies larger than Λ, in order to still have a good approximation. [10].

How does one construct an effective field theory? It is necessary to connect the observables calculated in such a low energy theory to the fundamental theory. The way this is achieved is by considering the most general Lagrangian that exhibits all the symmetries of the underlying theory. According to Weinberg, this yields the "*most general possible S-matrix consistent with analyticity, perturbative unitarity, cluster decomposition and the assumed symmetry principles*" [65]. Therefore it is of great importance to understand the symmetries of the fundamental theory, which we discussed in Section 2.2 for the case of QCD.

There are three main types of effective field theories. First, a theory with complete decoupling of heavy fields. In other words, heavy fields φ with a mass $m_\varphi > \Lambda$ that is greater than some cut-off are integrated out. An example of this would be the Fermi theory of weak interactions. Second, partial decoupling of heavy fields. In this case, only the high-momentum modes are integrated out. A prominent example is heavy quark effective theory (HQET). Third, a theory with spontaneous symmetry breaking. Here, we only consider the energy regime where the symmetry is already broken. An example of this kind of theory is chiral perturbation theory, which will be the topic of the next chapter.

2.5. Vacuum chiral perturbation theory

Chiral perturbation theory [10, 33] is an effective field theory, therefore its most fundamental quantity is the Lagrangian, which exhibits all symmetries of QCD and enters the partition function Z, which contains the information of all possible interactions. The partition function, or generating functional, is defined as the transition amplitude between two asymptotic *in*- and *out*-states, and can be written as the exponential of the functional of all connected Green functions W:

$$\mathcal{Z}[J] = \mathrm{e}^{\mathrm{i}W[J]} = \langle \Omega_{\mathrm{out}} | \Omega_{\mathrm{in}} \rangle_J . \tag{2.35}$$

In the main part of this thesis, we will take these asymptotic states to describe Fermi seas of non-interacting protons and neutrons at times $t \to \pm\infty$. In this section however, we will focus on in-vacuum chiral perturbation theory and review the fundamental points.

In the next two sections, we will discuss the chiral field U and the chiral Lagrangian.

2.5.1. The chiral field

Chiral perturbation theory is an effective theory to describe Nambu–Goldstone bosons, in our case, the pions. However, the field we use to construct the Lagrangian is not the pion field itself, but rather a non-linear parametrization of the pion field, called the chiral field $U(\pi)$.

Non-linear realization of chiral symmetry

In this section we closely follow Refs. [7, 10] to discuss the non-linear realization of chiral symmetry, which was originally developed by Callan, Coleman, Wess and Zumino [20, 21, 66, 67]. The goal of this section is to find a convenient way to represent the Nambu–Goldstone fields, with which we can build a Lagrangian that is invariant under chiral transformations.

General considerations for an arbitrary symmetry group. We start by defining a set of vectors Φ, the components of which are the Nambu–Goldstone (NG) fields ϕ_i, where $i = 1, .., n$. These functions $\phi_i(x)$ are smooth functions from Minkowski space $\mathbb{R}^{3,1}$ to the real numbers:

$$M_1 \equiv \{\Phi \in \mathbb{R}^n \mid \phi_i : \mathbb{R}^{3,1} \to \mathbb{R} \text{ are smooth functions}\}. \tag{2.36}$$

We want to find a bijective function $\varphi(g, \Phi)$, which takes an element $g \in G$ of the symmetry group and a configuration of NG fields and then returns a new configuration of NG fields,

$$\varphi(g, \Phi) : (G, M_1) \to M_1. \tag{2.37}$$

By finding this function, we know how an element of the abstract group G acts on the vector Φ of NG fields.

We demand two basic properties for this function φ. First, that the identity element $e \in G$ returns the same vector Φ, and second, that a composite transformation $g_1 g_2 \in G$ acts successively via φ:

$$\varphi(e, \Phi) = \Phi, \tag{2.38a}$$

$$\varphi(g_1 g_2, \Phi) = \varphi(g_1, \varphi(g_2, \Phi)). \tag{2.38b}$$

In the case of spontaneous symmetry breaking, the symmetry group G gets broken down to a subgroup $H \leq G$. By definition, this elements of this subgroup H must leave the ground state of the theory invariant. Let $\Phi = 0$ be the origin of M_1, which we interpret as the ground state. Then,

$$\varphi(h, 0) = 0 \quad \forall \quad h \in H. \tag{2.39}$$

In the following, we want to investigate the action of an element of the quotient space G/H on vectors in M_1, so we define the *left coset* of an element $g \in G$ with respect to a subgroup

$H \leq G$ as the set $gH \equiv \{gh|\ h \in H\}$. Since the identity is element of the group H (compare Eqs. (2.38a) and (2.39)), g itself is part of its coset. Furthermore, the set of all left cosets of group elements g with respect to a subgroup H defines the quotient space G/H. We state without proof that cosets either completely overlap or separate in completely disjoint cosets.

If we let an element $gh \in G/H$ of the quotient space act on the ground state, it will lead us to the same vector in M_1, independent of which $h \in H$ we choose. That is, all elements (so-called representatives) of a given coset gH lead to the same vector Φ_g:

$$\varphi(gh, 0) = \varphi(g, \varphi(h, 0)) = \varphi(g, 0) \equiv \Phi_g \in M_1. \tag{2.40}$$

Next we will show that φ is injective with respect to elements of different cosets, i.e. with respect to G/H. For g and g' belonging to different cosets ($g' \notin gH$, that is, g' cannot be written as $g' \neq gh$ for any $h \in H$, in particular since $e \in H$, $g' \neq g$), the respective output of the function $\Phi_g = \varphi(g, 0)$ and $\Phi_{g'} = \varphi(g', 0)$ will be different. To show this we use proof by contradiction: let us assume that g and g' belong to different cosets, $g' \notin gH$, but that $\Phi_g = \varphi(g, 0) = \varphi(g', 0) = \Phi_{g'}$. By using this, we can calculate:

$$0 = \varphi(e, 0) = \varphi(g^{-1}g, 0) = \varphi(g^{-1}, \varphi(g, 0)) \overset{(*)}{=} \varphi(g^{-1}, \varphi(g', 0)) = \varphi(g^{-1}g', 0), \tag{2.41}$$

where $(*)$ marks where we use our assumption. Since the last expression must be equal to 0, this means that $g^{-1}g'$ must be an element of H (since only elements of H leave the vacuum invariant). However, this means that $g^{-1}g' \in H \leftrightarrow g' \in gH$, which contradicts our assumption. This shows that two different $\Phi_g \neq \Phi_{g'}$ can be backtracked to different cosets, meaning that the cosets are in fact completely disjunct and that φ is invertible. This property of invertibility is important, because now we can start with a given configuration of the NG fields $\tilde{\Phi} = \varphi(\tilde{g}, 0) = \varphi(\tilde{g}h, 0)$ and uniquely determine the coset that $\tilde{g}h$ belongs to. One element $\tilde{g}h \in \tilde{g}H$ is called a representative of this coset.

Now what happens when we want to let a general group element $g \in G$ act on $\tilde{\Phi}$? By having this unique relationship between $\tilde{\Phi}$ and $\tilde{g}H$, we can investigate this. Instead of asking how g affects Φ, we know how g acts on $\tilde{g}H$, since they form a group:

$$\Phi_{\tilde{g}} \xrightarrow{g} \Phi'_{\tilde{g}} = \varphi(g, \tilde{\Phi}) = \varphi(g, \varphi(\tilde{g}h, 0)) = \varphi(g\tilde{g}h, 0) \equiv \Phi_{g\tilde{g}}. \tag{2.42}$$

We see that the transformation $\Phi_{\tilde{g}} \xrightarrow{g} \Phi'_{\tilde{g}}$ corresponds to letting g act on $\Phi_{\tilde{g}}$'s coset, $\tilde{g}H \to g\tilde{g}H$, thus creating a different coset $(g\tilde{g})H$, which (as we showed) is completely disjoint from the previous one. In other words, this way lets g transform one Φ to a strictly different Φ'. We can represent this situation using a commutative diagram:

$$\begin{tikzcd}
\Phi_{\tilde{g}} \arrow[rr, "g", "\text{unknown how to do}"'] \arrow[d, "\text{search for unique coset}"', "\varphi^{-1}"] & & \Phi'_{\tilde{g}} \\
\tilde{g}H \arrow[rr, "g", "\text{binary group operation}"'] & & g\tilde{g}H \arrow[u, "\varphi", "\text{new coset specifies a new } \Phi'"']
\end{tikzcd}$$

So instead of going from Φ to Φ', which we do not know how to do, we identify the unique coset $\tilde{g}H$ that is related to $\Phi_{\tilde{g}}$. Since this coset is part of the group G, we know how to let g act on this based on the binary group operation that defines G and then we can use φ to identify the new vector Φ' based on $g\tilde{g}H$.

Application to QCD. QCD's chiral symmetry and its spontaneous breaking are described by the following groups,

$$G = \mathrm{SU}(N)_L \times \mathrm{SU}(N)_R \quad \overset{\chi\mathrm{SB}}{\to} \quad H = \mathrm{SU}(N)_V, \tag{2.43}$$

which are given by

$$G = \{(L, R) \mid L \in \mathrm{SU}(N), R \in \mathrm{SU}(N)\}, \tag{2.44a}$$

$$H = \{(V, V) \mid V \in \mathrm{SU}(N)\}, \tag{2.44b}$$

where H is the diagonal subgroup of G. According to the Nambu–Goldstone theorem [62–64], this leads to massless Nambu–Goldstone bosons ϕ_i ($i = 1, .., N^2 - 1$) that live in the coset space G/H. However, the chiral transformations are elements of the larger group G. How the Nambu–Goldstone boson, i.e. the pion, transforms under an element $g \in G$, will be the topic from this point on.

Let us consider an element $\tilde{g} = (\tilde{L}, \tilde{R}) \in G$. Its left coset $\tilde{g}H$ contains all pairs $(\tilde{L}V, \tilde{R}V)$ where $V \in \mathrm{SU}(N)$. Since all coset representatives lead to the same NG boson configuration, we are free to choose a certain $(V, V) \in H$. A common convention is to choose V such that the first element of the pair $(\tilde{L}V, \tilde{R}V)$ is the identity matrix, i.e. $V = \tilde{L}^\dagger$. For a given $\tilde{g} = (\tilde{L}, \tilde{R}) \in G$, its coset will be represented by $(\mathbb{1}, \tilde{R}\tilde{L}^\dagger)$, and this can be identified by just one matrix $U \equiv \tilde{R}\tilde{L}^\dagger$ (since the other one is $\mathbb{1}$ by convention). This U is now uniquely connected to a certain configuration of NG bosons.

According to the commutative diagram depicted above, the question how the NG bosons transform can be answered by investigating how the coset transforms. A general chiral transformation $g = (L, R)$ acts on the coset $\tilde{g}H$ in the following way:

$$g \circ \tilde{g}H \quad \to \quad (L, R) \circ (\tilde{L}V, \tilde{R}V) = (L\tilde{L}V, R\tilde{R}V), \tag{2.45}$$

and again, we choose V such that the first element becomes the identity matrix: $L\tilde{L}V \stackrel{!}{=} \mathbb{1} \leftrightarrow V = \tilde{L}^\dagger L^\dagger$. The new coset representative is therefore $(\mathbb{1}, U') = (\mathbb{1}, R\tilde{R}\tilde{L}^\dagger L^\dagger)$ and we can read off the transformation behavior of U:

$$U \stackrel{g=(L,R)}{\longrightarrow} RUL^\dagger. \tag{2.46}$$

Let us summarize what we have got so far. The NG fields are collected in a vector $\Phi = (\phi_1, .., \phi_n)$ where ϕ_i are smooth functions from Minkowski space to the real numbers. We know in an abstract way that Φ can be represented by the left coset $\tilde{g}H$ for a particular $\tilde{g} \in G$ and as a representative of this coset we chose U. Now we want to make this connection less abstract and really get a connection between the NG fields and the object whose chiral transformation properties we know, U.

First, let us write the NG fields ϕ_i in a matrix, as opposed to a vector in $\mathbb{R}^n$. We define a set M_2, which contains matrices ϕ that act as functions from Minkowski space to Hermitian and traceless $n \times n$ matrices (the set of which is denoted by $\mathcal{H}(n)$):

$$M_2 \equiv \{\phi : \mathbb{R}^{3,1} \to \mathcal{H}(n) \mid \phi \,\text{contains smooth functions}\}. \tag{2.47}$$

A way to represent elements of $\mathcal{H}(2)$ is using an expansion in the Pauli matrices:

$$\phi = \phi_i \tau^i = \begin{pmatrix} \phi_3 & \phi_1 - \mathrm{i}\phi_2 \\ \phi_1 + \mathrm{i}\phi_2 & -\phi_3 \end{pmatrix}. \tag{2.48}$$

These ϕ_i are exactly what we will call the mathematical (or Cartesian) basis of the pions. One can extract one field ϕ_i out of the matrix ϕ by using $\phi_i = \frac{1}{2}\,\mathrm{Tr}_F\{\tau^i\phi\}$. As a side note, since the physical basis is defined as $\pi^\pm = (\phi_1 \mp \mathrm{i}\phi_2)/\sqrt{2}$ and $\pi^0 = \phi^3$, we could alternatively write ϕ as:

$$\phi = \begin{pmatrix} \pi^0 & \sqrt{2}\pi^+ \\ \sqrt{2}\pi^- & -\pi^0 \end{pmatrix}. \tag{2.49}$$

Second, we want to create a connection between the matrix ϕ and the matrix U. To do so, we define the set M_3 as the set of functions U from Minkowski space to $\mathrm{SU}(N)$:

$$M_3 \equiv \{U : \mathbb{R}^{3,1} \to \mathrm{SU}(N) \mid U = U[\phi] \text{ with } \phi \in M_2\}. \tag{2.50}$$

The simplest parametrization is $U[\phi] = \exp(\mathrm{i}\phi/F_0)$ with F_0 a dimensionful parameter to render the argument of the exponential function dimensionless. Since a bosonic field has units of energy, F_0 also has units of energy.

Finally, we identify this functional $U[\phi]$ with the coset representative $(\mathbb{1}, U) \in \tilde{g}H$ for the particular $\tilde{g}$ belonging to ϕ. To achieve this, we claim that our original φ (which took an element $g \in G$ and $\Phi \in \mathbb{R}^n$ as input to define the operation of g on Φ) now takes a $g \in G$ and a $U \in M_3$ as input and transforms it according to the behavior we already found in Eq. (2.46). Mathematically this can be written as:

$$\varphi : G \otimes M_3 \to M_3 \quad \text{with } \varphi[g, U] = \varphi[(L, R), U] = RUL^\dagger. \tag{2.51}$$

To verify that this is really a proper transformation for the NG boson fields, we need to check three things: (i) is $RUL^\dagger \in M_3$? (ii) Is $\varphi[e, U] = U$ fulfilled? (iii) Is $\varphi[g_1 g_2, U] = \varphi[g_1, \varphi[g_2, U]]$ fulfilled? The last two properties are the ones we initially demanded for the mapping φ in Eqs. (2.38a) and (2.38b).

(i) Since $U \in M_3$, it is a SU(N) function, taking $x^\mu \in \mathbb{R}^{3,1}$ as input. Therefore we can multiply the matrices $R, L^\dagger \in \mathrm{SU}(N)$ on it, yielding again a SU(N) matrix, since SU(N) is closed under matrix multiplication. Therefore, $RUL^\dagger$ is truly an element of M_3.

(ii) Yes: $\varphi[(\mathbb{1}, \mathbb{1}), U] = \mathbb{1}U\mathbb{1}^\dagger = \mathbb{1}U\mathbb{1} = U$.

(iii) We check both sides of the equation separately:

$$\begin{aligned}\varphi[g_1 g_2, U] &= \varphi[(L_1 L_2, R_1 R_2), U] = R_1 R_2 U L_2^\dagger L_1^\dagger,\\ \varphi[g_1, \varphi[g_2, U]] &= \varphi[(L_1, R_1), \varphi[(L_2, R_2), U]] = \varphi[(L_1, R_1), R_2 U L_1^\dagger] = R_1 R_2 U L_2^\dagger L_1^\dagger,\end{aligned}$$

so both sides are equal.

We note that φ is not a group representation, because M_3 is no vector space.

As a final check, we can confirm that vector chiral rotations leave the vacuum invariant, whereas axial-vector chiral rotations do not, thus confirming the implementation of spontaneous chiral symmetry breaking. The vacuum, i.e. the ground state, corresponds to $\phi = 0$, therefore $U[0] = \mathbb{1}$ should hold:

$$\varphi[(V, V), U[0]] = V\mathbb{1}V^\dagger = VV^\dagger = \mathbb{1}, \tag{2.52a}$$

$$\varphi[(A, A^\dagger), U[0]] = A^\dagger \mathbb{1} A^\dagger = A^\dagger A^\dagger \neq \mathbb{1}. \tag{2.52b}$$

Concluding this discussion, we found a (non-linear) realization of the NG fields in terms of SU(N) matrices, we know how these matrices transform and can thereby construct a Lagrangian that is invariant under the chiral transformation $U \to RUL^\dagger$. There are actually many possible parametrizations for the chiral field $U[\phi]$, which should all lead to the same physics. In the next section, we present the parametrization used in this thesis and the chirally invariant Lagrangian built from U.

2.5.2. The chiral Lagrangian

The first part of the Lagrangian contains only the pion field and external sources. It is called the chiral Lagrangian and is given by [9, 10]:

$$\mathcal{L}_{\pi}^{(2)} = \frac{f^2}{4}\,\mathrm{Tr}\left\{D_\mu U^\dagger D^\mu U + \chi^\dagger U + \chi U^\dagger\right\}, \tag{2.53}$$

where the trace is taken over spinor- and flavor indices[8] and the superscript (2) stands for second order in the chiral counting. The chiral field U contains the three pions, the field χ contains scalar and pseudoscalar external fields, and the covariant derivative D_μ contains vector and axial-vector external fields. We will now discuss these three quantities in more detail:

- U is the chiral field, which can be expressed in terms of the pion fields [68, 69],

$$U = \exp\left[\mathrm{i}\boldsymbol{\pi}\frac{y(\pi^2)}{2\sqrt{\pi^2}}\right] = \cos\left(\frac{y(\pi^2)}{2}\right) + \mathrm{i}\frac{\boldsymbol{\pi}}{\sqrt{\pi^2}}\sin\left(\frac{y(\pi^2)}{2}\right), \tag{2.54}$$

$$U^\dagger = \exp\left[-\mathrm{i}\boldsymbol{\pi}\frac{y(\pi^2)}{2\sqrt{\pi^2}}\right] = \cos\left(\frac{y(\pi^2)}{2}\right) - \mathrm{i}\frac{\boldsymbol{\pi}}{\sqrt{\pi^2}}\sin\left(\frac{y(\pi^2)}{2}\right), \tag{2.55}$$

  where $\boldsymbol{\pi} = \pi^a\tau^a$ and $\boldsymbol{\pi}^2 = \pi^a\tau^a\pi^b\tau^b = \pi^a\pi^a\mathbb{1} = \pi^2\mathbb{1}$, and the function $y(\pi^2)$ satisfies

$$y - \sin(y) = \frac{4}{3}\left(\frac{\pi^2}{f^2}\right)^{3/2}. \tag{2.56}$$

  The advantage of this parametrization is that the soft-pion theorems of chiral symmetry (e.g. the Adler zero condition [70]) are automatically fulfilled, even beyond tree-level calculations, i.e., involving pion loops. As demonstrated by Refs. [22, 69], loop amplitudes containing pions explicitly depend on the choice of the parametrization of the chiral field. Furthermore, for a general choice of the chiral field U, soft-pion theorems are only fulfilled at tree-level. However, when a certain parametrization is used (i.e. the one employed in the present work), Charap and Gerstein *et al.* showed that the resulting loop amplitudes agree with the soft-pion theorems. If one chooses the standard parametrization, one would have to use e.g. the background field method (see e.g. Refs. [30, 71]) in order to ensure chiral invariance.

  We discuss in Appendix B.1 how to deal with the function $y(\pi^2)$ and how to evaluate trigonometric functions containing $y(\pi^2)$. Finally, τ^a are the Pauli matrices. Useful identities involving the Pauli matrices are listed in Appendix B.4.1. The chiral field can be expanded like this:

$$U(\pi) = \mathbb{1} + \mathrm{i}\frac{\boldsymbol{\pi}}{f} - \frac{1}{2}\frac{\pi^2}{f^2} - \frac{\mathrm{i}}{10}\frac{\boldsymbol{\pi}\pi^2}{f^3} - \frac{1}{40}\frac{(\pi^2)^2}{f^4} + \cdots, \tag{2.57a}$$

$$U^\dagger(\pi) = \mathbb{1} - \mathrm{i}\frac{\boldsymbol{\pi}}{f} - \frac{1}{2}\frac{\pi^2}{f^2} + \frac{\mathrm{i}}{10}\frac{\boldsymbol{\pi}\pi^2}{f^3} - \frac{1}{40}\frac{(\pi^2)^2}{f^4} + \cdots. \tag{2.57b}$$

[8] E.g.: the gamma matrices carry spinor indices, $\gamma^\mu_{\alpha\beta}$, and the Pauli matrices carry flavor indices, τ^a_{ij}.

- D_μ is the covariant derivative, given by:

$$D_\mu U = \partial_\mu U - \mathrm{i} r_\mu U + \mathrm{i} U \ell_\mu, \tag{2.58a}$$

$$D_\mu U^\dagger = \partial_\mu U^\dagger + \mathrm{i} U^\dagger r_\mu - \mathrm{i} \ell_\mu U^\dagger, \tag{2.58b}$$

where $r_\mu = \frac{1}{2}(v_\mu + a_\mu)$ and $\ell_\mu = \frac{1}{2}(v_\mu - a_\mu)$. In these expressions, $v_\mu = v^a_\mu \frac{\tau^a}{2}$ and $a_\mu = a^a_\mu \frac{\tau^a}{2}$ are the external vector and axial-vector fields ($a = 1, 2, 3$). The partial derivative of U is given by:

$$\begin{aligned}\partial_\mu U = {} & \frac{\pi^i \partial_\mu \pi^i}{f^2}\left[-f^2 y' \sin(y/2)\right] + \mathrm{i}\frac{\partial_\mu \boldsymbol{\pi}}{f}\sqrt{\frac{f^2}{\pi^2}}\sin(y/2) \\ & + \mathrm{i}\frac{\boldsymbol{\pi}\pi^i \partial_\mu \pi^i}{f^3}\left[f^2 y' \sqrt{\frac{f^2}{\pi^2}}\cos(y/2) - \left(\frac{f^2}{\pi^2}\right)^{3/2}\sin(y/2)\right],\end{aligned} \tag{2.59a}$$

$$\begin{aligned}\partial_\mu U^\dagger = {} & \frac{\pi^i \partial_\mu \pi^i}{f^2}\left[-f^2 y' \sin(y/2)\right] - \mathrm{i}\frac{\partial_\mu \boldsymbol{\pi}}{f}\sqrt{\frac{f^2}{\pi^2}}\sin(y/2) \\ & - \mathrm{i}\frac{\boldsymbol{\pi}\pi^i \partial_\mu \pi^i}{f^3}\left[f^2 y' \sqrt{\frac{f^2}{\pi^2}}\cos(y/2) - \left(\frac{f^2}{\pi^2}\right)^{3/2}\sin(y/2)\right],\end{aligned} \tag{2.59b}$$

and it can be expanded like this:

$$\partial_\mu U = \mathrm{i}\frac{\partial_\mu \boldsymbol{\pi}}{f} - \frac{\pi^a \partial_\mu \pi^a}{f^2}\mathbb{1} - \mathrm{i}\frac{\partial_\mu \boldsymbol{\pi}\pi^2 + 2\partial_\mu \pi^a \pi^a \boldsymbol{\pi}}{10 f^3} - \frac{\partial_\mu \pi^a \pi^a \pi^2}{10 f^4}\mathbb{1} + \ldots, \tag{2.60a}$$

$$\partial_\mu U^\dagger = -\mathrm{i}\frac{\partial_\mu \boldsymbol{\pi}}{f} - \frac{\pi^a \partial_\mu \pi^a}{f^2}\mathbb{1} + \mathrm{i}\frac{\partial_\mu \boldsymbol{\pi}\pi^2 + 2\partial_\mu \pi^a \pi^a \boldsymbol{\pi}}{10 f^3} - \frac{\partial_\mu \pi^i \pi^i \pi^2}{10 f^4}\mathbb{1} + \ldots. \tag{2.60b}$$

Here, we use the convention that the derivative only acts on the object directly next to it: $\partial_\mu f g \equiv (\partial_\mu f) g$.

- The field χ contains the external scalar ($s = s^a \tau^a$, $a = 0, 1, 2, 3$) and pseudoscalar ($p = p^a \tau^a$, $a = 0, 1, 2, 3$) currents,

$$\chi = 2B_0(s + \mathrm{i}p), \qquad \chi^\dagger = 2B_0(s - \mathrm{i}p), \tag{2.61}$$

and B_0 is a low-energy constant (LEC).

The only LEC in the pion sector is B_0. Since it usually appears with a factor of the quark mass m, we replace both with $B_0 m \to m_\pi^2/2$, as discussed in Ref. [72], which follows from the pion mass term in the Lagrangian.

In order to evaluate the pion sector of the chiral Lagrangian, we first identify the necessary terms:

$$\mathcal{L}_\pi^{(2)} = \frac{f^2}{4}\operatorname{Tr}_F\left\{D_\mu U^\dagger D^\mu U\right\} + \frac{f^2}{4}\operatorname{Tr}_F\left\{\chi^\dagger U + \chi U^\dagger\right\} \tag{2.62}$$

$$\begin{aligned} &= \frac{f^2}{4}\operatorname{Tr}_F\left\{\partial_\mu U^\dagger \partial^\mu U\right\} - \mathrm{i}\frac{f^2}{4}\operatorname{Tr}_F\left\{(U\partial^\mu U^\dagger + U^\dagger\partial^\mu U)v_\mu\right\} \\ &\quad - \mathrm{i}\frac{f^2}{4}\operatorname{Tr}_F\left\{(U\partial^\mu U^\dagger - U^\dagger\partial^\mu U)a_\mu\right\} + \frac{f^2}{8}\operatorname{Tr}_F\{v_\mu v^\mu\} + \frac{f^2}{8}\operatorname{Tr}_F\{a_\mu a^\mu\} \\ &\quad - \frac{f^2}{8}\operatorname{Tr}_F\left\{U^\dagger(v_\mu + a_\mu)U(v^\mu - a^\mu)\right\} + \frac{f^2}{4}\operatorname{Tr}_F\left\{\chi^\dagger U + \chi U^\dagger\right\}. \end{aligned} \tag{2.63}$$

Here we used the following equations, which are due to $UU^\dagger = U^\dagger U = \mathbb{1}$:

$$\partial_\mu U^\dagger U = -U^\dagger\partial_\mu U, \qquad \partial_\mu U U^\dagger = -U\partial_\mu U^\dagger. \tag{2.64}$$

The necessary terms are as follows. The term with two derivatives can be written as:

$$\begin{aligned} \partial_\mu U^\dagger \partial^\mu U = {}& \frac{\partial_\mu \pi^i \partial^\mu \pi^i}{f^2}\left[\frac{f^2}{\pi^2}\sin^2\left(\frac{y}{2}\right)\right] \\ &+ \frac{\pi^i \partial\pi^i \pi^j \partial\pi^j}{f^4}\left[(f^2 y')^2\sin^2\left(\frac{y}{2}\right) + f^2 y'\frac{f^2}{\pi^2}\sin(y) - 2\left(\frac{f^2}{\pi^2}\right)^2\sin^2\left(\frac{y}{2}\right)\right] \\ &+ \frac{\pi^i\pi^i\pi^j\partial_\mu\pi^j\pi^k\partial^\mu\pi^k}{f^6}\left[f^2 y'\sqrt{\frac{f^2}{\pi^2}}\cos\left(\tfrac{y}{2}\right) - \left(\frac{f^2}{\pi^2}\right)^{3/2}\sin\left(\tfrac{y}{2}\right)\right]^2. \end{aligned} \tag{2.65}$$

The terms with one derivative yield:

$$\begin{aligned} U\partial_\mu U^\dagger = {}& \mathrm{i}\frac{\partial_\mu \boldsymbol{\pi}}{f}\left[-\sqrt{\frac{f^2}{\pi^2}}\frac{\sin(y)}{2}\right] + \frac{\pi^i\partial_\mu\pi^i}{f^2}\left[\frac{f^2}{\pi^2}\sin^2\left(\tfrac{y}{2}\right) - f^2 y'\frac{\sin(y)}{2}\right] \\ &+ \mathrm{i}\frac{\epsilon^{abc}\pi^a\partial_\mu\pi^b\tau^c}{f^2}\frac{f^2}{\pi^2}\sin^2\left(\tfrac{y}{2}\right) + \mathrm{i}\frac{\boldsymbol{\pi}\pi^i\partial_\mu\pi^i}{f^3}\left[\left(\frac{f^2}{\pi^2}\right)^{3/2}\frac{\sin(y)}{2} - \frac{1}{\tan^2\left(\frac{y}{2}\right)} - 1\right] \\ &+ \frac{\pi^i\pi^i\pi^j\partial_\mu\pi^j}{f^4}\left[\sqrt{\frac{f^2}{\pi^2}}\frac{1}{\tan\left(\frac{y}{2}\right)} - \left(\frac{f^2}{\pi^2}\right)^2\sin^4\left(\tfrac{y}{2}\right)\right], \end{aligned} \tag{2.66a}$$

$$\begin{aligned} U^\dagger\partial_\mu U = {}& \mathrm{i}\frac{\partial_\mu \boldsymbol{\pi}}{f}\left[\sqrt{\frac{f^2}{\pi^2}}\frac{\sin(y)}{2}\right] + \frac{\pi^i\partial_\mu\pi^i}{f^2}\left[\frac{f^2}{\pi^2}\sin^2\left(\tfrac{y}{2}\right) - f^2 y'\frac{\sin(y)}{2}\right] \\ &+ \mathrm{i}\frac{\epsilon^{abc}\pi^a\partial_\mu\pi^b\tau^c}{f^2}\frac{f^2}{\pi^2}\sin^2\left(\tfrac{y}{2}\right) - \mathrm{i}\frac{\boldsymbol{\pi}\pi^i\partial_\mu\pi^i}{f^3}\left[\left(\frac{f^2}{\pi^2}\right)^{3/2}\frac{\sin(y)}{2} - \frac{1}{\tan^2\left(\frac{y}{2}\right)} - 1\right] \\ &+ \frac{\pi^i\pi^i\pi^j\partial_\mu\pi^j}{f^4}\left[\sqrt{\frac{f^2}{\pi^2}}\frac{1}{\tan\left(\frac{y}{2}\right)} - \left(\frac{f^2}{\pi^2}\right)^2\sin^4\left(\tfrac{y}{2}\right)\right], \end{aligned} \tag{2.66b}$$

and the terms involving Pauli matrices give:

$$U^\dagger\tau^a U\tau^b = \delta^{ab} + \mathrm{i}\epsilon^{abc}\tau^c\cos^2(\tfrac{y}{2}) + \frac{\epsilon^{abc}\pi^c}{f}\left[\sqrt{\frac{f^2}{\pi^2}}\sin(y)\right] + \mathrm{i}\frac{\pi^b\tau^a - \pi^a\tau^b}{f}\left[\sqrt{\frac{f^2}{\pi^2}}\sin(y)\right] + \mathrm{i}\epsilon^{abc}\tau^c\sin^2(y/2), \tag{2.67a}$$

$$\tau^a U = \tau^a\cos(y/2) + \mathrm{i}\frac{\tau^a\boldsymbol{\pi}}{\sqrt{\pi^2}}\sin(y/2) \quad (a = 0,1,2,3), \tag{2.67b}$$

$$\tau^a U^\dagger = \tau^a\cos(y/2) - \mathrm{i}\frac{\tau^a\boldsymbol{\pi}}{\sqrt{\pi^2}}\sin(y/2) \quad (a = 0,1,2,3). \tag{2.67c}$$

Now we list the terms in the Lagrangian. First, the terms involving only pions are:

$$\frac{f^2}{4}\mathrm{Tr}_F\left\{\partial_\mu U^\dagger\partial^\mu U\right\} = \partial_\mu\pi^i\partial^\mu\pi^i\left[\frac{1}{2}\frac{f^2}{\pi^2}\sin^2\left(\frac{y}{2}\right)\right] + \frac{\pi^i\partial\pi^i\pi^j\partial\pi^j}{f^2}\left[\frac{1}{2\sin^2(y/2)}\frac{\pi^2}{f^2} + \frac{1}{\tan(y/2)}\sqrt{\frac{f^2}{\pi^2}} - \left(\frac{f^2}{\pi^2}\right)^2\sin^2\left(\frac{y}{2}\right)\right] + \frac{\pi^i\pi^i\pi^j\partial_\mu\pi^j\pi^k\partial^\mu\pi^k}{f^4}\frac{1}{2}\left[\frac{\cos\left(\frac{y}{2}\right)}{\sin^2(y/2)} - \left(\frac{f^2}{\pi^2}\right)^{3/2}\sin\left(\frac{y}{2}\right)\right]^2. \tag{2.68}$$

Note that, since $\left[\frac{1}{2}\frac{f^2}{\pi^2}\sin^2\left(\frac{y}{2}\right)\right]$ is equal to 1/2 to first order, this term correctly reproduces the usual Lagrangian for a real scalar field. Next, the terms involving one vector- or axial-vector external source field:

$$-\mathrm{i}\frac{f^2}{4}\mathrm{Tr}_F\left\{(U\partial^\mu U^\dagger + U^\dagger\partial^\mu U)v_\mu\right\} = \epsilon^{abc}\pi^a\partial^\mu\pi^b v_\mu^c\left[\frac{1}{2}\frac{f^2}{\pi^2}\sin^2(y/2)\right], \tag{2.69a}$$

$$-\mathrm{i}\frac{f^2}{4}\mathrm{Tr}_F\left\{(U\partial^\mu U^\dagger - U^\dagger\partial^\mu U)a_\mu\right\} = f a_\mu^a\partial^\mu\pi^a\left[-\frac{1}{4}\sqrt{\frac{f^2}{\pi^2}}\sin(y)\right] + \frac{\pi^a\pi^i\partial^\mu\pi^i}{f}a_\mu^a\left[\left(\frac{f^2}{\pi^2}\right)^{3/2}\frac{1}{4}\sin(y) - \frac{1}{2\tan^2(\frac{y}{2})} - \frac{1}{2}\right]. \tag{2.69b}$$

Next, the terms involving two vector- and axial-vector external source fields:

$$\frac{f^2}{8}\mathrm{Tr}_F\{v_\mu v^\mu\} = \frac{f^2}{8}v_\mu^a v_a^\mu, \tag{2.70a}$$

$$\frac{f^2}{8}\mathrm{Tr}_F\{a_\mu a^\mu\} = \frac{f^2}{8}a_\mu^a a_a^\mu, \tag{2.70b}$$

$$-\frac{f^2}{8}\mathrm{Tr}_F\left\{U^\dagger(v_\mu + a_\mu)U(v^\mu - a^\mu)\right\} = -\frac{f^2}{8}v_\mu^a v_a^\mu + \frac{f^2}{8}a_\mu^a a_a^\mu - f\epsilon^{abc}a_\mu^a v_b^\mu\pi^c\left[\sqrt{\frac{f^2}{\pi^2}}\frac{\sin(y)}{4}\right]. \tag{2.70c}$$

Note that the term in Eq. (2.70a) will cancel with the first term of Eq. (2.70c). This reflects gauge invariance: invariance under a local transformation is only realized in the vector transformations, the axial-vector transformations do not leave the Lagrangian invariant. For a local (i.e. gauge) transformation, the associated vector field cannot have a mass term without breaking gauge invariance. Therefore, since the vector transformations respect chiral symmetry, a mass term for the vector field is forbidden by gauge invariance. On the other hand, a mass term for the external axial-vector field Eq. (2.70b) is allowed.

Finally, the terms containing scalar and pseudoscalar sources reads:

$$\frac{f^2}{4}\,\mathrm{Tr}_F\left\{\chi^\dagger U + \chi U^\dagger\right\} = 2f^2 B_0 m\cos(y/2) + 2fB_0 p^i\pi^i\sqrt{\frac{\pi^2}{f^2}}\sin(y/2). \tag{2.71}$$

For the first term, we introduce the quark mass by replacing $s^0 = m$. Since we assume isospin symmetry, this quark mass is the average of the up and down quark mass, $m = (m_u + m_d)/2$.

3. In-Medium Chiral Perturbation Theory

In order to describe the interactions between the pions and the surrounding nuclear matter, we use in-medium chiral perturbation theory. In Section 3.1, we show how the nucleon field can be integrated out of the generating functional to arrive at an in-medium formulation of chiral perturbation theory. In Section 3.2, we discuss the πN interaction Lagrangian and review the low-energy constants that parametrize the interactions strengths In Section 3.3, we show how to implement isospin-asymmetric nuclear matter, and close this chapter in Section 3.4 by listing the Feynman rules that underly all further calculations within the scope of this thesis.

3.1. The nucleon field

Let us start by investigating the nucleon field. First, we show how the bilinear nucleon field can be integrated out using the path integral formalism. Then, we show the Lagrangian in detail, including its various low-energy constants (LECs).

3.1.1. Integration of the nucleon field

As originally demonstrated in Ref. [33], and further developed by Ref. [34], we will now show how we deal with the nucleon fields in this thesis. By assuming a bilinear nucleon term in the Lagrangian, we are able to integrate it out and treat it as a background field. We will closely follow Ref. [33] in order to arrive at an expression for the generating functional that allows us to systematically introduce pion-nucleon interactions within the framework of chiral perturbation theory.

Let us start by defining the ground state of the in-medium theory. At asymptotic times, $t \to \pm\infty$, the ground state is taken to be a Fermi-sea of non-interacting nucleons. The number of momentum states in this Fermi sea is determined by the proton and neutron densities $\rho_{p,n}$, which uniquely determine the respective Fermi momentum $k_F^{(p,n)} = (3\pi^2\rho_{p,n})^{1/3}$:

$$|\Omega_{\text{in}}\rangle = \lim_{t\to-\infty} \prod_i^{|\boldsymbol{p}_i|\le k_F^p} \prod_j^{|\boldsymbol{p}_j|\le k_F^n} a_p^\dagger(\boldsymbol{p}_i) a_n^\dagger(\boldsymbol{p}_j)|0\rangle, \tag{3.1a}$$

$$|\Omega_{\text{out}}\rangle = \lim_{t\to\infty} \prod_i^{|\boldsymbol{p}_i|\le k_F^p} \prod_j^{|\boldsymbol{p}_j|\le k_F^n} a_p^\dagger(\boldsymbol{p}_i) a_n^\dagger(\boldsymbol{p}_j)|0\rangle. \tag{3.1b}$$

By collecting proton and neutron fields in the two-component isospin doublet $N = (p, n)^T$, we can define the generating functional using the the path integral formulation of quantum field theory:

$$\mathcal{Z}[J, \eta, \bar{\eta}] = \langle \Omega_{\text{out}} | \Omega_{\text{in}} \rangle_{J,\eta,\bar{\eta}} = \lim_{\substack{t \to -\infty \\ t' \to \infty}} \int \mathcal{D}U \mathcal{D}\bar{N} \mathcal{D}N \langle \Omega_{\text{out}} | N(t') \rangle \\ \times \mathrm{e}^{\mathrm{i} \int_t^{t'} \mathrm{d}\tau \int \mathrm{d}^3\boldsymbol{x} [\mathcal{L}_{\pi\pi} + \bar{N} D N + \bar{\eta} N + \bar{N} \eta]} \langle N(t) | \Omega_{\text{in}} \rangle. \tag{3.2}$$

Here, J is a collection of external scalar, pseudoscalar, vector and axial-vector sources $J = \{s, p, v, a\}$ appearing in the pionic Lagrangian $\mathcal{L}_{\pi\pi}$, and U is the unitary 2×2 matrix containing the pion fields as defined in Eq. (2.54). The nucleons obey the free Dirac equation,

$$(\mathrm{i}\partial\!\!\!/ + m_N) N = 0, \tag{3.3}$$

using an isospin-averaged mass for both the proton and the neutron: $m_N = (m_p + m_n)/2$. The state $|N(t)\rangle$ denotes a state with a fixed number of nucleons. This means, the path integral describes the propagation of one, two, ... nucleons in the nuclear matter (this will be the first of three expansions of the generating functional). In analogy to the expression $\langle \boldsymbol{p} | \phi_0(\boldsymbol{x}) | 0 \rangle = \mathrm{e}^{-\mathrm{i}\boldsymbol{p}\cdot\boldsymbol{x}}$ from a scalar quantum field theory, we will derive an equivalent expression later.

In order to calculate the partition function $\mathcal{Z}$, we first turn our attention to the ground state nucleon wave functions $\langle \Omega_{\text{in/out}} | N_{t \to \mp\infty} \rangle$ in isospin-symmetric nuclear matter. In the final expression for Z, it is easy to modify the necessary terms for isospin-asymmetric nuclear matter. To evaluate this, we would like to write the fermionic nucleon fields in terms of their creation and annihilation operators. Before we do that, let us mention that we summarized our conventions for calculations involving spinors in Appendix A.3.

The nucleon field and its time derivative can be written in terms of their Fourier modes as follows:

$$N(x) = \sum_s \int \frac{\mathrm{d}^3\boldsymbol{p}}{(2\pi)^3} \frac{1}{\sqrt{2E_p}} \left[a^s_{\boldsymbol{p}} u^s_{\boldsymbol{p}} \mathrm{e}^{-\mathrm{i}px} + b^{s\dagger}_{\boldsymbol{p}} v^s_{\boldsymbol{p}} \mathrm{e}^{\mathrm{i}px} \right], \tag{3.4a}$$

$$\dot{N}(x) = \sum_s \int \frac{\mathrm{d}^3\boldsymbol{p}}{(2\pi)^3} \frac{1}{\sqrt{2E_p}} \left[a^s_{\boldsymbol{p}} u^s_{\boldsymbol{p}} \mathrm{e}^{-\mathrm{i}px} (-\mathrm{i}E_p) + b^{s\dagger}_{\boldsymbol{p}} v^s_{\boldsymbol{p}} \mathrm{e}^{\mathrm{i}px} (\mathrm{i}E_p) \right]. \tag{3.4b}$$

With these expressions, we can isolate the annihilation operator $a^s_{\boldsymbol{p}}$ by first taking a linear combination,

$$N(x) + \frac{\mathrm{i}}{E_p} \dot{N}(x) = \sum_s \int \frac{\mathrm{d}^3\boldsymbol{p}}{(2\pi)^3} \frac{1}{\sqrt{2E_p}} \left[2 a^s_{\boldsymbol{p}} u^s_{\boldsymbol{p}} \mathrm{e}^{-\mathrm{i}px} \right], \tag{3.5}$$

multiplying with $\bar{u}$ from the left and using $\bar{u}u = 2m_N$,

$$\bar{u}^{s'}_{\boldsymbol{p}} \left[N(x) + \frac{\mathrm{i}}{E_p} \dot{N}(x) \right] = \int \frac{\mathrm{d}^3\boldsymbol{p}}{(2\pi)^3} \frac{4m_N}{\sqrt{2E_p}} a^{s'}_{\boldsymbol{p}} \mathrm{e}^{-\mathrm{i}px}, \tag{3.6}$$

and then performing a Fourier transform:

$$a_{\boldsymbol{p}}^s = \frac{\sqrt{2E_p}}{4m_N} \mathrm{e}^{\mathrm{i}E_p t} \int \mathrm{d}^3\boldsymbol{x}\, \mathrm{e}^{-\mathrm{i}\boldsymbol{p}\boldsymbol{x}} \bar{u}_{\boldsymbol{p}}^s \left[N(x) + \frac{\mathrm{i}}{E_p} \dot{N}(x) \right]. \tag{3.7}$$

Next, we need to express $\dot{N}$ in terms of N. To do so, we use the Dirac equation:

$$[\mathrm{i}\partial\!\!\!/ - m_N] N(x) = 0 \quad \rightarrow \quad \dot{N}(x) = -[\mathrm{i}m_N\gamma^0 + \gamma^0\gamma^i\partial_i] N(x), \tag{3.8}$$

where $\partial\!\!\!/ = \gamma^0\partial_t + \gamma^i\partial_i$. Similarly, we can write an equation for the adjoint spinor:

$$\dot{\bar{N}}(x) = \bar{N}(x)[\mathrm{i}m_N\gamma^0 + \gamma^0\gamma^i \overleftarrow{\partial}_i]. \tag{3.9}$$

With this, we can compute the ground state nucleon functionals as follows:

$$\begin{aligned}
\langle \Omega_{\text{out}} | N(+\infty) \rangle &= \lim_{t\to+\infty} \langle 0 | \prod_n a_{\boldsymbol{p}_n} | N(t) \rangle & (3.10\text{a}) \\
&= \lim_{t\to+\infty} \langle 0 | \prod_n \frac{\sqrt{2E_{p_n}}}{4m_N} \mathrm{e}^{\mathrm{i}E_{p_n} t} \int \mathrm{d}^3\boldsymbol{x}_n\, \mathrm{e}^{-\mathrm{i}\boldsymbol{p}_n\boldsymbol{x}_n} \bar{u}_{\boldsymbol{p}_n}^s \\
&\qquad \times \left[N(x_n) + \frac{\mathrm{i}}{E_{p_n}} \dot{N}(x_n) \right] | N(t) \rangle & (3.10\text{b}) \\
&= \lim_{t\to+\infty} \prod_n \frac{E_{p_n}}{2m_N} \mathrm{e}^{\mathrm{i}E_{p_n} t} \int \mathrm{d}^3\boldsymbol{x}_n\, \mathrm{e}^{-\mathrm{i}\boldsymbol{p}_n\boldsymbol{x}_n} \bar{u}_{\boldsymbol{p}_n}^s \left[N(x_n) + \frac{\mathrm{i}}{E_{p_n}} \dot{N}(x_n) \right], & (3.10\text{c})
\end{aligned}$$

and similarly,

$$\langle N(-\infty) | \Omega_{\text{in}} \rangle = \lim_{t\to-\infty} \prod_n \frac{E_{p_n}}{2m_N} \mathrm{e}^{-\mathrm{i}E_{p_n} t} \int \mathrm{d}^3\boldsymbol{x}_n\, \mathrm{e}^{\mathrm{i}\boldsymbol{p}_n\boldsymbol{x}_n} \left[\bar{N}(x_n) - \frac{\mathrm{i}}{E_{p_n}} \dot{\bar{N}}(x_n) \right] \gamma^0 u_{\boldsymbol{p}_n}^s. \tag{3.11}$$

And by using Eqs. (3.8) and (3.9), these expressions are:

$$\begin{aligned}
\langle \Omega_{\text{out}} | N(+\infty) \rangle &= \lim_{t\to+\infty} \prod_n \frac{E_{p_n}}{2m_N} \int \mathrm{d}^3\boldsymbol{x}_n\, \mathrm{e}^{\mathrm{i}p_n x_n} \bar{u}_{\boldsymbol{p}_n}^s \\
&\qquad \times \left[1 - \frac{\mathrm{i}}{E_{p_n}} \left(\mathrm{i}m_N\gamma^0 + \gamma^0\gamma^i\partial_i \right) \right] N(x_n), & (3.12\text{a}) \\
\langle N(-\infty) | \Omega_{\text{in}} \rangle &= \lim_{t\to-\infty} \prod_n \frac{E_{p_n}}{2m_N} \int \mathrm{d}^3\boldsymbol{x}_n\, \mathrm{e}^{-\mathrm{i}p_n x_n} \\
&\qquad \times \left[\bar{N}(x_n) - \frac{\mathrm{i}}{E_{p_n}} \left(\mathrm{i}m_N \bar{N}(x_n)\gamma^0 + \partial_i \bar{N}(x_n)\gamma^0\gamma^i \right) \right] \gamma^0 u_{\boldsymbol{p}_n}^s. & (3.12\text{b})
\end{aligned}$$

We can now use these expressions in the generating functional Eq. (3.2), while also replacing the nucleon fields with functional derivatives with respect to the fermionic sources η:

$$N(x)\, \mathrm{e}^{\mathrm{i}\int \mathrm{d}^4y\, \bar{\eta}(y) N(y)} = \frac{\delta}{\mathrm{i}\delta\bar{\eta}(x)} \mathrm{e}^{\mathrm{i}\int \mathrm{d}^4y\, \bar{\eta}(y) N(y)}, \tag{3.13a}$$

$$\bar{N}(x)\, \mathrm{e}^{\mathrm{i}\int \mathrm{d}^4y\, \bar{N}(y)\eta(y)} = \frac{\mathrm{i}\delta}{\delta\eta(x)} \mathrm{e}^{\mathrm{i}\int \mathrm{d}^4y\, \bar{N}(y)\eta(y)}, \tag{3.13b}$$

such that the generating functional is:

$$
\begin{aligned}
\langle \Omega_{\text{out}} | \Omega_{\text{in}} \rangle_{J,\eta,\bar{\eta}} = \lim_{\substack{t \to -\infty \\ t' \to +\infty}} \int \mathcal{D}U \mathcal{D}\bar{N} \mathcal{D}N \mathrm{e}^{\mathrm{i} \int \mathrm{d}^4 x \, \mathcal{L}_{\pi\pi}} \\
\times \left\{ \prod_n \frac{E_{p_n}}{2m_N} \int \mathrm{d}^3 \boldsymbol{x}_n \, \mathrm{e}^{\mathrm{i} p_n x_n} \bar{u}^s_{\boldsymbol{p}_n} \left[1 - \frac{\mathrm{i}}{E_{p_n}} \left(\mathrm{i} m_N \gamma^0 + \gamma^0 \gamma^i \partial_i \right) \right] \frac{\delta}{\mathrm{i} \delta \bar{\eta}(x_n)} \right\} \\
\times \, \mathrm{e}^{\mathrm{i} \int \mathrm{d}^4 x [\bar{N} D N + \bar{\eta} N + \bar{N} \eta]} \\
\times \left\{ \prod_m \frac{E_{p_m}}{2m_N} \int \mathrm{d}^3 \boldsymbol{y}_m \, \mathrm{e}^{-\mathrm{i} q_m y_m} \right. \\
\times \left. \left[\frac{\mathrm{i} \overleftarrow{\delta}}{\delta \eta(y_m)} - \frac{\mathrm{i}}{E_{q_m}} \left(\mathrm{i} m_N \frac{\mathrm{i} \overleftarrow{\delta}}{\delta \eta(y_m)} \gamma^0 + \partial_j \frac{\mathrm{i} \overleftarrow{\delta}}{\delta \eta(y_m)} \gamma^0 \gamma^j \right) \right] \gamma^0 u^s_{\boldsymbol{q}_m} \right\}.
\end{aligned}
\tag{3.14}
$$

Here, we use the following symbols: $x^\mu = (t, \boldsymbol{x})$, $y^\mu = (t', \boldsymbol{y})$, $p^\mu = (E_p, \boldsymbol{p})$, and $q^\mu = (E_q, \boldsymbol{q})$.

It is now possible to perform the integration over $\mathcal{D}\bar{N}\mathcal{D}N$, which results in a functional determinant of the inverse nucleon propagator:

$$
\int \mathcal{D}\bar{N} \mathcal{D}N \, \mathrm{e}^{\mathrm{i} \int \mathrm{d}^4 x \, [\bar{N} D N + \bar{\eta} N + \bar{N} \eta]} = \det(D) \, \mathrm{e}^{\mathrm{i} \int \mathrm{d}^4 x \, \mathrm{d}^4 y \, \bar{\eta}(x) D^{-1}(x,y) \eta(y)},
\tag{3.15}
$$

which leads to:

$$
\begin{aligned}
\langle \Omega_{\text{out}} | \Omega_{\text{in}} \rangle_{J,\eta,\bar{\eta}} = \lim_{\substack{t \to -\infty \\ t' \to +\infty}} \int \mathcal{D}U \, \det(D) \, \mathrm{e}^{\mathrm{i} \int \mathrm{d}^4 x \, \mathcal{L}_{\pi\pi}} \\
\times \left\{ \prod_n \frac{E_{p_n}}{2m_N} \int \mathrm{d}^3 \boldsymbol{x}_n \, \mathrm{e}^{\mathrm{i} p_n x_n} \bar{u}^s_{\boldsymbol{p}_n} \left[1 - \frac{\mathrm{i}}{E_{p_n}} \left(\mathrm{i} m_N \gamma^0 + \gamma^0 \gamma^i \partial_i \right) \right] \frac{\delta}{\mathrm{i} \delta \bar{\eta}(x_n)} \right\} \\
\times \, \mathrm{e}^{\mathrm{i} \int \mathrm{d}^4 x \, \mathrm{d}^4 y \, \bar{\eta}(x) D^{-1}(x,y) \eta(y)} \\
\times \left\{ \prod_m \frac{E_{p_m}}{2m_N} \int \mathrm{d}^3 \boldsymbol{y}_m \, \mathrm{e}^{-\mathrm{i} q_m y_m} \right. \\
\times \left. \left[\frac{\mathrm{i} \overleftarrow{\delta}}{\delta \eta(y_m)} - \frac{\mathrm{i}}{E_{q_m}} \left(\mathrm{i} m_N \frac{\mathrm{i} \overleftarrow{\delta}}{\delta \eta(y_m)} \gamma^0 + \partial_j \frac{\mathrm{i} \overleftarrow{\delta}}{\delta \eta(y_m)} \gamma^0 \gamma^j \right) \right] \gamma^0 u^s_{\boldsymbol{q}_m} \right\}.
\end{aligned}
\tag{3.16}
$$

Let us consider now only the $\mathrm{d}^3 \boldsymbol{x}_n$ integration:

$$
I_x = \int \mathrm{d}^3 \boldsymbol{x}_n \, \mathrm{e}^{\mathrm{i} p_n x_n} \bar{u}^s_{\boldsymbol{p}_n} \left[1 - \frac{\mathrm{i}}{E_{p_n}} \left(\mathrm{i} m_N \gamma^0 + \gamma^0 \gamma^i \partial_i \right) \right] \frac{\delta}{\mathrm{i} \delta \bar{\eta}(x_n)}.
\tag{3.17}
$$

We perform a partial integration on the last term, such that the derivative acts on the exponential function:

$$
I_x = \int \mathrm{d}^3 \boldsymbol{x}_n \, \mathrm{e}^{\mathrm{i} p_n x_n} \bar{u}^s_{\boldsymbol{p}_n} \left[1 - \frac{\mathrm{i}}{E_{p_n}} \left(\mathrm{i} m_N \gamma^0 - \gamma^0 \gamma^i \overleftarrow{\partial}_i \right) \right] \frac{\delta}{\mathrm{i} \delta \bar{\eta}(x_n)}
\tag{3.18a}
$$

$$
= \int \mathrm{d}^3 \boldsymbol{x}_n \, \mathrm{e}^{\mathrm{i} p_n x_n} \bar{u}^s_{\boldsymbol{p}_n} \left[1 - \frac{\mathrm{i}}{E_{p_n}} \left(\mathrm{i} m_N \gamma^0 + \mathrm{i} \gamma^0 \gamma^i (\boldsymbol{p}_n)_i \right) \right] \frac{\delta}{\mathrm{i} \delta \bar{\eta}(x_n)},
\tag{3.18b}
$$

where $(\boldsymbol{p}_n)_i$ denotes the i-th component of $\boldsymbol{p}_n$. Next, we can use the Dirac equation $\bar{u}(\not{p}-m)=0$ to compute:

$$\bar{u}^s_{\boldsymbol{p}_n}\left[1-\frac{\mathrm{i}}{E_{p_n}}\left(\mathrm{i}m_N\gamma^0+\mathrm{i}\gamma^0\gamma^i(\boldsymbol{p}_n)_i\right)\right]=\frac{2m_N}{E_{p_n}}\bar{u}^s_{\boldsymbol{p}_n}\gamma^0, \tag{3.19}$$

and similarly for the $\mathrm{d}^3\mathbf{y}_m$ integration. The result is a much simpler expression for the generating functional:

$$\begin{aligned}\langle\Omega_{\text{out}}|\Omega_{\text{in}}\rangle_{J,\eta,\bar{\eta}}=\lim_{\substack{t\to-\infty\\ t'\to+\infty}}&\int\mathcal{D}U\ \det(D)\,\mathrm{e}^{\mathrm{i}\int\mathrm{d}^4x\,\mathcal{L}_{\pi\pi}}\left[\prod_n\int\mathrm{d}^3\boldsymbol{x}_n\,\mathrm{e}^{\mathrm{i}p_nx_n}\bar{u}^s_{\boldsymbol{p}_n}\gamma^0\frac{\delta}{\mathrm{i}\delta\bar{\eta}(x_n)}\right]\\ &\times\mathrm{e}^{\mathrm{i}\int\mathrm{d}^4x\,\mathrm{d}^4y\,\bar{\eta}(x)D^{-1}(x,y)\eta(y)}\left[\prod_m\int\mathrm{d}^3\boldsymbol{y}_m\,\mathrm{e}^{-\mathrm{i}q_my_m}\frac{\mathrm{i}\overleftarrow{\delta}}{\delta\eta(y_m)}u^s_{\boldsymbol{q}_m}\right].\end{aligned} \tag{3.20}$$

In order to set the sources η, $\bar{\eta}$ to zero, we act with the left-derivatives $\delta/\delta\bar{\eta}$ on the exponential function, which brings down factors of $D^{-1}\eta$:

$$\frac{\delta}{\mathrm{i}\delta\bar{\eta}(x_n)}\mathrm{e}^{\mathrm{i}\int\mathrm{d}^4x\,\mathrm{d}^4y\,\bar{\eta}(x)D^{-1}(x,y)\eta(y)}=\int\mathrm{d}^4z_{n'}\,D^{-1}(x_n,z_{n'})\eta(z_{n'}). \tag{3.21}$$

We let all right-derivatives $\overleftarrow{\delta}/\delta\eta$ act on this source and can then set the sources to zero, which makes the exponential function vanish:

$$\begin{aligned}\langle\Omega_{\text{out}}|\Omega_{\text{in}}\rangle_{J,\eta,\bar{\eta}}=\lim_{\substack{t\to-\infty\\ t'\to+\infty}}&\int\mathcal{D}U\ \det(D)\,\mathrm{e}^{\mathrm{i}\int\mathrm{d}^4x\,\mathcal{L}_{\pi\pi}}\\ &\times\left[\prod_n\int\mathrm{d}^3\boldsymbol{x}_n\,\mathrm{e}^{\mathrm{i}p_nx_n}\int\mathrm{d}^4z_{n'}\,\bar{u}^s_{\boldsymbol{p}_n}\gamma^0D^{-1}(x_n,z_{n'})\eta(z_{n'})\right]\\ &\left.\times\,\mathrm{e}^{\mathrm{i}\int\mathrm{d}^4x\,\mathrm{d}^4y\,\bar{\eta}(x)D^{-1}(x,y)\eta(y)}\qquad\right\}=1\\ &\times\left[\prod_m\int\mathrm{d}^3\boldsymbol{y}_m\,\mathrm{e}^{-\mathrm{i}q_my_m}\frac{\mathrm{i}\overleftarrow{\delta}}{\delta\eta(y_m)}u^s_{\boldsymbol{q}_m}\right].\end{aligned} \tag{3.22}$$

Since there are numerous copies of η and $\overleftarrow{\delta}/\delta\eta$, and they all anti-commute, we might get a minus sign, depending on the number of permutations. If σ denotes e.g. $\sigma=(2,3,1)$, which is an even permutation of $(1,2,3)$, we define:

$$\epsilon(\sigma)\equiv\begin{cases}+1 & \text{if } \sigma \text{ is an even permutation,}\\ -1 & \text{if } \sigma \text{ is an odd permutation,}\end{cases} \tag{3.23}$$

and can write the generating functional as:

$$\begin{aligned}\mathcal{Z}[J]=\lim_{\substack{t\to-\infty\\ t'\to+\infty}}&\int\mathcal{D}U\,\det(D)\,\mathrm{e}^{\mathrm{i}\int\mathrm{d}^4x\,\mathcal{L}_{\pi\pi}}\\ &\times\sum_\sigma\epsilon(\sigma)\prod_n\int\mathrm{d}^3\boldsymbol{x}_n\,\mathrm{d}^3\boldsymbol{y}_{\sigma_n}\,\mathrm{e}^{\mathrm{i}(p_nx_n-q_{\sigma_n}y_{\sigma_n})}\bar{u}^s_{\boldsymbol{p}_n}\gamma^0D^{-1}(x_n,y_{\sigma_n})u^s_{\boldsymbol{q}_{\sigma_n}}.\end{aligned} \tag{3.24}$$

We define $D = D_0 - A$, where $D_0 = \mathrm{i}\not{\partial} - m_N$ is the free Dirac operator and A represents the difference to the full operator D. Later on, A will give us πN interactions, but it is not necessary to assign this meaning to A yet. Since D^{-1} appears in the generating functional, we can do the following manipulation:

$$\begin{aligned} && A &= D_0 - D \qquad\qquad | \leftarrow D^{-1} && (3.25\text{a})\\ D_0^{-1} \rightarrow | && AD^{-1} &= D_0 D^{-1} - \mathbb{1} && (3.25\text{b})\\ && D_0^{-1} A D^{-1} &= D^{-1} - D_0^{-1}. && (3.25\text{c}) \end{aligned}$$

This gives us an expansion of the full nucleon propagator (similar to a Dyson series):

$$\begin{aligned} D^{-1} &= D_0^{-1} + D_0^{-1} A D^{-1} && (3.26\text{a})\\ &= D_0^{-1} + D_0^{-1} A D_0^{-1} + D_0^{-1} A D_0^{-1} A D_0^{-1} + \dots, && (3.26\text{b}) \end{aligned}$$

and the path integral can be expanded:

$$\begin{aligned} \mathcal{Z}[J] = \lim_{\substack{t\to-\infty\\ t'\to+\infty}} \int \mathcal{D}U \det(D)\, \mathrm{e}^{\mathrm{i}\int \mathrm{d}^4x \mathcal{L}_{\pi\pi}} \sum_\sigma \epsilon(\sigma) \prod_n \int \mathrm{d}^3\boldsymbol{x}_n\, \mathrm{d}^3\boldsymbol{y}_{\sigma_n}\, \mathrm{e}^{\mathrm{i}(p_n x_n - q_{\sigma_n} y_{\sigma_n})} \bar{u}^s_{\boldsymbol{p}_n} \gamma^0 \\ \times \left[D_0^{-1}(x_n, y_{\sigma_n}) + \int \mathrm{d}^4z\, \mathrm{d}^4z'\, D_0^{-1}(x_n, z) A(z, z') D_0^{-1}(z', y_{\sigma_n}) + \dots \right] u^s_{\boldsymbol{q}_{\sigma_n}}. \qquad (3.27) \end{aligned}$$

We will now use the following relation,

$$\lim_{t\to\infty} \int \mathrm{d}^3\boldsymbol{x}\, \mathrm{e}^{\mathrm{i}px} u^\dagger_{\boldsymbol{p}} D_0^{-1}(x, x') = -\mathrm{i}\mathrm{e}^{\mathrm{i}px'} \bar{u}_{\boldsymbol{p}}, \qquad (3.28)$$

which is derived step-by-step in Ref. [33]. This enables us to perform the $\mathrm{d}^3\boldsymbol{x}_n$ and $\mathrm{d}^3\boldsymbol{y}_{\sigma_n}$ integrations. For instance, the first (D_0^{-1}) and second ($D_0^{-1} A D_0^{-1}$) terms in the expansion become:

$$\begin{aligned} (\mathrm{I}) &= \lim_{\substack{t\to-\infty\\ t'\to+\infty}} \prod_n \int \mathrm{d}^3\boldsymbol{x}_n\, \mathrm{d}^3\boldsymbol{y}_{\sigma_n}\, \mathrm{e}^{\mathrm{i}(p_n x_n - q_{\sigma_n} y_{\sigma_n})} u^{s\dagger}_{\boldsymbol{p}_n} D_0^{-1}(x_n, y_{\sigma_n}) u^s_{\boldsymbol{q}_{\sigma_n}} && (3.29\text{a})\\ &= \lim_{t'\to-\infty} \prod_n \int \mathrm{d}^3\boldsymbol{y}_{\sigma_n}\, \mathrm{e}^{-\mathrm{i}q_{\sigma_n} y_{\sigma_n}} (-\mathrm{i}) \mathrm{e}^{\mathrm{i}p_n y_{\sigma_n}} \bar{u}^s_{\boldsymbol{p}_n} u^s_{\boldsymbol{q}_{\sigma_n}} && (3.29\text{b})\\ &= \lim_{t'\to-\infty} \prod_n (2\pi)^3 \delta^{(3)}(\boldsymbol{p}_n - \boldsymbol{q}_{\sigma_n}) \delta_{n,\sigma_n} (-\mathrm{i}) \underbrace{\mathrm{e}^{\mathrm{i}(p^0_n - q^0_{\sigma_n})t'}}_{1} \bar{u}^s_{\boldsymbol{p}_n} u^s_{\boldsymbol{q}_{\sigma_n}}. && (3.29\text{c}) \end{aligned}$$

Since the three-components of the momenta are the same, the respective energies E_p and E_q will also be equal, therefore the exponential vanishes. Then, the limit over t' is trivial. The second term is:

$$\begin{aligned} (\mathrm{II}) &= \lim_{\substack{t\to-\infty\\ t'\to+\infty}} \prod_n \int \mathrm{d}^3\boldsymbol{x}_n\, \mathrm{d}^3\boldsymbol{y}_{\sigma_n}\, \mathrm{e}^{\mathrm{i}(p_n x_n - q_{\sigma_n} y_{\sigma_n})} u^{s\dagger}_{\boldsymbol{p}_n} \\ &\qquad \times \int \mathrm{d}^4z\, \mathrm{d}^4z'\, D_0^{-1}(x_n, z) A(z, z') D^{-1}(z', y_{\sigma_n}) u^s_{\boldsymbol{q}_{\sigma_n}} && (3.30\text{a})\\ &= \prod_n \int \mathrm{d}^4z_n\, \mathrm{d}^4z_{\sigma_n}\, (-\mathrm{i})^2 \mathrm{e}^{\mathrm{i}(p_n z_n - q_{\sigma_n} z_{\sigma_n})} \bar{u}^s_{\boldsymbol{p}_n} A(z_n, z_{\sigma_n}) u^s_{\boldsymbol{q}_{\sigma_n}}, && (3.30\text{b}) \end{aligned}$$

and so on for the following terms. In summary, we can write the generating functional as:

$$\begin{aligned}\mathcal{Z}[J] = \int \mathcal{D}U \det(D)\, \mathrm{e}^{\mathrm{i}\int \mathrm{d}^4x\, \mathcal{L}_{\pi\pi}} \sum_{\sigma} \epsilon(\sigma) \prod_{n} \int \mathrm{d}^3\boldsymbol{z}_n\, \mathrm{d}^3\boldsymbol{z}'_{\sigma_n}\, \mathrm{e}^{-\mathrm{i}\boldsymbol{p}_n\boldsymbol{z}_n} \bar{u}^s_{\boldsymbol{p}_n} \\ \times \Bigg[\delta^{(3)}(\boldsymbol{z}_n - \boldsymbol{z}'_{\sigma_n})\delta_{n,\sigma_n} - \mathrm{i}\int \mathrm{d}t\, \mathrm{d}t'\, \mathrm{e}^{\mathrm{i}E_{p_n}t} A(z_n, z'_{\sigma_n}) \mathrm{e}^{-\mathrm{i}E_{q_{\sigma_n}}t'} \\ - \mathrm{i}\int \mathrm{d}t\, \mathrm{d}t' \int \mathrm{d}^4w\, \mathrm{d}^4w'\, \mathrm{e}^{\mathrm{i}E_{p_n}t} A(z_n, w) D_0^{-1}(w, w') A(w', z'_{\sigma_n}) \mathrm{e}^{-\mathrm{i}E_{q_{\sigma_n}}t'} + \ldots\Bigg] \\ \times\, \mathrm{e}^{+\mathrm{i}\boldsymbol{q}_{\sigma_n}\boldsymbol{z}'_{\sigma_n}} u^s_{\boldsymbol{q}_{\sigma_n}}, \end{aligned} \tag{3.31}$$

where the second and higher terms have a relative factor of $(-\mathrm{i})$ compared to the first one, because in the first term, only one copy of D_0^{-1} was removed. Also, t and t' are now integration variables: $z^\mu = (t, \boldsymbol{z})$, $z'^\mu = (t', \boldsymbol{z}')$.

If we compare this expression with the Leibniz formula for a determinant of an $n \times n$ matrix M,

$$\det(M) = \sum_{\sigma} \epsilon(\sigma) \prod_{i=1}^{n} a_{i\sigma_i}, \tag{3.32}$$

we can write the terms inside the path integral as a functional determinant:

$$\mathcal{Z}[J] = \int \mathcal{D}U \det(D)\, \mathrm{e}^{\mathrm{i}\int \mathrm{d}^4x\, \mathcal{L}_{\pi\pi}} \widetilde{\det}\mathcal{F}, \tag{3.33}$$

where the tilde over the determinant means that our basis functions are $\mathrm{e}^{\mathrm{i}\boldsymbol{p}\boldsymbol{z}} u_{\boldsymbol{p}}$ with $|\boldsymbol{p}| < k_F$, i.e. only states below the Fermi momentum. The operator $\mathcal{F}$ is equal to:

$$\mathcal{F} = \mathbb{1}_3 - \mathrm{i}\int \mathrm{d}t\, \mathrm{d}t'\, \mathrm{e}^{\mathrm{i}H_0 t} A[\mathbb{1}_4 - D_0^{-1}A]^{-1} \mathrm{e}^{-\mathrm{i}H_0 t'}, \tag{3.34}$$

where $\mathbb{1}_3 = \delta^{(3)}(\boldsymbol{z}_n - \boldsymbol{z}_m)\delta_{nm}$, $\mathbb{1}_4 = \delta^{(4)}(z_n - z_m)\delta_{nm}$, and H_0 is defined such that when it acts on the basis functions, we get:

$$\mathrm{e}^{-\mathrm{i}H_0 t'} \left[\mathrm{e}^{\mathrm{i}\boldsymbol{p}\boldsymbol{z}'} u_{\boldsymbol{p}}\right] = \mathrm{e}^{-\mathrm{i}E_p t'} \mathrm{e}^{\mathrm{i}\boldsymbol{p}\boldsymbol{z}'} u_{\boldsymbol{p}} = \mathrm{e}^{-\mathrm{i}pz'} u_{\boldsymbol{p}}, \tag{3.35a}$$

$$\left[\mathrm{e}^{-\mathrm{i}\boldsymbol{p}\boldsymbol{z}} \bar{u}_{\boldsymbol{p}}\right] \mathrm{e}^{\mathrm{i}H_0 t'} = \mathrm{e}^{-\mathrm{i}\boldsymbol{p}\boldsymbol{z}} \bar{u}_{\boldsymbol{p}} \mathrm{e}^{\mathrm{i}E_p t} = \mathrm{e}^{\mathrm{i}pz} \bar{u}_{\boldsymbol{p}}, \tag{3.35b}$$

and finally, $A[\mathbb{1}_4 - D_0^{-1}A]^{-1}$ is an abbreviated way to denote this infinite series:

$$A[\mathbb{1}_4 - D_0^{-1}A]^{-1} = A + D_0^{-1}AD_0^{-1} + D_0^{-1}AD_0^{-1}AD_0^{-1} + \ldots \tag{3.36}$$

The next step is to use Jacobi's formula $\det \mathrm{e}^M = \mathrm{e}^{\mathrm{Tr}\, M}$ to write $\widetilde{\det}\,\mathcal{F}$ as $\exp\left(\widetilde{\mathrm{Tr}} \ln \mathcal{F}\right)$, where the tilde on the trace has a similar meaning:

$$\widetilde{\mathrm{Tr}} = \int \frac{\mathrm{d}^4p}{(2\pi)^4} (2\pi)\delta(p^2 - m_N^2)\Theta(p^0) \int \mathrm{d}^3\boldsymbol{x}\, \mathrm{d}^3\boldsymbol{y} = \int \frac{\mathrm{d}^3\boldsymbol{p}}{(2\pi)^3} \frac{1}{2E_p} \int \mathrm{d}^3\boldsymbol{x}\, \mathrm{d}^3\boldsymbol{y}\,, \tag{3.37}$$

and the generating functional is:

$$\mathcal{Z}[J] = \int \mathcal{D}U \det(D)\, \mathrm{e}^{\mathrm{i}\int \mathrm{d}^4x\, \mathcal{L}_{\pi\pi}} \mathrm{e}^{\int \frac{\mathrm{d}^3\boldsymbol{p}}{(2\pi)^3}\frac{1}{2E_p}\int \mathrm{d}^3\boldsymbol{x}\,\mathrm{d}^3\boldsymbol{y}\,\mathrm{e}^{-\mathrm{i}\boldsymbol{p}\boldsymbol{x}}\bar{u}_{\boldsymbol{p}}\ln(\mathcal{F})\mathrm{e}^{\mathrm{i}\boldsymbol{p}\boldsymbol{y}}u_{\boldsymbol{p}}}. \tag{3.38}$$

We can expand the logarithm as follows,

$$\ln(1-\mathrm{i}x) = -\mathrm{i}x + \frac{x^2}{2} + \frac{\mathrm{i}x^3}{3} - \frac{x^4}{4} + \mathcal{O}(x^5), \tag{3.39}$$

which yields the following expression:

$$\begin{aligned}\mathcal{Z}[J] = &\int \mathcal{D}U \det(D)\, \mathrm{e}^{\mathrm{i}\int \mathrm{d}^4x\, \mathcal{L}_{\pi\pi}} \\ &\times \exp\Bigg(-\mathrm{i}\int \frac{\mathrm{d}^3\boldsymbol{p}}{(2\pi)^3}\frac{1}{2E_p}\int \mathrm{d}^3\boldsymbol{x}\,\mathrm{d}^3\boldsymbol{y}\,\mathrm{e}^{\mathrm{i}p(x-y)}\bar{u}_{\boldsymbol{p}}A[\mathbb{1}_4 - D_0^{-1}A]^{-1}u_{\boldsymbol{p}} \\ &\quad + \frac{1}{2}\int \frac{\mathrm{d}^3\boldsymbol{p}}{(2\pi)^3}\frac{1}{2E_p}\frac{\mathrm{d}^3\boldsymbol{q}}{(2\pi)^3}\frac{1}{2E_q}\int \mathrm{d}^3\boldsymbol{x}\,\mathrm{d}^3\boldsymbol{y}\,\mathrm{d}^3\boldsymbol{x}'\,\mathrm{d}^3\boldsymbol{y}' \\ &\quad\times \mathrm{e}^{\mathrm{i}px}\bar{u}_{\boldsymbol{p}}A[\mathbb{1}_4 - D_0^{-1}A]^{-1}\mathrm{e}^{-\mathrm{i}qx'}u_{\boldsymbol{q}}\mathrm{e}^{\mathrm{i}qy'}\bar{u}_{\boldsymbol{q}}A[\mathbb{1}_4 - D_0^{-1}A]^{-1}\mathrm{e}^{-\mathrm{i}py}u_{\boldsymbol{p}} + \ldots\Bigg).\end{aligned} \tag{3.40}$$

Note that this expression includes three different expansions:

1. $\ln(\mathcal{F})$, which corresponds to an increasing number of in-medium nucleon propagations with increasing order of expansion,
2. $A[\mathbb{1}_4 - D_0^{-1}A]^{-1} = A + AD_0^{-1}A + \ldots$, which is called expanding the nonlocal vertex $\mathrm{i}\Gamma$, and also
3. $A = A^{(1)} + A^{(2)} + \ldots$, which corresponds to expanding the operator A in powers of the chiral momentum.

Finally, we can rearrange the terms in the exponential function like this:

$$\boldsymbol{v}^T M\boldsymbol{w} = v_i M_{ij} w_j = M_{ij} w_j v_i = \mathrm{Tr}\left\{M(\boldsymbol{w}\otimes\boldsymbol{v})\right\}, \tag{3.41}$$

and use the spinor outer product,

$$\sum_{s=1}^{2} u_{\boldsymbol{p}}^s \bar{u}_{\boldsymbol{p}}^s = \not{p} + m_N, \tag{3.42}$$

to get:

$$\begin{aligned}\mathcal{Z}[J] = &\int \mathcal{D}U \det(D)\, \mathrm{e}^{\mathrm{i}\int \mathrm{d}^4x\, \mathcal{L}_{\pi\pi}} \\ &\times \exp\Bigg(-\mathrm{i}\int \widetilde{\mathrm{d}p}\int \mathrm{d}^3\boldsymbol{x}\,\mathrm{d}^3\boldsymbol{y}\,\mathrm{e}^{\mathrm{i}p(x-y)}\,\mathrm{Tr}\Big\{A[\mathbb{1}_4 - D_0^{-1}A]^{-1}(\not{p} + m_N)\Big\} \\ &\quad + \frac{1}{2}\int \widetilde{\mathrm{d}p}\,\widetilde{\mathrm{d}q}\int \mathrm{d}^3(\boldsymbol{x},\boldsymbol{y},\boldsymbol{x}',\boldsymbol{y}')\,\mathrm{e}^{\mathrm{i}p(x-y)}\mathrm{e}^{-\mathrm{i}q(x'-y')} \\ &\quad\times \mathrm{Tr}\Big\{A[\mathbb{1}_4 - D_0^{-1}A]^{-1}(\not{p} + m_N)A[\mathbb{1}_4 - D_0^{-1}A]^{-1}(\not{q} + m_N)\Big\} + \ldots\Bigg),\end{aligned} \tag{3.43}$$

where we used the abbreviation:

$$\int \widetilde{\mathrm{d}p} \equiv \int \frac{\mathrm{d}^3\boldsymbol{p}}{(2\pi)^3}\frac{1}{2E_p}. \tag{3.44}$$

Although we will show our results in powers of ρ/ρ_0, we note that this is just a convenient normalization of the nucleon density to the normal nuclear density ρ_0. The *expansion parameter* in this perturbation theory is k_F/m_N, where k_F denotes the nucleons' Fermi momentum and m_N is the nucleon mass. For instance, at normal nuclear density $\rho = \rho_0$ and in isospin-symmetric nuclear matter, the Fermi momentum is $k_F \approx 270$ MeV, which leads to $k_F/m_N \approx 0.29$, even though $\rho/\rho_0 = 1$ is of order unity.

Isospin-asymmetric nuclear matter. We can now extend this to isospin-asymmetric nuclear matter in a straight-forward way. Let us go back to Eq. (3.38):

$$\mathcal{Z}[J] = \int \mathcal{D}U \det(D)\, \mathrm{e}^{\mathrm{i}\int \mathrm{d}^4x\, \mathcal{L}_{\pi\pi}} \mathrm{e}^{\int \widetilde{\mathrm{d}p} \int \mathrm{d}^3\boldsymbol{x}\, \mathrm{d}^3\boldsymbol{y}\, \mathrm{e}^{-\mathrm{i}\boldsymbol{p}\boldsymbol{x}} \bar{u}_{\boldsymbol{p}} \ln(\mathcal{F}) \mathrm{e}^{\mathrm{i}\boldsymbol{p}\boldsymbol{y}} u_{\boldsymbol{p}}}.$$

If we distinguish between the two isospin components of the spinors $u_{\boldsymbol{p}}^{s,1}$ and $u_{\boldsymbol{p}}^{s,2}$ for protons and neutrons, respectively, we can write the generating functional like this:

$$\begin{aligned}\mathcal{Z}[J] = &\int \mathcal{D}U \det(D)\, \mathrm{e}^{\mathrm{i}\int \mathrm{d}^4x\, \mathcal{L}_{\pi\pi}} \\ &\times \exp\left(\int_0^{k_F^p} \widetilde{\mathrm{d}p} \int \mathrm{d}^3\boldsymbol{x}\, \mathrm{d}^3\boldsymbol{y}\, \mathrm{e}^{-\mathrm{i}\boldsymbol{p}(\boldsymbol{x}-\boldsymbol{y})} \bar{u}_{\boldsymbol{p}}^1 \ln(\mathcal{F}) u_{\boldsymbol{p}}^1 + \int_0^{k_F^n} \widetilde{\mathrm{d}p} \int \mathrm{d}^3\boldsymbol{x}\, \mathrm{d}^3\boldsymbol{y}\, \mathrm{e}^{-\mathrm{i}\boldsymbol{p}(\boldsymbol{x}-\boldsymbol{y})} \bar{u}_{\boldsymbol{p}}^2 \ln(\mathcal{F}) u_{\boldsymbol{p}}^2\right),\end{aligned} \tag{3.45}$$

where we integrate up to the proton Fermi momentum in the first term and up to the neutron Fermi momentum in the second term. This is equivalent to introducing the 2×2 matrix $n(\boldsymbol{p})$:

$$n(\boldsymbol{p}) \equiv \begin{pmatrix} \Theta(k_F^p - |\boldsymbol{p}|) & 0 \\ 0 & \Theta(k_F^n - |\boldsymbol{p}|) \end{pmatrix}, \tag{3.46}$$

and putting it next to every factor of $(\not{p} + m_N)$ inside a trace:

$$(\not{p} + m_N) \quad \to \quad (\not{p} + m_N) n(\boldsymbol{p}), \tag{3.47}$$

such that the generating functional for isospin-asymmetric nuclear matter reads:

$$\begin{aligned}\mathcal{Z}[J] = &\int \mathcal{D}U \det(D)\, \mathrm{e}^{\mathrm{i}\int \mathrm{d}^4x\, \mathcal{L}_{\pi\pi}} \\ &\times \exp\Bigg(-\mathrm{i} \int \widetilde{\mathrm{d}p} \int \mathrm{d}^3\boldsymbol{x}\, \mathrm{d}^3\boldsymbol{y}\, \mathrm{e}^{\mathrm{i}p(x-y)}\, \mathrm{Tr}\left\{ A[\mathbb{1}_4 - D_0^{-1}A]^{-1} (\not{p} + m_N) n(\boldsymbol{p}) \right\} \\ &\quad + \frac{1}{2} \int \widetilde{\mathrm{d}p}\, \widetilde{\mathrm{d}q} \int \mathrm{d}^3(\boldsymbol{x}, \boldsymbol{y}, \boldsymbol{x}', \boldsymbol{y}')\, \mathrm{e}^{\mathrm{i}p(x-y)} \mathrm{e}^{-\mathrm{i}q(x'-y')} \\ &\quad \times \mathrm{Tr}\left\{ A[\mathbb{1}_4 - D_0^{-1}A]^{-1} (\not{p} + m_N) n(\boldsymbol{p}) A[\mathbb{1}_4 - D_0^{-1}A]^{-1} (\not{q} + m_N) n(\boldsymbol{q}) \right\} \\ &+ \ldots \Bigg).\end{aligned} \tag{3.48}$$

The fermion determinant $\det(D)$, which came from the integration over $\mathcal{D}\bar{N}\mathcal{D}N$ corresponds to closed fermion loops in vacuum. These contributions should be included in counter terms, and we therefore set $\det(D) = 1$ in the following.

In the course of this calculation, we assumed the ground state to be a Fermi sea of non-interacting nucleons. This is important, because nucleon-nucleon interactions are important to correctly implement diagrams proportional to the square of the nucleon density, i.e. which are $\mathcal{O}(\rho^2)$. The scope of our calculations is therefore up to $\mathcal{O}(\rho^{5/3})$, which corresponds to $\mathcal{O}(k_F^5)$ when expressed in terms of the Fermi momentum.

3.2. The pion-nucleon Lagrangian

In the previous section, we established the expansion in Fermi sea insertions, which introduces the in-medium aspect to our calculations. In this section, we will focus on the operator $A \equiv D_0 - D$, which is the source for pion-nucleon interactions [34].

The nucleon Lagrangian in its bilinear form reads

$$\mathcal{L}_{\pi N} = \bar{N}(\mathrm{i}\gamma^\mu \partial_\mu - m_N - A)N, \quad A = \sum_{i=1} A^{(i)}, \quad N = \begin{pmatrix} p \\ n \end{pmatrix}, \tag{3.49}$$

where $A^{(i)}$ is of chiral order $\mathcal{O}(p^i)$. The first term, $A^{(1)}$ reads,

$$A^{(1)} = -\mathrm{i}\gamma^\mu \Gamma_\mu - \mathrm{i}g_A \gamma^\mu \gamma^5 \Delta_\mu, \tag{3.50}$$

where we need the following quantities:

- The vector current Γ_μ is given by:

$$\Gamma_\mu = \frac{1}{2}[u^\dagger, \partial_\mu u] - \frac{\mathrm{i}}{2} u^\dagger (v_\mu + a_\mu) u - \frac{\mathrm{i}}{2} u (v_\mu - a_\mu) u^\dagger \tag{3.51a}$$

$$= \frac{1}{2}\left[u^\dagger \partial_\mu u + u \partial_\mu u^\dagger\right] - \frac{\mathrm{i}}{4} v_\mu^a \left[u^\dagger \tau^a u + u \tau^a u^\dagger\right] - \frac{\mathrm{i}}{4} a_\mu^a \left[u^\dagger \tau^a u - u \tau^a u^\dagger\right]. \tag{3.51b}$$

- The axial-vector current is defined as:

$$\Delta_\mu = \frac{1}{2}\left\{u^\dagger \Big[\partial_\mu - \mathrm{i}(v_\mu + a_\mu)\Big] u - u \Big[\partial_\mu - \mathrm{i}(v_\mu - a_\mu)\Big] u^\dagger \right\} \tag{3.52a}$$

$$= \frac{1}{2}\left[u^\dagger \partial_\mu u - u \partial_\mu u^\dagger\right] - \frac{\mathrm{i}}{4} v_\mu^a \left[u^\dagger \tau^a u - u \tau^a u^\dagger\right] - \frac{\mathrm{i}}{4} a_\mu^a \left[u^\dagger \tau^a u + u \tau^a u^\dagger\right]. \tag{3.52b}$$

- The square root of the chiral field is defined as $u^2 = U$:

$$u(\pi) = \cos\left(\frac{y(\pi^2)}{4}\right) + \mathrm{i}\frac{\boldsymbol{\pi}}{\sqrt{\pi^2}} \sin\left(\frac{y(\pi^2)}{4}\right), \tag{3.53a}$$

$$u^\dagger(\pi) = \cos\left(\frac{y(\pi^2)}{4}\right) - \mathrm{i}\frac{\boldsymbol{\pi}}{\sqrt{\pi^2}} \sin\left(\frac{y(\pi^2)}{4}\right), \tag{3.53b}$$

and it can be expanded as:

$$u = \mathbb{1} + \mathrm{i}\frac{\boldsymbol{\pi}}{2f} - \frac{\pi^2}{8f^2}\mathbb{1} + \mathrm{i}\frac{\boldsymbol{\pi}\pi^2}{80f^3} - \frac{9\pi^4}{640f^4}\mathbb{1} + \ldots, \tag{3.54a}$$

$$u^\dagger = \mathbb{1} - \mathrm{i}\frac{\boldsymbol{\pi}}{2f} - \frac{\pi^2}{8f^2}\mathbb{1} - \mathrm{i}\frac{\boldsymbol{\pi}\pi^2}{80f^3} - \frac{9\pi^4}{640f^4}\mathbb{1} + \ldots. \tag{3.54b}$$

Its derivatives are:

$$\begin{aligned}\partial_\mu u = {} & \frac{\pi^i\partial_\mu\pi^i}{f^2}\left[-\frac{f^2y'}{2}\sin\left(\tfrac{y}{4}\right)\right] + \mathrm{i}\frac{\partial_\mu\boldsymbol{\pi}}{f}\left[\sqrt{\frac{f^2}{\pi^2}}\sin\left(\tfrac{y}{4}\right)\right] \\ & + \mathrm{i}\frac{\boldsymbol{\pi}\pi^i\partial_\mu\pi^i}{f^3}\left[\frac{f^2y'}{2}\sqrt{\frac{f^2}{\pi^2}}\cos\left(\tfrac{y}{4}\right) - \left(\frac{f^2}{\pi^2}\right)^{3/2}\sin\left(\tfrac{y}{4}\right)\right],\end{aligned} \tag{3.55a}$$

$$\begin{aligned}\partial_\mu u^\dagger = {} & \frac{\pi^i\partial_\mu\pi^i}{f^2}\left[-\frac{f^2y'}{2}\sin\left(\tfrac{y}{4}\right)\right] - \mathrm{i}\frac{\partial_\mu\boldsymbol{\pi}}{f}\left[\sqrt{\frac{f^2}{\pi^2}}\sin\left(\tfrac{y}{4}\right)\right] \\ & - \mathrm{i}\frac{\boldsymbol{\pi}\pi^i\partial_\mu\pi^i}{f^3}\left[\frac{f^2y'}{2}\sqrt{\frac{f^2}{\pi^2}}\cos\left(\tfrac{y}{4}\right) - \left(\frac{f^2}{\pi^2}\right)^{3/2}\sin\left(\tfrac{y}{4}\right)\right],\end{aligned} \tag{3.55b}$$

which can be expanded to:

$$\partial_\mu u = \mathrm{i}\frac{\partial_\mu\boldsymbol{\pi}}{2f} - \frac{\pi^a\partial_\mu\pi^a}{4f^2}\mathbb{1} + \mathrm{i}\frac{\partial_\mu\boldsymbol{\pi}\pi^2 + 2\partial_\mu\pi^a\pi^a\boldsymbol{\pi}}{80f^3} - \frac{\partial_\mu\pi^a\pi^a\pi^2}{160f^4}\mathbb{1} + \ldots, \tag{3.56a}$$

$$\partial_\mu u^\dagger = -\mathrm{i}\frac{\partial_\mu\boldsymbol{\pi}}{2f} - \frac{\pi^a\partial_\mu\pi^a}{4f^2}\mathbb{1} - \mathrm{i}\frac{\partial_\mu\boldsymbol{\pi}\pi^2 + 2\partial_\mu\pi^a\pi^a\boldsymbol{\pi}}{80f^3} - \frac{\partial_\mu\pi^a\pi^a\pi^2}{160f^4}\mathbb{1} + \ldots. \tag{3.56b}$$

With these definitions in place, we can calculate the explicit expressions for the operator $A^{(1)}$. In order to calculate the vector and axial-vector currents, we need the following expressions:

$$\begin{aligned}u^\dagger\partial_\mu u = {} & \mathrm{i}\frac{\partial_\mu\boldsymbol{\pi}}{f}\left[\sqrt{\frac{f^2}{\pi^2}}\frac{\sin(y/2)}{2}\right] + \mathrm{i}\frac{\boldsymbol{\pi}\pi^i\partial_\mu\pi^i}{f^3}\left[\frac{f^2y'}{2}\sqrt{\frac{f^2}{\pi^2}} - \left(\frac{f^2}{\pi^2}\right)^{3/2}\frac{\sin(y/2)}{2}\right] \\ & + \mathrm{i}\frac{\epsilon^{abc}\tau^c\pi^a\partial_\mu\pi^b}{f^2}\left[\frac{f^2}{\pi^2}\sin^2\left(\tfrac{y}{4}\right)\right],\end{aligned} \tag{3.57a}$$

$$\begin{aligned}u\partial_\mu u^\dagger = {} & \mathrm{i}\frac{\partial_\mu\boldsymbol{\pi}}{f}\left[-\sqrt{\frac{f^2}{\pi^2}}\frac{\sin(y/2)}{2}\right] - \mathrm{i}\frac{\boldsymbol{\pi}\pi^i\partial_\mu\pi^i}{f^3}\left[\frac{f^2y'}{2}\sqrt{\frac{f^2}{\pi^2}} - \left(\frac{f^2}{\pi^2}\right)^{3/2}\frac{\sin(y/2)}{2}\right] \\ & + \mathrm{i}\frac{\epsilon^{abc}\tau^c\pi^a\partial_\mu\pi^b}{f^2}\left[\frac{f^2}{\pi^2}\sin^2\left(\tfrac{y}{4}\right)\right],\end{aligned} \tag{3.57b}$$

$$u^\dagger\tau^a u = \tau^a\cos(y/2) + \frac{\boldsymbol{\pi}\pi^a}{f^2}\left[2\frac{f^2}{\pi^2}\sin^2\left(\tfrac{y}{4}\right)\right] - \frac{\epsilon^{abc}\pi^b\tau^c}{f}\left[\sqrt{\frac{f^2}{\pi^2}}\sin\left(\tfrac{y}{2}\right)\right], \tag{3.57c}$$

$$u\tau^a u^\dagger = \tau^a\cos(y/2) + \frac{\boldsymbol{\pi}\pi^a}{f^2}\left[2\frac{f^2}{\pi^2}\sin^2\left(\tfrac{y}{4}\right)\right] + \frac{\epsilon^{abc}\pi^b\tau^c}{f}\left[\sqrt{\frac{f^2}{\pi^2}}\sin\left(\tfrac{y}{2}\right)\right]. \tag{3.57d}$$

Next, the following linear combinations of Eqs. (3.57a) to (3.57d) are necessary to calculate the vector and axial-vector currents:

$$u^\dagger\partial_\mu u + u\partial_\mu u^\dagger = \mathrm{i}\frac{\epsilon^{abc}\tau^c\pi^a\partial_\mu\pi^b}{f^2}\left[2\frac{f^2}{\pi^2}\sin^2\left(\tfrac{y}{4}\right)\right], \tag{3.58a}$$

$$u^\dagger\partial_\mu u - u\partial_\mu u^\dagger = \mathrm{i}\frac{\partial_\mu\boldsymbol{\pi}}{f}\left[\sqrt{\frac{f^2}{\pi^2}}\sin\left(\tfrac{y}{2}\right)\right] + \mathrm{i}\frac{\boldsymbol{\pi}\pi^i\partial_\mu\pi^i}{f^3}\left[f^2y'\sqrt{\frac{f^2}{\pi^2}} - \left(\frac{f^2}{\pi^2}\right)^{3/2}\sin\left(\tfrac{y}{2}\right)\right], \tag{3.58b}$$

$$u^\dagger\tau^a u + u\tau^a u^\dagger = 2\tau^a\cos(y/2) + \frac{\boldsymbol{\pi}\pi^a}{f^2}\left[4\frac{f^2}{\pi^2}\sin^2\left(\tfrac{y}{4}\right)\right], \tag{3.58c}$$

$$u^\dagger\tau^a u - u\tau^a u^\dagger = -\frac{\epsilon^{abc}\pi^b\tau^c}{f}\left[2\sqrt{\frac{f^2}{\pi^2}}\sin\left(\tfrac{y}{2}\right)\right]. \tag{3.58d}$$

Finally, the vector current reads:

$$\begin{aligned}\Gamma_\mu = {} & \mathrm{i}\frac{\epsilon^{abc}\tau^c\pi^a\partial_\mu\pi^b}{f^2}\left[\frac{f^2}{\pi^2}\sin^2\left(\tfrac{y}{4}\right)\right] - \mathrm{i}v^a_\mu\tau^a\frac{\cos(y/2)}{2} - \mathrm{i}\frac{\boldsymbol{\pi}\pi^a}{f^2}v^a_\mu\left[\frac{f^2}{\pi^2}\sin^2\left(\tfrac{y}{4}\right)\right] \\ & + \frac{\mathrm{i}\epsilon^{abc}a^a_\mu\pi^b\tau^c}{f}\left[\frac{1}{2}\sqrt{\frac{f^2}{\pi^2}}\sin\left(\tfrac{y}{2}\right)\right],\end{aligned} \tag{3.59}$$

and can be expanded as follows:

$$\Gamma_\mu = \mathrm{i}\frac{\epsilon^{abc}\tau^c\pi^a\partial_\mu\pi^b}{4f^2} - \frac{\mathrm{i}}{2}v^a_\mu\tau^a + \frac{\mathrm{i}}{4}v^a_\mu\tau^a\frac{\pi^2}{f^2} - \mathrm{i}\frac{\boldsymbol{\pi}\pi^a}{4f^2}v^a_\mu + \frac{\mathrm{i}\epsilon^{abc}a^a_\mu\pi^b\tau^c}{2f} + \mathcal{O}(1/f^3). \tag{3.60}$$

The axial-vector current is given by:

$$\begin{aligned}\Delta_\mu = {} & \mathrm{i}\frac{\partial_\mu\boldsymbol{\pi}}{f}\left[\sqrt{\frac{f^2}{\pi^2}}\frac{\sin(y/2)}{2}\right] + \mathrm{i}\frac{\boldsymbol{\pi}\pi^i\partial_\mu\pi^i}{f^3}\left[\frac{f^2y'}{2}\sqrt{\frac{f^2}{\pi^2}} - \left(\frac{f^2}{\pi^2}\right)^{3/2}\frac{\sin(y/2)}{2}\right] \\ & + \frac{\mathrm{i}\epsilon^{abc}v^a_\mu\pi^b\tau^c}{f}\left[\frac{1}{2}\sqrt{\frac{f^2}{\pi^2}}\sin\left(\tfrac{y}{2}\right)\right] - \mathrm{i}a^a_\mu\tau^a\frac{\cos(y/2)}{2} - \mathrm{i}\frac{\boldsymbol{\pi}\pi^a}{f^2}a^a_\mu\left[\frac{f^2}{\pi^2}\sin^2\left(\tfrac{y}{4}\right)\right],\end{aligned} \tag{3.61}$$

which can be expanded like this:

$$\Delta_\mu = \mathrm{i}\frac{\partial_\mu\boldsymbol{\pi}}{2f} + \frac{\mathrm{i}\epsilon^{abc}v^a_\mu\pi^b\tau^c}{2f} - \frac{\mathrm{i}}{2}a^a_\mu\tau^a + \frac{\mathrm{i}}{4}a^a_\mu\tau^a\frac{\pi^2}{f^2} - \mathrm{i}\frac{\boldsymbol{\pi}\pi^a}{4f^2}a^a_\mu + \mathcal{O}(1/f^3). \tag{3.62}$$

Higher order interactions. The second-order term, $A^{(2)}$ is given by,

$$\begin{aligned}A^{(2)} = {} & -c_1\,\mathrm{Tr}_F\{\chi_+\} + \frac{c_2}{2m_N^2}\,\mathrm{Tr}_F\{u_\mu u_\nu\}\,D^\mu D^\nu - \frac{c_3}{2}\,\mathrm{Tr}_F\{u_\mu u^\mu\} + \frac{c_4}{2}\gamma^\mu\gamma^\nu[u_\mu, u_\nu] \\ & - c_5\hat{\chi}_+ - \frac{\mathrm{i}c_6}{8m_N}\gamma^\mu\gamma^\nu F^+_{\mu\nu} - \frac{\mathrm{i}c_7}{8m_N}\gamma^\mu\gamma^\nu\,\mathrm{Tr}_F\left\{F^+_{\mu\nu}\right\},\end{aligned} \tag{3.63}$$

where the following terms are introduced:

- χ_+ contains scalar and pseudoscalar fields, as well as the pion fields:

$$\chi_+ = u\chi^\dagger u + u^\dagger \chi u^\dagger. \tag{3.64}$$

- u_μ is proportional to the axial-vector current:

$$u_\mu = 2\mathrm{i}\Delta_\mu. \tag{3.65}$$

- D_μ is a covariant derivative, acting on a spinor ψ as:

$$D_\mu\psi = \partial_\mu\psi + \Gamma_\mu\psi. \tag{3.66}$$

- $\hat{\chi}_+$ is the traceless version of χ_+, defined as:

$$\hat{\chi}_+ = \chi_+ - \frac{1}{2}\,\mathrm{Tr}_F\{\chi_+\}\,, \tag{3.67}$$

  where the coefficient 1/2 is equal to $\mathrm{Tr}_F\{\mathbb{1}\}^{-1}$ such that $\hat{\chi}_+$ becomes traceless:

$$\mathrm{Tr}_F\{\hat{\chi}_+\} = \mathrm{Tr}_F\{\chi_+\} - \frac{1}{\mathrm{Tr}_F\{\mathbb{1}\}}\,\mathrm{Tr}_F\{\chi_+\}\,\mathrm{Tr}_F\{\mathbb{1}\} = 0. \tag{3.68}$$

- $F^+_{\mu\nu}$ is a field strength tensor, defined in terms of the left- and right-handed currents:

$$F^+_{\mu\nu} = u^\dagger F^R_{\mu\nu} u + u F^L_{\mu\nu} u^\dagger, \tag{3.69a}$$
$$F^R_{\mu\nu} = \partial_\mu r_\nu - \partial_\nu r_\mu - \mathrm{i}[r_\nu, r_\mu], \tag{3.69b}$$
$$F^L_{\mu\nu} = \partial_\mu l_\nu - \partial_\nu l_\mu - \mathrm{i}[l_\nu, l_\mu], \tag{3.69c}$$

  where $r_\mu = (v_\mu + a_\mu)/2$ and $l_\mu = (v_\mu - a_\mu)/2$.

In this thesis, we will need the interactions that are parametrized by the LECs $c_{1,2,3,4}$. For the term proportional to c_1, we need the trace over χ_+. However, this is exactly equivalent to a term of the pion Lagrangian, Eq. (2.71):

$$\mathrm{Tr}_F\{\chi_+\} = \mathrm{Tr}_F\left\{u\chi^\dagger u + u^\dagger\chi u^\dagger\right\} = \mathrm{Tr}_F\left\{\chi^\dagger u^2 + \chi(u^\dagger)^2\right\} = \mathrm{Tr}_F\left\{\chi^\dagger U + \chi U^\dagger\right\}. \tag{3.70}$$

For the terms proportional to $c_{2,3,4}$, we need u_μ. By definition, this is proportional to the axial-vector current Δ_μ in Eq. (3.61):

$$\begin{aligned} u_\mu = 2\mathrm{i}\Delta_\mu = \frac{\partial_\mu\boldsymbol{\pi}}{f}\left[-\sqrt{\frac{f^2}{\pi^2}}\sin(y/2)\right] - \frac{\boldsymbol{\pi}\pi^i\partial_\mu\pi^i}{f^3}\left[f^2y'\sqrt{\frac{f^2}{\pi^2}} - \left(\frac{f^2}{\pi^2}\right)^{3/2}\sin(y/2)\right] \\ - \frac{\epsilon^{abc}v^a_\mu\pi^b\tau^c}{f}\left[\sqrt{\frac{f^2}{\pi^2}}\sin\left(\frac{y}{2}\right)\right] + a^a_\mu\tau^a\cos(y/2) + \frac{\boldsymbol{\pi}\pi^a}{f^2}a^a_\mu\left[2\frac{f^2}{\pi^2}\sin^2\left(\frac{y}{4}\right)\right]. \end{aligned} \tag{3.71}$$

Further terms can be calculated in a similar way, but are irrelevant to the present thesis.

3.2.1. Low energy constants

In this work, we assume that in-vacuum loop effects are renormalized into counter-terms in the chiral Lagrangian, which means that we take the low energy constants (LECs) to be fixed in vacuum.

In the following sections, we will need numerical values for the LECs $c_{1,2,3,4}$. One usually obtains the values for the LECs of an effective field theory by comparing with experiments. In this section, we give an overview how to determine these LECs via experimental methods.

The LEC c_1 is related to the πN sigma term [6, 46]:

$$c_1 = -\frac{1}{4m_\pi^2}\left[\sigma_{\pi N}(0) + \frac{9g_A^2 m_\pi^3}{64\pi f^2}\right]. \tag{3.72}$$

A sigma term is a scalar form factor that indicates the strength of certain matrix elements inside a proton p. In particular, the πN sigma term is defined as:

$$\sigma_{\pi N}(t) = \frac{m_u + m_d}{2}\langle p(k')|\bar{u}u + \bar{d}d|p(k)\rangle, \tag{3.73}$$

where $t = (k' - k)^2$ is the momentum transfer, and $m_{u,d}$ the light quark masses [6].

The LEC c_2 is connected to the isospin-even S wave πN scattering length a^+ [6, 46]:

$$c_2 = \frac{f^2}{2m_\pi^2}\left[4\pi(1 + m_\pi/m_N)a^+ - \frac{3g_A^2 m_\pi^3}{64\pi f^4}\right] + 2c_1 - c_3 + \frac{g_A^2}{2m_N}. \tag{3.74}$$

For incoming and outgoing pions π^a_{in} and π^b_{out}, the on-shell πN forward scattering amplitude can be written as [6]:

$$T^{ba} = T^+(\omega)\delta^{ab} + T^-(\omega)\mathrm{i}\epsilon^{bac}\tau^c, \tag{3.75}$$

where $\omega = n\cdot q$, where n_μ denotes the frame of the nucleon, and q_μ is the pion's four-momentum. Under the exchange $a \leftrightarrow b$, which implies $q \leftrightarrow -q$, the functions $T^\pm$ are either even or odd, $T^\pm(\omega) = \pm T^\pm(-\omega)$. Furthermore, one can define the relevant scattering lengths as [6]:

$$a^\pm = \frac{1}{4\pi}\left(1 + \frac{m_\pi}{m_N}\right)^{-1} T^\pm(m_\pi). \tag{3.76}$$

Depending on the total isospin of the πN system being 1/2 or 3/2, the S-wave scattering lengths are given by [6]:

$$a_{1/2} = a^+ + 2a^-, \qquad\qquad a_{3/2} = a^+ - a^-. \tag{3.77}$$

The LEC c_3 is related to the nucleon axial-vector polarizability α_A [6, 46]:

$$c_3 = -\frac{f^2}{2}\left[\alpha_A + \frac{g_A^2 m_\pi}{8f^4}\left(\frac{77}{48} + g_A^2\right)\right]. \tag{3.78}$$

The axial polarizability α_A describes the change of the nucleon's axial charge g_A in nuclear matter and is defined according to Eq. (3.83) in Ref. [6]:

$$\alpha_A = 2\frac{\partial}{\partial t}\bar{A}^+(m_N^2 + m_\pi^2 - t/2\,, m_N^2 + m_\pi^2 - t/2)\Big|_{t=0}. \tag{3.79}$$

Here, A^+ is a component of the isospin-even πN scattering amplitude $T^+_{\pi N} = A^+(\nu,t) + \not{q}B^+(\nu,t)$ with the pion momentum q^μ. The arguments of A and B are $\nu \equiv (s-u)/(4m_N)$ and the invariant momentum transfer squared, $t = (k'-k)^2$. Furthermore, the bar reminds of the fact that the nucleon Born term (proportional to $g_{\pi N}^2$) has already been subtracted. The nucleon isovector charges g_i are defined via the following matrix element [73]:

$$\langle p|\bar{u}\Gamma_i d|n\rangle = g_i \bar{u}_p \Gamma_i u_n, \tag{3.80}$$

which is connected to β-decay. Here, $\Gamma_S = 1$, $\Gamma_A = \gamma^\mu\gamma^5$, and $\Gamma_T = \sigma^{\mu\nu}$. The relations Eqs. (3.72), (3.74) and (3.78) are obtained from $\mathcal{O}(q^2)$ calculations in chiral perturbation theory, taken from Ref. [6].

c_4 is related to P-wave pion-nucleon scattering [6, 10, 74]. The comparatively large values of $c_{2,3}(c_4)$ are connected to $\Delta(1232)$ (ρ) exchange processes [75]. The numerical values of these LECs are the topic of the next section.

For completeness, we note that the LEC c_5 is related to how the strong interactions create a proton-neutron mass difference, and $c_{6,7}$ can be obtained from the anomalous magnetic moments of the proton and the neutron [75], however their numeric values are not important for this work.

3.2.2. Determination of low-energy constants

The relation of LECs to experimental methods is discussed in detail in Section 3.2.1. In this section, we will list the different options for their numerical values summarized in Tables 3.1 and 3.2.

The first set of $c_{1,2,3,4}$ is taken from a textbook reference, Ref. [10]. The second set is taken from Ref. [72], where experimental data was used to fix the values of the LECs. The LEC c_1 was chosen in connection to the πN sigma term:

$$c_1 = -\frac{\sigma_{\pi N}}{4m_\pi^2}, \tag{3.81}$$

with an empirical value $\sigma_{\pi N} \approx 45$ MeV. We note that other references suggest a possibly larger value of $\sigma_{\pi N} \approx 60$ MeV. The LECs c_2 and c_3 were chosen in connection to the isoscalar πN scattering length a^+:

$$4\pi\left[1 + \frac{m_\pi}{m_N}\right]a^+ = \frac{2m_\pi^2}{f_\pi^2}\left[2c_1 - c_2 - c_3 + \frac{g_A^2}{8m_N}\right], \tag{3.82}$$

LEC	**Set 1** [10]	**Set 2** [72]	**Set 3** [77]
c_1	-0.90	-0.59	-0.61
c_2	3.30	3.30	2.97
c_3	-4.70	-4.43	-4.05
c_4	1.75	1.75	1.85

Table 3.1.: The SU(2) LECs are listed in units of 10^{-3} MeV^{-1}.

where $a^+ = (7.6 \pm 3.1) \times 10^{-3} m_\pi^{-1}$. This means that only the linear combination $c_2 + c_3$ is determined. In order to get separate values for c_2 and c_3, we used the value for c_2 from the first set and were then able to determine c_3. Also, since the LEC c_4 only plays a role in isospin-asymmetric nuclear matter, this LEC was not determined in Ref. [72]. Hence, we also take this value from the first set. The third set corresponds to fitting data to πp elastic differential cross sections, using data from Ref. [76] and performed in K. Aoki's PhD thesis [77] with $\chi^2/N = 3.9$. Note that due to a different convention in the chiral Lagrangian, we have to divide their value of c_4 by two in order to be consistent.

SU(3) LECs. For the SU(3) low-energy constants, we consider four sets of values, as summarized in Table 3.2.

The first two sets were obtained by fitting to lattice QCD data of octet baryon masses, as reviewed by Ref. [78]. The difference between the first and second set lies in the number of masses that were considered for the fit. The third set was obtained by Ref. [79] via fitting to experimental baryon octet data, this was also summarized by [80]. Since they only determined b_D and b_F, we use the relation[1] between SU(2) and SU(3) LECs, $2b_0 + b_D + b_F = 2c_1$, to fix b_0. The fourth set is taken from Ref. [81]. There, the authors performed a fit to K^+p elastic differential cross sections, using experimental data from Ref. [82].

Other LECs. Furthermore, we use physical values for the pion decay constant $f_\pi = 92.4$ MeV, and the axial coupling $g_A = 1.26$. We also use isospin-averaged values for the pion mass, $m_\pi = 138$ MeV, and the nucleon mass, $m_N = 939$ MeV. In the SU(3) calculations, we use the eta mass $m_\eta = 548$ MeV. We will also use these values for the quark masses: $m_u = 2.16$ MeV, $m_d = 4.67$ MeV, and $m_s = 93$ MeV. These values lead to:

$$\frac{\delta m}{m} \approx -\frac{1}{3}, \qquad\qquad \frac{m_s}{m} \approx 27.2, \tag{3.83}$$

where $m = (m_u + m_d)/2$ and $\delta m = (m_u - m_d)/2$, which play a role in the explicit isospin breaking effects.

[1]This was determined by comparing the results for $\langle \bar{u}u + \bar{d}d \rangle^*_{\mathrm{SU(2)}}$ and $\langle \bar{u}u + \bar{d}d \rangle^*_{\mathrm{SU(3)}}$ in Section 4.4.3.

LEC	**Set 1** [78]	**Set 2** [78]	**Set 3** [79]	**Set 4** [81]
b_0	-0.609	-0.714	0.064	-0.054
b_D	0.225	0.222	0.060	0.064
b_F	-0.404	-0.428	-0.190	-0.209

Table 3.2.: The SU(3) LECs are listed in units of 10^{-3} MeV^{-1}.

3.3. Isospin-asymmetric nuclear matter

In order to describe asymmetric nuclear matter, we assume a different Fermi momentum for the proton and the neutron. They will be denoted k_F^p and k_F^n, respectively, and depend on the proton and neutron densities:

$$k_F^p = (3\pi^2\rho_p)^{1/3}, \qquad\qquad k_F^n = (3\pi^2\rho_n)^{1/3}. \tag{3.84}$$

Instead of the two variables $\{\rho_p, \rho_n\}$, we will use the total nucleon density $\rho = \rho_p + \rho_n$ and the ratio of neutron-to-proton densities $r = \rho_n/\rho_p$. One can calculate the individual densities via:

$$\rho_p = \frac{\rho}{1+r}, \qquad\qquad \rho_n = \frac{r\rho}{1+r}. \tag{3.85}$$

In order to restrict the in-medium nucleons' momenta to always be below their respective Fermi momenta, we include the matrix $n(\boldsymbol{p})$, which reads:

$$n(\boldsymbol{p}) = \begin{pmatrix} \Theta(k_F^p - |\boldsymbol{p}|) & 0 \\ 0 & \Theta(k_F^n - |\boldsymbol{p}|) \end{pmatrix}. \tag{3.86}$$

A simple nucleon loop will then include the factor $\mathrm{Tr}_F\{n(\boldsymbol{p})\}$, which leads to two separate integrations, once over momenta below the proton's Fermi momentum and another over momenta below the neutron's Fermi momenta.

The physical effect that asymmetric nuclear matter has on the pion is that the charged and uncharged pions will behave differently. We perform our calculations in the so-called mathematical basis of the pions, $\pi^a \in \{\pi^1, \pi^2, \pi^3\}$. Depending on the ratio r of neutrons and protons in the nuclear matter, the different pion components are affected differently. Therefore, after transforming to the physical basis, $\{\pi^\pm, \pi^0\}$, the charged pions and the neutral pions' properties will not be equal. More details on the transformation between the mathematical basis and the physical basis can be found in Appendix B.2.

Finally, let us mention numeric values. We will express the nucleon density in terms of the normal nuclear density $\rho_0 \approx 0.17\,\mathrm{fm}^{-3}$, which is the typical density for heavy nuclei. The densities inside neutron stars are around $2\rho_0$, but could go as high as $9\rho_0$ in their center [83]. In heavy nuclei, the ratio of neutrons to protons is around $r \approx 1.5$. For instance, the stable lead nucleus ^{208}Pb has 82 protons and 126 neutrons. In neutron stars, the neutron-to-proton ratio is about $r \approx 10$ [84].

3.4. In-medium Feynman rules

Finally in this section, we collect the Feynman rules [33, 72] that we use throughout this thesis.

1. For n nucleon loops (i.e. fermionic loops), we include a factor $(-1)^n$, due to the anti-commutating nature of fermionic variables [85]. Furthermore, for m Fermi sea insertions, include a factor $(-1)^m/m$. This m counts the number of in-medium nucleon propagators in a given diagram.

2. An internal pion of momentum p^μ is to be replaced by:

$$a \overset{\pi(p)}{\dashrightarrow} b \quad = \lim_{\epsilon\to 0} \frac{\mathrm{i}}{p^2 - m_\pi^2 + \mathrm{i}\epsilon} \delta^{ab}, \tag{3.87}$$

   where m_π is the in vacuum pion mass.

3. An internal nucleon line for a nucleon of momentum p^μ propagating in vacuum gets replaced by:

$$\xrightarrow{N(p)} \quad = \lim_{\epsilon\to 0} \frac{\mathrm{i}(\not{p} + m_N)}{p^2 - m_N^2 + \mathrm{i}\epsilon}, \tag{3.88}$$

   where m_N is the nucleon mass.

4. An internal nucleon line for a nucleon of momentum p^μ propagating *in-medium* gets replaced by:

$$\overset{N(p)}{\boldsymbol{\longrightarrow}} \quad = (\not{p} + m_N)\, 2\pi\, \delta(p^2 - m_N^2)\Theta(p^0) n(\boldsymbol{p}), \tag{3.89}$$

   so that after integrating over this momentum we get:

$$\begin{aligned} &\int \frac{\mathrm{d}^4 p}{(2\pi)^4} (\not{p} + m_N)\, 2\pi\, \delta(p^2 - m_N^2)\Theta(p^0) n(\boldsymbol{p}) \\ &\qquad = \int \frac{\mathrm{d}^3 \boldsymbol{p}}{(2\pi)^3} \frac{1}{2E(\boldsymbol{p})} (\not{p} + m_N)\, n(\boldsymbol{p}) \Big|_{p^0 \to E(\boldsymbol{p})}, \end{aligned} \tag{3.90}$$

   where $E(\boldsymbol{p}) = (\boldsymbol{p}^2 + m_N^2)^{1/2}$. For the in-medium nucleons, we make use of the matrix $n(\boldsymbol{p})$, which is a matrix in isospin space, that takes care of keeping the momentum of the nucleon below the respective Fermi momentum:

$$n(\boldsymbol{p}) = \begin{pmatrix} \Theta(k_F^p - |\boldsymbol{p}|) & 0 \\ 0 & \Theta(k_F^n - |\boldsymbol{p}|) \end{pmatrix}. \tag{3.91}$$

5. A vertex that includes nucleon lines gets a factor $[-\mathrm{i}A_{\phi\cdots\chi}]$, where $\phi\cdots\chi$ represents all the fields that interact with the nucleon. We calculate this vertex factor by taking the functional derivative of the operator A in Eqs. (3.50) and (3.63) with respect to $\phi\cdots\chi$ in momentum space,

$$A_{\phi\cdots\chi} = \frac{\delta}{\delta\phi}\cdots\frac{\delta}{\delta\chi}A, \tag{3.92}$$

   where an incoming momentum gets replaced by $\partial^\mu \to -\mathrm{i}p^\mu$ and an exiting momentum will be replaced with $\partial^\mu \to \mathrm{i}p^\mu$:

$$\frac{\delta}{\delta\varphi(p_{\mathrm{in}})}[\partial^\mu\varphi] = -\mathrm{i}p^\mu_{\mathrm{in}}, \qquad \frac{\delta}{\delta\varphi(p_{\mathrm{out}})}[\partial^\mu\varphi] = \mathrm{i}p^\mu_{\mathrm{out}}. \tag{3.93}$$

6. For a vertex that does *not* connect to any nucleons, we use the pionic Lagrangian $\mathcal{L}_\pi^{(2)}$ in Eq. (2.53). Similar to the case with A, we now get a factor of $[+\mathrm{i}\mathcal{L}_{\phi\cdots\chi}]$, where $\phi\cdots\chi$ represents all the fields that interact at this vertex. Again, we calculate this vertex factor by taking the functional derivative of the Lagrangian with respect to $\phi\cdots\chi$ in momentum space,

$$\mathcal{L}_{\phi\cdots\chi} = \frac{\delta}{\delta\phi}\cdots\frac{\delta}{\delta\chi}\mathcal{L}_\pi^{(2)}, \tag{3.94}$$

   where an incoming momentum gets replaced by $\partial^\mu \to -\mathrm{i}p^\mu$ and an exiting momentum will be replaced with $\partial^\mu \to \mathrm{i}p^\mu$.

7. Finally, we integrate over all internal momenta,

$$\int \frac{\mathrm{d}^4p}{(2\pi)^4}, \tag{3.95}$$

   and sum over all Dirac and spinor indices, which often leads to taking the trace of some expression. We do this in opposite direction as the arrows on fermionic propagators are pointing.

Another rule comes from the fact that we treat external currents as dynamical fields in our approach. For reasons explained in Section 5.5, we have to include a factor of $(-\mathrm{i})$ for every external current in a given diagram.

4. In-Medium Quark Condensate

In this chapter, we demonstrate how to compute the density dependence of the in-medium quark condensate. We will first consider the SU(2) case in Section 4.1, where we show how to calculate the condensate devising the chiral Ward identity. In Section 4.2, we apply in-medium chiral perturbation theory up to next-to-leading order and present our results in Section 4.3. In Section 4.4, we present a simple extension to the SU(3) case, where we can perform a first-order (linear density) estimation of the quantities $\langle \bar{u}u - \bar{d}d \rangle^*$ and $\langle \bar{s}s \rangle^*$.

4.1. Using the SU(2) chiral Ward identity

In this section, we show how to calculate the nuclear density dependence of the in-medium quark condensate. To do this, we follow Ref. [68] and use the chiral Ward identity. We start with the divergence of the following time-ordered product:

$$\partial^\mu [\mathsf{T} A^a_\mu(x) P^b(0)] = \partial^\mu [A^a_\mu(x) P^b(0)\Theta(x^0) + P^b(0) A^a_\mu(x)\Theta(-x^0)]. \tag{4.1}$$

Using $\partial_\mu \Theta(x^0 - y^0) = \delta(x^0 - y^0)\delta_{\mu 0}$, we write:

$$\begin{aligned} \partial^\mu [\mathsf{T} A^a_\mu(x) P^b(0)] &= \partial^\mu A^a_\mu(x) P^b(0)\Theta(x^0) + A^a_0(x) P^b(0)\delta(x^0) \\ &\quad + P^b(0)\partial^\mu A^a_\mu(x)\Theta(-x^0) - P^b(0) A^a_0(x)\delta(x^0) \qquad (4.2\text{a}) \\ &= \mathsf{T}[\partial^\mu A^a_\mu(x) P^b(0)] + \delta(x^0)[A^a_0(x), P^b(0)]. \qquad (4.2\text{b}) \end{aligned}$$

We can use the partially-conserved axial current (PCAC) relation $\partial^\mu A^a_\mu(x) = m P^a(x)$ with m the quark mass, which yields:

$$\partial^\mu [\mathsf{T} A^a_\mu(x) P^b(0)] = m \mathsf{T}[P^a(x) P^b(0)] + \delta(x^0)[A^a_0(x), P^b(0)]. \tag{4.3}$$

Next we evaluate the whole equation between the in-medium vacuum $|\Omega\rangle$,

$$\partial^\mu \langle \Omega | \mathsf{T} A^a_\mu(x) P^b(0) | \Omega \rangle = m \langle \Omega | \mathsf{T} P^a(x) P^b(0) | \Omega \rangle + \delta(x^0) \langle \Omega | [A^a_0(x), P^b(0)] | \Omega \rangle, \tag{4.4}$$

and write the equation in terms of the pseudoscalar two-point correlation function $\Pi^{ab}(x,0)$ as well as the pseudoscalar-axial-vector correlation function $\Pi^{ab}_{5\mu}(x,0)$:

$$\partial^\mu \Pi^{ab}_{5\mu}(x,0) = m \Pi^{ab}(x,0) + \delta(x^0) \langle \Omega | [A^a_0(x), P^b(0)] | \Omega \rangle. \tag{4.5}$$

We then multiply the whole equation by $\exp(\mathrm{i}q\cdot(x-0))$ and integrate over d^4x in order to write this in terms of Fourier transformed momentum space correlation functions:

$$\int \mathrm{d}^4x\, \mathrm{e}^{\mathrm{i}q\cdot x}\partial^\mu \Pi^{ab}_{5\mu}(x,0) = m\int \mathrm{d}^4x\, \mathrm{e}^{\mathrm{i}q\cdot x}\Pi^{ab}(x,0) + \int \mathrm{d}^4x\, \mathrm{e}^{\mathrm{i}q\cdot x}\delta(x^0)\langle\Omega|[A^a_0(x),P^b(0)]|\Omega\rangle \tag{4.6a}$$

$$= m\int \mathrm{d}^4x\, \mathrm{e}^{\mathrm{i}q\cdot x}\Pi^{ab}(x,0) + \int \mathrm{d}^3\boldsymbol{x}\, \mathrm{e}^{-\mathrm{i}\boldsymbol{q}\cdot\boldsymbol{x}}\langle\Omega|[A^a_0(x),P^b(0)]|\Omega\rangle. \tag{4.6b}$$

After a partial integration on the left-hand side of the equation, we use the momentum space correlation functions $\Pi(q)$ and $\Pi_{5\mu}$:

$$-\mathrm{i}q^\mu\Pi^{ab}_{5\mu}(q) = m\Pi^{ab}(q) + \int \mathrm{d}^3\boldsymbol{x}\, \mathrm{e}^{-\mathrm{i}\boldsymbol{q}\cdot\boldsymbol{x}}\langle\Omega|[A^a_0(x),P^b(0)]|\Omega\rangle. \tag{4.7}$$

Now we take the soft limit $q^\mu \to 0$ and perform the $\mathrm{d}^3\boldsymbol{x}$ integration over the axial-vector current, which gives the corresponding conserved Noether charge according to $Q^a_5 = \int \mathrm{d}^3\boldsymbol{x} A^a_0(x)$:

$$-\mathrm{i}\lim_{q\to 0} q^\mu\Pi^{ab}_{5\mu}(q) = m\Pi^{ab}(0) + \langle\Omega|[Q^a_5,P^b(0)]|\Omega\rangle. \tag{4.8}$$

In order to continue, we employ the SU(2) chiral transformation behavior of the pseudoscalar current[1], $[Q^a_5,P^b(0)] = -\mathrm{i}\delta^{ab}\bar{q}q(x)$, to write the equation like this:

$$m\Pi^{ab}(0) + \mathrm{i}\lim_{q\to 0} q^\mu\Pi^{ab}_{5\mu}(q) = \mathrm{i}\delta^{ab}\langle\Omega|\bar{q}q|\Omega\rangle. \tag{4.9}$$

So by calculating the pseudoscalar two-point correlation function in chiral perturbation theory, we can infer the density dependence of the in-medium quark condensate.

We will write down the result for the in-medium condensate in terms of a ratio of the in-medium value compared to the in-vacuum value. Therefore, the expression for the vacuum condensate is useful,

$$\langle\bar{q}q\rangle_0 \equiv \langle\bar{u}u+\bar{d}d\rangle_0 = -2f^2B_0, \tag{4.10}$$

such that a multiplication by the quark mass and division by the vacuum condensate amounts to:

$$\frac{m}{\langle\bar{q}q\rangle_0} = -\frac{m}{2f^2B_0}, \tag{4.11}$$

which we will often use in Section 4.2. Note that here in the SU(2) case, $\langle\bar{q}q\rangle_0 = \langle\bar{u}u+\bar{d}d\rangle_0 = -2f^2B_0$, where as in the SU(3) case, $\langle\bar{q}q\rangle_0 = \langle\bar{u}u+\bar{d}d+\bar{s}s\rangle_0 = -3f^2B_0$.

[1] Since we are only considering SU(2) here, the right-hand side only involves δ^{ab} and the isoscalar scalar current. For SU(3), the right-hand side would be $2/3\delta^{ab}\bar{q}q + d^{abc}\bar{q}\lambda^c q$ where d^{abc} are SU(3)'s totally symmetric structure constants.

4.2. Calculation of the SU(2) quark condensate

As described in Section 4.1, we will now show how to calculate the pseudoscalar two-point correlation function $\Pi^{ab}(0)$, which can be used to calculate the density dependence of the in-medium quark condensate according to Eq. (4.9):

$$m\Pi^{ab}(0) + \mathrm{i}\lim_{q\to 0} q^\mu \Pi^{ab}_{5\mu}(q) = \mathrm{i}\delta^{ab}\langle\Omega|\bar{q}q|\Omega\rangle.$$

The second term on the left-hand side of the equation vanishes in the soft limit. This is because there are no zero-mass modes in our system which could provide a factor of $1/q^2$ with their propagator in a diagram of $\Pi^{ab}_{5\mu}$. Hence, we only need to calculate Π^{ab}. In an expansion of the quark mass, the quark condensate starts at $\mathcal{O}(m^0)$, but the left-hand side of the equation looks proportional to $\mathcal{O}(m)$. However, the soft limit leads to pion propagators $1/m_\pi^2$ in the pseudoscalar correlation function, and since $m_\pi^2 \propto m$, the expansion in the quark mass of the left-hand side indeed starts at $\mathcal{O}(m^0)$.

We have to consider diagrams with two external pseudoscalar lines. The meaning of the different lines in the diagrams and the corresponding Feynman rules are discussed in Section 3.4. These diagrams follow from the expansion schemes, as discussed in Section 3.1.1. In particular, we treat each expansion as follows: First, we expand $\ln(\mathcal{F})$ up to second order, which means we can have diagrams with up to two in-medium nucleon propagators. Second, we expand $A[\mathbb{1}_4 - D_0^{-1}A]^{-1}$ also to second order, which means we can have in-vacuum nucleon propagators between two vertices. This happens for instance in the first type of diagrams. We will not include a diagram with an in-vacuum nucleon propagator if a purely in-vacuum loop can be contracted to a vertex, since we use experimental data for our LECs and those only-vacuum contributions are already renormalized to yield these numerical values. Third, we include πN interactions up to second order $A = A^{(1)} + A^{(2)}$. We furthermore restrict our calculations to diagrams proportional to $\mathcal{O}(k_F^5) = \mathcal{O}(\rho^{5/3})$, since one would have to include nucleon-nucleon interactions in the Lagrangian in order to be able to discuss $\mathcal{O}(\rho^2)$ terms. These considerations lead to the diagrams in Tables 4.1 to 4.5.

These tables are organized as follows. For each type of diagram, there can be an interaction from $A^{(1)}$ or $A^{(2)}$. Hence, for each diagram we investigate all possible cases of interactions, $i \in \{1, 2\}$ for one vertex or $(i, j) \in \{11, 12, 21, 22\}$ for two vertices. If such a vertex does not exist (because there is no corresponding term in the Lagrangian) we disregard the whole diagram. Still, some diagrams might vanish in the course of the calculation, which will be shown later on. In summary, we will calculate three type-2 diagrams, two type-3 diagrams, seven type-4 diagrams and one type-5 diagram:

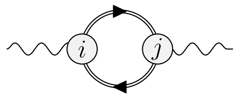

i	$\cancel{1}^{(1)}$	$\cancel{1}^{(1)}$	$\cancel{2}^{(2)}$	$\cancel{2}^{(2)}$
j	$\cancel{1}^{(1)}$	$\cancel{2}^{(2)}$	$\cancel{1}^{(1)}$	$\cancel{2}^{(2)}$

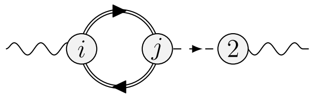

i	$\cancel{1}^{(1)}$	$\cancel{1}^{(1)}$	$\cancel{2}^{(2)}$	$\cancel{2}^{(2)}$
j	1	$\cancel{2}^{(3)}$	1	$\cancel{2}^{(3)}$

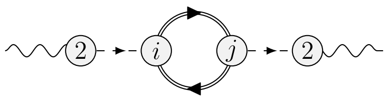

i	$\cancel{1}^{(4)}$	1	$\cancel{2}^{(3)}$	$\cancel{2}^{(3)}$
j	$\cancel{1}^{(4)}$	$\cancel{2}^{(3)}$	1	$\cancel{2}^{(3)}$

Table 4.1.: Type 1 Π^{ab} diagrams. The superscript (1) denotes that the corresponding diagram vanishes because of $A_p^{(1)} = 0$, (2) because of $A_p^{(2)} = 0$, (3) because of $A_\pi^{(2)} = 0$ and (4) because $A_\pi^{(1)} \overset{q \to 0}{=} 0$ in the soft limit. In total, no diagram remains.

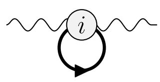

i	$\cancel{1}^{(1)}$	$\cancel{2}^{(2)}$

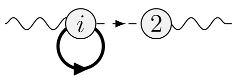

i	$\cancel{1}^{(3)}$	2

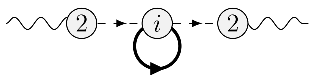

i	1	2

Table 4.2.: Type 2 Π^{ab} diagrams. The superscript (1) denotes that the corresponding diagram vanishes because of $A_{pp}^{(1)} = 0$, (2) because of $A_{pp}^{(2)} = 0$, and (3) because of $A_{\pi p}^{(1)} = 0$. In total, three diagrams remain.

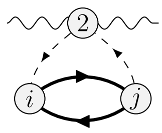

no contribution because $\mathcal{L}_{\pi\pi pp}^{(2)} = 0$

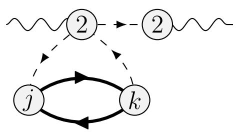

i	1	1	$\cancel{2}^{(1)}$	$\cancel{2}^{(1)}$
j	1	$\cancel{2}^{(1)}$	1	$\cancel{2}^{(1)}$

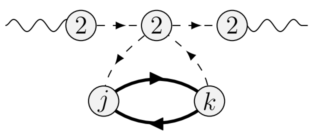

i	1	1	$\cancel{2}^{(1)}$	$\cancel{2}^{(1)}$
j	1	$\cancel{2}^{(1)}$	1	$\cancel{2}^{(1)}$

Table 4.3.: Type 3 Π^{ab} diagrams. The superscript (1) denotes that the corresponding diagram vanishes because of $A_\pi^{(2)} = 0$. In total, two diagrams remain.

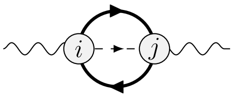

i	$\cancel{1}^{(1)}$	$\cancel{1}^{(1)}$	2	2
j	$\cancel{1}^{(1)}$	2	$\cancel{1}^{(1)}$	2

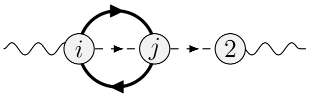

i	$\cancel{1}^{(1)}$	$\cancel{1}^{(1)}$	2	2
j	1	2	1	2

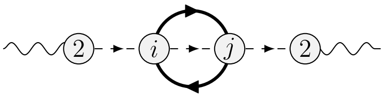

i	1	1	2	2
j	1	2	1	2

Table 4.4.: Type 4 Π^{ab} diagrams. The superscript (1) denotes that the corresponding diagram vanishes because of $A^{(1)}_{\pi p} = 0$. In total, seven diagrams remain. We will see that all type-4 diagrams will precisely cancel each other in the soft limit.

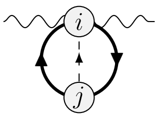

i	$\cancel{1}^{(1)}$	$\cancel{1}^{(1)}$	$\cancel{2}^{(2)}$	$\cancel{2}^{(2)}$
j	1	$\cancel{2}^{(3)}$	1	$\cancel{2}^{(3)}$

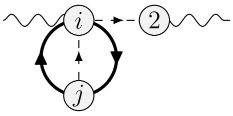

i	$\cancel{1}^{(4)}$	$\cancel{1}^{(4)}$	$\cancel{2}^{(5)}$	$\cancel{2}^{(5)}$
j	1	$\cancel{2}^{(3)}$	1	$\cancel{2}^{(3)}$

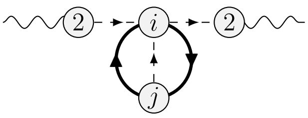

i	1	1	$\cancel{2}^{(6)}$	$\cancel{2}^{(6)}$
j	1	$\cancel{2}^{(3)}$	1	$\cancel{2}^{(3)}$

Table 4.5.: Type 5 Π^{ab} diagrams. The superscript (1) denotes that the corresponding diagram vanishes because of $A^{(1)}_{\pi pp} = 0$, (2) because of $A^{(2)}_{\pi pp} = 0$, (3) because of $A^{(2)}_{\pi} = 0$, (4) because of $A^{(1)}_{\pi^2 p} = 0$, (5) because of $A^{(2)}_{\pi^2 p} = 0$, and (6) because of $A^{(2)}_{\pi^3} = 0$. In total, one diagram remains.

4.2.1. One-loop diagrams of type 2

First Diagram

The first diagram for the in-medium pseudoscalar correlation function is:

$\Pi^{ab}_{2,1}(0):\quad p^a$ 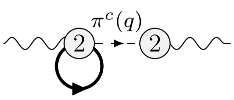 p^b (4.12)

In terms of an integral expression, this can be translated to[2]:

$$\Pi^{ab}_{2,1}(0) = \lim_{q^\mu\to 0}(-1)^L\frac{(-1)^n}{n}(-\mathrm{i})^2\int\frac{\mathrm{d}^3\boldsymbol{p}}{(2\pi)^3}\frac{1}{2E_p}\,\mathrm{Tr}\left\{[-\mathrm{i}A^{(2)}_{\pi p}]^{ac}(\not{p}+m_N)n(\boldsymbol{p})\right\}\frac{\mathrm{i}\delta^{ac}}{q^2-m_\pi^2}[\mathrm{i}\mathcal{L}^{(2)}_{\pi p}]^{cb}. \tag{4.13}$$

In this diagram, we have one fermionic loop, $L = 1$, one Fermi-sea propagator, $n = 1$, and two external currents in the correlation function, thus we get a factor of $(-\mathrm{i})^2$. The relevant terms in the Lagrangian, which contain the necessary information about the vertices in the present diagram, are:

$$A^{(2)}_{\pi p} = -\frac{8c_1B_0}{f}p^i\pi^i, \tag{4.14a}$$

$$\mathcal{L}^{(2)}_{\pi p} = 2fB_0\pi^ip^i. \tag{4.14b}$$

In order to use these interactions in the Feynman rules, we perform a functional differentiation with respect to the interacting fields to get the vertex factors:

$$[-\mathrm{i}A^{(2)}_{\pi p}]^{ac} = \frac{8\mathrm{i}c_1B_0}{f}\delta^{ac}, \tag{4.15a}$$

$$[\mathrm{i}\mathcal{L}^{(2)}_{\pi p}]^{cb} = 2\mathrm{i}fB_0\delta^{bc}. \tag{4.15b}$$

The trace in spinor space yields:

$$\mathrm{Tr}_S\left\{\not{p}+m_N\right\} = 4m_N. \tag{4.16}$$

In order to efficiently calculate the traces of Dirac gamma matrices, we employed the Mathematica package `FeynCalc` [86–88] for several calculations in this and the next chapter. The trace in isospin space yields:

$$\mathrm{Tr}_F\{n(\boldsymbol{p})\} = \Theta^p_{\boldsymbol{p}} + \Theta^n_{\boldsymbol{p}}. \tag{4.17}$$

We can take the soft limit without problems, which gives us:

$$\Pi^{ab}_{2,1}(0) = -\mathrm{i}\delta^{ab}\frac{32c_1B_0^2m_N}{m_\pi^2}\int\frac{\mathrm{d}^3\boldsymbol{p}}{(2\pi)^3}\frac{1}{E_p}(\Theta^p_{\boldsymbol{p}}+\Theta^n_{\boldsymbol{p}}). \tag{4.18}$$

Now we change to spherical coordinates, $\mathrm{d}^3\boldsymbol{p} = 4\pi p^2\,\mathrm{d}p$, and have our result for the first diagram:

$$\Pi^{ab}_{2,1}(0) = -\mathrm{i}\delta^{ab}\frac{16c_1B_0^2m_N}{\pi^2m_\pi^2}\int\mathrm{d}p\frac{p^2}{E_p}(\Theta^p_{\boldsymbol{p}}+\Theta^n_{\boldsymbol{p}}). \tag{4.19}$$

[2]Note the difference between the external isovector pseudoscalar field p^a and the nucleon momentum $p^\mu = (E_p,\boldsymbol{p})$, since both are denoted by the letter "p".

In order to account for the fact that the nucleon loop can be attached to either vertex, we include a factor of two:

$$\Pi^{ab}_{2,1}(0) = -\mathrm{i}\delta^{ab}\frac{32c_1B_0^2m_N}{\pi^2m_\pi^2}\int \mathrm{d}p\frac{p^2}{E_p}(\Theta^p_{\boldsymbol{p}}+\Theta^n_{\boldsymbol{p}}). \tag{4.20}$$

The result for the first diagram is:

$$\frac{m\Pi^{ab}_{2,1}(0)}{\langle\bar{q}q\rangle_0} = \mathrm{i}\delta^{ab}\frac{8c_1m_N}{\pi^2f^2}\int \mathrm{d}p\frac{p^2}{E_p}[\Theta^p_{\boldsymbol{p}}+\Theta^n_{\boldsymbol{p}}]. \tag{4.21}$$

Here we used the relation for the LEC B_0 in order to replace $B_0m \to m_\pi^2/2$.

Second Diagram

The second type-2 diagram is:

$\Pi^{ab}_{2,2}(0):$

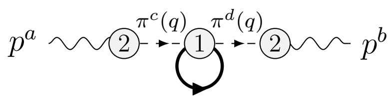

(4.22)

In terms of an integral expression, this can be translated to:

$$\begin{aligned}\Pi^{ab}_{2,2}(0) = &\lim_{q^\mu\to 0}(-\mathrm{i})^2[\mathrm{i}\mathcal{L}^{(2)}_{\pi p}]^{ac}\frac{\mathrm{i}}{q^2-m_\pi^2}(-1)\frac{(-1)}{1}\\ &\times\int\frac{\mathrm{d}^3\boldsymbol{p}}{(2\pi)^3}\frac{1}{2E_p}\,\mathrm{Tr}\left\{[-\mathrm{i}A^{(1)}_{\pi\pi}]^{cd}(\not{p}+m_N)n(\boldsymbol{p})\right\}\frac{\mathrm{i}}{q^2-m_\pi^2}[\mathrm{i}\mathcal{L}^{(2)}_{\pi p}]^{db}.\end{aligned} \tag{4.23}$$

The relevant term in the Lagrangian is:

$$A^{(1)}_{\pi\pi} = \frac{1}{4f^2}\gamma^\mu\pi^i\partial_\mu\pi^j\epsilon^{ijk}\tau^k. \tag{4.24}$$

Since we take the soft limit $q^\mu\to 0$, this diagram will vanish because the vertex is proportional to the pion momentum.

Third Diagram

The third and last type-2 diagram is:

$\Pi^{ab}_{2,3}(0):$

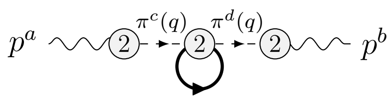

(4.25)

In terms of an integral expression, this can be translated to:

$$\begin{aligned}\Pi^{ab}_{2,3}(0) = &\lim_{q^\mu\to 0}(-\mathrm{i})^2[\mathrm{i}\mathcal{L}^{(2)}_{\pi p}]^{ac}\frac{\mathrm{i}}{q^2-m_\pi^2}(-1)\frac{(-1)}{1}\\ &\times\int\frac{\mathrm{d}^3\boldsymbol{p}}{(2\pi)^3}\frac{1}{2E_p}\,\mathrm{Tr}\left\{[-\mathrm{i}A^{(2)}_{\pi\pi}]^{cd}(\not{p}+m_N)n(\boldsymbol{p})\right\}\frac{\mathrm{i}}{q^2-m_\pi^2}[\mathrm{i}\mathcal{L}^{(2)}_{\pi p}]^{db}.\end{aligned} \tag{4.26}$$

The relevant term in the Lagrangian is:

$$A^{(2)}_{\pi\pi} = \frac{4B_0 c_1 m}{f^2}\pi^i\pi^i + \frac{c_2}{f^2 m_N^2}\partial_\mu\pi^i\partial_\nu\pi^i\partial^\mu\partial^\nu - \frac{c_3}{f^2}\partial_\mu\pi^i\partial^\mu\pi^i + \frac{\mathrm{i}c_4}{f^2}\epsilon^{ijk}\tau^k\gamma^\mu\gamma^\nu\partial_\mu\pi^i\partial_\nu\pi^j. \quad (4.27)$$

In the soft limit, only the first term will be relevant. The vertex factor in the soft limit is:

$$[-\mathrm{i}A^{(2)}_{\pi\pi}]^{cd} = -\frac{8\mathrm{i}c_1 B_0 m}{f^2}\delta^{cd}. \quad (4.28)$$

The trace simplifies to:

$$\mathrm{Tr}\left\{[-\mathrm{i}A^{(2)}_{\pi\pi}]^{cd}(\not{p} + m_N)n(\boldsymbol{p})\right\} = -\frac{32\mathrm{i}c_1 B_0 m m_N}{f^2}\delta^{cd}[\Theta^p_{\boldsymbol{p}} + \Theta^n_{\boldsymbol{p}}]. \quad (4.29)$$

The diagram therefore yields:

$$\Pi^{ab}_{2,3}(0) = \mathrm{i}\delta^{ab}\frac{32B_0^2 m_N c_1 B_0 m}{\pi^2 m_\pi^4}\int \mathrm{d}p\frac{p^2}{E(p)}[\Theta^p_{\boldsymbol{p}} + \Theta^n_{\boldsymbol{p}}], \quad (4.30)$$

and the result is:

$$\frac{m\Pi^{ab}_{2,3}(0)}{\langle\bar{q}q\rangle_0} = -\mathrm{i}\delta^{ab}\frac{4c_1 m_N}{\pi^2 f^2}\int \mathrm{d}p\frac{p^2}{E(p)}[\Theta^p_{\boldsymbol{p}} + \Theta^n_{\boldsymbol{p}}], \quad (4.31)$$

where we used the relation for the LEC B_0 in order to replace $B_0 m \to m_\pi/2$. In total, we can write for the LO diagrams:

$$\frac{\langle\bar{q}q\rangle^*}{\langle\bar{q}q\rangle_0} = 1 + \frac{4c_1}{f^2}\rho + \mathcal{O}(\rho^{4/3}) \quad (4.32)$$

4.2.2. Two-loop diagrams of type 3

First Diagram

The next diagram is:

$\Pi^{ab}_{3,1}(0)$:

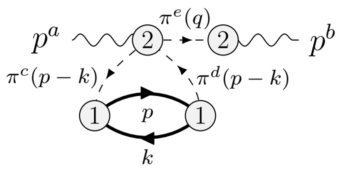

(4.33)

In terms of an integral expression, this can be translated to:

$$\begin{aligned}\Pi^{ab}_{3,1}(0) = \lim_{q^\mu\to 0}(-1)^L\frac{(-1)^n}{n}(-\mathrm{i})^2\frac{1}{2}\int\frac{\mathrm{d}^3\boldsymbol{p}}{(2\pi)^3}\frac{\mathrm{d}^3\boldsymbol{k}}{(2\pi)^3}\frac{1}{4p_0k_0}[\mathrm{i}\mathcal{L}^{(2)}_{\pi^3p}]^{acde}\left[\frac{\mathrm{i}}{(p-k)^2-m_\pi^2}\right]^2 \\ \times \mathrm{Tr}\left\{[-\mathrm{i}A^{(1)}_\pi]^c(\not{k}+m_N)n(\boldsymbol{k})[-\mathrm{i}A^{(1)}_\pi]^d(\not{p}+m_N)n(\boldsymbol{p})\right\} \\ \times\frac{\mathrm{i}}{q^2-m_\pi^2}[\mathrm{i}\mathcal{L}^{(2)}_{\pi p}]^{eb}. \quad (4.34)\end{aligned}$$

The relevant terms in the Lagrangian are:

$$\mathcal{L}^{(2)}_{\pi^3 p} = -\frac{B_0}{5f} p^i \pi^i \pi^j \pi^j, \tag{4.35a}$$

$$A^{(1)}_{\pi} = \frac{g_A}{2f} \gamma^\mu \gamma^5 \partial_\mu \pi^i \tau^i, \tag{4.35b}$$

$$\mathcal{L}^{(2)}_{\pi p} = 2f B_0 \pi^i p^i, \tag{4.35c}$$

and the vertex factors are:

$$[\mathrm{i}\mathcal{L}^{(2)}_{\pi^3 p}]^{abcd} = -\frac{2\mathrm{i}B_0}{5f}(\delta^{ac}_{de} + \delta^{ad}_{ce} + \delta^{ae}_{cd}), \tag{4.36a}$$

$$[-\mathrm{i}A^{(1)}_{\pi}]^{c} = -\frac{g_A}{2f}(\not{p} - \not{k})\gamma^5 \tau^c, \tag{4.36b}$$

$$[-\mathrm{i}A^{(1)}_{\pi}]^{d} = \frac{g_A}{2f}(\not{p} - \not{k})\gamma^5 \tau^d, \tag{4.36c}$$

$$[\mathrm{i}\mathcal{L}^{(2)}_{\pi p}]^{eb} = 2\mathrm{i} f B_0 \delta^{be}. \tag{4.36d}$$

The trace in spinor space is:

$$\mathrm{Tr}_S\Big\{(\not{p} - \not{k})\gamma^5(\not{k} + m_N)(\not{p} - \not{k})\gamma^5(\not{p} + m_N)\Big\} = 16 m_N^2 (p_0 k_0 - pk\cos\theta - m_N^2), \tag{4.37}$$

where we used $p^2 = m_N^2 = k^2$ since both nucleons are on the mass shell. The trace in isospin space is:

$$\begin{aligned}(\delta^{ac}_{de} + \delta^{ad}_{ce} + \delta^{ae}_{cd})\,\mathrm{Tr}_F\Big\{\tau^c n(\boldsymbol{k})\tau^d n(\boldsymbol{p})\Big\} = {}& (\Theta^p_{\boldsymbol{p}}\Theta^p_{\boldsymbol{k}} + 4\Theta^p_{\boldsymbol{p}}\Theta^n_{\boldsymbol{k}} + 4\Theta^n_{\boldsymbol{p}}\Theta^p_{\boldsymbol{k}} + \Theta^n_{\boldsymbol{p}}\Theta^n_{\boldsymbol{k}})\delta^{ab} \\ & + 2(\Theta^p_{\boldsymbol{p}} - \Theta^n_{\boldsymbol{p}})(\Theta^p_{\boldsymbol{k}} - \Theta^n_{\boldsymbol{k}})\delta^{a3}_{b3},\end{aligned} \tag{4.38}$$

where $\Theta^x_{\boldsymbol{y}}$ is an abbreviation for $\Theta(k^x_F - |\boldsymbol{y}|)$, the Heaviside step function that ensures that the nucleon's momentum stays below the Fermi momentum. The diagram, after accounting for the fact that the nucleon loop can be attached on either vertex (i.e. multiplying by 2), is given by:

$$\begin{aligned}\Pi^{ab}_{3,1}(0) = {}& -\mathrm{i}\frac{g_A^2 B_0^2 m_N^2}{20\pi^4 f^2 m_\pi^2}\int \mathrm{d}p\,\mathrm{d}k\,\mathrm{d}\cos\theta \frac{p^2k^2}{p_0k_0}\frac{p_0k_0 - pk\cos\theta - m_N^2}{(2m_N^2 - m_\pi^2 - 2p_0k_0 + 2pk\cos\theta)^2} \\ & \times \begin{cases} (\Theta^p_{\boldsymbol{p}}\Theta^p_{\boldsymbol{k}} + 4\Theta^p_{\boldsymbol{p}}\Theta^n_{\boldsymbol{k}} + 4\Theta^n_{\boldsymbol{p}}\Theta^p_{\boldsymbol{k}} + \Theta^n_{\boldsymbol{p}}\Theta^n_{\boldsymbol{k}})\delta^{ab} \\ 0 \\ 2(\Theta^p_{\boldsymbol{p}} - \Theta^n_{\boldsymbol{p}})(\Theta^p_{\boldsymbol{k}} - \Theta^n_{\boldsymbol{k}})\delta^{a3}_{b3} \end{cases},\end{aligned} \tag{4.39}$$

and the result including the quark mass is:

$$\begin{aligned}\frac{m\Pi^{ab}_{3,1}(0)}{\langle\bar{q}q\rangle_0} = {}& \mathrm{i}\frac{g_A^2 m_N^2}{5(2\pi f)^4}\int \mathrm{d}p\,\mathrm{d}k\,\mathrm{d}\cos\theta \frac{p^2k^2}{p_0k_0}\frac{p_0k_0 - pk\cos\theta - m_N^2}{(2m_N^2 - m_\pi^2 - 2p_0k_0 + 2pk\cos\theta)^2} \\ & \times \begin{cases} (\Theta^p_{\boldsymbol{p}}\Theta^p_{\boldsymbol{k}} + 4\Theta^p_{\boldsymbol{p}}\Theta^n_{\boldsymbol{k}} + 4\Theta^n_{\boldsymbol{p}}\Theta^p_{\boldsymbol{k}} + \Theta^n_{\boldsymbol{p}}\Theta^n_{\boldsymbol{k}})\delta^{ab} \\ 0 \\ 2(\Theta^p_{\boldsymbol{p}} - \Theta^n_{\boldsymbol{p}})(\Theta^p_{\boldsymbol{k}} - \Theta^n_{\boldsymbol{k}})\delta^{a3}_{b3} \end{cases}.\end{aligned} \tag{4.40}$$

Second Diagram

The next diagram is:

$$\Pi^{ab}_{3,2}(0): \tag{4.41}$$

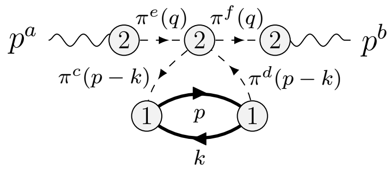

In terms of an integral expression, this can be translated to:

$$\begin{aligned}\Pi^{ab}_{3,2}(0) = \lim_{q^\mu\to 0}(-1)^L\frac{(-1)^n}{n}(-\mathrm{i})^2\frac{\mathrm{i}}{q^2-m_\pi^2}[\mathrm{i}\mathcal{L}^{(2)}_{\pi p}]^{ae}\frac{1}{2}\int\frac{\mathrm{d}^3\boldsymbol{p}}{(2\pi)^3}\frac{\mathrm{d}^3\boldsymbol{k}}{(2\pi)^3}\frac{1}{4E_pE_k}\\ \times[\mathrm{i}\mathcal{L}^{(2)}_{\pi^4}]^{cdef}\left[\frac{\mathrm{i}}{(p-k)^2-m_\pi^2}\right]^2\\ \times\mathrm{Tr}\left\{[-\mathrm{i}A^{(1)}_\pi]^c(\not{k}+m_N)n(\boldsymbol{k})[-\mathrm{i}A^{(1)}_\pi]^d(\not{p}+m_N)n(\boldsymbol{p})\right\}\\ \times\frac{\mathrm{i}}{q^2-m_\pi^2}[\mathrm{i}\mathcal{L}^{(2)}_{\pi p}]^{fb}.\end{aligned}\tag{4.42}$$

The relevant terms in the Lagrangian are:

$$\mathcal{L}^{(2)}_{\pi^4} = \frac{1}{10f^2}\partial_\mu\pi^i\partial^\mu\pi^j\pi^k\pi^l(3\delta^{ik}\delta^{jl}-\delta^{ij}\delta kl)-\frac{B_0m}{20f^2}\pi^i\pi^i\pi^j\pi^j, \tag{4.43a}$$

$$A^{(1)}_\pi = \frac{g_A}{2f}\gamma^\mu\gamma^5\partial_\mu\pi^i\tau^i, \tag{4.43b}$$

$$\mathcal{L}^{(2)}_{\pi p} = 2fB_0\pi^ip^i, \tag{4.43c}$$

and the vertex factors are:

$$\begin{aligned}[\mathrm{i}\mathcal{L}^{(2)}_{\pi^4}]^{efcd} = -\frac{\mathrm{i}}{5f^2}\Bigg[&2[(p-k)^2+q_0^2]\delta^{ef}_{cd}\\ &-\Big[3[(p-k)^2+q_0^2]-10(p_0-k_0)q_0\Big]\delta^{ec}_{fd}\\ &-\Big[3[(p-k)^2+q_0^2]+10(p_0-k_0)q_0\Big]\delta^{ed}_{fc}\\ &+2B_0m(\delta^{ab}_{cd}+\delta^{ac}_{bd}+\delta^{ed}_{fc})\Bigg],\end{aligned}\tag{4.44a}$$

$$[-\mathrm{i}A^{(1)}_\pi]^c = -\frac{g_A}{2f}(\not{p}-\not{k})\gamma^5\tau^c, \tag{4.44b}$$

$$[-\mathrm{i}A^{(1)}_\pi]^d = \frac{g_A}{2f}(\not{p}-\not{k})\gamma^5\tau^d, \tag{4.44c}$$

$$[\mathrm{i}\mathcal{L}^{(2)}_{\pi p}]^{ae} = 2\mathrm{i}fB_0\delta^{ae}. \tag{4.44d}$$

For later convenience, we write the four-pion vertex in the following way:

$$[\mathrm{i}\mathcal{L}^{(2)}_{\pi^4}]^{efcd} = -\frac{\mathrm{i}}{5f^2}[v_1\delta^{ef}_{cd}+v_2\delta^{ec}_{fd}+v_3\delta^{ed}_{fc}], \tag{4.45a}$$

$$v_1 = 2(p-k)^2 + 2q_0^2 + 2B_0 m, \tag{4.45b}$$

$$v_2 = -3(p-k)^2 - 3q_0^2 + 10(p_0-k_0)q_0 + 2B_0 m, \tag{4.45c}$$

$$v_3 = -3(p-k)^2 - 3q_0^2 - 10(p_0-k_0)q_0 + 2B_0 m. \tag{4.45d}$$

The trace in spinor space is:

$$\mathrm{Tr}_S\Big\{(\not{p}-\not{k})\gamma^5(\not{k}+m_N)(\not{p}-\not{k})\gamma^5(\not{p}+m_N)\Big\} = 16m_N^2(p_0k_0 - pk\cos\theta - m_N^2), \tag{4.46}$$

where we used $p^2 = m_N^2 = k^2$ since both nucleons are on the mass shell. The trace in isospin space is:

$$[\mathrm{i}\mathcal{L}_{\pi^4}^{(2)}]^{efcd}\,\mathrm{Tr}_F\Big\{\tau^c n(\boldsymbol{k})\tau^d n(\boldsymbol{p})\Big\} = -\frac{\mathrm{i}}{5f^2} \times \begin{cases} v_1(\Theta^p_{\boldsymbol{p}}\Theta^p_{\boldsymbol{k}} + \Theta^n_{\boldsymbol{p}}\Theta^n_{\boldsymbol{k}})\delta^{ef} + (2v_1+v_2+v_3)(\Theta^p_{\boldsymbol{p}}\Theta^n_{\boldsymbol{k}} + \Theta^n_{\boldsymbol{p}}\Theta^p_{\boldsymbol{k}})\delta^{ef} \\ (v_2-v_3)(\Theta^p_{\boldsymbol{p}}\Theta^n_{\boldsymbol{k}} - \Theta^n_{\boldsymbol{p}}\Theta^p_{\boldsymbol{k}})\mathrm{i}\epsilon^{ef3} \\ (v_2+v_3)(\Theta^p_{\boldsymbol{p}}\Theta^p_{\boldsymbol{k}} - \Theta^p_{\boldsymbol{p}}\Theta^n_{\boldsymbol{k}} - \Theta^n_{\boldsymbol{p}}\Theta^p_{\boldsymbol{k}} + \Theta^n_{\boldsymbol{p}}\Theta^n_{\boldsymbol{k}})\delta^{e3}_{f3} \end{cases}. \tag{4.47}$$

With this, the diagram is given by:

$$\Pi^{ab}_{3,2}(0) = -\lim_{q^\mu\to 0}\frac{1}{q^2-m_\pi^2}\frac{16\mathrm{i}g_A^2B_0^2m_N^2}{80f^2}\int\frac{\mathrm{d}^3\boldsymbol{p}}{(2\pi)^3}\frac{\mathrm{d}^3\boldsymbol{k}}{(2\pi)^3}\frac{1}{E_pE_k} \times\left[\frac{1}{(p-k)^2-m_\pi^2}\right]^2\frac{p_0k_0-pk\cos\theta-m_N^2}{q^2-m_\pi^2} \times \begin{cases} v_1(\Theta^p_{\boldsymbol{p}}\Theta^p_{\boldsymbol{k}} + \Theta^n_{\boldsymbol{p}}\Theta^n_{\boldsymbol{k}})\delta^{ab} + (2v_1+v_2+v_3)(\Theta^p_{\boldsymbol{p}}\Theta^n_{\boldsymbol{k}} + \Theta^n_{\boldsymbol{p}}\Theta^p_{\boldsymbol{k}})\delta^{ab} \\ (v_2-v_3)(\Theta^p_{\boldsymbol{p}}\Theta^n_{\boldsymbol{k}} - \Theta^n_{\boldsymbol{p}}\Theta^p_{\boldsymbol{k}})\mathrm{i}\epsilon^{ab3} \\ (v_2+v_3)(\Theta^p_{\boldsymbol{p}}\Theta^p_{\boldsymbol{k}} - \Theta^p_{\boldsymbol{p}}\Theta^n_{\boldsymbol{k}} - \Theta^n_{\boldsymbol{p}}\Theta^p_{\boldsymbol{k}} + \Theta^n_{\boldsymbol{p}}\Theta^n_{\boldsymbol{k}})\delta^{a3}_{b3} \end{cases}. \tag{4.48}$$

We now take the soft limit, where the vertex functions simplify to:

$$v_1 = 2(p-k)^2 + 2B_0 m, \tag{4.49a}$$

$$v_2 = -3(p-k)^2 + 2B_0 m, \tag{4.49b}$$

$$v_3 = -3(p-k)^2 + 2B_0 m, \tag{4.49c}$$

hence $v_2 - v_3 = 0$, and the diagrams yields:

$$\Pi^{ab}_{3,2}(0) = -\frac{\mathrm{i}g_A^2B_0^2m_N^2}{40\pi^4f^2m_\pi^4}\int\mathrm{d}p\,\mathrm{d}k\,\mathrm{d}\cos\theta\,\frac{p^2k^2}{E_pE_k}\frac{E_pE_k-pk\cos\theta-m_N^2}{(2m_N^2-m_\pi^2-2E_pE_k+2pk\cos\theta)^2} \times \begin{cases} v_1(\Theta^p_{\boldsymbol{p}}\Theta^p_{\boldsymbol{k}} + \Theta^n_{\boldsymbol{p}}\Theta^n_{\boldsymbol{k}})\delta^{ab} + (2v_1+v_2+v_3)(\Theta^p_{\boldsymbol{p}}\Theta^n_{\boldsymbol{k}} + \Theta^n_{\boldsymbol{p}}\Theta^p_{\boldsymbol{k}})\delta^{ab} \\ 0 \\ (v_2+v_3)(\Theta^p_{\boldsymbol{p}}\Theta^p_{\boldsymbol{k}} - \Theta^p_{\boldsymbol{p}}\Theta^n_{\boldsymbol{k}} - \Theta^n_{\boldsymbol{p}}\Theta^p_{\boldsymbol{k}} + \Theta^n_{\boldsymbol{p}}\Theta^n_{\boldsymbol{k}})\delta^{a3}_{b3} \end{cases}. \tag{4.50}$$

We now use $B_0 m = m_\pi^2/2$ and divide by the vacuum condensate $\langle \bar{q}q \rangle_0 = -2f^2 B_0$. The result for this diagram is:

$$\frac{m\Pi^{ab}_{3,2}(0)}{\langle \bar{q}q \rangle_0} = \mathrm{i}\frac{g_A^2 m_N^2}{10(2\pi f)^4 m_\pi^2} \int \mathrm{d}p\,\mathrm{d}k\,\mathrm{d}\cos\theta\, \frac{p^2k^2}{E_pE_k} \frac{E_pE_k - pk\cos\theta - m_N^2}{(2m_N^2 - m_\pi^2 - 2E_pE_k + 2pk\cos\theta)^2}$$
$$\times \begin{cases} v_1(\Theta^p_{\boldsymbol{p}}\Theta^p_{\boldsymbol{k}} + \Theta^n_{\boldsymbol{p}}\Theta^n_{\boldsymbol{k}})\delta^{ab} + (2v_1 + v_2 + v_3)(\Theta^p_{\boldsymbol{p}}\Theta^n_{\boldsymbol{k}} + \Theta^n_{\boldsymbol{p}}\Theta^p_{\boldsymbol{k}})\delta^{ab} \\ 0 \\ (v_2 + v_3)(\Theta^p_{\boldsymbol{p}}\Theta^p_{\boldsymbol{k}} - \Theta^p_{\boldsymbol{p}}\Theta^n_{\boldsymbol{k}} - \Theta^n_{\boldsymbol{p}}\Theta^p_{\boldsymbol{k}} + \Theta^n_{\boldsymbol{p}}\Theta^n_{\boldsymbol{k}})\delta^{a3}_{b3} \end{cases}, \tag{4.51}$$

and we abbreviate:

$$v_1 = 2(p-k)^2 + m_\pi^2, \tag{4.52a}$$
$$2v_1 + v_2 + v_3 = -2(p-k)^2 + 4m_\pi^2, \tag{4.52b}$$
$$v_2 + v_3 = -6(p-k)^2 + 2m_\pi^2, \tag{4.52c}$$

where $(p-k)^2 = 2m_N^2 - 2p_0k_0 + 2pk\cos\theta$.

4.2.3. Two-loop diagrams of type 4

First diagram

The next diagram is:

$\Pi^{ab}_{4,1}(0): \quad p^a$ 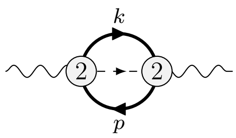

p^b (4.53)

In terms of an integral expression, this can be translated to:

$$\Pi^{ab}_{4,1}(0) = \lim_{q^\mu \to 0} (-1)^L \frac{(-1)^n}{n} (-\mathrm{i})^2 \int \frac{\mathrm{d}^3\boldsymbol{p}}{(2\pi)^3} \frac{\mathrm{d}^3\boldsymbol{k}}{(2\pi)^3} \frac{1}{4E_pE_k} \frac{\mathrm{i}}{(p-k)^2 - m_\pi^2}$$
$$\times \mathrm{Tr}\left\{ [-\mathrm{i}A^{(2)}_{\pi p}]^{ac} (\not{p} + m_N) n(\boldsymbol{p}) [-\mathrm{i}A^{(2)}_{\pi p}]^{cb} (\not{k} + m_N) n(\boldsymbol{k}) \right\}, \tag{4.54}$$

where $L = 1$ and $n = 2$ and the virtual pion π^c has momentum $p^\mu - k^\mu$ going to the right. The relevant term in the Lagrangian is:

$$A^{(2)}_{\pi p} = -\frac{8c_1 B_0}{f} p^i \pi^i, \tag{4.55}$$

and the vertex factors are:

$$[-\mathrm{i}A^{(2)}_{\pi p}]^{ac} = \mathrm{i}\frac{8c_1 B_0}{f}\delta^{ac}, \tag{4.56a}$$

$$[-\mathrm{i}A^{(2)}_{\pi p}]^{cb} = \mathrm{i}\frac{8c_1B_0}{f}\delta^{bc}. \tag{4.56b}$$

The trace yields:

$$\begin{aligned}
&\mathrm{Tr}\left\{[-\mathrm{i}A^{(2)}_{\pi p}]^{ac}(\not{p}+m_N)n(\boldsymbol{p})[-\mathrm{i}A^{(2)}_{\pi p}]^{cb}(\not{k}+m_N)n(\boldsymbol{k})\right\} \\
&\quad = -\frac{256c_1^2B_0^2}{f^2}(E_pE_k - \boldsymbol{p}\cdot\boldsymbol{k} + m_N^2)(\Theta^p_{\boldsymbol{p}}+\Theta^n_{\boldsymbol{p}})(\Theta^p_{\boldsymbol{k}}+\Theta^n_{\boldsymbol{k}})\delta^{ab},
\end{aligned} \tag{4.57}$$

and the diagram is given by:

$$\begin{aligned}
\Pi^{ab}_{4,1}(0) = -\mathrm{i}\delta^{ab}\frac{32c_1^2B_0^2}{f^2}\int\frac{\mathrm{d}^3\boldsymbol{p}}{(2\pi)^3}\frac{\mathrm{d}^3\boldsymbol{k}}{(2\pi)^3}\frac{1}{E_pE_k}\frac{E_pE_k-\boldsymbol{p}\cdot\boldsymbol{k}+m_N^2}{(p-k)^2-m_\pi^2} \\
\times(\Theta^p_{\boldsymbol{p}}+\Theta^n_{\boldsymbol{p}})(\Theta^p_{\boldsymbol{k}}+\Theta^n_{\boldsymbol{k}}).
\end{aligned} \tag{4.58}$$

Second diagram

The next diagram is:

$\Pi^{ab}_{4,2}(0)$: p^a 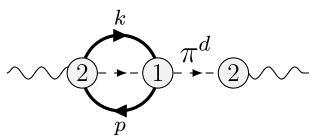 p^b (4.59)

In terms of an integral expression, this can be written as:

$$\begin{aligned}
\Pi^{ab}_{4,2}(0) = 2\lim_{q^\mu\to 0}(-1)^L\frac{(-1)^n}{n}(-\mathrm{i})^2\int\frac{\mathrm{d}^3\boldsymbol{p}}{(2\pi)^3}\frac{\mathrm{d}^3\boldsymbol{k}}{(2\pi)^3}\frac{1}{4E_pE_k}\frac{\mathrm{i}}{(q+p-k)^2-m_\pi^2} \\
\times\mathrm{Tr}\left\{[-\mathrm{i}A^{(2)}_{\pi p}]^{ac}(\not{p}+m_N)n(\boldsymbol{p})[-\mathrm{i}A^{(1)}_{\pi\pi}]^{cd}(\not{k}+m_N)n(\boldsymbol{k})\right\} \\
\times\frac{\mathrm{i}}{q^2-m_\pi^2}[\mathrm{i}\mathcal{L}^{(2)}_{\pi p}]^{db},
\end{aligned} \tag{4.60}$$

where $L=1$ and $n=2$ and the virtual pion π^c has momentum $q^\mu+p^\mu-k^\mu$. We also have to include a factor of 2, since the pion can be attached left or right. The relevant terms in the Lagrangian are:

$$A^{(2)}_{\pi p} = -\frac{8c_1B_0}{f}p^i\pi^i, \tag{4.61a}$$

$$A^{(1)}_{\pi\pi} = \frac{1}{4f^2}\gamma^\mu\pi^i\partial_\mu\pi^j\epsilon^{ijk}\tau^k, \tag{4.61b}$$

$$\mathcal{L}^{(2)}_{\pi p} = 2fB_0\pi^ip^i, \tag{4.61c}$$

and the vertex factors in the soft limit are:

$$[-\mathrm{i}A^{(2)}_{\pi p}]^{ac} = \mathrm{i}\frac{8c_1B_0}{f}\delta^{ac}, \tag{4.62a}$$

$$[-\mathrm{i}A^{(1)}_{\pi\pi}]^{cd} = \frac{1}{4f^2}(2\not{q} + \not{p} - \not{k})\epsilon^{cdk}\tau^k, \tag{4.62b}$$

$$[\mathrm{i}\mathcal{L}^{(2)}_{\pi p}]^{db} = 2\mathrm{i}fB_0\delta^{bd}. \tag{4.62c}$$

The trace in Dirac spinor space yields:

$$\mathrm{Tr}_S\Big\{(\not{p} + m_N)(2\not{q} + \not{p} - \not{k})(\not{k} + m_N)\Big\} = 4m_N q_0(E_p + E_k), \tag{4.63}$$

which vanishes in the soft limit.

Third diagram

The next diagram is:

$\Pi^{ab}_{4,3}(0)$:

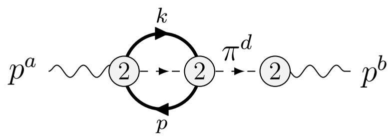

(4.64)

In terms of an integral expression, this equals:

$$\begin{aligned}
\Pi^{ab}_{4,3}(0) = 2\lim_{q^\mu\to 0}(-1)^L\frac{(-1)^n}{n}(-\mathrm{i})^2\int\frac{\mathrm{d}^3\boldsymbol{p}}{(2\pi)^3}\frac{\mathrm{d}^3\boldsymbol{k}}{(2\pi)^3}\frac{1}{4E_pE_k}\frac{\mathrm{i}}{(q+p-k)^2-m_\pi^2}& \\
\times\,\mathrm{Tr}\Big\{[-\mathrm{i}A^{(2)}_{\pi p}]^{ac}(\not{p}+m_N)n(\boldsymbol{p})[-\mathrm{i}A^{(1)}_{\pi\pi}]^{cd}(\not{k}+m_N)n(\boldsymbol{k})\Big\}& \\
\times\,\frac{\mathrm{i}}{q^2-m_\pi^2}[\mathrm{i}\mathcal{L}^{(2)}_{\pi p}]^{db},&
\end{aligned} \tag{4.65}$$

where $L = 1$ and $n = 2$ and the virtual pion π^c has momentum $q^\mu + p^\mu - k^\mu$. We also have to include a factor of 2, since the pion can be attached left or right. The relevant terms in the Lagrangian are:

$$A^{(2)}_{\pi p} = -\frac{8c_1B_0}{f}p^i\pi^i, \tag{4.66a}$$

$$\begin{aligned}
A^{(2)}_{\pi\pi} = {}& \frac{4B_0c_1m}{f^2}\pi^i\pi^i + \frac{c_2}{f^2m_N^2}\partial_\mu\pi^i\partial_\nu\pi^i\partial^\mu\partial^\nu - \frac{c_3}{f^2}\partial_\mu\pi^i\partial^\mu\pi^i \\
&+ \frac{\mathrm{i}c_4}{f^2}\epsilon^{ijk}\tau^k\gamma^\mu\gamma^\nu\partial_\mu\pi^i\partial_\nu\pi^j,
\end{aligned} \tag{4.66b}$$

$$\mathcal{L}^{(2)}_{\pi p} = 2fB_0\pi^ip^i, \tag{4.66c}$$

and the vertex factors in the soft limit are:

$$[-\mathrm{i}A^{(2)}_{\pi p}]^{ac} = \mathrm{i}\frac{8c_1B_0}{f}\delta^{ac}, \tag{4.67a}$$

$$[-\mathrm{i}A^{(2)}_{\pi\pi}]^{cd} = -\mathrm{i}\frac{8c_1B_0m}{f^2}\delta^{cd}, \tag{4.67b}$$

$$[\mathrm{i}\mathcal{L}^{(2)}_{\pi p}]^{db} = 2\mathrm{i}fB_0\delta^{bd}. \tag{4.67c}$$

In the soft limit, the trace yields:

$$\begin{aligned}
&\mathrm{Tr}\left\{[-\mathrm{i}A_{\pi p}^{(2)}]^{ac}(\not{p}+m_N)n(\boldsymbol{p})[-\mathrm{i}A_{\pi\pi}^{(1)}]^{cd}(\not{k}+m_N)n(\boldsymbol{k})\right\} \\
&\quad = \frac{256c_1^2B_0^2m}{f^3}(E_pE_k-\boldsymbol{p}\cdot\boldsymbol{k}+m_N^2)(\Theta_{\boldsymbol{p}}^p+\Theta_{\boldsymbol{p}}^n)(\Theta_{\boldsymbol{k}}^p+\Theta_{\boldsymbol{k}}^n)\delta^{ad}.
\end{aligned} \tag{4.68}$$

With this, the diagram is given by:

$$\begin{aligned}
\Pi_{4,3}^{ab}(0) = \mathrm{i}\delta^{ab}\frac{128c_1^2B_0^3m}{f^2m_\pi^2}\int\frac{\mathrm{d}^3\boldsymbol{p}}{(2\pi)^3}\frac{\mathrm{d}^3\boldsymbol{k}}{(2\pi)^3}\frac{1}{E_pE_k}\frac{E_pE_k-\boldsymbol{p}\cdot\boldsymbol{k}+m_N^2}{(p-k)^2-m_\pi^2} \\
\times(\Theta_{\boldsymbol{p}}^p+\Theta_{\boldsymbol{p}}^n)(\Theta_{\boldsymbol{k}}^p+\Theta_{\boldsymbol{k}}^n).
\end{aligned} \tag{4.69}$$

After using $B_0m = m_\pi^2/2$, we get:

$$\begin{aligned}
\Pi_{4,3}^{ab}(0) = \mathrm{i}\delta^{ab}\frac{64c_1^2B_0^2}{f^2}\int\frac{\mathrm{d}^3\boldsymbol{p}}{(2\pi)^3}\frac{\mathrm{d}^3\boldsymbol{k}}{(2\pi)^3}\frac{1}{E_pE_k}\frac{E_pE_k-\boldsymbol{p}\cdot\boldsymbol{k}+m_N^2}{(p-k)^2-m_\pi^2} \\
\times(\Theta_{\boldsymbol{p}}^p+\Theta_{\boldsymbol{p}}^n)(\Theta_{\boldsymbol{k}}^p+\Theta_{\boldsymbol{k}}^n),
\end{aligned} \tag{4.70}$$

i.e. $\Pi_{4,1}^{ab}(0)$ and $\Pi_{4,3}^{ab}(0)$ are related by:

$$-2\Pi_{4,1}^{ab}(0) = \Pi_{4,3}^{ab}(0). \tag{4.71}$$

Fourth diagram

The next diagram is:

$\Pi_{4,4}^{ab}(0)$: p^a 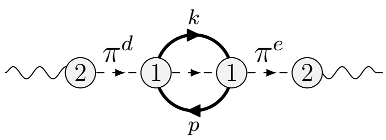 p^b (4.72)

In terms of an integral expression, this can be translated to:

$$\begin{aligned}
\Pi_{4,4}^{ab}(0) = \lim_{q^\mu\to 0}(-1)^L\frac{(-1)^n}{n}(-\mathrm{i})^2[\mathrm{i}\mathcal{L}_{\pi p}^{(2)}]^{ad}\frac{\mathrm{i}}{q^2-m_\pi^2}\int\frac{\mathrm{d}^3\boldsymbol{p}}{(2\pi)^3}\frac{\mathrm{d}^3\boldsymbol{k}}{(2\pi)^3}\frac{1}{4E_pE_k}\frac{\mathrm{i}}{(q+p-k)^2-m_\pi^2} \\
\times\mathrm{Tr}\left\{[-\mathrm{i}A_{\pi\pi}^{(1)}]^{dc}(\not{p}+m_N)n(\boldsymbol{p})[-\mathrm{i}A_{\pi\pi}^{(1)}]^{ce}(\not{k}+m_N)n(\boldsymbol{k})\right\} \\
\times\frac{\mathrm{i}}{q^2-m_\pi^2}[\mathrm{i}\mathcal{L}_{\pi p}^{(2)}]^{eb},
\end{aligned} \tag{4.73}$$

where $L=1$ and $n=2$ and the virtual pion π^c has momentum $q^\mu+p^\mu-k^\mu$. The relevant terms in the Lagrangian are:

$$A_{\pi\pi}^{(1)} = \frac{1}{4f^2}\gamma^\mu\pi^i\partial_\mu\pi^j\epsilon^{ijk}\tau^k, \tag{4.74a}$$

$$\mathcal{L}_{\pi p}^{(2)} = 2fB_0\pi^ip^i. \tag{4.74b}$$

In the soft limit, the relevant vertices are:

$$[-\mathrm{i}A^{(1)}_{\pi\pi}]^{dc} = \frac{1}{4f^2}(\not{p} - \not{k})\epsilon^{dck}\tau^k, \tag{4.75a}$$

$$[-\mathrm{i}A^{(1)}_{\pi\pi}]^{ce} = \frac{1}{4f^2}(\not{p} - \not{k})\epsilon^{cel}\tau^l, \tag{4.75b}$$

$$[\mathrm{i}\mathcal{L}^{(2)}_{\pi p}]^{ab} = 2\mathrm{i}fB_0\delta^{ab}. \tag{4.75c}$$

The trace yields zero in the soft limit, i.e. this diagram vanishes:

$$\Pi^{ab}_{4,4}(0) = 0. \tag{4.76}$$

Fifth diagram

The next diagram is:

$\Pi^{ab}_{4,5}(0)$:

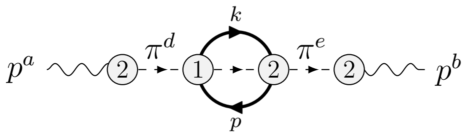

(4.77)

In terms of an integral expression, this can be written as:

$$\Pi^{ab}_{4,5}(0) = \lim_{q^\mu \to 0}(-1)^L \frac{(-1)^n}{n}(-\mathrm{i})^2[\mathrm{i}\mathcal{L}^{(2)}_{\pi p}]^{ad}\frac{\mathrm{i}}{q^2 - m_\pi^2}\int \frac{\mathrm{d}^3\boldsymbol{p}}{(2\pi)^3}\frac{\mathrm{d}^3\boldsymbol{k}}{(2\pi)^3}\frac{1}{4E_pE_k}\frac{\mathrm{i}}{(q+p-k)^2 - m_\pi^2}$$
$$\times \operatorname{Tr}\left\{[-\mathrm{i}A^{(1)}_{\pi\pi}]^{dc}(\not{p} + m_N)n(\boldsymbol{p})[-\mathrm{i}A^{(2)}_{\pi\pi}]^{ce}(\not{k} + m_N)n(\boldsymbol{k})\right\}$$
$$\times \frac{\mathrm{i}}{q^2 - m_\pi^2}[\mathrm{i}\mathcal{L}^{(2)}_{\pi p}]^{eb}, \tag{4.78}$$

where $L = 1$ and $n = 2$ and the virtual pion π^c has momentum $q^\mu + p^\mu - k^\mu$. The relevant terms in the Lagrangian are:

$$A^{(1)}_{\pi\pi} = \frac{1}{4f^2}\gamma^\mu\pi^i\partial_\mu\pi^j\epsilon^{ijk}\tau^k, \tag{4.79a}$$

$$A^{(2)}_{\pi\pi} = \frac{4B_0c_1m}{f^2}\pi^i\pi^i + \frac{c_2}{f^2m_N^2}\partial_\mu\pi^i\partial_\nu\pi^i\partial^\mu\partial^\nu - \frac{c_3}{f^2}\partial_\mu\pi^i\partial^\mu\pi^i$$
$$+ \frac{\mathrm{i}c_4}{f^2}\epsilon^{ijk}\tau^k\gamma^\mu\gamma^\nu\partial_\mu\pi^i\partial_\nu\pi^j, \tag{4.79b}$$

$$\mathcal{L}^{(2)}_{\pi p} = 2fB_0\pi^ip^i. \tag{4.79c}$$

In the soft limit, the relevant vertices are:

$$[-\mathrm{i}A^{(1)}_{\pi\pi}]^{dc} = \frac{1}{4f^2}(\not{p} - \not{k})\epsilon^{dck}\tau^k, \tag{4.80a}$$

$$[-\mathrm{i}A^{(2)}_{\pi\pi}]^{ce} = -\mathrm{i}\frac{8c_1B_0m}{f^2}\delta^{ce}, \tag{4.80b}$$

$$[\mathrm{i}\mathcal{L}^{(2)}_{\pi p}]^{ab} = 2\mathrm{i}fB_0\delta^{ab}. \tag{4.80c}$$

The trace yields zero in the soft limit, i.e. this diagram vanishes:

$$\Pi^{ab}_{4,5}(0) = 0. \tag{4.81}$$

Sixth diagram

The next diagram is:

$$\Pi^{ab}_{4,6}(0): \tag{4.82}$$

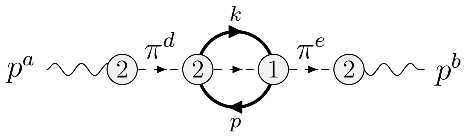

In terms of an integral expression, this diagram is given by:

$$\begin{aligned}\Pi^{ab}_{4,6}(0) = \lim_{q^\mu \to 0} (-1)^L \frac{(-1)^n}{n} (-\mathrm{i})^2 [\mathrm{i}\mathcal{L}^{(2)}_{\pi p}]^{ad} \frac{\mathrm{i}}{q^2 - m_\pi^2} \int \frac{\mathrm{d}^3\boldsymbol{p}}{(2\pi)^3} \frac{\mathrm{d}^3\boldsymbol{k}}{(2\pi)^3} \frac{1}{4E_p E_k} \frac{\mathrm{i}}{(q+p-k)^2 - m_\pi^2} \\ \times \operatorname{Tr}\left\{[-\mathrm{i}A^{(2)}_{\pi\pi}]^{dc}(\not{p} + m_N) n(\boldsymbol{p}) [-\mathrm{i}A^{(1)}_{\pi\pi}]^{ce} (\not{k} + m_N) n(\boldsymbol{k})\right\} \\ \times \frac{\mathrm{i}}{q^2 - m_\pi^2} [\mathrm{i}\mathcal{L}^{(2)}_{\pi p}]^{eb},\end{aligned} \tag{4.83}$$

where $L = 1$ and $n = 2$ and the virtual pion π^c has momentum $q^\mu + p^\mu - k^\mu$. The relevant terms in the Lagrangian are:

$$A^{(1)}_{\pi\pi} = \frac{1}{4f^2} \gamma^\mu \pi^i \partial_\mu \pi^j \epsilon^{ijk} \tau^k, \tag{4.84a}$$

$$\begin{aligned}A^{(2)}_{\pi\pi} = \frac{4B_0 c_1 m}{f^2} \pi^i \pi^i + \frac{c_2}{f^2 m_N^2} \partial_\mu \pi^i \partial_\nu \pi^i \partial^\mu \partial^\nu - \frac{c_3}{f^2} \partial_\mu \pi^i \partial^\mu \pi^i \\ + \frac{\mathrm{i}c_4}{f^2} \epsilon^{ijk} \tau^k \gamma^\mu \gamma^\nu \partial_\mu \pi^i \partial_\nu \pi^j,\end{aligned} \tag{4.84b}$$

$$\mathcal{L}^{(2)}_{\pi p} = 2f B_0 \pi^i p^i. \tag{4.84c}$$

In the soft limit, the relevant vertices are:

$$[-\mathrm{i}A^{(2)}_{\pi\pi}]^{dc} = -\mathrm{i}\frac{8c_1 B_0 m}{f^2} \delta^{dc}, \tag{4.85a}$$

$$[-\mathrm{i}A^{(1)}_{\pi\pi}]^{ce} = \frac{1}{4f^2} (\not{p} - \not{k}) \epsilon^{cel} \tau^l, \tag{4.85b}$$

$$[\mathrm{i}\mathcal{L}^{(2)}_{\pi p}]^{ab} = 2\mathrm{i} f B_0 \delta^{ab}. \tag{4.85c}$$

The trace yields zero in the soft limit, i.e. this diagram vanishes:

$$\Pi^{ab}_{4,6}(0) = 0. \tag{4.86}$$

Seventh diagram

The next diagram is:

$$\Pi^{ab}_{4,7}(0): \tag{4.87}$$

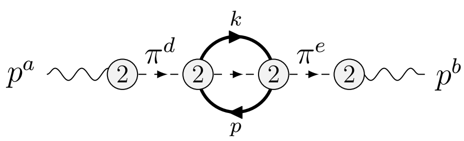

In terms of an integral expression, this can be translated to:

$$\Pi_{4,7}^{ab}(0) = \lim_{q^\mu\to 0}(-1)^L\frac{(-1)^n}{n}(-\mathrm{i})^2[\mathrm{i}\mathcal{L}_{\pi p}^{(2)}]^{ad}\frac{\mathrm{i}}{q^2-m_\pi^2}\int\frac{\mathrm{d}^3\boldsymbol{p}}{(2\pi)^3}\frac{\mathrm{d}^3\boldsymbol{k}}{(2\pi)^3}\frac{1}{4E_pE_k}\frac{\mathrm{i}}{(q+p-k)^2-m_\pi^2}$$
$$\times \operatorname{Tr}\left\{[-\mathrm{i}A_{\pi\pi}^{(2)}]^{dc}(\not p+m_N)n(\boldsymbol{p})[-\mathrm{i}A_{\pi\pi}^{(2)}]^{ce}(\not k+m_N)n(\boldsymbol{k})\right\}$$
$$\times\frac{\mathrm{i}}{q^2-m_\pi^2}[\mathrm{i}\mathcal{L}_{\pi p}^{(2)}]^{eb}, \tag{4.88}$$

where $L=1$ and $n=2$ and the virtual pion π^c has momentum $q^\mu+p^\mu-k^\mu$. The relevant terms in the Lagrangian are:

$$A_{\pi\pi}^{(2)} = \frac{4B_0c_1m}{f^2}\pi^i\pi^i + \frac{c_2}{f^2m_N^2}\partial_\mu\pi^i\partial_\nu\pi^i\partial^\mu\partial^\nu - \frac{c_3}{f^2}\partial_\mu\pi^i\partial^\mu\pi^i$$
$$+\frac{\mathrm{i}c_4}{f^2}\epsilon^{ijk}\tau^k\gamma^\mu\gamma^\nu\partial_\mu\pi^i\partial_\nu\pi^j, \tag{4.89a}$$

$$\mathcal{L}_{\pi p}^{(2)} = 2fB_0\pi^ip^i. \tag{4.89b}$$

In the soft limit, the relevant vertices are:

$$[-\mathrm{i}A_{\pi\pi}^{(2)}]^{dc} = -\mathrm{i}\frac{8c_1B_0m}{f^2}\delta^{dc}, \tag{4.90a}$$

$$[-\mathrm{i}A_{\pi\pi}^{(1)}]^{ce} = -\mathrm{i}\frac{8c_1B_0m}{f^2}\delta^{ce}, \tag{4.90b}$$

$$[\mathrm{i}\mathcal{L}_{\pi p}^{(2)}]^{ab} = 2\mathrm{i}fB_0\delta^{ab}. \tag{4.90c}$$

The trace yields:

$$\operatorname{Tr}\left\{[-\mathrm{i}A_{\pi\pi}^{(2)}]^{dc}(\not p+m_N)n(\boldsymbol{p})[-\mathrm{i}A_{\pi\pi}^{(2)}]^{ce}(\not k+m_N)n(\boldsymbol{k})\right\}$$
$$= -\frac{256c_1^2B_0^2m^2}{f^4}(E_pE_k-\boldsymbol{p}\cdot\boldsymbol{k}+m_N^2)(\Theta_{\boldsymbol{p}}^p+\Theta_{\boldsymbol{p}}^n)(\Theta_{\boldsymbol{k}}^p+\Theta_{\boldsymbol{k}}^n)\delta^{de}. \tag{4.91}$$

With this, the last type-4 diagram is given by:

$$\Pi_{4,7}^{ab}(0) = -\mathrm{i}\delta^{ab}\frac{128c_1^2B_0^4m^2}{f^2m_\pi^4}\int\frac{\mathrm{d}^3\boldsymbol{p}}{(2\pi)^3}\frac{\mathrm{d}^3\boldsymbol{k}}{(2\pi)^3}\frac{1}{E_pE_k}\frac{E_pE_k-\boldsymbol{p}\cdot\boldsymbol{k}+m_N^2}{(p-k)^2-m_\pi^2}$$
$$\times(\Theta_{\boldsymbol{p}}^p+\Theta_{\boldsymbol{p}}^n)(\Theta_{\boldsymbol{k}}^p+\Theta_{\boldsymbol{k}}^n). \tag{4.92}$$

Finally we use $B_0m = m_\pi^2/2$ again and get:

$$\Pi_{4,7}^{ab}(0) = -\mathrm{i}\delta^{ab}\frac{32c_1^2B_0^2}{f^2}\int\frac{\mathrm{d}^3\boldsymbol{p}}{(2\pi)^3}\frac{\mathrm{d}^3\boldsymbol{k}}{(2\pi)^3}\frac{1}{E_pE_k}\frac{E_pE_k-\boldsymbol{p}\cdot\boldsymbol{k}+m_N^2}{(p-k)^2-m_\pi^2}$$
$$\times(\Theta_{\boldsymbol{p}}^p+\Theta_{\boldsymbol{p}}^n)(\Theta_{\boldsymbol{k}}^p+\Theta_{\boldsymbol{k}}^n). \tag{4.93}$$

Thus, in the soft limit, we have:

$$\Pi_{4,1}^{ab}(0) = \Pi_{4,7}^{ab}(0). \tag{4.94}$$

Cancellation in the soft limit

In summary, these are the results for the type-4 diagrams in the soft limit:

$$\Pi_{4,1} = -\frac{1}{2}\Pi_{4,3}, \tag{4.95a}$$

$$\Pi_{4,2} = \Pi_{4,4} = \Pi_{4,5} = \Pi_{4,6} = 0, \tag{4.95b}$$

$$\Pi_{4,7} = \Pi_{4,1}, \tag{4.95c}$$

which means that $\sum\limits_{i=1}^{7} \Pi_{4,i} = \Pi_{4,1} + \Pi_{4,3} + \Pi_{4,7} = 0$ and thus all type-4 diagrams vanish.

4.2.4. Two-loop diagrams of type 5

The only diagram in this group is:

$\Pi_5^{ab}(0)$: 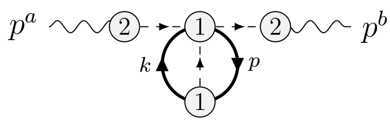

(4.96)

In terms of an integral expression, this can be translated to:

$$\begin{aligned}\Pi_5^{ab}(0) = \lim_{q^\mu \to 0} &(-\mathrm{i})^2(-1)^L \frac{(-1)^n}{n} [\mathrm{i}\mathcal{L}_{\pi p}^{(2)}]^{ad} \frac{\mathrm{i}}{q^2 - m_\pi^2} \int \frac{\mathrm{d}^3\boldsymbol{p}}{(2\pi)^3} \frac{\mathrm{d}^3\boldsymbol{k}}{(2\pi)^3} \frac{1}{4E_pE_k} \\ &\times \mathrm{Tr}\left\{[-\mathrm{i}A_{\pi^3}^{(1)}]^{dec}(\not{k} + m_N)n(\boldsymbol{k})[-\mathrm{i}A_\pi^{(1)}]^c(\not{p} + m_N)n(\boldsymbol{p})\right\} \frac{\mathrm{i}}{(p-k)^2 + m_\pi^2} \\ &\times \frac{\mathrm{i}}{q^2 - m_\pi^2}[\mathrm{i}\mathcal{L}_{\pi p}^{(2)}]^{eb},\end{aligned} \tag{4.97}$$

where $L = 1$, $n = 2$ and we have to replace $p^0 = \sqrt{\boldsymbol{p}^2 + m_N^2}$ and $k^0 = \sqrt{\boldsymbol{k}^2 + m_N^2}$. The pion momentum is $p^\mu - k^\mu$, going in the upwards direction. The relevant terms in the Lagrangian are:

$$A_\pi^{(1)} = \frac{g_A}{2f}\gamma^\mu\gamma^5\partial_\mu\pi^i\tau^i, \tag{4.98a}$$

$$A_{\pi^3}^{(1)} = \frac{g_A}{20f^3}\gamma^\mu\gamma^5\left[3\pi^i\pi^j\partial_\mu\pi^j - \pi^j\pi^j\partial_\mu\pi^i\right]\tau^i, \tag{4.98b}$$

$$\mathcal{L}_{\pi p}^{(2)} = 2fB_0\pi^i p^i, \tag{4.98c}$$

and the vertices are:

$$[-\mathrm{i}A_{\pi^3}^{(1)}]^{dec} = \frac{g_A}{20f^3}\left[\delta_{ec}^{id}(5\not{q} - 3\not{p} + 3\not{k}) + \delta_{dc}^{ie}(-5\not{q} - 3\not{p} + 3\not{k}) + \delta_{de}^{ic}2(\not{p} - \not{k})\right]\gamma^5\tau^i, \tag{4.99a}$$

$$[-\mathrm{i}A_\pi^{(1)}]^c = \frac{g_A}{2f}(\not{p} - \not{k})\gamma^5\tau^c, \tag{4.99b}$$

$$[\mathrm{i}\mathcal{L}_{\pi p}^{(2)}]^{ab} = 2\mathrm{i}fB_0\delta^{ab}. \tag{4.99c}$$

The results for the traces are (we simplify using $p^2 = m_N^2 = k^2$):

$$\begin{aligned}
&\mathrm{Tr}_S\Big\{(5\not{q} - 3\not{p} + 3\not{k})\gamma^5(\not{k} + m_N)(\not{p} - \not{k})\gamma^5(\not{p} + m_N)\Big\} \\
&\qquad = 8m_N^2(6m_N^2 - 5q_0(E_p - E_k) - 6E_pE_k + 6\boldsymbol{p}\cdot\boldsymbol{k}), && (4.100a) \\
&\mathrm{Tr}_S\Big\{(-5\not{q} - 3\not{p} + 3\not{k})\gamma^5(\not{k} + m_N)(\not{p} - \not{k})\gamma^5(\not{p} + m_N)\Big\} \\
&\qquad = 8m_N^2(6m_N^2 + 5q_0(E_p - E_k) - 6E_pE_k + 6\boldsymbol{p}\cdot\boldsymbol{k}), && (4.100b) \\
&\mathrm{Tr}_S\Big\{2(\not{p} - \not{k})\gamma^5(\not{k} + m_N)(\not{p} - \not{k})\gamma^5(\not{p} + m_N)\Big\} = 32m_N^2(E_pE_k - \boldsymbol{p}\cdot\boldsymbol{k} - m_N^2). && (4.100c)
\end{aligned}$$

After taking the soft limit, we get:

$$\begin{aligned}
\Pi_5^{ab}(0) = {}& \frac{\mathrm{i}4m_N^2B_0^2g_A^2}{10(2\pi)^4f^2m_\pi^4}\int \mathrm{d}p\,\mathrm{d}k\,\mathrm{d}(\cos\theta)\,\frac{p^2k^2}{E_pE_k}\frac{E_pE_k - pk\cos\theta - m_N^2}{2m_N^2 - 2E_pE_k + 2pk\cos\theta + m_\pi^2} \\
&\times(\Theta_{\boldsymbol{p}}^p\Theta_{\boldsymbol{k}}^p - \Theta_{\boldsymbol{p}}^p\Theta_{\boldsymbol{k}}^n - \Theta_{\boldsymbol{p}}^n\Theta_{\boldsymbol{k}}^p + \Theta_{\boldsymbol{p}}^n\Theta_{\boldsymbol{k}}^n)\begin{cases}2\delta^{ab} \\ 0 \\ -6\delta_{b3}^{a3}\end{cases}.
\end{aligned} \tag{4.101}$$

Finally, we include the quark mass and divide by the vacuum condensate:

$$\begin{aligned}
\frac{m\Pi_5^{ab}(0)}{\langle\bar{q}q\rangle_0} = {}& \mathrm{i}\frac{g_A^2m_N^2}{10(2\pi f)^4m_\pi^2}\int \mathrm{d}p\,\mathrm{d}k\,\mathrm{d}\cos\theta\frac{p^2k^2}{p_0k_0}\frac{p_0k_0 - pk\cos\theta - m_N^2}{2m_N^2 - m_\pi^2 - 2p_0k_0 + 2pk\cos\theta} \\
&\times(\Theta_{\boldsymbol{p}}^p\Theta_{\boldsymbol{k}}^p - \Theta_{\boldsymbol{p}}^p\Theta_{\boldsymbol{k}}^n - \Theta_{\boldsymbol{p}}^n\Theta_{\boldsymbol{k}}^p + \Theta_{\boldsymbol{p}}^n\Theta_{\boldsymbol{k}}^n)\begin{cases}-2\delta^{ab} \\ 0 \\ 6\delta_{b3}^{a3}\end{cases},
\end{aligned} \tag{4.102}$$

where we also used the relation $B_0m = m_\pi^2/2$.

4.2.5. Cancellation of symmetry breaking terms

By calculating the two-point pseudoscalar correlation functions, we got terms proportional to δ^{ab}, but also terms proportional to $\delta^{a3}\delta^{b3}$. According to SU(2) chiral symmetry, the δ_{b3}^{a3} terms break this symmetry. However, if we add all diagrams, then these terms precisely cancel each other:

$$\delta_{b3}^{a3}: \qquad \Pi_{3,1} + \Pi_{3,2} + \Pi_5 = 0, \tag{4.103}$$

where we already included a factor of 2 inside of $\Pi_{3,1}$ in order to account for the two vertices that the nucleon loop can attach to.

The results of the corresponding diagrams (only the terms proportional to $\delta^{a3}\delta^{b3}$) are as follows:

$$\begin{aligned}\frac{m\Pi^{ab}_{3,1}(0)}{\langle\bar{q}q\rangle_0} &= \mathrm{i}\frac{g_A^2 m_N^2}{10(2\pi f)^4 m_\pi^2}\int \mathrm{d}p\,\mathrm{d}k\,\mathrm{d}\cos\theta \frac{p^2k^2}{p_0k_0}\frac{4m_\pi^2(p_0k_0 - pk\cos\theta - m_N^2)}{(2m_N^2 - m_\pi^2 - 2p_0k_0 + 2pk\cos\theta)^2} \\ &\quad\times (\Theta^p_{\boldsymbol{p}} - \Theta^n_{\boldsymbol{p}})(\Theta^p_{\boldsymbol{k}} - \Theta^n_{\boldsymbol{k}})\delta^{a3}_{b3}, \qquad (4.104a)\\ \frac{m\Pi^{ab}_{3,2}(0)}{\langle\bar{q}q\rangle_0} &= \mathrm{i}\frac{g_A^2 m_N^2}{10(2\pi f)^4 m_\pi^2}\int \mathrm{d}p\,\mathrm{d}k\,\mathrm{d}\cos\theta \frac{p^2k^2}{p_0k_0}\frac{p_0k_0 - pk\cos\theta - m_N^2}{(2m_N^2 - m_\pi^2 - 2p_0k_0 + 2pk\cos\theta)^2} \\ &\quad\times (v_2+v_3)(\Theta^p_{\boldsymbol{p}} - \Theta^n_{\boldsymbol{p}})(\Theta^p_{\boldsymbol{k}} - \Theta^n_{\boldsymbol{k}})\delta^{a3}_{b3}. \qquad (4.104b)\end{aligned}$$

Here we used the relation for the LEC B_0 in order to replace $B_0 m \to m_\pi^2/2$. The vertex functions simplify a bit for $q^\mu = 0$:

$$v_2 + v_3 = -6(p-k)^2 + 2m_\pi^2, \tag{4.105}$$

where $(p-k)^2 = 2m_N^2 - 2p^\mu k_\mu$. The last contribution proportional to $\delta^{a3}\delta^{b3}$ is:

$$\begin{aligned}\frac{m\Pi^{ab}_{5}(0)}{\langle\bar{q}q\rangle_0} &= \mathrm{i}\frac{g_A^2 m_N^2}{10(2\pi f)^4 m_\pi^2}\int \mathrm{d}p\,\mathrm{d}k\,\mathrm{d}\cos\theta \frac{p^2k^2}{p_0k_0}\frac{p^\mu k_\mu - m_N^2}{2m_N^2 - m_\pi^2 - 2p_0k_0 + 2pk\cos\theta} \\ &\quad\times 6(\Theta^p_{\boldsymbol{p}} - \Theta^n_{\boldsymbol{p}})(\Theta^p_{\boldsymbol{k}} - \Theta^n_{\boldsymbol{k}})\delta^{a3}_{b3}, \qquad (4.106)\end{aligned}$$

where $p^\mu k_\mu = p_0k_0 - pk\cos\theta$. Since the coefficients are the same in these terms, we can start by adding the integrands:

$$\begin{aligned}\text{Integrands} &= \frac{4m_\pi^2(p_0k_0 - pk\cos\theta - m_N^2)}{2m_N^2 - m_\pi^2 - 2p_0k_0 + 2pk\cos\theta} + \frac{(2m_\pi^2 - 6(p-k)^2)(p_0k_0 - pk\cos\theta - m_N^2)}{2m_N^2 - m_\pi^2 - 2p_0k_0 + 2pk\cos\theta} \\ &\quad + 6(p_0k_0 - pk\cos\theta - m_N^2). \qquad (4.107)\end{aligned}$$

We can combine the two fractions and use $(p-k)^2 = 2m_N^2 - 2p^\mu k_\mu$:

$$\begin{aligned}\text{Integrands} &= \frac{(6m_\pi^2 - 12m_N^2 + 12p_0k_0 - 12pk\cos\theta)(p_0k_0 - pk\cos\theta - m_N^2)}{2m_N^2 - m_\pi^2 - 2p_0k_0 + 2pk\cos\theta} \\ &\quad + 6(p_0k_0 - pk\cos\theta - m_N^2). \qquad (4.108)\end{aligned}$$

Finally, we cancel the left bracket in the numerator and all of the denominator to yield -6, which leads to:

$$-6(p_0k_0 - pk\cos\theta - m_N^2) + 6(p_0k_0 - pk\cos\theta - m_N^2) = 0, \tag{4.109}$$

i.e. the symmetry breaking terms precisely cancel each other.

4.3. Results: quark condensate

For the in-medium quark condensate, the integrals in Section 4.2 are solved numerically using Python [89–91] and the result yields the density dependence of the quark condensate, which is presented in Fig. 4.1. We perform these calculations for three sets of low-energy constants, which we discuss in detail in Section 3.2.2. In summary, set 1 is taken from a textbook reference, set 2 was obtained in Ref. [68] by comparing to experimental data, and set 3 was obtained in Ref. [77] by fitting to scattering data.

Our computed value of the quark condensate at normal nuclear density, which shows a reduction of 34–35% (LEC sets 2, 3) shows good agreement with Ref. [35], where the in-medium behavior of the quark condensate was shown to be: $\langle\bar{q}q\rangle^*/\langle\bar{q}q\rangle_0 \approx (b_1/b_1^*)^{1/2}[1-\frac{1}{2}\beta\rho] \approx 1 - 0.37\,\rho/\rho_0$. Here, the parameters take on the following values $b_1/b_1^*|_{\rho=\rho_0} \approx 0.79 \pm 0.05$ and $\beta \approx (2.17 \pm 0.04)$ fm^3, which were obtained from experimental data from deeply bound pionic atoms and isospin-singlet πN-scattering amplitudes, respectively. Our results are also in good agreement with results obtained in Ref. [92] which are summarized by Ref. [93]. They are also consistent with Refs. [50, 94]. Ref. [95] uses methods of the functional renormalization group including fluctuations beyond the mean-field approximation and arrives at the result that the quark condensate is reduced by only around 20% at normal nuclear density.

The density dependence of the in-medium quark condensate shows a linear behavior, since the next-to-leading order contributions in the density expansion, which lead to $\mathcal{O}(\rho^{4/3})$ and $\mathcal{O}(\rho^{5/3})$ behavior, are much smaller. The contributions of the individual diagrams are shown in Fig. 4.2. The right two figures show that the next-to-leading order diagrams have rather tiny contributions to the quark condensate. This is because the Fermi momentum is small compared to the nucleon mass in low densities and the Fermi motion expansion could be convergent. In this sense, the nucleon-nucleon correlation, which plays a role from $\mathcal{O}(\rho^2)$, should be important and bring a new scale parameter.

This work is built on the foundation of Ref. [68], where the in-medium quark condensate was calculated for isospin-symmetric nuclear matter. In this work, we found several new diagrams which are necessary contributions to the in-medium quark condensate. In particular, the third type of diagram in Table 4.2 with $i = 1$, the second type of diagram in Table 4.4 with $i = 1$ as well as the third type of diagram in Table 4.4 with $i \neq j$. Furthermore, diagrams like the one in Table 4.5 were not considered at all in Ref. [68]. Comparing to Ref. [92] and related works, we include interactions from $A^{(2)}$, but omit 2π-exchange and Δ-excitation processes, as they contribute beyond $\mathcal{O}(\rho^{5/3})$. In order to include such processes, Ref. [92] uses a nucleon-nucleon potential obtained from lattice QCD data.

Despite being a small contribution, the isospin-asymmetry of the surrounding nuclear matter plays a role in the in-medium quark condensate. As shown in Fig. 4.3, for normal nuclear density $\rho = \rho_0$, different values for the neutron-to-proton ratio have a small effect on the in-medium quark condensate. In particular, when plotted logarithmically, one can clearly see that the plot is symmetric around the point $\rho_n/\rho_p = 1$, which represents isospin symmetric nuclear matter. This means, the in-medium quark condensate behaves the same for a certain ratio ρ_n/ρ_p and for the inverse ratio $(\rho_n/\rho_p)^{-1}$ because of isospin symmetry. This can also be seen on the far left and far right ends of the plot, which correspond to proton matter and neutron matter, respectively. Furthermore, there is no significant effect if we treat protons and neutrons with different masses $m_p \neq m_n$.

For interactions between nucleons the Δ baryons might be an important ingredient, as suggested by Ref. [92], however in this work we do not consider dynamical Δ interactions. Since some Δ contributions are already implicitly included in the low-energy constants, our calculations are expected to be valid as long as dynamical Δ interactions are not required. Otherwise, one would have to include the Δ fields in the Lagrangian and investigate their in-medium effects.

4.4. A simple SU(3) extension

In this section, we perform a simple extension to SU(3). This is not a “true” in-medium chiral perturbation theory, as we simply use an in-vacuum chiral SU(3) Lagrangian. In order to estimate the effects of nuclear matter, we investigate diagrams with meson-nucleon interactions and then manually restrict the proton and neutron momenta to be below their respective Fermi momenta.

The details on how to extend our formalism to SU(3) can be found in Appendix A.1. In Sections 4.4.1 and 4.4.3 to 4.4.5, we will show the explicit calculations for the quark condensates $\langle \bar{u}u - \bar{d}d \rangle^*$, $\langle \bar{u}u + \bar{d}d \rangle^*$, $\langle \bar{u}u + \bar{s}s \rangle^*$, and $\langle \bar{d}d + \bar{s}s \rangle^*$. Finally, in Section 4.4.6, we present our results.

4.4.1. Up minus down quark condensate with explicit isospin breaking

In this section, we present an estimation of the isospin splitting of the quark condensate in nuclear matter, i.e., the quantity $\langle \bar{u}u - \bar{d}d \rangle^*$ in leading order of the density expansion. This splitting arises due to explicit isospin breaking, which we will consider via $m_u \neq m_d$ in the Lagrangian and $\rho_p \neq \rho_n$ in the nuclear matter. There is also isospin breaking via different hadron masses, like $m_p \neq m_n$, however since these effects yield minor corrections, $(m_n - m_p)/(m_n + m_p) \approx 10^{-4}$, we neglect them, and instead use isospin-averaged masses. We also omit SU(3) breaking in the meson decay constant.

The present calculation is an estimate for two reasons. First, the values of the LECs are not fixed by scattering data, and second, there are no dynamic meson loops included, i.e., this is a linear-density approximation. In order to compute $\langle \bar{u}u - \bar{d}d \rangle^*$, we need to extend our formalism

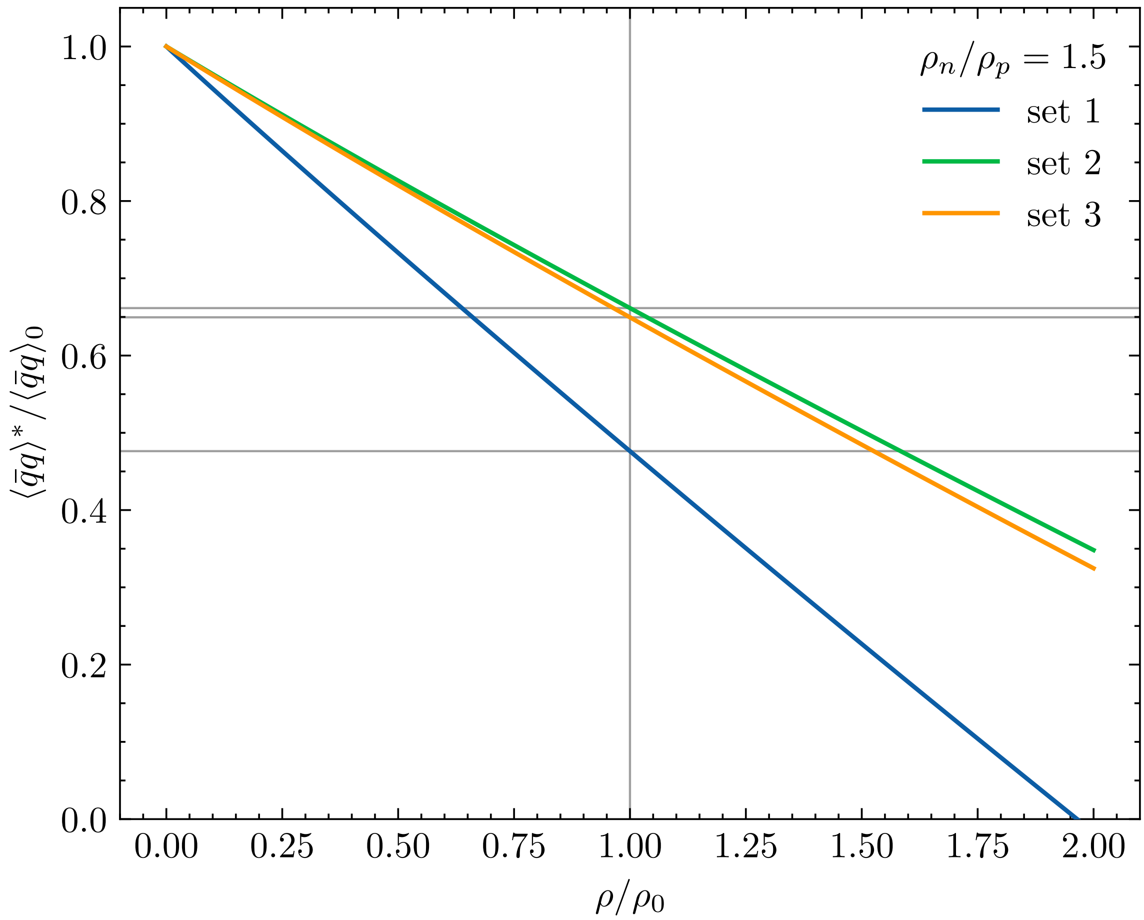

Figure 4.1.: Density dependence of the in-medium quark condensate, normalized to the vacuum condensate. The ratio of neutrons to protons is given by ρ_n/ρ_p. At normal nuclear density, $\rho = \rho_0$, the quark condensate is reduced by about 52% (set 1) and 34–35% (sets 2,3) compared to its vacuum value.

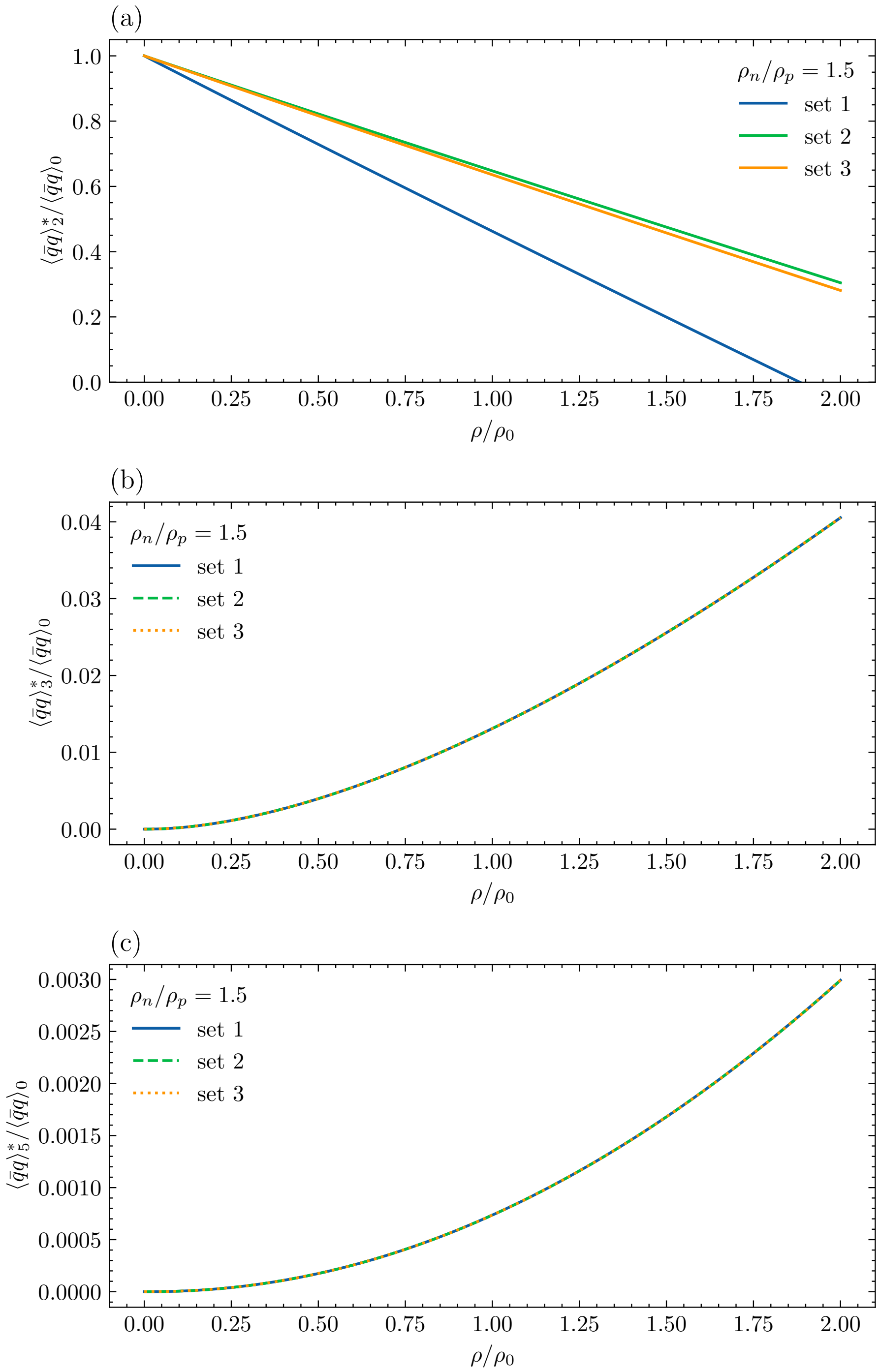

Figure 4.2.: Density dependence of the contributions to the in-medium quark condensate, normalized to the vacuum condensate. The ratio of neutrons to protons is given by ρ_n/ρ_p. Fig. 4.1 shows the sum of these three contributions. (a) The leading order contributions corresponding to Eqs. (4.21) and (4.31). (b) The next-to-leading order contributions corresponding to Eqs. (4.40) and (4.51). (c) The next-to-leading order contributions corresponding to Eq. (4.102).

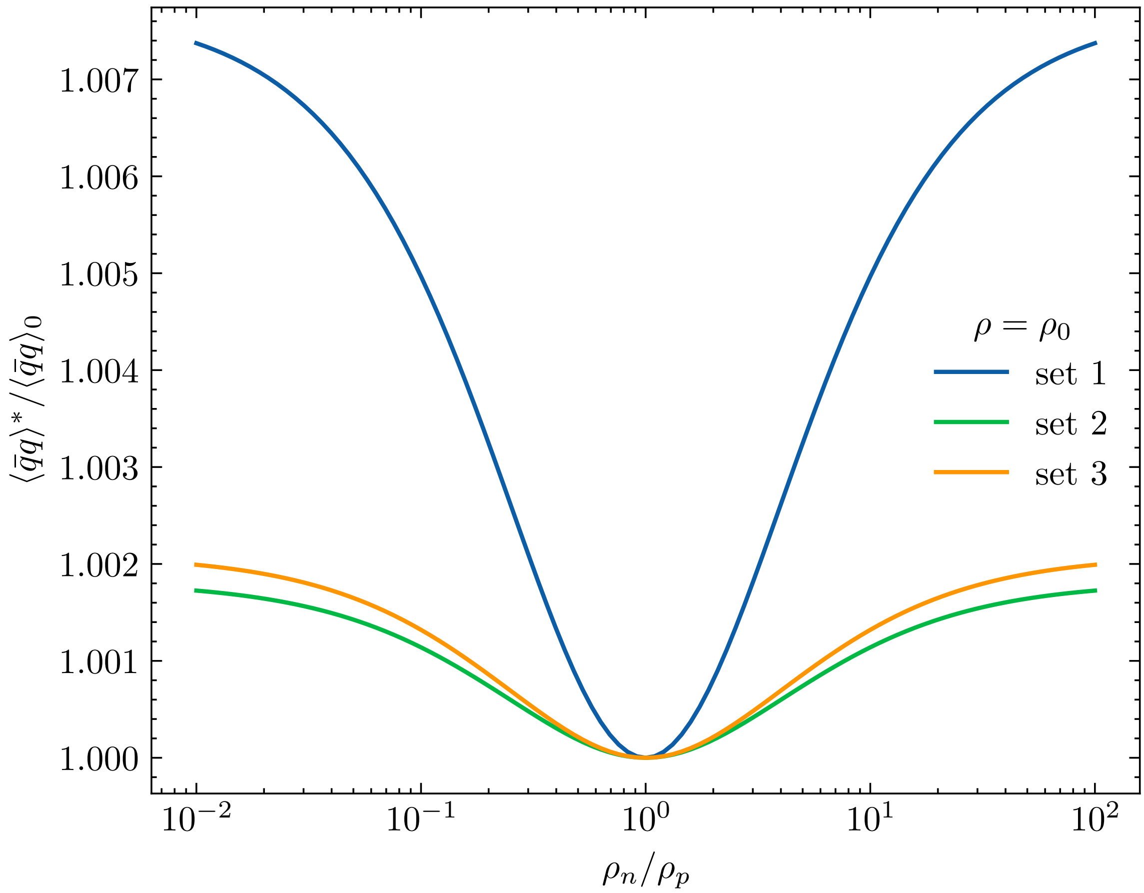

Figure 4.3.: Density dependence of the in-medium quark condensate, normalized to the vacuum condensate. The ratio of neutrons to protons is given by ρ_n/ρ_p. The in-medium quark condensate at a fixed density is symmetric around the point $\rho_n/\rho_p = 1$ under the exchange $\rho_n \leftrightarrow \rho_p$. The far left of these plots correspond to proton matter, whereas the far right corresponds to neutron matter.

to SU(3), since the SU(2) chiral transformation of a pseudoscalar current can only yield the sum $\bar{u}u + \bar{d}d$.

In the pionic part of the SU(3) Lagrangian,

$$\mathcal{L}_\pi^{(2)} = \frac{f^2}{4} \operatorname{Tr} \left\{ D_\mu U^\dagger D^\mu U + \chi^\dagger U + \chi U^\dagger \right\}, \tag{4.110}$$

we introduce the quark mass isospin breaking via the scalar source in $\chi = 2B_0(s + \mathrm{i}p)$, as discussed in Eq. (A.24).

Chiral Ward identity with explicit isospin breaking

We start with

$$\partial^\mu [\mathsf{T} A_\mu^a(x) P^b(0)] = \mathsf{T}[\partial^\mu A_\mu^a(x) P^b(0)] + \delta(x^0)[A_0^a(x), P^b(0)]. \tag{4.111}$$

We can use the partially-conserved axial current (PCAC) relation:

$$\partial^\mu A_\mu^a(x) = \mathrm{i}\bar{q} \left\{ M, \frac{\lambda_a}{2} \right\} \gamma^5 q, \tag{4.112}$$

with the quark mass matrix $M = diag(m + \delta m, m - \delta m, m_s)$. We need:

$$\begin{aligned} \partial^\mu A_\mu^3(x) = \mathrm{i}\bar{q}\{M, \frac{\lambda_3}{2}\}\gamma^5 q = \mathrm{i}\bar{q} \left[\delta m \sqrt{\frac{2}{3}} \lambda^0 + m\lambda^3 + \frac{\delta m}{\sqrt{3}} \lambda^8 \right] \gamma^5 q \\ = \delta m \sqrt{\frac{2}{3}} P^0 + m P^3 + \frac{\delta m}{\sqrt{3}} P^8. \end{aligned} \tag{4.113}$$

If we choose $a = 3$ and $b = 8$ and take the vacuum expectation value, we get:

$$\partial^\mu \Pi_{5\mu}^{38}(x, 0) = \delta m \sqrt{\frac{2}{3}} \Pi^{08}(x, 0) + m\Pi^{38}(x, 0) + \frac{\delta m}{\sqrt{3}} \Pi^{88}(x, 0) + \delta(x^0)\langle\Omega|[A_0^3(x), P^8(0)]|\Omega\rangle. \tag{4.114}$$

We perform a Fourier transformation and take the soft limit:

$$0 = \delta m \sqrt{\frac{2}{3}} \Pi^{08}(0) + m\Pi^{38}(0) + \frac{\delta m}{\sqrt{3}} \Pi^{88}(0) + \int \mathrm{d}^3\boldsymbol{x}\, \langle\Omega|[A_0^3(x), P^8(0)]|\Omega\rangle. \tag{4.115}$$

After integrating we use the commutator: $[Q_5^3, P^8(0)] = -\frac{\mathrm{i}}{\sqrt{3}} S^3(0) = -\frac{\mathrm{i}}{\sqrt{3}} [\bar{u}u - \bar{d}d]$:

$$\frac{\mathrm{i}}{\sqrt{3}} \langle \bar{u}u - \bar{d}d \rangle^* = \delta m \sqrt{\frac{2}{3}} \Pi^{08}(0) + m\Pi^{38}(0) + \frac{\delta m}{\sqrt{3}} \Pi^{88}(0). \tag{4.116}$$

So in order to calculate the difference of the quark condensates, we need to calculate:

$$\langle \bar{u}u - \bar{d}d \rangle^* = -\mathrm{i}\sqrt{3} m\Pi^{38}(0) - \mathrm{i}\sqrt{2}\delta m\Pi^{08}(0) - \mathrm{i}\delta m\Pi^{88}(0). \tag{4.117}$$

Diagrams

We treat the $\pi^0\eta$ mixing as perturbations in our calculations, i.e. we introduce a $\pi^0\eta$ vertex. Every $\pi^0\eta$ mixing from the Lagrangian due to $\delta m \neq 0$,

$$\mathrm{i}\mathcal{L}_{\pi^0\eta_8} = -\frac{2\mathrm{i}B_0\,\delta m}{\sqrt{3}}, \tag{4.118}$$

gives us a correction depending on whether the new propagator belongs to the π^0 or the η_8:

$$\text{additional pion:} \quad \times\frac{2}{\sqrt{3}}B_0 m\,\frac{\delta m}{m}\frac{1}{m_\pi^2} \approx 0.2 \tag{4.119a}$$

$$\text{additional eta:} \quad \times\frac{2}{\sqrt{3}}B_0 m\,\frac{\delta m}{m}\frac{1}{m_\eta^2} \approx 0.012 \tag{4.119b}$$

using $m_\pi = 138$ MeV and $m_\eta = 548$ MeV. We will in the following consider all diagrams with additional pions coming from this π^0-η_8 mixing, since the large mass of the η_8 leads to a suppression of new η_8 propagators in the soft limit.

The diagrams for Π^{38} are as follows:

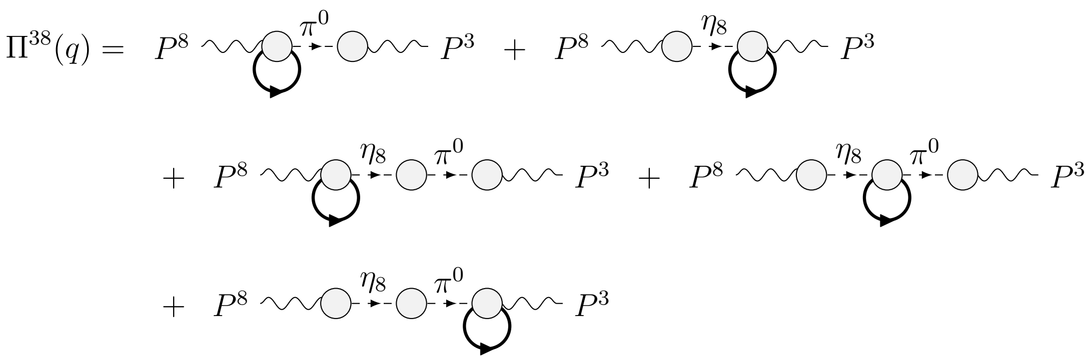

(4.120)

The necessary interactions are:

$$\mathrm{i}\mathcal{L}_{\bar{N}Np^8\pi^0} = \pm\frac{4\mathrm{i}B_0(b_D+b_F)}{\sqrt{3}f}, \tag{4.121a}$$

$$\mathrm{i}\mathcal{L}_{\bar{N}Np^3\eta} = \pm\frac{4\mathrm{i}B_0(b_D+b_F)}{\sqrt{3}f}, \tag{4.121b}$$

$$\mathrm{i}\mathcal{L}_{\bar{N}Np^3\pi^0} = \frac{4\mathrm{i}B_0(2b_0+b_D+b_F)}{f}, \tag{4.121c}$$

$$\mathrm{i}\mathcal{L}_{\bar{N}N\pi^0\eta} = -\frac{4\mathrm{i}B_0\delta m(2b_0+b_D+b_F)}{\sqrt{3}f^2} \mp \frac{4\mathrm{i}B_0 m(b_D+b_F)}{\sqrt{3}f^2}, \tag{4.121d}$$

$$\mathrm{i}\mathcal{L}_{\bar{N}Np^8\eta} = \frac{4\mathrm{i}B_0(6b_0+5b_D-3b_F)}{3f}, \tag{4.121e}$$

$$\mathrm{i}\mathcal{L}_{p^3\pi^0} = \mathrm{i}\mathcal{L}_{p^8\eta} = 2\mathrm{i}B_0 f. \tag{4.121f}$$

The first diagram yields:

$$\Pi_1^{38} = (-\mathrm{i})^2 \int \frac{\mathrm{d}^3\boldsymbol{p}}{(2\pi)^3} \frac{1}{2E_p} \operatorname{Tr}\left\{[\mathrm{i}\mathcal{L}_{\bar{N}Np^8\pi^0}](\not{p} + m_N)n(\boldsymbol{p})\right\} \frac{\mathrm{i}}{-m_\pi^2}[\mathrm{i}\mathcal{L}_{p^3\pi^0}] \tag{4.122a}$$

$$= -\mathrm{i}\frac{8m_N B_0^2(b_D + b_F)}{\sqrt{3}\pi^2 m_\pi^2} \int \mathrm{d}p\, \frac{p^2}{E_p}[\Theta_{\boldsymbol{p}}^p - \Theta_{\boldsymbol{p}}^n], \tag{4.122b}$$

the second diagram results in:

$$\Pi_2^{38} = (-\mathrm{i})^2 \int \frac{\mathrm{d}^3\boldsymbol{p}}{(2\pi)^3} \frac{1}{2E_p} \operatorname{Tr}\left\{[\mathrm{i}\mathcal{L}_{\bar{N}Np^3\eta}](\not{p} + m_N)n(\boldsymbol{p})\right\} \frac{\mathrm{i}}{-m_\eta^2}[\mathrm{i}\mathcal{L}_{p^8\eta}] \tag{4.123a}$$

$$= -\mathrm{i}\frac{8m_N B_0^2(b_D + b_F)}{\sqrt{3}\pi^2 m_\eta^2} \int \mathrm{d}p\, \frac{p^2}{E_p}[\Theta_{\boldsymbol{p}}^p - \Theta_{\boldsymbol{p}}^n]. \tag{4.123b}$$

The third diagram is given by:

$$\Pi_3^{38} = (-\mathrm{i})^2 \int \frac{\mathrm{d}^3\boldsymbol{p}}{(2\pi)^3} \frac{1}{2E_p} \operatorname{Tr}\left\{[\mathrm{i}\mathcal{L}_{\bar{N}Np^8\eta}](\not{p} + m_N)n(\boldsymbol{p})\right\} \frac{\mathrm{i}}{-m_\eta^2}[\mathrm{i}\mathcal{L}_{\pi^0\eta}]\frac{\mathrm{i}}{-m_\pi^2}[\mathrm{i}\mathcal{L}_{p^3\pi^0}] \tag{4.124a}$$

$$= \mathrm{i}\frac{16m_N B_0^3\delta m(6b_0 + 5b_D - 3b_F)}{3\sqrt{3}\pi^2 m_\pi^2 m_\eta^2} \int \mathrm{d}p\, \frac{p^2}{E_p}[\Theta_{\boldsymbol{p}}^p + \Theta_{\boldsymbol{p}}^n], \tag{4.124b}$$

the fourth diagram yields:

$$\Pi_4^{38} = (-\mathrm{i})^2 \int \frac{\mathrm{d}^3\boldsymbol{p}}{(2\pi)^3} \frac{1}{2E_p} \operatorname{Tr}\left\{[\mathrm{i}\mathcal{L}_{\bar{N}N\pi^0\eta}](\not{p} + m_N)n(\boldsymbol{p})\right\} \frac{\mathrm{i}}{-m_\eta^2}[\mathrm{i}\mathcal{L}_{p^8\eta}]\frac{\mathrm{i}}{-m_\pi^2}[\mathrm{i}\mathcal{L}_{p^3\pi^0}] \tag{4.125a}$$

$$= \mathrm{i}\frac{16B_0^3\delta m(2b_0 + b_D + b_F)m_N}{\sqrt{3}\pi^2 m_\pi^2 m_\eta^2} \int \mathrm{d}p\, \frac{p^2}{E_p}[\Theta_{\boldsymbol{p}}^p + \Theta_{\boldsymbol{p}}^n] + \mathrm{i}\frac{8B_0^2 m_N(b_D + b_F)}{\sqrt{3}\pi^2 m_\eta^2} \int \mathrm{d}p\, \frac{p^2}{E_p}[\Theta_{\boldsymbol{p}}^p - \Theta_{\boldsymbol{p}}^n], \tag{4.125b}$$

and the fifth diagram results in:

$$\Pi_5^{38} = (-\mathrm{i})^2[\mathrm{i}\mathcal{L}_{p^8\eta}]\frac{\mathrm{i}}{-m_\eta^2}[\mathrm{i}\mathcal{L}_{\pi^0\eta}]\frac{\mathrm{i}}{-m_\pi^2} \int \frac{\mathrm{d}^3\boldsymbol{p}}{(2\pi)^3} \frac{1}{2E_p} \operatorname{Tr}\left\{[\mathrm{i}\mathcal{L}_{\bar{N}Np^3\pi^0}](\not{p} + m_N)n(\boldsymbol{p})\right\} \tag{4.126a}$$

$$= \mathrm{i}\frac{16m_N B_0^3\delta m(2b_0 + b_D + b_F)}{\sqrt{3}\pi^2 m_\eta^2 m_\pi^2} \int \mathrm{d}p\, \frac{p^2}{E_p}[\Theta_{\boldsymbol{p}}^p + \Theta_{\boldsymbol{p}}^n]. \tag{4.126b}$$

The result of all diagrams, divided by the vacuum condensate, is as follows:

$$-\mathrm{i}\sqrt{3}\frac{m\Pi_1^{38}}{\langle\bar{q}q\rangle_0} = \frac{2m_N(b_D + b_F)}{f^2\pi^2} \int \mathrm{d}p\, \frac{p^2}{E_p}[\Theta_{\boldsymbol{p}}^p - \Theta_{\boldsymbol{p}}^n], \tag{4.127a}$$

$$-\mathrm{i}\sqrt{3}\frac{m\Pi_2^{38}}{\langle\bar{q}q\rangle_0} = \frac{4m_N B_0 m(b_D + b_F)}{\pi^2 f^2 m_\eta^2} \int \mathrm{d}p\, \frac{p^2}{E_p}[\Theta_{\boldsymbol{p}}^p - \Theta_{\boldsymbol{p}}^n], \tag{4.127b}$$

$$-\mathrm{i}\sqrt{3}\frac{m\Pi_3^{38}}{\langle\bar{q}q\rangle_0} = -\frac{4m_N B_0\delta m(6b_0 + 5b_D - 3b_F)}{3f^2\pi^2 m_\eta^2} \int \mathrm{d}p\, \frac{p^2}{E_p}[\Theta_{\boldsymbol{p}}^p + \Theta_{\boldsymbol{p}}^n], \tag{4.127c}$$

$$-\mathrm{i}\sqrt{3}\frac{m\Pi_4^{38}}{\langle\bar{q}q\rangle_0} = -\frac{8B_0^2 m\delta m(2b_0+b_D+b_F)m_N}{\pi^2 f^2 m_\pi^2 m_\eta^2}\int \mathrm{d}p\,\frac{p^2}{E_p}[\Theta_{\boldsymbol{p}}^p+\Theta_{\boldsymbol{p}}^n]$$
$$-\frac{4B_0 m m_N(b_D+b_F)}{\pi^2 f^2 m_\eta^2}\int \mathrm{d}p\,\frac{p^2}{E_p}[\Theta_{\boldsymbol{p}}^p-\Theta_{\boldsymbol{p}}^n], \tag{4.127d}$$
$$-\mathrm{i}\sqrt{3}\frac{m\Pi_5^{38}}{\langle\bar{q}q\rangle_0} = -\frac{4m_N B_0\delta m(2b_0+b_D+b_F)}{f^2\pi^2 m_\eta^2}\int \mathrm{d}p\,\frac{p^2}{E_p}[\Theta_{\boldsymbol{p}}^p+\Theta_{\boldsymbol{p}}^n], \tag{4.127e}$$

where we used $B_0 m = m_\pi^2/2$ and divided by $\langle\bar{q}q\rangle_0 = -2f^2B_0$.

The diagrams for Π^{08} are:

$$\Pi^{08}(q) = \tag{4.128}$$

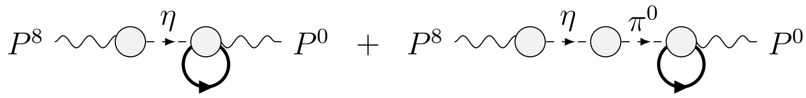

and the interactions are:

$$\mathrm{i}\mathcal{L}_{p^0\pi^0} = \mathrm{i}\mathcal{L}_{p^0\eta} = 0, \tag{4.129a}$$
$$\mathrm{i}\mathcal{L}_{\bar{N}Np^0\eta} = -\frac{4\mathrm{i}\sqrt{2}B_0(b_D-3b_F)}{3f}, \tag{4.129b}$$
$$\mathrm{i}\mathcal{L}_{\bar{N}Np^0\pi^0} = \pm\frac{4\mathrm{i}\sqrt{\frac{2}{3}}B_0(b_D+b_F)}{f}, \tag{4.129c}$$
$$\mathrm{i}\mathcal{L}_{p^8\eta} = 2\mathrm{i}B_0 f. \tag{4.129d}$$

The first diagram yields:

$$\Pi_1^{08} = (-\mathrm{i})^2\int\frac{\mathrm{d}^3\boldsymbol{p}}{(2\pi)^3}\frac{1}{2E_p}\,\mathrm{Tr}\left\{[\mathrm{i}\mathcal{L}_{\bar{N}Np^0\eta}](\not{p}+m_N)n(\boldsymbol{p})\right\}\frac{\mathrm{i}}{-m_\eta^2}[\mathrm{i}\mathcal{L}_{p^8\eta}] \tag{4.130a}$$
$$= \mathrm{i}\frac{8\sqrt{2}m_N B_0^2(b_D-3b_F)}{3\pi^2 m_\eta^2}\int \mathrm{d}p\,\frac{p^2}{E_p}[\Theta_{\boldsymbol{p}}^p+\Theta_{\boldsymbol{p}}^n], \tag{4.130b}$$

and the second diagram results in:

$$\Pi_2^{08} = (-\mathrm{i})^2[\mathrm{i}\mathcal{L}_{p^8\eta}]\frac{\mathrm{i}}{-m_\eta^2}[\mathrm{i}\mathcal{L}_{\pi^0\eta}]\frac{\mathrm{i}}{-m_\pi^2}\int\frac{\mathrm{d}^3\boldsymbol{p}}{(2\pi)^3}\frac{1}{2E_p}\,\mathrm{Tr}\left\{[\mathrm{i}\mathcal{L}_{\bar{N}Np^0\pi^0}](\not{p}+m_N)n(\boldsymbol{p})\right\} \tag{4.131a}$$
$$= \mathrm{i}\frac{16\sqrt{2}m_N B_0^3\delta m(b_D+b_F)}{3\pi^2 m_\eta^2 m_\pi^2}\int \mathrm{d}p\,\frac{p^2}{E_p}[\Theta_{\boldsymbol{p}}^p-\Theta_{\boldsymbol{p}}^n]. \tag{4.131b}$$

The result is as follows:

$$-\mathrm{i}\sqrt{2}\frac{\delta m\Pi_1^{08}}{\langle\bar{q}q\rangle_0} = -\frac{8m_N B_0\delta m(b_D-3b_F)}{3\pi^2 m_\eta^2 f^2}\int \mathrm{d}p\,\frac{p^2}{E_p}[\Theta_{\boldsymbol{p}}^p+\Theta_{\boldsymbol{p}}^n], \tag{4.132a}$$
$$-\mathrm{i}\sqrt{2}\frac{\delta m\Pi_2^{08}}{\langle\bar{q}q\rangle_0} = -\frac{16m_N B_0^2(\delta m)^2(b_D+b_F)}{3f^2\pi^2 m_\eta^2 m_\pi^2}\int \mathrm{d}p\,\frac{p^2}{E_p}[\Theta_{\boldsymbol{p}}^p-\Theta_{\boldsymbol{p}}^n], \tag{4.132b}$$

where we used $B_0 m = m_\pi^2/2$ and divided by $\langle\bar{q}q\rangle_0 = -2f^2B_0$.

The diagrams for Π^{88} are:

$\Pi^{88}(q) = 2$

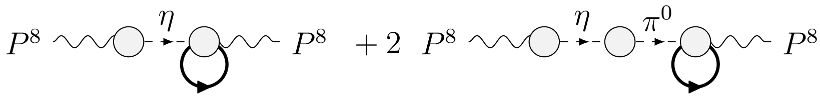

$+$

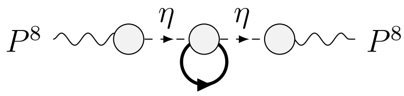

(4.133)

and the interactions are:

$$\mathrm{i}\mathcal{L}_{p^8\pi^0} = 0, \tag{4.134a}$$

$$\mathrm{i}\mathcal{L}_{p^8\eta} = 2\mathrm{i}B_0 f, \tag{4.134b}$$

$$\mathrm{i}\mathcal{L}_{\bar{N}Np^8\eta} = \frac{4\mathrm{i}B_0(6b_0 + 5b_D - 3b_F)}{3f}, \tag{4.134c}$$

$$\mathrm{i}\mathcal{L}_{\bar{N}Np^8\pi^0} = \pm\frac{4\mathrm{i}B_0(b_D + b_F)}{\sqrt{3}f}, \tag{4.134d}$$

$$\mathrm{i}\mathcal{L}_{\bar{N}N\eta^8\eta^8} = -\frac{2\mathrm{i}B_0[m(2b_0 + b_D + b_F) + 4m_s(b_0 + b_D - b_F))}{3f^2} \mp \frac{2\mathrm{i}B_0\delta m(b_D + b_F)}{3f^2}. \tag{4.134e}$$

The first diagram gives:

$$\Pi_1^{88} = (-\mathrm{i})^2 \int \frac{\mathrm{d}^3\boldsymbol{p}}{(2\pi)^3}\frac{1}{2E_p}\,\mathrm{Tr}\left\{[\mathrm{i}\mathcal{L}_{\bar{N}Np^8\eta}](\not{p} + m_N)n(\boldsymbol{p})\right\}\frac{\mathrm{i}}{-m_\eta^2}[\mathrm{i}\mathcal{L}_{p^8\eta}] \tag{4.135a}$$

$$= -\mathrm{i}\frac{8m_N B_0^2(6b_0 + 5b_D - 3b_F)}{3\pi^2 m_\eta^2}\int \mathrm{d}p\,\frac{p^2}{E_p}[\Theta_{\boldsymbol{p}}^p + \Theta_{\boldsymbol{p}}^n], \tag{4.135b}$$

the second diagram yields:

$$\Pi_2^{88} = (-\mathrm{i})^2[\mathrm{i}\mathcal{L}_{p^8\eta}]\frac{\mathrm{i}}{-m_\eta^2}[\mathrm{i}\mathcal{L}_{\pi^0\eta}]\frac{\mathrm{i}}{-m_\pi^2}\int\frac{\mathrm{d}^3\boldsymbol{p}}{(2\pi)^3}\frac{1}{2E_p}\,\mathrm{Tr}\left\{[\mathrm{i}\mathcal{L}_{\bar{N}Np^8\pi^0}](\not{p} + m_N)n(\boldsymbol{p})\right\} \tag{4.136a}$$

$$= \mathrm{i}\frac{16m_N B_0^3\delta m(b_D + b_F)}{3\pi^2 m_\eta^2 m_\pi^2}\int \mathrm{d}p\,\frac{p^2}{E_p}[\Theta_{\boldsymbol{p}}^p - \Theta_{\boldsymbol{p}}^n], \tag{4.136b}$$

and the third diagram yields:

$$\Pi_3^{88} = (-\mathrm{i})^2\int\frac{\mathrm{d}^3\boldsymbol{p}}{(2\pi)^3}\frac{1}{2E_p}\,\mathrm{Tr}\left\{[\mathrm{i}\mathcal{L}_{\bar{N}N\eta\eta}](\not{p} + m_N)n(\boldsymbol{p})\right\}\frac{\mathrm{i}}{-m_\eta^2}[\mathrm{i}\mathcal{L}_{p^8\eta}]\frac{\mathrm{i}}{-m_\eta^2}[\mathrm{i}\mathcal{L}_{p^8\eta}] \tag{4.137a}$$

$$= \mathrm{i}\frac{8m_N B_0^2\left[B_0 m(2b_0 + b_D + b_F) + 4B_0 m_s(b_0 + b_D - b_F)\right]}{3\pi^2 m_\eta^4}\int \mathrm{d}p\,\frac{p^2}{E_p}[\Theta_{\boldsymbol{p}}^p + \Theta_{\boldsymbol{p}}^n] \tag{4.137b}$$

$$\begin{aligned} &= \mathrm{i}\frac{8m_N B_0^3[m(2b_0 + b_D + b_F) + 4m_s(b_0 + b_D - b_F))}{3\pi^2 m_\eta^4}\int \mathrm{d}p\,\frac{p^2}{E_p}[\Theta_{\boldsymbol{p}}^p + \Theta_{\boldsymbol{p}}^n] \\ &\quad + \mathrm{i}\frac{8m_N B_0^3\delta m(b_D + b_F)}{3\pi^2 m_\eta^4}\int \mathrm{d}p\,\frac{p^2}{E_p}[\Theta_{\boldsymbol{p}}^p - \Theta_{\boldsymbol{p}}^n]. \end{aligned} \tag{4.137c}$$

These diagrams give the following contribution to the quark condensate:

$$-\mathrm{i}\frac{\delta m\Pi_1^{88}}{\langle\bar{q}q\rangle_0}\times 2 = \frac{8m_N B_0\delta m(6b_0+5b_D-3b_F)}{3f^2\pi^2 m_\eta^2}\int \mathrm{d}p\,\frac{p^2}{E_p}[\Theta_{\boldsymbol{p}}^p+\Theta_{\boldsymbol{p}}^n], \tag{4.138a}$$

$$-\mathrm{i}\frac{\delta m\Pi_2^{88}}{\langle\bar{q}q\rangle_0}\times 2 = -\frac{16m_N B_0^2(\delta m)^2(b_D+b_F)}{3f^2\pi^2 m_\eta^2 m_\pi^2}\int \mathrm{d}p\,\frac{p^2}{E_p}[\Theta_{\boldsymbol{p}}^p-\Theta_{\boldsymbol{p}}^n], \tag{4.138b}$$

$$\begin{aligned}-\mathrm{i}\frac{\delta m\Pi_3^{88}}{\langle\bar{q}q\rangle_0} &= -\frac{4m_N B_0^2\delta m[m(2b_0+b_D+b_F)+4m_s(b_0+b_D-b_F))}{3f^2\pi^2 m_\eta^4}\int \mathrm{d}p\,\frac{p^2}{E_p}[\Theta_{\boldsymbol{p}}^p+\Theta_{\boldsymbol{p}}^n]\\ &\quad -\frac{4m_N B_0^2(\delta m)^2(b_D+b_F)}{3f^2\pi^2 m_\eta^4}\int \mathrm{d}p\,\frac{p^2}{E_p}[\Theta_{\boldsymbol{p}}^p-\Theta_{\boldsymbol{p}}^n],\end{aligned} \tag{4.138c}$$

where we used $B_0 m = m_\pi^2/2$ and divided by $\langle\bar{q}q\rangle_0 = -2f^2B_0$.

In the soft limit and omitting terms beyond $\mathcal{O}(\rho)$ and $\mathcal{O}(\delta m)$, which means omitting terms with triple isospin breaking, the three results for Π^{38}, Π^{08} and Π^{88} can be summarized:

$$\sqrt{3}\frac{m\Pi^{38}}{\mathrm{i}\langle\bar{q}q\rangle_0} = \frac{2\rho}{f^2}(b_D+b_F)\frac{1-r}{1+r}-\frac{2\rho}{f^2}(18b_0+11b_D+3b_F)\frac{\delta m}{m+2m_s}, \tag{4.139a}$$

$$\sqrt{2}\frac{\delta m\Pi^{08}}{\mathrm{i}\langle\bar{q}q\rangle_0} = -\frac{4\rho(b_D-3b_F)}{f^2}\frac{\delta m}{m+2m_s}, \tag{4.139b}$$

$$\frac{\delta m\Pi^{88}}{\mathrm{i}\langle\bar{q}q\rangle_0} = \frac{\rho}{f^2}\left[2(9b_0+7b_D-3b_F)+\frac{m_\pi^2}{m_\eta^2}(b_D-3b_F)\right]\frac{\delta m}{m+2m_s}. \tag{4.139c}$$

4.4.2. Results: difference of light quark condensates

In agreement with the Vafa–Witten theorem [96], our results only depend on the difference of proton and neutron densities in the absence of explicit isospin breaking ($\delta m = 0$), since isospin symmetry is not spontaneously broken in QCD. We in fact find that all contributions with $\delta m = 0$ contain the difference of nucleon densities and contributions of order (δm) contain the sum of nucleon densities:

$$\underbrace{\langle\bar{u}u-\bar{d}d\rangle^*}_{\text{isospin-odd}} = \underbrace{(...)\underbrace{[\Theta^p-\Theta^n]}_{\text{odd}} + (...)\underbrace{\delta m}_{\text{odd}}\underbrace{[\Theta^p+\Theta^n]}_{\text{even}}}_{1\times\text{ isospin breaking}} + \underbrace{(...)\underbrace{(\delta m)^2}_{\text{even}}\underbrace{[\Theta^p-\Theta^n]}_{\text{odd}}}_{3\times\text{ isospin breaking}} + \dots. \tag{4.140}$$

We further used a quark mass ratio of $\delta m/m \approx -1/3$ (equivalent to $m_u/m_d \approx 0.46$) and $m_s/m \approx 27.2$ and the following leading order relations of meson masses with relation to B_0:

$$m_\pi^2 = 2B_0 m, \qquad\qquad m_\eta^2 = \frac{2}{3}B_0(m+2m_s), \tag{4.141}$$

with $m_\pi = 138$ MeV and $m_\eta = 548$ MeV.

The results of Π^{38}, Π^{08} and Π^{88} are shown in Figs. 4.4 and 4.5. The density dependence of $\langle\bar{u}u-\bar{d}d\rangle^*$ is one order of magnitude smaller than the density dependence of $\langle\bar{u}u+\bar{d}d\rangle^*$.

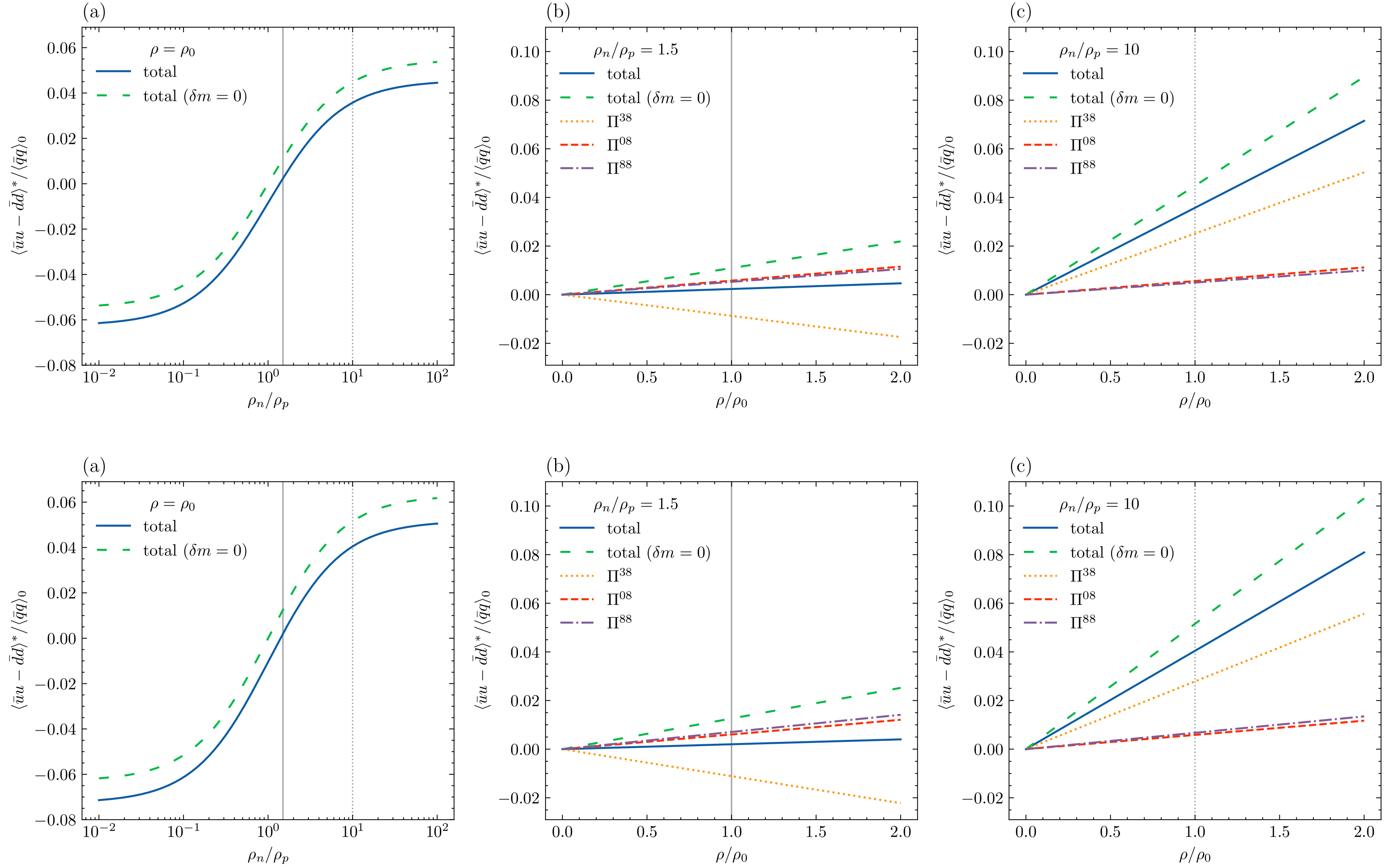

Figure 4.4.: Top to bottom: LEC sets 1 and 2 of Table 3.2. (a) The dependence of $\langle \bar{u}u - \bar{d}d \rangle^*$ on the neutron-to-proton ratio. (b) The dependence of $\langle \bar{u}u - \bar{d}d \rangle^*$ on the nucleon density for a nucleon ratio of $\rho_n/\rho_p = 1.5$. (c) Same as before, here with a ratio $\rho_n/\rho_p = 10$.

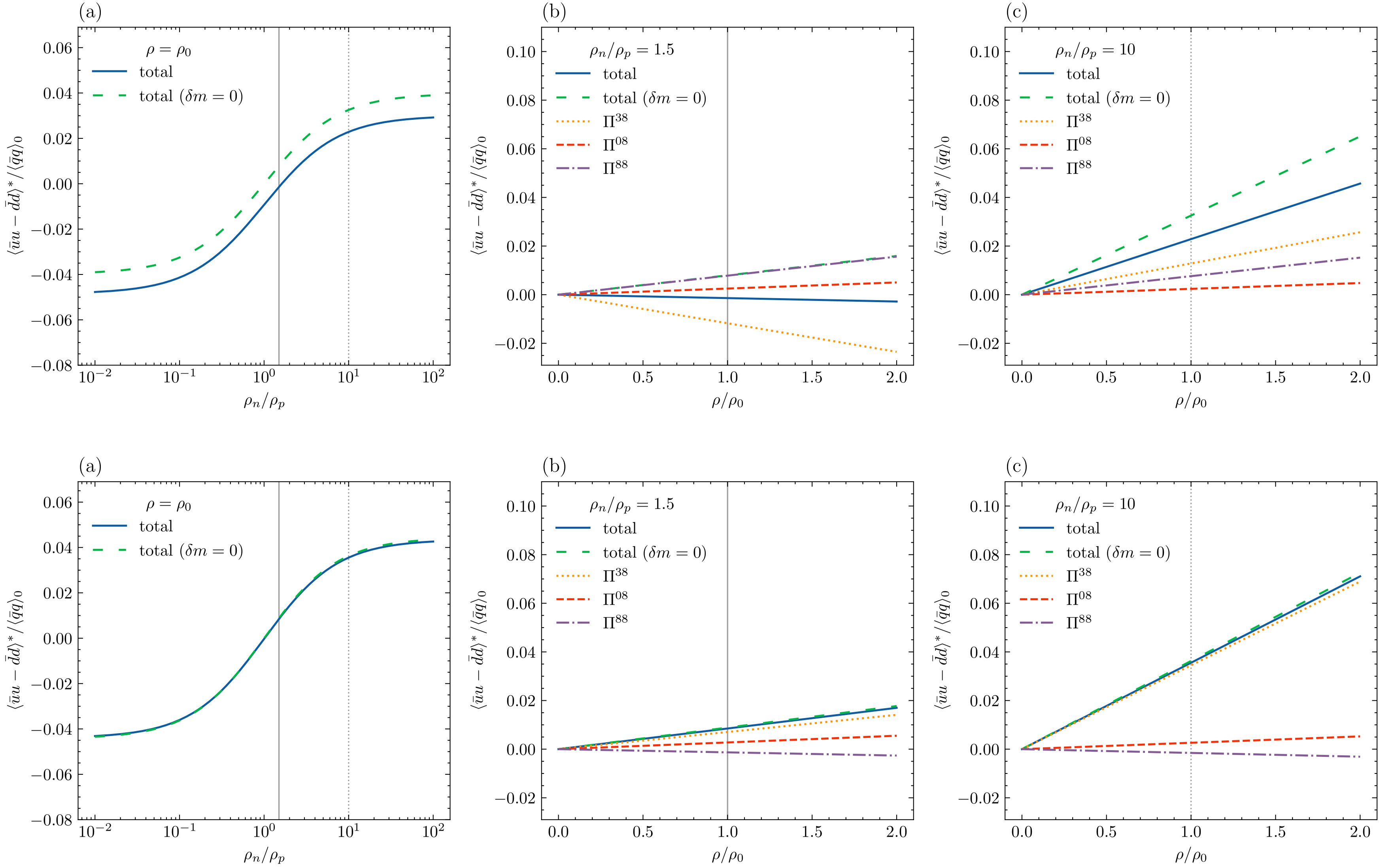

Figure 4.5.: Top to bottom: LEC sets 3 and 4 of Table 3.2. (a) The dependence of $\langle \bar{u}u - \bar{d}d \rangle^*$ on the neutron-to-proton ratio. (b) The dependence of $\langle \bar{u}u - \bar{d}d \rangle^*$ on the nucleon density for a nucleon ratio of $\rho_n/\rho_p = 1.5$. (c) Same as before, here with a ratio $\rho_n/\rho_p = 10$.

This is because the coefficient in $\langle\bar{u}u - \bar{d}d\rangle^*$ is smaller by a factor of 10 than the coefficient in $\langle\bar{u}u + \bar{d}d\rangle^*$, e.g. for the LEC set 1:

$$b_D + b_F \approx -0.18 \text{ GeV}^{-1}, \tag{4.142a}$$

$$2b_0 + b_D + b_F \approx -1.4 \quad \text{GeV}^{-1}. \tag{4.142b}$$

We illustrate the effects of explicit isospin breaking by also plotting the result for $\delta m = 0$. Figures 4.4 and 4.5 (a) show the dependence of $\langle\bar{u}u - \bar{d}d\rangle^*$ on the neutron-to-proton ratio. The isospin breaking due to $m_u \neq m_d$ leads to a reduction of around 1% at normal nuclear density, almost independent of nucleon ratios. Interestingly, the LEC set 4 exhibits no difference between explicit isospin breaking or its absence. Figures 4.4 and 4.5 (b) show the dependence of $\langle\bar{u}u - \bar{d}d\rangle^*$ on the nucleon density, in particular the three contributions to $\langle\bar{u}u - \bar{d}d\rangle^*$ as well as their sum are shown. For a nucleon ratio of $\rho_n/\rho_p = 1.5$, the up and down quark condensates are almost the same. Figures 4.4 and 4.5 (c) also show the density dependence and was calculated using a nucleon ratio $\rho_n/\rho_p = 10$.

Although the explicit isospin breaking due to non-equal quark masses in the Lagrangian provides a numerically smaller effect than the isospin breaking from the surrounding nuclear matter at e.g. $\rho_n/\rho_p = 1.5$,

$$\frac{1}{150} \approx \left|\frac{\delta m}{m + 2m_s}\right| \ll \left|\frac{1-r}{1+r}\right| = \frac{1}{5}, \tag{4.143}$$

this is compensated by the large number of diagrams due to $\delta m \neq 0$, which leads to a large contribution via the LECs (LEC set 1):

$$-(b_D + b_F)\frac{1-r}{1+r} \approx 0.04 \text{ GeV}^{-1}, \tag{4.144a}$$

$$(18b_0 + 11b_D + 3b_F)\frac{\delta m}{m + 2m_s} \approx 0.06 \text{ GeV}^{-1}. \tag{4.144b}$$

Here we note that the coefficients of the LECs in Eq. (4.144b) are one order of magnitude larger than the ones in Eq. (4.144a). This is significant, especially since b_0 is larger than the other LECs b_D and b_F, which gets further enhanced by the factor of 18. Hence, the effects of isospin breaking in the Lagrangian and in the nuclear matter are of similar size in our calculations. Still, there exists a possible ambiguity in the determination of b_0, which is often absorbed in the chiral limit octet baryon masses m_0. It is possible to extract a value for b_0 from scattering experiments, although such experimental data is scarce. Such an issue is absent in the LECs b_D and b_F, which are determined via Gell-Mann–Okubo mass relations.

For a nucleon ratio of 1.5, i.e. the one most accessible to experiments via heavy nuclei, the up and down quark condensates behave almost the same with increasing density, see Figs. 4.4 and 4.5 (a). The effect of explicit isospin breaking in the Lagrangian leads to an almost constant

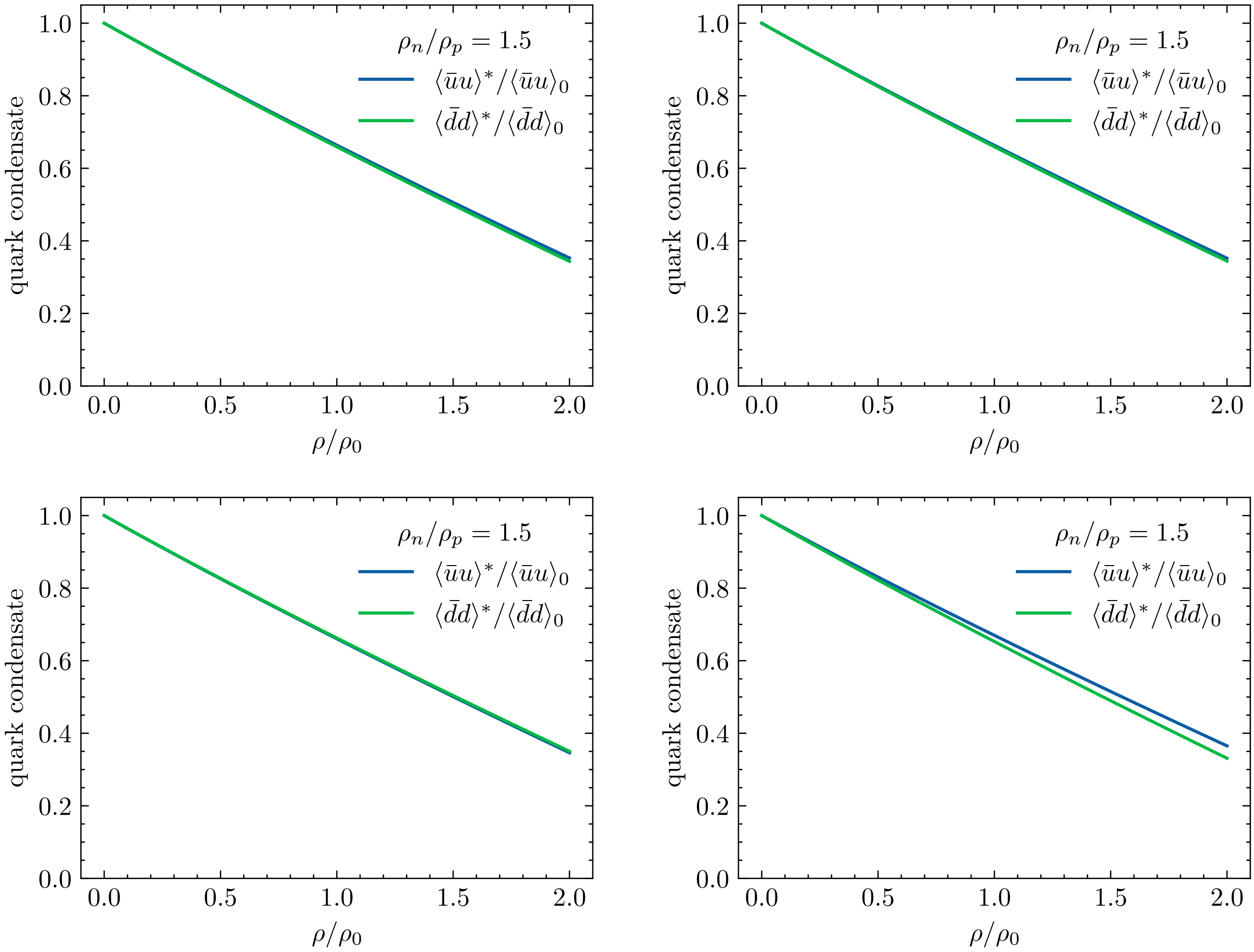

Figure 4.6.: Top row: LEC sets 1 and 2, bottom row: LEC sets 3 and 4 from Table 3.2. The result for $\langle\bar{u}u + \bar{d}d\rangle^*$ was obtained from the SU(2) LEC set 2 in Table 3.1. In three out of four cases, the up and down quark condensates behave almost the same in nuclear matter with $\rho_n/\rho_p = 1.5$, which is typical for heavy nuclei.

reduction of 1% along all nucleon ratios, but the splitting of up and down quark condensates increases due to the isospin breaking of the surrounding nuclear matter.

It would be interesting to discuss the experimental determination of the coefficients $b_D + b_F$ etc., appearing in our results. As is well-known, the parameter c_1 is determined by the πN-σ term, which is obtained by taking the soft limit in πN scattering, $\lim_{p\to 0} T_{\pi N}(p) = -\sigma_{\pi N}/f^2$. In a similar way, the SU(3) coefficients could be extracted from the $\eta N \to \pi^0 N$ scattering amplitudes in the soft limit. Nevertheless, it would be difficult, because the η meson mass is so large that a theoretical extrapolation to the soft limit would have a large uncertainty. In addition, in $\eta N \to \pi^0 N$ scattering, the contribution of the $N(1535)$ nucleon resonance is known to dominate the amplitude around the threshold. The resonance contribution should therefore be counted in the extrapolation.

Finally, we also show the up and down quark condensates separately in Fig. 4.6 by combining the results for $\langle \bar{u}u + \bar{d}d \rangle *$ and $\langle \bar{u}u - \bar{d}d \rangle^*$.

4.4.3. Up plus down quark condensate

In the following, we set $\delta m = 0$ again. In order to calculate $\langle \bar{u}u + \bar{d}d \rangle^*$, we need these diagrams:

$\Pi^{33}(q) =$ 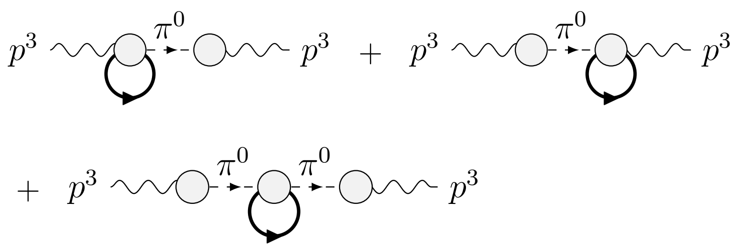

(4.145)

The necessary vertex factors are:

$$[\mathrm{i}\mathcal{L}_{P^3\pi^0}] = 2\mathrm{i}B_0 f, \tag{4.146a}$$
$$\mathcal{L}_{\bar{N}Np^3\pi^0} = \frac{4B_0(2b_0 + b_D + b_F)}{f}, \tag{4.146b}$$
$$[\mathrm{i}\mathcal{L}_{\bar{N}N\pi^0\pi^0}] = -\frac{4\mathrm{i}B_0 m(2b_0 + b_D + b_F)}{f^2}, \tag{4.146c}$$

which we obtained from Eq. (A.18).

First diagram (nucleon loop on the left)

$$\Pi_1^{33}(0) = (-1)^L \frac{(-1)^1}{1!} (-\mathrm{i})^2 \int \frac{\mathrm{d}^3\boldsymbol{p}}{(2\pi)^3} \frac{1}{2p_0} \,\mathrm{Tr}\left\{ [\mathrm{i}\mathcal{L}_{\bar{N}Np^3\phi^3}](\not{p} + m_N) n(\boldsymbol{p}) \right\} \frac{\mathrm{i}}{-m_\pi^2} [\mathrm{i}\mathcal{L}_{p^3\phi^3}] \tag{4.147}$$

The necessary vertices are:

$$[\mathrm{i}\mathcal{L}_{\bar{N}N\pi^0p^3}] = \frac{4\mathrm{i}B_0(2b_0 + b_D + b_F)}{f}, \tag{4.148a}$$
$$[\mathrm{i}\mathcal{L}_{p^a\phi^b}] = 2\mathrm{i}B_0 f \delta^{ab}. \tag{4.148b}$$

The result of this diagram is:

$$\Pi_1^{33}(0) = -\frac{8\mathrm{i}B_0^2(2b_0 + b_D + b_F)m_N}{\pi^2 m_\pi^2} \int \mathrm{d}p \,\frac{p^2}{p_0} (\Theta_{\boldsymbol{p}}^p + \Theta_{\boldsymbol{p}}^n). \tag{4.149}$$

We divide by $\langle \bar{u}u + \bar{d}d \rangle_0 = -2B_0 f^2$:

$$\begin{aligned} \frac{\langle \bar{u}u + \bar{d}d \rangle_1^*}{\langle \bar{u}u + \bar{d}d \rangle_0} &= \frac{-\mathrm{i}m}{-2f^2 B_0} \Pi_1^{33}(0) \\ &= \frac{4B_0 m(2b_0 + b_D + b_F)m_N}{\pi^2 m_\pi^2 f^2} \int \mathrm{d}p \,\frac{p^2}{p_0} (\Theta_{\boldsymbol{p}}^p + \Theta_{\boldsymbol{p}}^n), \end{aligned} \tag{4.150}$$

and use $mB_0 = m_\pi^2/2$:

$$\frac{\langle \bar{u}u + \bar{d}d \rangle_1^*}{\langle \bar{u}u + \bar{d}d \rangle_0} = \frac{2(2b_0 + b_D + b_F)m_N}{\pi^2 f^2} \int \mathrm{d}p \, \frac{p^2}{p_0} (\Theta_{\boldsymbol{p}}^p + \Theta_{\boldsymbol{p}}^n). \tag{4.151}$$

Second diagram (nucleon loop on the right)

Due to symmetry, this result is the same as the first diagram:

$$\frac{\langle \bar{u}u + \bar{d}d \rangle_2^*}{\langle \bar{u}u + \bar{d}d \rangle_0} = \frac{\langle \bar{u}u + \bar{d}d \rangle_1^*}{\langle \bar{u}u + \bar{d}d \rangle_0} \tag{4.152}$$

Third diagram (nucleon loop in the middle)

$$\Pi_3^{33}(0) = (-1)^L \frac{(-1)^1}{1!} (-\mathrm{i})^2 \int \frac{\mathrm{d}^3\boldsymbol{p}}{(2\pi)^3} \frac{1}{2p_0} [\mathrm{i}\mathcal{L}_{p^3\Phi^3}] \frac{\mathrm{i}}{-m_\pi^2} \operatorname{Tr}\left\{ [\mathrm{i}\mathcal{L}_{\bar{N}N\phi^3\phi^3}](\not{p} + m_N) n(\boldsymbol{p}) \right\} \frac{\mathrm{i}}{-m_\pi^2} [\mathrm{i}\mathcal{L}_{p^3\Phi^3}] \tag{4.153}$$

The relevant vertices are:

$$[\mathrm{i}\mathcal{L}_{p^a\phi^b}] = 2\mathrm{i}B_0 f \delta^{ab}, \tag{4.154a}$$

$$[\mathrm{i}\mathcal{L}_{\bar{N}N\pi^0\pi^0}] = -\frac{4\mathrm{i}B_0 m(2b_0 + b_D + b_F)}{f^2}. \tag{4.154b}$$

We can simplify this to:

$$\Pi_3^{33}(0) = \frac{16\mathrm{i}B_0^3 m(2b_0 + b_D + b_F)m_N}{\pi^2 m_\pi^4} \int \mathrm{d}p \, \frac{p^2}{p_0} (\Theta_{\boldsymbol{p}}^p + \Theta_{\boldsymbol{p}}^n), \tag{4.155}$$

and divide by $\langle \bar{u}u + \bar{d}d \rangle_0 = -2B_0 f^2$:

$$\begin{aligned} \frac{\langle \bar{u}u + \bar{d}d \rangle_3^*}{\langle \bar{u}u + \bar{d}d \rangle_0} &= \frac{-\mathrm{i}m}{-2f^2 B_0} \Pi_3^{33}(0) \\ &= -\frac{8B_0^2 m^2(2b_0 + b_D + b_F)m_N}{\pi^2 m_\pi^4 f^2} \int \mathrm{d}p \, \frac{p^2}{p_0} (\Theta_{\boldsymbol{p}}^p + \Theta_{\boldsymbol{p}}^n). \end{aligned} \tag{4.156}$$

Finally we use $mB_0 = m_\pi^2/2$:

$$\frac{\langle \bar{u}u + \bar{d}d \rangle_3^*}{\langle \bar{u}u + \bar{d}d \rangle_0} = -\frac{2(2b_0 + b_D + b_F)m_N}{\pi^2 f^2} \int \mathrm{d}p \, \frac{p^2}{p_0} (\Theta_{\boldsymbol{p}}^p + \Theta_{\boldsymbol{p}}^n). \tag{4.157}$$

Result

The calculations of the previous sections showed that:

$$\frac{\langle \bar{u}u + \bar{d}d \rangle_1^*}{\langle \bar{u}u + \bar{d}d \rangle_0} = \frac{\langle \bar{u}u + \bar{d}d \rangle_2^*}{\langle \bar{u}u + \bar{d}d \rangle_0} = -\frac{\langle \bar{u}u + \bar{d}d \rangle_3^*}{\langle \bar{u}u + \bar{d}d \rangle_0}, \tag{4.158}$$

so only the first diagram remains after summing over all three:

$$\frac{\langle \bar{u}u + \bar{d}d\rangle^*}{\langle \bar{u}u + \bar{d}d\rangle_0} = \frac{2(2b_0 + b_D + b_F)m_N}{\pi^2 f^2} \int \mathrm{d}p\, \frac{p^2}{p_0}(\Theta^p_{\boldsymbol{p}} + \Theta^n_{\boldsymbol{p}}). \tag{4.159}$$

In the large-m_N limit (see Appendix B.4.5 for details), we can evaluate this to:

$$\frac{\langle \bar{u}u + \bar{d}d\rangle^*}{\langle \bar{u}u + \bar{d}d\rangle_0} \overset{m_N\to\infty}{=} \frac{2\rho(2b_0 + b_D + b_F)}{f^2}. \tag{4.160}$$

Comparing this to the linear-density result of the SU(2) calculation in Eqs. (4.21) and (4.31) (i.e. only the type-2 diagrams):

$$\frac{\langle \bar{q}q\rangle^*_{\mathrm{LO}}}{\langle \bar{q}q\rangle_0} = \frac{4c_1 m_N}{\pi^2 f^2} \int \mathrm{d}p \frac{p^2}{E(\boldsymbol{p})}[\Theta^p_{\boldsymbol{p}} + \Theta^n_{\boldsymbol{p}}] \overset{m_N\to\infty}{=} \frac{4c_1\rho}{f^2} \tag{4.161}$$

we can relate the following SU(2) and SU(3) LECs:

$$2b_0 + b_D + b_F = 2c_1. \tag{4.162}$$

4.4.4. Up plus strange quark condensate

In order to calculate $\langle \bar{u}u + \bar{s}s\rangle^*$, we need these diagrams:

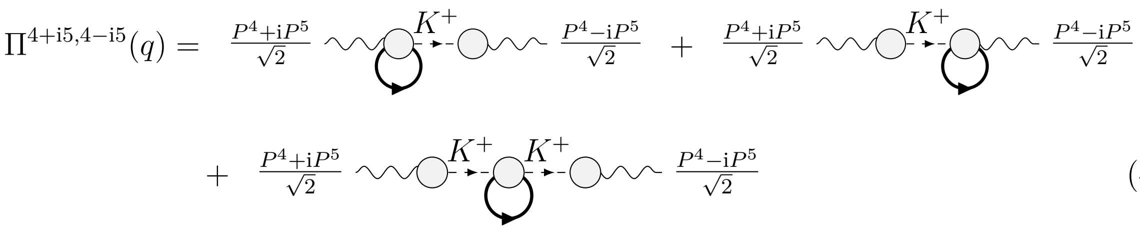

(4.163)

The necessary vertex factors are derived in Appendix A.1.4:

$$[\mathrm{i}\mathcal{L}_{\frac{P^4+\mathrm{i}P^5}{\sqrt{2}}K^-}] = 2\mathrm{i}B_0 f, \tag{4.164a}$$

$$[\mathrm{i}\mathcal{L}_{\frac{P^4-\mathrm{i}P^5}{\sqrt{2}}K^+}] = 2\mathrm{i}B_0 f, \tag{4.164b}$$

$$[\mathrm{i}\mathcal{L}_{\bar{p}p\frac{P^4+\mathrm{i}P^5}{\sqrt{2}}K^+}] = \frac{8\mathrm{i}B_0(b_0+b_D)}{f}, \tag{4.164c}$$

$$[\mathrm{i}\mathcal{L}_{\bar{n}n\frac{P^4+\mathrm{i}P^5}{\sqrt{2}}K^+}] = \frac{4\mathrm{i}B_0(2b_0+b_D-b_F)}{f}, \tag{4.164d}$$

$$[\mathrm{i}\mathcal{L}_{\bar{p}p\frac{P^4-\mathrm{i}P^5}{\sqrt{2}}K^-}] = \frac{8\mathrm{i}B_0(b_0+b_D)}{f}, \tag{4.164e}$$

$$[\mathrm{i}\mathcal{L}_{\bar{n}n\frac{P^4-\mathrm{i}P^5}{\sqrt{2}}K^-}] = \frac{4\mathrm{i}B_0(2b_0+b_D-b_F)}{f}, \tag{4.164f}$$

$$[\mathrm{i}\mathcal{L}_{\bar{p}pK^+K^-}] = -\frac{4\mathrm{i}B_0(m+m_s)(b_0+b_D)}{f^2}, \tag{4.164g}$$

$$[\mathrm{i}\mathcal{L}_{\bar{n}nK^+K^-}] = -\frac{2\mathrm{i}B_0(m+m_s)(2b_0+b_D-b_F)}{f^2}. \tag{4.164h}$$

First diagram (nucleon loop on the left)

The first diagram can be written like this:

$$\Pi_1(0) = (-1)(-1)(-\mathrm{i})^2 \int \frac{\mathrm{d}^3\boldsymbol{p}}{(2\pi)^3} \frac{1}{2p_0} \operatorname{Tr}\left\{(\not{p} + m_N)n(\boldsymbol{p})[\mathrm{i}\mathcal{L}_{\bar{N}N\frac{P^4+\mathrm{i}P^5}{\sqrt{2}}K^+}]\right\} \frac{\mathrm{i}}{-m_K^2}[\mathrm{i}\mathcal{L}_{\frac{P^4-\mathrm{i}P^5}{\sqrt{2}}K^+}]. \tag{4.165}$$

The necessary vertices for this diagram are:

$$[\mathrm{i}\mathcal{L}_{\frac{P^4-\mathrm{i}P^5}{\sqrt{2}}K^+}] = 2\mathrm{i}B_0 f, \tag{4.166a}$$

$$[\mathrm{i}\mathcal{L}_{\bar{p}p\frac{P^4+\mathrm{i}P^5}{\sqrt{2}}K^+}] = \frac{8\mathrm{i}B_0(b_0+b_D)}{f}, \tag{4.166b}$$

$$[\mathrm{i}\mathcal{L}_{\bar{n}n\frac{P^4+\mathrm{i}P^5}{\sqrt{2}}K^+}] = \frac{4\mathrm{i}B_0(2b_0+b_D-b_F)}{f}. \tag{4.166c}$$

We can simplify this to:

$$\begin{aligned}\Pi_1(0) &= -\frac{2B_0 f m_N}{\pi^2 m_K^2}\int \mathrm{d}p\,\frac{p^2}{p_0}\operatorname{Tr}\left\{n(\boldsymbol{p})[\mathrm{i}\mathcal{L}_{\bar{N}N\frac{P^4+\mathrm{i}P^5}{\sqrt{2}}K^+}]\right\}\\ &= -\frac{2B_0 f m_N}{\pi^2 m_K^2}\int \mathrm{d}p\,\frac{p^2}{p_0}\left[\Theta^p_{\boldsymbol{p}}[\mathrm{i}\mathcal{L}_{\bar{p}p\frac{P^4+\mathrm{i}P^5}{\sqrt{2}}K^+}] + \Theta^n_{\boldsymbol{p}}[\mathrm{i}\mathcal{L}_{\bar{n}n\frac{P^4+\mathrm{i}P^5}{\sqrt{2}}K^+}]\right]\\ &= -\frac{8\mathrm{i}B_0^2 m_N}{\pi^2 m_K^2}\int \mathrm{d}p\,\frac{p^2}{p_0}\left[2(b_0+b_D)\Theta^p_{\boldsymbol{p}} + (2b_0+b_D-b_F)\Theta^n_{\boldsymbol{p}}\right].\end{aligned} \tag{4.167}$$

We recall Eq. (4.9) and divide by the vacuum condensate $\langle\bar{u}u+\bar{s}s\rangle_0 = -2B_0f^2$:

$$\begin{aligned}\frac{\langle\bar{u}u+\bar{s}s\rangle_1^*}{\langle\bar{u}u+\bar{s}s\rangle_0} &= \frac{-\mathrm{i}\frac{m+m_s}{2}\Pi_1(0)}{-2B_0f^2}\\ &= \frac{2B_0(m+m_s)m_N}{\pi^2f^2m_K^2}\int \mathrm{d}p\,\frac{p^2}{p_0}\left[2(b_0+b_D)\Theta^p_{\boldsymbol{p}} + (2b_0+b_D-b_F)\Theta^n_{\boldsymbol{p}}\right].\end{aligned} \tag{4.168}$$

Lastly, we use $B_0(m+m_s) = m_K^2$:

$$\frac{\langle\bar{u}u+\bar{s}s\rangle_1^*}{\langle\bar{u}u+\bar{s}s\rangle_0} = \frac{2m_N}{\pi^2f^2}\int \mathrm{d}p\,\frac{p^2}{p_0}\left[2(b_0+b_D)\Theta^p_{\boldsymbol{p}} + (2b_0+b_D-b_F)\Theta^n_{\boldsymbol{p}}\right]. \tag{4.169}$$

Second diagram (nucleon loop on the right)

Since K^+ and K^- have the same mass and the vertices are also the same, this is the same as the first diagram:

$$\frac{\langle\bar{u}u+\bar{s}s\rangle_2^*}{\langle\bar{u}u+\bar{s}s\rangle_0} = \frac{\langle\bar{u}u+\bar{s}s\rangle_1^*}{\langle\bar{u}u+\bar{s}s\rangle_0}. \tag{4.170}$$

Third diagram (nucleon loop in the middle)

The diagram can be written as:

$$\Pi_3(0) = (-1)(-1)(-\mathrm{i})^2 \int \frac{\mathrm{d}^3\boldsymbol{p}}{(2\pi)^3} \frac{1}{2p_0} [\mathrm{i}\mathcal{L}_{\frac{P^4+\mathrm{i}P^5}{\sqrt{2}}K^-}] \frac{\mathrm{i}}{-m_K^2} \operatorname{Tr}\left\{(\not{p} + m_N) n(\boldsymbol{p}) [\mathrm{i}\mathcal{L}_{\bar{N}NK^+K^-}]\right\} \\ \times \frac{\mathrm{i}}{-m_K^2} [\mathrm{i}\mathcal{L}_{\frac{P^4-\mathrm{i}P^5}{\sqrt{2}}K^+}]. \tag{4.171}$$

The vertices are:

$$[\mathrm{i}\mathcal{L}_{\frac{P^4+\mathrm{i}P^5}{\sqrt{2}}K^-}] = 2\mathrm{i}B_0 f, \tag{4.172a}$$

$$[\mathrm{i}\mathcal{L}_{\frac{P^4-\mathrm{i}P^5}{\sqrt{2}}K^+}] = 2\mathrm{i}B_0 f, \tag{4.172b}$$

$$[\mathrm{i}\mathcal{L}_{\bar{p}pK^+K^-}] = -\frac{4\mathrm{i}B_0(m+m_s)(b_0+b_D)}{f^2}, \tag{4.172c}$$

$$[\mathrm{i}\mathcal{L}_{\bar{n}nK^+K^-}] = -\frac{2\mathrm{i}B_0(m+m_s)(2b_0+b_D-b_F)}{f^2}. \tag{4.172d}$$

We can simplify this to:

$$\Pi_3(0) = \frac{8\mathrm{i}B_0^3(m+m_s)m_N}{\pi^2 m_K^4} \int \mathrm{d}p\, \frac{p^2}{p_0} \left[2(b_0+b_D)\Theta_{\boldsymbol{p}}^p + (2b_0+b_D-b_F)\Theta_{\boldsymbol{p}}^n\right]. \tag{4.173}$$

We recall Eq. (4.9) and divide by the vacuum condensate $\langle \bar{u}u + \bar{s}s\rangle_0 = -2B_0 f^2$:

$$\frac{\langle \bar{u}u+\bar{s}s\rangle_3^*}{\langle \bar{u}u+\bar{s}s\rangle_0} = \frac{-\mathrm{i}\frac{m+m_s}{2}\Pi_3(0)}{-2B_0f^2} \\ = -\frac{2B_0^2(m+m_s)^2 m_N}{\pi^2 m_K^4 f^2} \int \mathrm{d}p\, \frac{p^2}{p_0} \left[2(b_0+b_D)\Theta_{\boldsymbol{p}}^p + (2b_0+b_D-b_F)\Theta_{\boldsymbol{p}}^n\right]. \tag{4.174}$$

Lastly, we use $B_0(m+m_s) = m_K^2$:

$$\frac{\langle \bar{u}u+\bar{s}s\rangle_3^*}{\langle \bar{u}u+\bar{s}s\rangle_0} = -\frac{2m_N}{\pi^2 f^2} \int \mathrm{d}p\, \frac{p^2}{p_0} \left[2(b_0+b_D)\Theta_{\boldsymbol{p}}^p + (2b_0+b_D-b_F)\Theta_{\boldsymbol{p}}^n\right]. \tag{4.175}$$

Result

Since our calculations showed that:

$$\frac{\langle \bar{u}u+\bar{s}s\rangle_1^*}{\langle \bar{u}u+\bar{s}s\rangle_0} = \frac{\langle \bar{u}u+\bar{s}s\rangle_2^*}{\langle \bar{u}u+\bar{s}s\rangle_0} = -\frac{\langle \bar{u}u+\bar{s}s\rangle_3^*}{\langle \bar{u}u+\bar{s}s\rangle_0}, \tag{4.176}$$

the result is:

$$\frac{\langle \bar{u}u+\bar{s}s\rangle^*}{\langle \bar{u}u+\bar{s}s\rangle_0} = \frac{2m_N}{\pi^2 f^2} \int \mathrm{d}p\, \frac{p^2}{p_0} \left[2(b_0+b_D)\Theta_{\boldsymbol{p}}^p + (2b_0+b_D-b_F)\Theta_{\boldsymbol{p}}^n\right]. \tag{4.177}$$

We can expand this in the large m_N limit:

$$\frac{\langle \bar{u}u+\bar{s}s\rangle^*}{\langle \bar{u}u+\bar{s}s\rangle_0} = \frac{2\rho}{(1+r)f^2} \left[2(b_0+b_D) + r(2b_0+b_D-b_F)\right]. \tag{4.178}$$

4.4.5. Down plus strange quark condensate

In order to calculate $\langle \bar{d}d + \bar{s}s \rangle^*$, we need these diagrams:

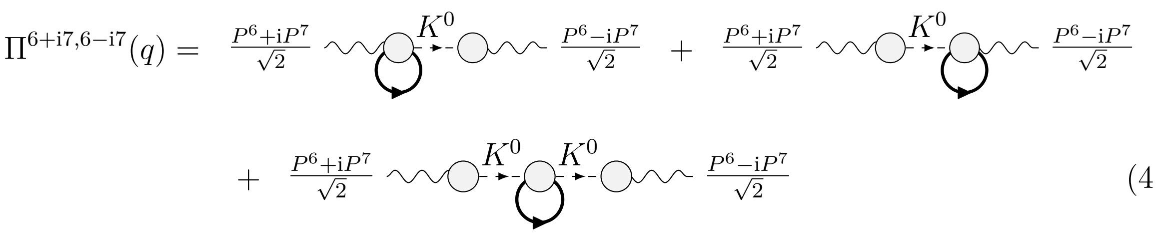

(4.179)

The necessary vertex factors are derived in Appendix A.1.4:

$$[\mathrm{i}\mathcal{L}_{\frac{P^6+\mathrm{i}P^7}{\sqrt{2}}\bar{K}^0}] = 2\mathrm{i}B_0 f, \tag{4.180a}$$

$$[\mathrm{i}\mathcal{L}_{\frac{P^6-\mathrm{i}P^7}{\sqrt{2}}K^0}] = 2\mathrm{i}B_0 f, \tag{4.180b}$$

$$[\mathrm{i}\mathcal{L}_{\bar{p}p\frac{P^6+\mathrm{i}P^7}{\sqrt{2}}K^0}] = \frac{4\mathrm{i}B_0(2b_0+b_D-b_F)}{f}, \tag{4.180c}$$

$$[\mathrm{i}\mathcal{L}_{\bar{n}n\frac{P^6+\mathrm{i}P^7}{\sqrt{2}}K^0}] = \frac{8\mathrm{i}B_0(b_0+b_D)}{f}, \tag{4.180d}$$

$$[\mathrm{i}\mathcal{L}_{\bar{p}p\frac{P^6-\mathrm{i}P^7}{\sqrt{2}}\bar{K}^0}] = \frac{4\mathrm{i}B_0(2b_0+b_D-b_F)}{f}, \tag{4.180e}$$

$$[\mathrm{i}\mathcal{L}_{\bar{n}n\frac{P^6-\mathrm{i}P^7}{\sqrt{2}}\bar{K}^0}] = \frac{8\mathrm{i}B_0(b_0+b_D)}{f}, \tag{4.180f}$$

$$[\mathrm{i}\mathcal{L}_{\bar{p}pK^0\bar{K}^0}] = -\frac{2\mathrm{i}B_0(m+m_s)(2b_0+b_D-b_F)}{f^2}, \tag{4.180g}$$

$$[\mathrm{i}\mathcal{L}_{\bar{n}nK^0\bar{K}^0}] = -\frac{4\mathrm{i}B_0(m+m_s)(b_0+b_D)}{f^2}. \tag{4.180h}$$

First diagram (nucleon loop on the left)

This is the first diagram:

$$\Pi_1(0) = (-1)(-1)(-\mathrm{i})^2 \int \frac{\mathrm{d}^3\boldsymbol{p}}{(2\pi)^3}\frac{1}{2p_0}\,\mathrm{Tr}\left\{(\not{p}+m_N)n(\boldsymbol{p})[\mathrm{i}\mathcal{L}_{\bar{N}N\frac{P^6+\mathrm{i}P^7}{\sqrt{2}}K^0}]\right\}\frac{\mathrm{i}}{-m_K^2}[\mathrm{i}\mathcal{L}_{\frac{P^6-\mathrm{i}P^7}{\sqrt{2}}K^0}]. \tag{4.181}$$

The necessary vertices are:

$$[\mathrm{i}\mathcal{L}_{\frac{P^6-\mathrm{i}P^7}{\sqrt{2}}K^0}] = 2\mathrm{i}B_0 f, \tag{4.182a}$$

$$[\mathrm{i}\mathcal{L}_{\bar{p}p\frac{P^6+\mathrm{i}P^7}{\sqrt{2}}K^0}] = \frac{4\mathrm{i}B_0(2b_0+b_D-b_F)}{f}, \tag{4.182b}$$

$$[\mathrm{i}\mathcal{L}_{\bar{n}n\frac{P^6+\mathrm{i}P^7}{\sqrt{2}}K^0}] = \frac{8\mathrm{i}B_0(b_0+b_D)}{f}. \tag{4.182c}$$

We can simplify this:

$$\begin{aligned}\Pi_1(0) &= -\frac{2B_0 f m_N}{\pi^2 m_K^2}\int \mathrm{d}p\,\frac{p^2}{p_0}\,\mathrm{Tr}\left\{n(\boldsymbol{p})[\mathrm{i}\mathcal{L}_{\bar{N}N\frac{P^6+\mathrm{i}P^7}{\sqrt{2}}K^0}]\right\}\\ &= -\frac{2B_0 f m_N}{\pi^2 m_K^2}\int \mathrm{d}p\,\frac{p^2}{p_0}\left[\Theta^p_{\boldsymbol{p}}[\mathrm{i}\mathcal{L}_{\bar{p}p\frac{P^6+\mathrm{i}P^7}{\sqrt{2}}K^0}] + \Theta^n_{\boldsymbol{p}}[\mathrm{i}\mathcal{L}_{\bar{n}n\frac{P^6+\mathrm{i}P^7}{\sqrt{2}}K^0}]\right]\\ &= -\frac{8\mathrm{i}B_0^2 m_N}{\pi^2 m_K^2}\int \mathrm{d}p\,\frac{p^2}{p_0}\left[(2b_0+b_D-b_F)\Theta^p_{\boldsymbol{p}} + 2(b_0+b_D)\Theta^n_{\boldsymbol{p}}\right].\end{aligned} \tag{4.183}$$

We recall Eq. (4.9) and divide by the vacuum condensate $\langle\bar{d}d+\bar{s}s\rangle_0 = -2B_0 f^2$:

$$\begin{aligned}\frac{\langle\bar{d}d+\bar{s}s\rangle_1^*}{\langle\bar{d}d+\bar{s}s\rangle_0} &= \frac{-\mathrm{i}\frac{m+m_s}{2}\Pi_1(0)}{-2B_0 f^2}\\ &= \frac{2B_0(m+m_s)m_N}{\pi^2 f^2 m_K^2}\int \mathrm{d}p\,\frac{p^2}{p_0}\left[(2b_0+b_D-b_F)\Theta^p_{\boldsymbol{p}} + 2(b_0+b_D)\Theta^n_{\boldsymbol{p}}\right].\end{aligned} \tag{4.184}$$

Finally, we use $B_0(m+m_s) = m_K^2$:

$$\frac{\langle\bar{d}d+\bar{s}s\rangle_1^*}{\langle\bar{d}d+\bar{s}s\rangle_0} = \frac{2m_N}{\pi^2 f^2}\int \mathrm{d}p\,\frac{p^2}{p_0}\left[(2b_0+b_D-b_F)\Theta^p_{\boldsymbol{p}} + 2(b_0+b_D)\Theta^n_{\boldsymbol{p}}\right]. \tag{4.185}$$

Second diagram (nucleon loop on the right)

Since K^0 and $\bar{K}^0$ have the same mass and the vertices are also the same, this is the same as the first diagram:

$$\frac{\langle\bar{d}d+\bar{s}s\rangle_2^*}{\langle\bar{d}d+\bar{s}s\rangle_0} = \frac{\langle\bar{d}d+\bar{s}s\rangle_1^*}{\langle\bar{d}d+\bar{s}s\rangle_0}. \tag{4.186}$$

Third diagram (nucleon loop in the middle)

The diagram is:

$$\begin{aligned}\Pi_3(0) = (-1)(-1)(-\mathrm{i})^2\int \frac{\mathrm{d}^3\boldsymbol{p}}{(2\pi)^3}\frac{1}{2p_0}[\mathrm{i}\mathcal{L}_{\frac{P^6+\mathrm{i}P^7}{\sqrt{2}}\bar{K}^0}]\frac{\mathrm{i}}{-m_K^2}\,\mathrm{Tr}\left\{(\not{p}+m_N)n(\boldsymbol{p})[\mathrm{i}\mathcal{L}_{\bar{N}NK^0\bar{K}^0}]\right\}\\ \times\frac{\mathrm{i}}{-m_K^2}[\mathrm{i}\mathcal{L}_{\frac{P^6-\mathrm{i}P^7}{\sqrt{2}}K^0}]\end{aligned} \tag{4.187}$$

The relevant vertices for this diagram are:

$$[\mathrm{i}\mathcal{L}_{\frac{P^6+\mathrm{i}P^7}{\sqrt{2}}\bar{K}^0}] = 2\mathrm{i}B_0 f, \tag{4.188a}$$

$$[\mathrm{i}\mathcal{L}_{\frac{P^6-\mathrm{i}P^7}{\sqrt{2}}K^0}] = 2\mathrm{i}B_0 f, \tag{4.188b}$$

$$[\mathrm{i}\mathcal{L}_{\bar{p}pK^0\bar{K}^0}] = -\frac{2\mathrm{i}B_0(m+m_s)(2b_0+b_D-b_F)}{f^2}, \tag{4.188c}$$

$$[\mathrm{i}\mathcal{L}_{\bar{n}nK^0\bar{K}^0}] = -\frac{4\mathrm{i}B_0(m+m_s)(b_0+b_D)}{f^2}. \tag{4.188d}$$

We can simplify this to:

$$\Pi_3(0) = \frac{8\mathrm{i}B_0^3(m+m_s)m_N}{\pi^2 m_K^4} \int \mathrm{d}p\, \frac{p^2}{p_0} \left[(2b_0+b_D-b_F)\Theta^p_{\boldsymbol{p}} + 2(b_0+b_D)\Theta^n_{\boldsymbol{p}}\right]. \tag{4.189}$$

We recall Eq. (4.9) and divide by the vacuum condensate $\langle \bar{d}d + \bar{s}s\rangle_0 = -2B_0 f^2$:

$$\begin{aligned}\frac{\langle \bar{d}d + \bar{s}s\rangle_3^*}{\langle \bar{d}d + \bar{s}s\rangle_0} &= \frac{-\mathrm{i}\frac{m+m_s}{2}\Pi_3(0)}{-2B_0 f^2} \\ &= -\frac{2B_0^2(m+m_s)^2 m_N}{\pi^2 m_K^4 f^2} \int \mathrm{d}p\, \frac{p^2}{p_0} \left[(2b_0+b_D-b_F)\Theta^p_{\boldsymbol{p}} + 2(b_0+b_D)\Theta^n_{\boldsymbol{p}}\right]. \end{aligned}\tag{4.190}$$

Lastly, we use $B_0(m+m_s) = m_K^2$ to remove the LEC B_0:

$$\frac{\langle \bar{d}d + \bar{s}s\rangle_3^*}{\langle \bar{d}d + \bar{s}s\rangle_0} = -\frac{2m_N}{\pi^2 f^2} \int \mathrm{d}p\, \frac{p^2}{p_0} \left[(2b_0+b_D-b_F)\Theta^p_{\boldsymbol{p}} + 2(b_0+b_D)\Theta^n_{\boldsymbol{p}}\right]. \tag{4.191}$$

Result

Since our calculations showed that:

$$\frac{\langle \bar{d}d + \bar{s}s\rangle_1^*}{\langle \bar{d}d + \bar{s}s\rangle_0} = \frac{\langle \bar{d}d + \bar{s}s\rangle_2^*}{\langle \bar{d}d + \bar{s}s\rangle_0} = -\frac{\langle \bar{d}d + \bar{s}s\rangle_3^*}{\langle \bar{d}d + \bar{s}s\rangle_0}, \tag{4.192}$$

the result is:

$$\frac{\langle \bar{d}d + \bar{s}s\rangle^*}{\langle \bar{d}d + \bar{s}s\rangle_0} = \frac{2m_N}{\pi^2 f^2} \int \mathrm{d}p\, \frac{p^2}{p_0} \left[(2b_0+b_D-b_F)\Theta^p_{\boldsymbol{p}} + 2(b_0+b_D)\Theta^n_{\boldsymbol{p}}\right], \tag{4.193}$$

and we can expand this in the large m_N limit:

$$\frac{\langle \bar{d}d + \bar{s}s\rangle^*}{\langle \bar{d}d + \bar{s}s\rangle_0} = \frac{2\rho}{(1+r)f^2} \left[(2b_0+b_D-b_F) + 2r(b_0+b_D)\right]. \tag{4.194}$$

4.4.6. Results: strange quark condensate

We isolate the strange condensate as follows:

$$\frac{\langle \bar{s}s\rangle^*}{\langle \bar{s}s\rangle_0} = \frac{\langle \bar{u}u + \bar{s}s\rangle^*}{\langle \bar{u}u + \bar{s}s\rangle_0} + \frac{\langle \bar{d}d + \bar{s}s\rangle^*}{\langle \bar{d}d + \bar{s}s\rangle_0} - \frac{\langle \bar{u}u + \bar{d}d\rangle^*}{\langle \bar{u}u + \bar{d}d\rangle_0}, \tag{4.195}$$

where we assume $\langle \bar{u}u\rangle_0 = \langle \bar{d}d\rangle_0 = \langle \bar{s}s\rangle_0$ for simplicity. If we use Eqs. (4.160), (4.178) and (4.194), this yields the linear density approximation:

$$\frac{\langle \bar{s}s\rangle^*}{\langle \bar{s}s\rangle_0} = \frac{4\rho}{f^2}\left[b_0+b_D-b_F\right]. \tag{4.196}$$

This expression is independent of the neutron-to-proton ratio. Since we assume isospin symmetry, the up and down quarks have the same mass. And because the strong interactions do

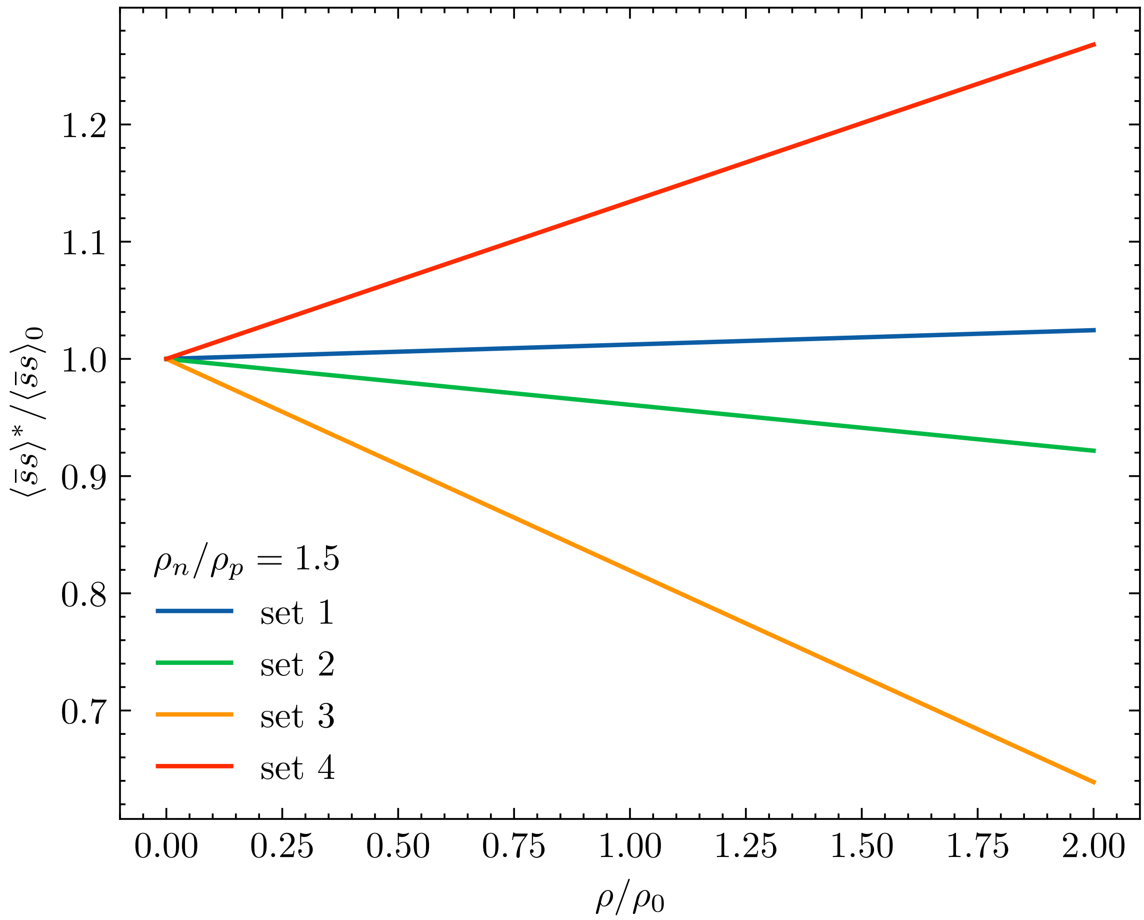

Figure 4.7.: Linear density approximation of the density dependence of the strange quark condensate in nuclear matter. According to Eq. (4.196), all results are independent of the nucleon ratio $r = \rho_n/\rho_p$ in the linear density approximation.

not distinguish between quark flavors, the strange quark cannot distinguish a proton from a neutron, hence the ratio does not play a role.

Looking at Fig. 4.7, we see that the results strongly depend on the choice of the low-energy constants. There are two main ways to determine the low-energy constants of an SU(3) chiral Lagrangian. First, one can calculate expressions for e.g. the octet baryon masses and fit them to either experimentally obtained data, or data obtained via lattice QCD calculations. Second, one can calculate certain quantities and fit them to scattering data. In fact, future research is planned to pursue the second option: By fitting to K^+N scattering data[3], we aim to determine a set of SU(3) LECs.

[3] K^+N scattering is preferable over K^-N scattering, since in K^+N scattering there cannot be a $\Lambda(1405)$ resonance due to baryon number conservation.

5. In-Medium Pion Properties

Since the dynamical breaking of QCD's chiral symmetry may be responsible for the bulk of all hadron masses, a potential partial restoration of chiral symmetry should lead to changes in various hadron properties. In order to investigate this, we compute the pion self-energy in isospin-asymmetric nuclear matter, which enables us to deduce the density dependence of the pion in-medium mass, as well as the pion in-medium wave function renormalization. We also investigate a different set of diagrams in order to compute the density dependence of the in-medium pion decay constant. This chapter presents the results of the corresponding diagrams, which will be discussed in the following chapter.

The first section, Section 5.1, follows Ref. [72] and defines the various in-medium pion properties that we aim to compute within the scope of this thesis. In Sections 5.2 and 5.3, we compute the diagrams for the self-energy and present our results for the in-medium pion mass. In Section 5.4, we show how to compute the wave function renormalization and discuss the results of our calculations. Next, in Section 5.5, we discuss the pion decay constant first in vacuum and then in nuclear matter. Afterwards, we calculate the required diagrams in Section 5.6 and discuss the results in Section 5.7.

5.1. In-medium pions

When the pion operator π^a with $a = 1, 2, 3$ acts on the in-medium vacuum $|\Omega\rangle$, it creates an in-medium pion state with mass m_π^* and wave function renormalization Z. In other words, this operator satisfies:

$$\langle \Omega | \pi^a | \pi^{*b}(p) \rangle = \delta^{ab} \sqrt{Z}, \tag{5.1}$$

where the in-medium pion state having momentum p^μ is denoted with $|\pi^{*a}(p)\rangle$. The in-vacuum pion state is conventionally normalized according to the covariant normalization:

$$\langle \pi^a(k) | \pi^b(p) \rangle = (2\pi)^3 2\omega_p \delta^{(3)}(\boldsymbol{p} - \boldsymbol{k}). \tag{5.2}$$

We now define the in-medium pion mass as the pole position of the in-medium pion propagator, where here and in the following equations the limit of $\epsilon \to 0$ has to be taken:

$$\langle \Omega | \pi^a \pi^b | \Omega \rangle = \frac{\mathrm{i}Z}{p_0^2 - v_\pi^2 \boldsymbol{p}^2 - m_\pi^{*2} + \mathrm{i}\epsilon}, \tag{5.3}$$

or written in terms of in-vacuum quantities,

$$\langle\Omega|\pi^a\pi^b|\Omega\rangle = \frac{\mathrm{i}}{p^2 - m_\pi^2 - \Sigma(p) + \mathrm{i}\epsilon}. \tag{5.4}$$

How the in-medium mass, wave function renormalization and velocity are related to the self-energy Σ is the topic of the next section.

The coupling of the in-medium pion state $|\pi^{*a}(p)\rangle$ to a pseudoscalar current is given by the in-medium coupling constant G_π^*:

$$\langle\Omega|P|\pi^*\rangle = G_\pi^*. \tag{5.5}$$

Since the pseudoscalar current is related to the pion field in vacuum via $P = \hat{G}_\pi \pi$, we can either calculate G_π^* to be:

$$G_\pi^* = \langle\Omega|P|\pi^*\rangle = \hat{G}_\pi\langle\Omega|\pi|\pi^*\rangle = \hat{G}_\pi\sqrt{Z}, \tag{5.6}$$

where we used Eq. (5.1) in the last equality. This can also be explicitly shown by using the LSZ reduction formula (roughly speaking, changing the pion from a state to an operator leads to an inverse propagator):

$$G_\pi^* = \langle\Omega|P|\pi^*\rangle = \left[\frac{\mathrm{i}\sqrt{Z}}{p_0^2 - v_\pi^2\boldsymbol{p}^2 - m_\pi^{*2} + \mathrm{i}\epsilon}\right]^{-1}\langle\Omega|P\pi|\Omega\rangle \tag{5.7a}$$

$$= \left[\frac{\mathrm{i}\sqrt{Z}}{p_0^2 - v_\pi^2\boldsymbol{p}^2 - m_\pi^{*2} + \mathrm{i}\epsilon}\right]^{-1}\hat{G}_\pi\langle\Omega|\pi\pi|\Omega\rangle \tag{5.7b}$$

$$= \left[\frac{\mathrm{i}\sqrt{Z}}{p_0^2 - v_\pi^2\boldsymbol{p}^2 - m_\pi^{*2} + \mathrm{i}\epsilon}\right]^{-1}\hat{G}_\pi\left[\frac{\mathrm{i}Z}{p_0^2 - v_\pi^2\boldsymbol{p}^2 - m_\pi^{*2} + \mathrm{i}\epsilon}\right] \tag{5.7c}$$

$$= \hat{G}\sqrt{Z}, \tag{5.7d}$$

which agrees with Eq. (5.6).

The connection between $\hat{G}_\pi$ and G_π^* can also be seen in the pseudoscalar two-point function,

$$\Pi = \langle\Omega|PP|\Omega\rangle = G_\pi^*\frac{\mathrm{i}}{p_0^2 - v_\pi^2\boldsymbol{p}^2 - m_\pi^{*2} + \mathrm{i}\epsilon}G_\pi^* + \text{other}, \tag{5.8}$$

where "other" stands for regular terms near the pion pole. This can also be written in terms of in-vacuum quantities:

$$\Pi = \hat{G}_\pi\frac{\mathrm{i}}{p^2 - m_\pi^2 - \Sigma + \mathrm{i}\epsilon}\hat{G}_\pi + \text{other}. \tag{5.9}$$

By using $G_\pi^* = \sqrt{Z}\hat{G}_\pi$, we can also write this as:

$$\Pi = \hat{G}_\pi\frac{\mathrm{i}Z}{p_0^2 - v_\pi^2\boldsymbol{p}^2 - m_\pi^{*2} + \mathrm{i}\epsilon}\hat{G}_\pi + \text{other}. \tag{5.10}$$

5.1.1. Pion mass and wave function renormalization

We start with the pseudoscalar two-point correlation function in nuclear matter:

$$\Pi^{ab}(x,y) = \langle \Omega | P^a(x) P^b(y) | \Omega \rangle. \tag{5.11}$$

This correlation function has a pole in momentum space when $p^2 = m_\pi^{*2}$. We can write this in terms of in-medium pion quantities,

$$\Pi = \langle \Omega | PP | \Omega \rangle = G_\pi^* \frac{\mathrm{i}}{p_0^2 - v_\pi^2 \boldsymbol{p}^2 - m_\pi^{*2} + \mathrm{i}\epsilon} G_\pi^* + \text{other}. \tag{5.12}$$

Here, G_π^* is defined as the pseudoscalar coupling between the pseudoscalar current and the pion, m_π^* and v_π are the pion's in-medium mass and velocity respectively and we disregard all other terms that might contribute to Π^{ab}, but have no divergence at the pion pole. Since we assume G_π^* not to have any singularity at the pion pole, we can extract the in-medium pion mass for $\boldsymbol{p} = 0$ using $p_0^2 = m_\pi^{*2}$ and the residue of this two-point correlation function can be interpreted as G_π^{*2}.

The pseudoscalar two-point correction function can also be written in terms of in-vacuum quantities,

$$\Pi = \hat{G}_\pi \frac{\mathrm{i}}{p^2 - m_\pi^2 - \Sigma + \mathrm{i}\epsilon} \hat{G}_\pi + \text{other}, \tag{5.13}$$

where m_π is the pion's vacuum mass, which we take to be $m_\pi = 138$ MeV. $\Sigma(p^2)$ is the pion's self-energy, where $\Sigma > 0$ leads to an increase in the in-medium pion mass. Lastly, quantities with a caret like $\hat{G}_\pi$ represent vertex corrections. In particular, $\hat{G}_\pi$ stands for the in-medium vertex correction of the pion-pseudoscalar vertex. These vertex corrections are calculated by drawing one-particle irreducible (1PI) diagrams. In Section 5.5, we will consider another such vertex correction, the correction to the pion decay constant.

We now expand the self-energy in Eq. (5.13) in a Taylor series around the point $p = (p^0, \boldsymbol{p}) = (m_\pi^{*2}, \mathbf{0})$:

$$\Sigma(p^2) = \Sigma(m_\pi^{*2}) + (p_0^2 - m_\pi^{*2}) \left.\frac{\partial \Sigma(p^2)}{\partial p_0^2}\right|_{p=(m_\pi^{*2},\mathbf{0})} + \boldsymbol{p}^2 \left.\frac{\partial \Sigma(p^2)}{\partial \boldsymbol{p}^2}\right|_{p=(m_\pi^{*2},\mathbf{0})} + \cdots \tag{5.14}$$

We can then write the fraction in Eq. (5.13) as:

$$\begin{aligned} &[p^2 - m_\pi^2 - \Sigma(p^2)]^{-1} \approx \\ &\quad \left[p_0^2 - \boldsymbol{p}^2 - m_\pi^2 - \Sigma(m_\pi^{*2}) - (p_0^2 - m_\pi^{*2}) \left.\frac{\partial \Sigma(p^2)}{\partial p_0^2}\right|_{p=(m_\pi^{*2},\mathbf{0})} - \boldsymbol{p}^2 \left.\frac{\partial \Sigma(p^2)}{\partial \boldsymbol{p}^2}\right|_{p=(m_\pi^{*2},\mathbf{0})} \right]^{-1}. \end{aligned} \tag{5.15}$$

First, we define the pion's in-medium mass:

$$m_\pi^{*2} = m_\pi^2 + \Sigma(m_\pi^{*2}), \tag{5.16}$$

and can simplify the expression in Eq. (5.15):

$$[p^2 - m_\pi^2 - \Sigma(p^2)]^{-1} \approx \left[(p_0^2 - m_\pi^{*2})\left(1 - \frac{\partial\Sigma(p^2)}{\partial p_0^2}\bigg|_{p=(m_\pi^{*2},\mathbf{0})}\right) - \boldsymbol{p}^2 - \boldsymbol{p}^2\frac{\partial\Sigma(p^2)}{\partial\boldsymbol{p}^2}\bigg|_{p=(m_\pi^{*2},\mathbf{0})}\right]^{-1}. \tag{5.17}$$

Then we define the pion's wave function renormalization Z in terms of the self-energy:

$$Z = \left(1 - \frac{\partial\Sigma(p^2)}{\partial p_0^2}\bigg|_{p=(m_\pi^{*2},\mathbf{0})}\right)^{-1}, \tag{5.18}$$

and write Eq. (5.15) as:

$$[p^2 - m_\pi^2 - \Sigma(p^2)]^{-1} \approx \left[(p_0^2 - m_\pi^{*2})\frac{1}{Z} - \boldsymbol{p}^2\left(1 + \frac{\partial\Sigma(p^2)}{\partial\boldsymbol{p}^2}\bigg|_{p=(m_\pi^{*2},\mathbf{0})}\right)\right]^{-1}. \tag{5.19}$$

Finally, we define the pion's in-medium velocity:

$$v_\pi^2 = \left(1 + \frac{\partial\Sigma(p^2)}{\partial\boldsymbol{p}^2}\bigg|_{p=(m_\pi^{*2},\mathbf{0})}\right) Z. \tag{5.20}$$

This lets us write the pseudoscalar two-point correlation function in Eq. (5.13) as:

$$\Pi = \hat{G}_\pi \frac{\mathrm{i}Z}{p_0^2 - v_\pi^2\boldsymbol{p}^2 - m_\pi^{*2} + \mathrm{i}\epsilon}\hat{G}_\pi + \text{other}, \tag{5.21}$$

where $\boldsymbol{p}_v = v_\pi\boldsymbol{p}$ is the pion's in-medium momentum. By comparing the pseudoscalar two-point function written completely in terms of in-medium quantities in Eq. (5.12) with this new expression, we can read off the relation between the in-medium pion-pseudoscalar vertex G_π^* and the in-medium correction to this vertex: $G_\pi^* = \sqrt{Z}\hat{G}_\pi$, which we discussed in the previous section.

The reason why we expanded the self-energy in order to arrive at Eq. (5.21), is that using chiral perturbation theory, we can calculate both the pion's self-energy, as well as the vertex correction $\hat{G}_\pi$. Thus, by using Eqs. (5.16), (5.18) and (5.20), it is possible to calculate the in-medium quantities m_π^*, Z and v_π.

5.2. Calculation of the in-medium pion self-energy

We discuss in detail how we chose the relevant diagrams in Section 4.2 and list them in Table 5.1. These tables are organized as follows. For each type of diagram, there can be an interaction from $A^{(1)}$ or $A^{(2)}$. Hence, for each diagram we investigate all possible cases of interactions, $i \in \{1, 2\}$ for one vertex or $(i, j) \in \{11, 12, 21, 22\}$ for two vertices. If such a vertex does not exist (because there is no corresponding term in the Lagrangian) we disregard the whole diagram. Still, some diagrams might vanish in the course of the calculation, which will be shown later on. In summary, we will calculate one type-1 diagram, two type-2 diagrams, one type-3 diagrams, four type-4 diagrams and one type-5 diagram:

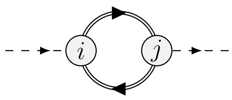

i	1	1	$\cancel{2}^{(1)}$	$\cancel{2}^{(1)}$
j	1	$\cancel{2}^{(1)}$	1	$\cancel{2}^{(1)}$

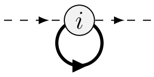

i	1	2

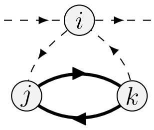

i	$\cancel{1}^{(3)}$	$\cancel{1}^{(3)}$	$\cancel{1}^{(3)}$	$\cancel{1}^{(3)}$	2	2	2	2
j	1	1	$\cancel{2}^{(1)}$	$\cancel{2}^{(1)}$	1	1	$\cancel{2}^{(1)}$	$\cancel{2}^{(1)}$
k	1	$\cancel{2}^{(1)}$	1	$\cancel{2}^{(1)}$	1	$\cancel{2}^{(1)}$	1	$\cancel{2}^{(1)}$

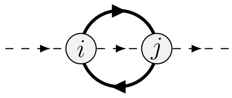

i	1	1	2	2
j	1	2	1	2

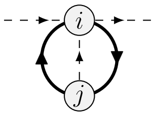

i	1	1	$\cancel{2}^{(2)}$	$\cancel{2}^{(2)}$
j	1	$\cancel{2}^{(1)}$	1	$\cancel{2}^{(1)}$

Table 5.1.: Self-energy diagrams. The superscript (1) denotes that the corresponding diagram vanishes because of $A_\pi^{(2)} = 0$, (2) because of $A_{\pi^3}^{(2)} = 0$, and (3) because of $\mathcal{L}_{\pi^4}^{(1)} = 0$. In total, nine diagrams remain. We will see that the type-4 diagrams are actually $\mathcal{O}(\rho^2)$, i.e. they are out of the scope of this thesis.

and the total self energy is given by the sum over all diagrams. For our calculations, we will fix the external momentum as $q^\mu = (q^0, \mathbf{0})^\mu$, i.e. we consider the pion at rest.

5.2.1. One-loop diagrams of type 1

This self-energy diagram is given by

$$-\mathrm{i}\Sigma_1^{ab}(q^0) = \quad \pi^a(q)$$ 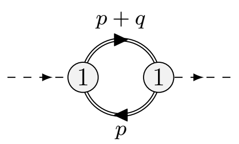 $$\pi^b(q) \tag{5.22}$$

This actually corresponds to four diagrams, one where there are two vacuum propagators, two with one vacuum- and one in-medium propagator, and one with two in-medium propagators. We discard the first one with only vacuum propagators, since we assume that the values for our LECs are already fixed in vacuum. We can also ignore the last one, since if both nucleons are on the mass-shell, this means $p^2 = m_N^2$ and $(p+q)^2 = p^2 + 2p_0q_0 + q_0^2 = m_N^2$, while also $p_0 > 0$ and $p_0 + q_0 > 0$. Using the first two equations, we get the relation $2p_0q_0 + q_0^2 = 0$, which we can solve for $p_0 = -q_0/2$. Since the external pion energy must be positive, $q_0 > 0$, this contradicts the requirement for the nucleon momentum $p_0 > 0$. Therefore we can discard this diagram.

The two remaining diagrams are:

$$-\mathrm{i}\Sigma^{ab}_{1a}(q^0) = \quad \pi^a(q)$$
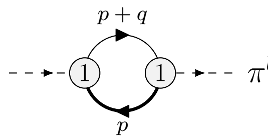
$$\pi^b(q) \quad , \tag{5.23a}$$

$$-\mathrm{i}\Sigma^{ab}_{1b}(q^0) = \quad \pi^a(q)$$
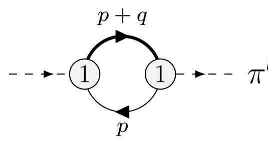
$$\pi^b(q) \quad . \tag{5.23b}$$

The thin line represents an in-vacuum propagator and the thick line represents the in-medium propagator. The diagrams in Eq. (5.23) illustrate the expansion of $A[\mathbb{1}_4 - D_0^{-1}A]^{-1}$ in second order to $AD_0^{-1}A$, i.e. including an in-vacuum propagator. This is equivalent to the so-called "conventional approach" of nuclear many-body calculations, which involves a Pauli-blocked nucleon propagator (which can only have momenta above the Fermi momentum), denoted here with a double-stroke line. This equivalence has been shown by Ref. [68].

These diagrams are now given by the following expressions:

$$\begin{aligned}
-\mathrm{i}\Sigma^{ab}_{1a}(q^0) = (-1)^L \frac{(-1)^n}{n} \int \frac{\mathrm{d}^3\boldsymbol{p}}{(2\pi)^3} \frac{1}{2E(\boldsymbol{p})} \frac{\mathrm{i}}{(p+q)^2 - m_N^2} \\
\times \operatorname{Tr}\left\{[-\mathrm{i}A^{(1)}_\pi]^a(\not{p} + m_N)n(\boldsymbol{p})[-\mathrm{i}A^{(1)}_\pi]^b(\not{p} + \not{q} + m_N)\right\}\Big|_{p^0 \to E(\boldsymbol{p})} \quad ,
\end{aligned} \tag{5.24a}$$

$$\begin{aligned}
-\mathrm{i}\Sigma^{ab}_{1b}(q^0) = (-1)^L \frac{(-1)^n}{n} \int \frac{\mathrm{d}^3\boldsymbol{p}}{(2\pi)^3} \frac{1}{2E(\boldsymbol{p}+\boldsymbol{q})} \frac{\mathrm{i}}{p^2 - m_N^2} \\
\times \operatorname{Tr}\left\{[-\mathrm{i}A^{(1)}_\pi]^a(\not{p} + m_N)[-\mathrm{i}A^{(1)}_\pi]^b(\not{p} + \not{q} + m_N)n(\boldsymbol{p}+\boldsymbol{q})\right\}\Big|_{p^0 \to E(\boldsymbol{p}) - q_0} \quad .
\end{aligned} \tag{5.24b}$$

The relevant term in the Lagrangian reads:

$$A^{(1)}_\pi = \frac{g_A}{2f}\gamma^\mu\gamma^5\partial_\mu\pi^i\tau^i, \tag{5.25}$$

and the vertex factors are for both diagrams:

$$[-\mathrm{i}A^{(1)}_\pi]^a = -\frac{g_A}{2f}\not{q}\gamma^5\tau^a, \tag{5.26a}$$

$$[-\mathrm{i}A^{(1)}_\pi]^b = \frac{g_A}{2f}\not{q}\gamma^5\tau^b. \tag{5.26b}$$

The trace in spinor space is the same for both diagrams:

$$\operatorname{Tr}_S\left\{\not{q}\gamma^5(\not{p} + m_N)\not{q}\gamma^5(\not{p} + \not{q} + m_N)\right\} = -4q_0^2(m_N^2 - p_0^2 - \boldsymbol{p}^2 - p_0q_0), \tag{5.27}$$

however, p_0 is to be replaced by different terms for the two diagrams. Since we assume a pion at rest, $\boldsymbol{q} = \boldsymbol{0}$, the traces in isospin space are similar:

$$\mathrm{Tr}_F\left\{\tau^b n(\boldsymbol{p})\tau^a\right\} = (\Theta_p^p + \Theta_p^n)\delta^{ab} + (\Theta_p^p - \Theta_p^n)\mathrm{i}\epsilon^{ab3}, \tag{5.28a}$$

$$\mathrm{Tr}_F\left\{\tau^b \tau^a n(\boldsymbol{p})\right\} = (\Theta_p^p + \Theta_p^n)\delta^{ab} - (\Theta_p^p - \Theta_p^n)\mathrm{i}\epsilon^{ab3}. \tag{5.28b}$$

Collecting all coefficients, we can write the sum of the two diagrams as:

$$\begin{aligned}\Sigma_1^{ab}(q) = \frac{g_A^2}{16\pi^2 f^2}\int \mathrm{d}p \frac{p^2}{E(p)} \\ \times \begin{cases} \left[\left.\frac{\mathrm{Tr}_S\{\cdots\}}{p_0^2-p^2+2p_0q_0+q_0^2-m_N^2}\right|_{p^0\to E(\boldsymbol{p})} + \left.\frac{\mathrm{Tr}_S\{\cdots\}}{p_0^2-p^2-m_N^2}\right|_{p^0\to E(\boldsymbol{p})-q_0} \right] (\Theta_p^p + \Theta_p^n)\,\delta^{ab} \\ \left[\left.\frac{\mathrm{Tr}_S\{\cdots\}}{p_0^2-p^2+2p_0q_0+q_0^2-m_N^2}\right|_{p^0\to E(\boldsymbol{p})} - \left.\frac{\mathrm{Tr}_S\{\cdots\}}{p_0^2-p^2-m_N^2}\right|_{p^0\to E(\boldsymbol{p})-q_0} \right] (\Theta_p^p - \Theta_p^n)\,\mathrm{i}\epsilon^{ab3} \end{cases} .\end{aligned} \tag{5.29}$$

The terms inside the integral can be simplified:

$$\left.\frac{\mathrm{Tr}_S\{\cdots\}}{p_0^2 - p^2 + 2p_0q_0 + q_0^2 - m_N^2}\right|_{p^0\to E(\boldsymbol{p})} + \left.\frac{\mathrm{Tr}_S\{\cdots\}}{p_0^2 - p^2 - m_N^2}\right|_{p^0\to E(\boldsymbol{p})-q_0} = \frac{16 m_N^2 q_0^2}{4E(p)^2 - q_0^2}, \tag{5.30a}$$

$$\left.\frac{\mathrm{Tr}_S\{\cdots\}}{p_0^2 - p^2 + 2p_0q_0 + q_0^2 - m_N^2}\right|_{p^0\to E(\boldsymbol{p})} - \left.\frac{\mathrm{Tr}_S\{\cdots\}}{p_0^2 - p^2 - m_N^2}\right|_{p^0\to E(\boldsymbol{p})-q_0} = \frac{8E(p)q_0(4p^2 - q_0^2)}{4E(p)^2 - q_0^2}, \tag{5.30b}$$

so that the first self-energy diagram is given by:

$$\Sigma_1^{ab}(q) = \frac{g_A^2 q_0^2}{4\pi^2 f^2}\int \mathrm{d}p \frac{p^2}{E(p)} \begin{cases} \frac{4m_N^2}{4E(p)^2-q_0^2}(\Theta_p^p + \Theta_p^n)\,\delta^{ab} \\ \frac{2E(p)}{q_0}\frac{4p^2-q_0^2}{4E(p)^2-q_0^2}(\Theta_p^p - \Theta_p^n)\,\mathrm{i}\epsilon^{ab3} \end{cases} . \tag{5.31}$$

After performing the first integral analytically, we can expand the diagonal part of the self-energy as follows:

$$\Sigma_1^{\mathrm{diag}}(q) = \frac{g_A^2 m_N q_0^2 \rho}{f^2(4m_N^2 - q_0^2)} + \mathcal{O}(\rho^{4/3}). \tag{5.32}$$

5.2.2. One-loop diagrams of type 2

Leading Order Interactions

The next self energy diagram is given by:

$$-\mathrm{i}\Sigma_{2a}^{ab}(q) = \tag{5.33a}$$

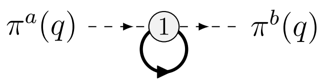

$$= (-1)^L \frac{(-1)^n}{n}\int \frac{\mathrm{d}^3\boldsymbol{p}}{(2\pi)^3}\frac{1}{2E(\boldsymbol{p})}\,\mathrm{Tr}\left\{[-\mathrm{i}A_{\pi\pi}^{(1)}]^{ab}(\not{p} + m_N)n(\boldsymbol{p})\right\}, \tag{5.33b}$$

with $L = 1$ and $n = 1$. The relevant term in the Lagrangian is:

$$A^{(1)}_{\pi\pi} = \frac{1}{4f^2}\gamma^\mu \pi^i \partial_\mu \pi^j \epsilon^{ijk}\tau^k. \tag{5.34}$$

The vertex reads,

$$[-\mathrm{i}A^{(1)}_{\pi\pi}]^{ab} = \frac{1}{2f^2}\not{q}\epsilon^{abc}\tau^c. \tag{5.35}$$

The traces are:

$$\mathrm{Tr}_S\left\{\not{q}(\not{p}+m)\right\} = 4p\cdot q = 4p_0 q_0, \tag{5.36a}$$

$$\mathrm{Tr}_F\left\{\tau^c n(\boldsymbol{p})\right\} = (\Theta^p_{\boldsymbol{p}} - \Theta^n_{\boldsymbol{p}})\delta^{c3}, \tag{5.36b}$$

and the diagram is given by:

$$\Sigma^{ab}_{2a}(q) = \frac{q_0}{f^2}\int\frac{\mathrm{d}^3\boldsymbol{p}}{(2\pi)^3}(\Theta^p_{\boldsymbol{p}} - \Theta^n_{\boldsymbol{p}})\mathrm{i}\epsilon^{ab3} \tag{5.37a}$$

$$= \frac{q_0}{2f^2}(\rho_p - \rho_n)\mathrm{i}\epsilon^{ab3}. \tag{5.37b}$$

Written in terms of the total density ρ and the neutron-to-proton ratio, the second diagram reads:

$$\Sigma^{ab}_{2a}(q) = \frac{q_0\,\rho}{2f^2}\frac{1-r}{1+r}\mathrm{i}\epsilon^{ab3}. \tag{5.38}$$

Next-to-leading order interactions

The next self energy diagram is given by

$$-\mathrm{i}\Sigma^{ab}_{2b}(q) = \tag{5.39a}$$

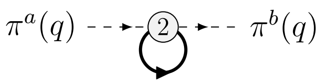

$$= (-1)^L\frac{(-1)^n}{n}\int\frac{\mathrm{d}^3\boldsymbol{p}}{(2\pi)^3}\frac{1}{2E(\boldsymbol{p})}\,\mathrm{Tr}\left\{[-\mathrm{i}A^{(2)}_{\pi\pi}]^{ab}(\not{p}+m_N)n(\boldsymbol{p})\right\}, \tag{5.39b}$$

where $(-1)^L$ accounts for $L = 1$ fermionic loop, $\frac{(-1)^n}{n}$ must be included for $n = 1$ Fermi-sea insertions. Also, since the nucleon is on its mass shell, p^0 must be replaced with $E(\boldsymbol{p})$. The relevant term in the Lagrangian reads:

$$A^{(2)}_{\pi\pi} = \frac{4B_0c_1m}{f^2}\pi^i\pi^i + \frac{c_2}{f^2m_N^2}\partial_\mu\pi^i\partial_\nu\pi^i\partial^\mu\partial^\nu - \frac{c_3}{f^2}\partial_\mu\pi^i\partial^\mu\pi^i + \frac{\mathrm{i}c_4}{f^2}\epsilon^{ijk}\tau^k\gamma^\mu\gamma^\nu\partial_\mu\pi^i\partial_\nu\pi^j, \tag{5.40}$$

and thus the vertex factor is:

$$[-\mathrm{i}A^{(2)}_{\pi\pi}]^{ab} = -\frac{8\mathrm{i}c_1B_0m}{f^2}\delta^{ab} + \frac{2\mathrm{i}c_2}{f^2m_N^2}(q\cdot p)^2\delta^{ab} + \frac{2\mathrm{i}c_3}{f^2}q^2\delta^{ab} + \frac{2c_4}{f^2}q^2\epsilon^{abk}\tau^k \tag{5.41a}$$

$$= -\frac{8\mathrm{i}c_1B_0m}{f^2}\delta^{ab} + \frac{2\mathrm{i}c_2}{f^2m_N^2}q_0^2E(\boldsymbol{p})^2\delta^{ab} + \frac{2\mathrm{i}c_3}{f^2}q_0^2\delta^{ab} + \frac{2c_4}{f^2}q_0^2\epsilon^{abk}\tau^k. \tag{5.41b}$$

The trace in spinor space is easily evaluated,

$$\mathrm{Tr}_S\left\{\not{p} + m_N\right\} = 4m_N, \tag{5.42}$$

and the for the trace in isospin space we have two different terms:

$$\mathrm{Tr}_F\{n(\boldsymbol{p})\} = \Theta^p_{\boldsymbol{p}} + \Theta^n_{\boldsymbol{p}}, \tag{5.43a}$$

$$\mathrm{Tr}_F\left\{\tau^k n(\boldsymbol{p})\right\} = (\Theta^p_{\boldsymbol{p}} - \Theta^n_{\boldsymbol{p}})\delta^{k3}. \tag{5.43b}$$

We can now split the self-energy into a diagonal part, proportional to δ^{ab}, and an off-diagonal part, proportional to $\mathrm{i}\epsilon^{ab3}$:

$$\Sigma^{ab}_{2b}(q) = \frac{2m_N q_0^2}{f^2\pi^2}\int \mathrm{d}p \frac{p^2}{E(p)} \begin{cases} \left(\frac{4c_1 B_0 m}{q_0^2} - \frac{c_2(p^2+m_N^2)}{m_N^2} - c_3\right)[\Theta^p_{\boldsymbol{p}} + \Theta^n_{\boldsymbol{p}}]\delta^{ab} \\ c_4[\Theta^p_{\boldsymbol{p}} - \Theta^n_{\boldsymbol{p}}]\mathrm{i}\epsilon^{ab3} \end{cases}. \tag{5.44}$$

One can now use the following integral results:

$$\int_0^A \mathrm{d}p\, p^2\sqrt{p^2+m_N^2} = \frac{1}{8}\left[A^2\sqrt{A^2+m_N^2}(2A^2+m_N^2) - m_N^4 \sinh^{-1}(A/m_N)\right], \tag{5.45a}$$

$$\int_0^A \mathrm{d}p\, \frac{p^2}{\sqrt{p^2+m_N^2}} = \frac{1}{2}\left[A\sqrt{A^2+m_N^2} - m_N^2\tanh^{-1}\left(\frac{A}{\sqrt{A^2+m_N^2}}\right)\right], \tag{5.45b}$$

to get an analytic result. For example, the diagonal part of the self-energy is given by:

$$\Sigma^{\mathrm{diag}}_2(q) = \frac{\rho(4c_1 m_\pi^2 - 2q_0^2(c_2+c_3))}{f^2} + \mathcal{O}(\rho^{4/3}). \tag{5.46}$$

5.2.3. Two-loop diagrams of type 3

The next self energy diagram is given by:

$$-\mathrm{i}\Sigma^{ab}_3(q) = \tag{5.47a}$$

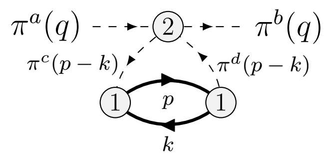

$$= (-1)^L\frac{(-1)^n}{n}\frac{1}{2}\int\frac{\mathrm{d}^3\boldsymbol{p}}{(2\pi^3)}\frac{\mathrm{d}^3\boldsymbol{k}}{(2\pi^3)}\frac{1}{4p_0k_0}[\mathrm{i}\mathcal{L}^{(2)}_{\pi^4}]^{abcd}\left[\frac{\mathrm{i}}{(p-k)^2-m_\pi^2}\right]^2$$

$$\times\ \mathrm{Tr}\left\{[-\mathrm{i}A^{(1)}_\pi]^c(\not{k}+m_N)n(\boldsymbol{k})[-\mathrm{i}A^{(1)}_\pi]^d(\not{p}+m_N)n(\boldsymbol{p})\right\}, \tag{5.47b}$$

where $(-1)^L$ accounts for $L=1$ fermionic loop, $\frac{(-1)^n}{n}$ must be included for $n=2$ Fermi-sea insertions. Additionally, we include a symmetry factor of $1/2$. Since the nucleons are on their mass shell, p^0 must be replaced with $\sqrt{\boldsymbol{p}^2+m_N^2}$ and k^0 by $\sqrt{\boldsymbol{k}^2+m_N^2}$. The relevant terms in the Lagrangian read:

$$\mathcal{L}_{\pi^4}^{(2)} = \frac{1}{10f^2}\partial_\mu\pi^i\partial^\mu\pi^j\pi^k\pi^l(3\delta^{ik}\delta^{jl}-\delta^{ij}\delta^{kl}) - \frac{mB_0}{20f^2}\pi^i\pi^i\pi^j\pi^j, \tag{5.48a}$$

$$A_\pi^{(1)} = \frac{g_A}{2f}\gamma^\mu\gamma^5\partial_\mu\pi^i\tau^i, \tag{5.48b}$$

and the corresponding vertex factors are:

$$\begin{aligned}[\mathrm{i}\mathcal{L}_{\pi^4}^{(2)}]^{abcd} = -\frac{\mathrm{i}}{5f^2}\Big[&2[(p-k)^2+q_0^2]\delta_{cd}^{ab}\\ &-\Big[3[(p-k)^2+q_0^2]-10(p_0-k_0)q_0\Big]\,\delta_{bd}^{ac}\\ &-\Big[3[(p-k)^2+q_0^2]+10(p_0-k_0)q_0\Big]\,\delta_{bc}^{ad}\\ &+2B_0m(\delta_{cd}^{ab}+\delta_{bd}^{ac}+\delta_{bc}^{ad})\Big],\end{aligned} \tag{5.49a}$$

$$[-\mathrm{i}A_\pi^{(1)}]^c = -\frac{g_A}{2f}(\not{p}-\not{k})\gamma^5\tau^c, \tag{5.49b}$$

$$[-\mathrm{i}A_\pi^{(1)}]^d = \frac{g_A}{2f}(\not{p}-\not{k})\gamma^5\tau^d. \tag{5.49c}$$

For later convenience, we write the four-pion vertex in the following way:

$$[\mathrm{i}\mathcal{L}_{\pi^4}^{(2)}]^{abcd} = -\frac{\mathrm{i}}{5f^2}[v_1\delta_{cd}^{ab}+v_2\delta_{bd}^{ac}+v_3\delta_{bc}^{ad}], \tag{5.50a}$$

$$v_1 = 2(p-k)^2+2q_0^2+2B_0m, \tag{5.50b}$$

$$v_2 = -3(p-k)^2-3q_0^2+10(p_0-k_0)q_0+2B_0m, \tag{5.50c}$$

$$v_3 = -3(p-k)^2-3q_0^2-10(p_0-k_0)q_0+2B_0m. \tag{5.50d}$$

The trace in spinor space is:

$$\mathrm{Tr}_S\Big\{(\not{p}-\not{k})\gamma^5(\not{k}+m_N)(\not{p}-\not{k})\gamma^5(\not{p}+m_N)\Big\} = 16m_N^2(p_0k_0-pk\cos\theta-m_N^2), \tag{5.51}$$

where we used $p^2=m_N^2=k^2$ since both nucleons are on the mass shell. The trace in isospin space is:

$$[\mathrm{i}\mathcal{L}_{\pi^4}^{(2)}]^{abcd}\,\mathrm{Tr}_F\Big\{\tau^c n(\boldsymbol{k})\tau^d n(\boldsymbol{p})\Big\} = -\frac{\mathrm{i}}{5f^2} \times\begin{cases} v_1(\Theta_{\boldsymbol{p}}^p\Theta_{\boldsymbol{k}}^p+\Theta_{\boldsymbol{p}}^n\Theta_{\boldsymbol{k}}^n)\delta^{ab}+(2v_1+v_2+v_3)(\Theta_{\boldsymbol{p}}^p\Theta_{\boldsymbol{k}}^n+\Theta_{\boldsymbol{p}}^n\Theta_{\boldsymbol{k}}^p)\delta^{ab}\\ (v_2-v_3)(\Theta_{\boldsymbol{p}}^p\Theta_{\boldsymbol{k}}^n-\Theta_{\boldsymbol{p}}^n\Theta_{\boldsymbol{k}}^p)\mathrm{i}\epsilon^{ab3}\\ (v_2+v_3)(\Theta_{\boldsymbol{p}}^p\Theta_{\boldsymbol{k}}^p-\Theta_{\boldsymbol{p}}^p\Theta_{\boldsymbol{k}}^n-\Theta_{\boldsymbol{p}}^n\Theta_{\boldsymbol{k}}^p+\Theta_{\boldsymbol{p}}^n\Theta_{\boldsymbol{k}}^n)\delta_{b3}^{a3}\end{cases}, \tag{5.52}$$

where $\Theta^x_{\boldsymbol{y}}$ is an abbreviation for $\Theta(k^x_F - |\boldsymbol{y}|)$, the Heaviside step function that ensures that the nucleon's momentum stays below the Fermi momentum. The third self-energy diagram can now be written as:

$$\Sigma^{ab}_3(q) = -\frac{g_A^2 m_N^2}{10(2\pi f)^4}\int \mathrm{d}p\,\mathrm{d}k\,\mathrm{d}\cos\theta \frac{p^2k^2}{p_0k_0}\frac{p_0k_0 - pk\cos\theta - m_N^2}{(2m_N^2 - m_\pi^2 - 2p_0k_0 + 2pk\cos\theta)^2}$$
$$\times\begin{cases} v_1(\Theta^p_{\boldsymbol{p}}\Theta^p_{\boldsymbol{k}} + \Theta^n_{\boldsymbol{p}}\Theta^n_{\boldsymbol{k}})\delta^{ab} + (2v_1 + v_2 + v_3)(\Theta^p_{\boldsymbol{p}}\Theta^n_{\boldsymbol{k}} + \Theta^n_{\boldsymbol{p}}\Theta^p_{\boldsymbol{k}})\delta^{ab} \\ (v_2 - v_3)(\Theta^p_{\boldsymbol{p}}\Theta^n_{\boldsymbol{k}} - \Theta^n_{\boldsymbol{p}}\Theta^p_{\boldsymbol{k}})\mathrm{i}\epsilon^{ab3} \\ (v_2 + v_3)(\Theta^p_{\boldsymbol{p}}\Theta^p_{\boldsymbol{k}} - \Theta^p_{\boldsymbol{p}}\Theta^n_{\boldsymbol{k}} - \Theta^n_{\boldsymbol{p}}\Theta^p_{\boldsymbol{k}} + \Theta^n_{\boldsymbol{p}}\Theta^n_{\boldsymbol{k}})\delta^{a3}_{b3} \end{cases}. \tag{5.53}$$

The vertex functions simplify a bit:

$$2v_1 + v_2 + v_3 = -2(p-k)^2 + 8B_0m, \tag{5.54a}$$
$$v_2 + v_3 = -6(p-k)^2 - 6q_0^2 + 4B_0m, \tag{5.54b}$$
$$v_2 - v_3 = 20(p_0 - k_0)q_0, \tag{5.54c}$$

where $(p-k)^2 = 2m_N^2 - 2p_0k_0 + 2pk\cos\theta$.

5.2.4. Two-loop diagrams of type 4

First diagram: (11)

$$-\mathrm{i}\Sigma^{ab}_{4,11}(q) =$$
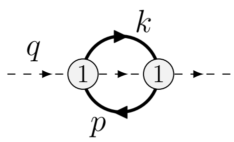

$$= (-1)\frac{(-1)^2}{2!}\int \frac{\mathrm{d}^3\boldsymbol{p}}{(2\pi)^3}\frac{\mathrm{d}^3\boldsymbol{k}}{(2\pi)^3}\frac{1}{4p_0k_0}\frac{\mathrm{i}}{(q+p-k)^2 - m_\pi^2}$$
$$\times \operatorname{Tr}\left\{[-\mathrm{i}A^{(1)}_{\pi\pi}]^{ac}(\not{p} + m_N)n(\boldsymbol{p})[-\mathrm{i}A^{(1)}_{\pi\pi}]^{cb}(\not{k} + m_N)n(\boldsymbol{k})\right\} \tag{5.55}$$

The vertex factors are:

$$[-\mathrm{i}A^{(1)}_{\pi\pi}]^{ac} = \frac{1}{4f^2}(2\not{q} - \not{k} + \not{p})\epsilon^{ack}\tau^k, \tag{5.56a}$$
$$[-\mathrm{i}A^{(1)}_{\pi\pi}]^{cb} = \frac{1}{4f^2}(2\not{q} - \not{k} + \not{p})\epsilon^{cbl}\tau^l. \tag{5.56b}$$

The result of the traces is:

$$\operatorname{Tr}\{\cdots\}^{ab} = \frac{16q_0^2}{(2f)^4}(p_0k_0 + \boldsymbol{p}\cdot\boldsymbol{k} + m_N^2)\begin{cases} -(\Theta^p_{\boldsymbol{p}}\Theta^p_{\boldsymbol{k}} + \Theta^p_{\boldsymbol{p}}\Theta^n_{\boldsymbol{k}} + \Theta^n_{\boldsymbol{p}}\Theta^p_{\boldsymbol{k}} + \Theta^n_{\boldsymbol{p}}\Theta^n_{\boldsymbol{k}})\;\delta^{ab} \\ (\Theta^p_{\boldsymbol{p}}\Theta^n_{\boldsymbol{k}} - \Theta^n_{\boldsymbol{p}}\Theta^p_{\boldsymbol{k}})\;\mathrm{i}\epsilon^{ab3} \\ (\Theta^p_{\boldsymbol{p}}\Theta^p_{\boldsymbol{k}} - \Theta^p_{\boldsymbol{p}}\Theta^n_{\boldsymbol{k}} - \Theta^n_{\boldsymbol{p}}\Theta^p_{\boldsymbol{k}} + \Theta^n_{\boldsymbol{p}}\Theta^n_{\boldsymbol{k}})\;\delta^{a3}_{b3} \end{cases}. \tag{5.57}$$

So the self-energy is given by:

$$\Sigma^{ab}_{4,11}(q) = \frac{q_0^2}{4(2\pi f)^4} \int \mathrm{d}p\,\mathrm{d}k\,\mathrm{d}(\cos\theta)\,\frac{p^2k^2}{p_0k_0}\frac{p_0k_0 + \boldsymbol{p}\cdot\boldsymbol{k} + m_N^2}{(q+p-k)^2 - m_\pi^2} \times \begin{cases} -(\Theta^p_{\boldsymbol{p}}\Theta^p_{\boldsymbol{k}} + \Theta^p_{\boldsymbol{p}}\Theta^n_{\boldsymbol{k}} + \Theta^n_{\boldsymbol{p}}\Theta^p_{\boldsymbol{k}} + \Theta^n_{\boldsymbol{p}}\Theta^n_{\boldsymbol{k}})\,\delta^{ab} \\ (\Theta^p_{\boldsymbol{p}}\Theta^n_{\boldsymbol{k}} - \Theta^n_{\boldsymbol{p}}\Theta^p_{\boldsymbol{k}})\,\mathrm{i}\epsilon^{ab3} \\ (\Theta^p_{\boldsymbol{p}}\Theta^p_{\boldsymbol{k}} - \Theta^p_{\boldsymbol{p}}\Theta^n_{\boldsymbol{k}} - \Theta^n_{\boldsymbol{p}}\Theta^p_{\boldsymbol{k}} + \Theta^n_{\boldsymbol{p}}\Theta^n_{\boldsymbol{k}})\,\delta^{a3}_{b3} \end{cases}. \tag{5.58}$$

If we expand this using the large-m_N expansion to first order, we get:

$$\Sigma^{ab}_{4,11}(q) = \frac{q_0^2}{2(2\pi f)^4} \int \mathrm{d}p\,\mathrm{d}k\,\mathrm{d}(\cos\theta)\,\frac{p^2k^2}{p^2 - 2\boldsymbol{p}\cdot\boldsymbol{k} + k^2 + m_\pi^2 - q_0^2} \times \begin{cases} (\Theta^p_{\boldsymbol{p}}\Theta^p_{\boldsymbol{k}} + \Theta^p_{\boldsymbol{p}}\Theta^n_{\boldsymbol{k}} + \Theta^n_{\boldsymbol{p}}\Theta^p_{\boldsymbol{k}} + \Theta^n_{\boldsymbol{p}}\Theta^n_{\boldsymbol{k}})\,\delta^{ab} \\ -(\Theta^p_{\boldsymbol{p}}\Theta^n_{\boldsymbol{k}} - \Theta^n_{\boldsymbol{p}}\Theta^p_{\boldsymbol{k}})\,\mathrm{i}\epsilon^{ab3} \\ -(\Theta^p_{\boldsymbol{p}}\Theta^p_{\boldsymbol{k}} - \Theta^p_{\boldsymbol{p}}\Theta^n_{\boldsymbol{k}} - \Theta^n_{\boldsymbol{p}}\Theta^p_{\boldsymbol{k}} + \Theta^n_{\boldsymbol{p}}\Theta^n_{\boldsymbol{k}})\,\delta^{a3}_{b3} \end{cases}. \tag{5.59}$$

We can perform the integration over $\mathrm{d}(\cos\theta)$:

$$\Sigma^{ab}_{4,11}(q) = \frac{q_0^2}{2(2\pi f)^4} \int \mathrm{d}p\,\mathrm{d}k\,pk\,\mathrm{arctanh}\left[\frac{2pk}{p^2 + k^2 + m_\pi^2 - q_0^2}\right] \times \begin{cases} (\Theta^p_{\boldsymbol{p}}\Theta^p_{\boldsymbol{k}} + \Theta^p_{\boldsymbol{p}}\Theta^n_{\boldsymbol{k}} + \Theta^n_{\boldsymbol{p}}\Theta^p_{\boldsymbol{k}} + \Theta^n_{\boldsymbol{p}}\Theta^n_{\boldsymbol{k}})\,\delta^{ab} \\ -(\Theta^p_{\boldsymbol{p}}\Theta^n_{\boldsymbol{k}} - \Theta^n_{\boldsymbol{p}}\Theta^p_{\boldsymbol{k}})\,\mathrm{i}\epsilon^{ab3} \\ -(\Theta^p_{\boldsymbol{p}}\Theta^p_{\boldsymbol{k}} - \Theta^p_{\boldsymbol{p}}\Theta^n_{\boldsymbol{k}} - \Theta^n_{\boldsymbol{p}}\Theta^p_{\boldsymbol{k}} + \Theta^n_{\boldsymbol{p}}\Theta^n_{\boldsymbol{k}})\,\delta^{a3}_{b3} \end{cases}. \tag{5.60}$$

Expanding the integrand reveals a $\mathcal{O}(p^2k^2)$ dependence,

$$pk\,\mathrm{arctanh}\left[\frac{2pk}{p^2 + k^2 + m_\pi^2 - q_0^2}\right] = p^2\left(\frac{2k^2}{m_\pi^2 - q_0^2} + O\left(k^3\right)\right) + O\left(p^3\right), \tag{5.61}$$

which means that after integrating this expression over $\mathrm{d}p$ and $\mathrm{d}k$, we get a $\mathcal{O}(p^3k^3)$ behavior, which corresponds to $\mathcal{O}(k_F^6) = \mathcal{O}(\rho^2)$. Hence, this diagram (and in fact all type-4 diagrams) are out of the scope of this thesis. We note that near $q_0 = m_\pi$, this expansion breaks down, because then, the quantity $p/(q_0 - m_\pi)$ is not a small quantity anymore.

Second diagram: (12)

The next self-energy diagram is:

$$-\mathrm{i}\Sigma^{ab}_{4,12}(q) =$$

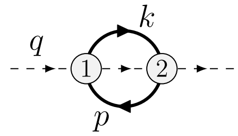

$$= (-1)\frac{(-1)^2}{2!}\int \frac{\mathrm{d}^3\boldsymbol{p}}{(2\pi)^3}\frac{\mathrm{d}^3\boldsymbol{k}}{(2\pi)^3}\frac{1}{4p_0k_0}\frac{\mathrm{i}}{(q+p-k)^2-m_\pi^2}$$
$$\times \operatorname{Tr}\left\{[-\mathrm{i}A^{(1)}_{\pi\pi}]^{ac}(\not{p}+m_N)n(\boldsymbol{p})[-\mathrm{i}A^{(2)}_{\pi\pi}]^{cb}(\not{k}+m_N)n(\boldsymbol{k})\right\}. \tag{5.62}$$

The vertex factors are:

$$[-\mathrm{i}A^{(1)}_{\pi\pi}]^{ac} = \frac{1}{4f^2}(2\not{q}-\not{k}+\not{p})\epsilon^{ack}\tau^k, \tag{5.63a}$$
$$[-\mathrm{i}A^{(2)}_{\pi\pi}]^{cb} = -\frac{\mathrm{i}}{f^2}\Big[C_R\delta^{bc} + c_4\mathrm{i}\epsilon^{cbl}\tau^l[\not{p}-\not{k},\not{q}]\Big], \tag{5.63b}$$
$$C_R \equiv 8c_1B_0m + \frac{2c_2}{m_N^2}q_0k_0(q_0k_0+p_0k_0-\boldsymbol{p}\cdot\boldsymbol{k}-k_0^2+\boldsymbol{k}^2) + 2c_3q_0(q_0+p_0-k_0).$$

The result of the traces is:

$$\operatorname{Tr}\{\ldots\} = \frac{6C_Rm_Nq_0(p_0+k_0)}{f^4}(\Theta^n_{\boldsymbol{p}}\Theta^n_{\boldsymbol{k}} - \Theta^p_{\boldsymbol{p}}\Theta^p_{\boldsymbol{k}})\mathrm{i}\epsilon^{ab3}$$
$$-\frac{4c_4m_Nq_0^2}{f^4}(\boldsymbol{p}^2-2\boldsymbol{p}\cdot\boldsymbol{k}+\boldsymbol{k}^2)\begin{cases}-(\Theta^p_{\boldsymbol{p}}+\Theta^n_{\boldsymbol{p}})(\Theta^p_{\boldsymbol{k}}+\Theta^n_{\boldsymbol{k}})\delta^{ab}\\ (\Theta^p_{\boldsymbol{p}}\Theta^n_{\boldsymbol{k}}-\Theta^n_{\boldsymbol{p}}\Theta^p_{\boldsymbol{k}})\mathrm{i}\epsilon^{ab3}\\ (\Theta^p_{\boldsymbol{p}}-\Theta^n_{\boldsymbol{p}})(\Theta^p_{\boldsymbol{k}}-\Theta^n_{\boldsymbol{k}})\delta^{a3}_{b3}\end{cases}. \tag{5.64}$$

We can simplify:

$$\Sigma^{ab}_{4,12}(q) = \frac{3m_Nq_0}{32\pi^4f^4}\int \mathrm{d}p\,\mathrm{d}k\,\mathrm{d}\cos\theta\frac{p^2k^2}{p_0k_0}\frac{C_R(p_0+k_0)}{q^2+2m_N^2+2q_0(p_0-k_0)-2p_0k_0+2pk\cos\theta-m_\pi^2}$$
$$\times(\Theta^n_{\boldsymbol{p}}\Theta^n_{\boldsymbol{k}}-\Theta^p_{\boldsymbol{p}}\Theta^p_{\boldsymbol{k}})\mathrm{i}\epsilon^{ab3}$$
$$+\frac{c_4m_Nq_0^2}{16\pi^4f^4}\int \mathrm{d}p\,\mathrm{d}k\,\mathrm{d}\cos\theta\frac{p^2k^2}{p_0k_0}\frac{p^2-2pk\cos\theta+k^2}{q^2+2m_N^2+2q_0(p_0-k_0)-2p_0k_0+2pk\cos\theta-m_\pi^2}$$
$$\times\begin{cases}(\Theta^p_{\boldsymbol{p}}+\Theta^n_{\boldsymbol{p}})(\Theta^p_{\boldsymbol{k}}+\Theta^n_{\boldsymbol{k}})\delta^{ab}\\ -(\Theta^p_{\boldsymbol{p}}\Theta^n_{\boldsymbol{k}}-\Theta^n_{\boldsymbol{p}}\Theta^p_{\boldsymbol{k}})\mathrm{i}\epsilon^{ab3}\\ -(\Theta^p_{\boldsymbol{p}}-\Theta^n_{\boldsymbol{p}})(\Theta^p_{\boldsymbol{k}}-\Theta^n_{\boldsymbol{k}})\delta^{a3}_{b3}\end{cases}. \tag{5.65}$$

We expand both terms in the large-m_N expansion and keep the leading order term:

$$\begin{aligned}
\Sigma^{ab}_{4,12}(q) = &\frac{3q_0(4c_1B_0m + c_2q_0^2 + c_3q_0^2)}{8\pi^4 f^4}\int \mathrm{d}p\,\mathrm{d}k\,\mathrm{d}\cos\theta \frac{p^2k^2}{p^2 - 2pk\cos\theta + k^2 + m_\pi^2 - q_0^2}\\
&\times (\Theta^p_{\boldsymbol{p}}\Theta^p_{\boldsymbol{k}} - \Theta^n_{\boldsymbol{p}}\Theta^n_{\boldsymbol{k}})\mathrm{i}\epsilon^{ab3}\\
&+ \frac{c_4q_0^2}{16\pi^4 f^4 m_N}\int \mathrm{d}p\,\mathrm{d}k\,\mathrm{d}\cos\theta \frac{p^2k^2(p^2 - 2pk\cos\theta + k^2)}{p^2 - 2pk\cos\theta + k^2 + m_\pi^2 - q_0^2}\\
&\times \begin{cases} -(\Theta^p_{\boldsymbol{p}} + \Theta^n_{\boldsymbol{p}})(\Theta^p_{\boldsymbol{k}} + \Theta^n_{\boldsymbol{k}})\delta^{ab}\\ (\Theta^p_{\boldsymbol{p}}\Theta^n_{\boldsymbol{k}} - \Theta^n_{\boldsymbol{p}}\Theta^p_{\boldsymbol{k}})\mathrm{i}\epsilon^{ab3}\\ (\Theta^p_{\boldsymbol{p}} - \Theta^n_{\boldsymbol{p}})(\Theta^p_{\boldsymbol{k}} - \Theta^n_{\boldsymbol{k}})\delta^{a3}_{b3}\end{cases}. \qquad (5.66)
\end{aligned}$$

If we set $q_0 = m_\pi$ and use $B_0m = m_\pi^2/2$:

$$\begin{aligned}
\Sigma^{ab}_{4,12} = &\frac{3m_\pi^3(2c_1 + c_2 + c_3)}{8\pi^4 f^4}\int \mathrm{d}p\,\mathrm{d}k\,\mathrm{d}\cos\theta \frac{p^2k^2}{p^2 - 2pk\cos\theta + k^2}\\
&\times (\Theta^p_{\boldsymbol{p}}\Theta^p_{\boldsymbol{k}} - \Theta^n_{\boldsymbol{p}}\Theta^n_{\boldsymbol{k}})\mathrm{i}\epsilon^{ab3}\\
&+ \frac{c_4m_\pi^2}{16\pi^4 f^4 m_N}\int \mathrm{d}p\,\mathrm{d}k\,\mathrm{d}\cos\theta\, p^2k^2 \begin{cases} -(\Theta^p_{\boldsymbol{p}} + \Theta^n_{\boldsymbol{p}})(\Theta^p_{\boldsymbol{k}} + \Theta^n_{\boldsymbol{k}})\delta^{ab}\\ (\Theta^p_{\boldsymbol{p}}\Theta^n_{\boldsymbol{k}} - \Theta^n_{\boldsymbol{p}}\Theta^p_{\boldsymbol{k}})\mathrm{i}\epsilon^{ab3}\\ (\Theta^p_{\boldsymbol{p}} - \Theta^n_{\boldsymbol{p}})(\Theta^p_{\boldsymbol{k}} - \Theta^n_{\boldsymbol{k}})\delta^{a3}_{b3}\end{cases}, \qquad (5.67)
\end{aligned}$$

hence this diagram also yields a $\mathcal{O}(\rho^2)$ dependence.

Third diagram: (21)

The next self-energy diagram is:

$$-\mathrm{i}\Sigma^{ab}_{4,21}(q) =$$

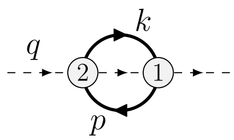

$$\begin{aligned}
&= (-1)\frac{(-1)^2}{2!}\int \frac{\mathrm{d}^3\boldsymbol{p}}{(2\pi)^3}\frac{\mathrm{d}^3\boldsymbol{k}}{(2\pi)^3}\frac{1}{4p_0k_0}\frac{\mathrm{i}}{(q + p - k)^2 - m_\pi^2}\\
&\quad\times \mathrm{Tr}\left\{[-\mathrm{i}A^{(2)}_{\pi\pi}]^{ac}(\not{p} + m_N)n(\boldsymbol{p})[-\mathrm{i}A^{(1)}_{\pi\pi}]^{cb}(\not{k} + m_N)n(\boldsymbol{k})\right\}. \qquad (5.68)
\end{aligned}$$

The vertex factors are:

$$[-\mathrm{i}A^{(2)}_{\pi\pi}]^{ac} = -\frac{\mathrm{i}}{f^2}\Big[C_L\delta^{ac} + c_4\mathrm{i}\epsilon^{cak}\tau^k[\not{p} - \not{k}, \not{q}]\Big], \qquad (5.69a)$$

$$C_L \equiv 8c_1B_0m + \frac{2c_2}{m_N^2}q_0p_0(q_0p_0 - p_0k_0 + \boldsymbol{p}\cdot\boldsymbol{k} + p_0^2 - \boldsymbol{p}^2) + 2c_3q_0(q_0 + p_0 - k_0),$$

$$[-\mathrm{i}A^{(1)}_{\pi\pi}]^{cb} = \frac{1}{4f^2}(2\not{q} - \not{k} + \not{p})\epsilon^{cbl}\tau^l. \qquad (5.69b)$$

The result of the traces is:

$$\mathrm{Tr}\,\{\ldots\} = \frac{6C_L m_N q_0(p_0+k_0)}{f^4}(\Theta^n_{\boldsymbol{p}}\Theta^n_{\boldsymbol{k}} - \Theta^p_{\boldsymbol{p}}\Theta^p_{\boldsymbol{k}})\mathrm{i}\epsilon^{ab3} + \frac{4c_4 m_N q_0^2}{f^4}(\boldsymbol{p}^2 - 2\boldsymbol{p}\cdot\boldsymbol{k} + \boldsymbol{k}^2)\begin{cases}(\Theta^p_{\boldsymbol{p}}+\Theta^n_{\boldsymbol{p}})(\Theta^p_{\boldsymbol{k}}+\Theta^n_{\boldsymbol{k}})\delta^{ab}\\ (\Theta^n_{\boldsymbol{p}}\Theta^p_{\boldsymbol{k}} - \Theta^p_{\boldsymbol{p}}\Theta^n_{\boldsymbol{k}})\mathrm{i}\epsilon^{ab3}\\ -(\Theta^p_{\boldsymbol{p}}-\Theta^n_{\boldsymbol{p}})(\Theta^p_{\boldsymbol{k}}-\Theta^n_{\boldsymbol{k}})\delta^{a3}_{b3}\end{cases}. \tag{5.70}$$

We can simplify this to:

$$\begin{aligned}\Sigma^{ab}_{4,21}(q) = {}& \frac{3C_L m_N q_0}{32\pi^4 f^4}\int \mathrm{d}p\,\mathrm{d}k\,\mathrm{d}\cos\theta \frac{p^2k^2}{p_0k_0}\frac{p_0+k_0}{q_0^2+2m_N^2+2q_0(p_0-k_0)-2p_0k_0+2pk\cos\theta - m_\pi^2}\\ &\times(\Theta^n_{\boldsymbol{p}}\Theta^n_{\boldsymbol{k}} - \Theta^p_{\boldsymbol{p}}\Theta^p_{\boldsymbol{k}})\mathrm{i}\epsilon^{ab3}\\ &+\frac{c_4 m_N q_0^2}{16\pi^4 f^4}\int \mathrm{d}p\,\mathrm{d}k\,\mathrm{d}\cos\theta \frac{p^2k^2}{p_0k_0}\frac{p^2-2pk\cos\theta+k^2}{q_0^2+2m_N^2+2q_0(p_0-k_0)-2p_0k_0+2pk\cos\theta - m_\pi^2}\\ &\times\begin{cases}(\Theta^p_{\boldsymbol{p}}+\Theta^n_{\boldsymbol{p}})(\Theta^p_{\boldsymbol{k}}+\Theta^n_{\boldsymbol{k}})\delta^{ab}\\ (\Theta^n_{\boldsymbol{p}}\Theta^p_{\boldsymbol{k}} - \Theta^p_{\boldsymbol{p}}\Theta^n_{\boldsymbol{k}})\mathrm{i}\epsilon^{ab3}\\ -(\Theta^p_{\boldsymbol{p}}-\Theta^n_{\boldsymbol{p}})(\Theta^p_{\boldsymbol{k}}-\Theta^n_{\boldsymbol{k}})\delta^{a3}_{b3}\end{cases},\end{aligned} \tag{5.71}$$

and expand both terms in the large-m_N expansion while keeping the leading order terms:

$$\begin{aligned}\Sigma^{ab}_{4,21}(q) = {}& \frac{3q_0(4c_1B_0m + c_2q_0^2 + c_3q_0^2)}{8\pi^4 f^4}\int \mathrm{d}p\,\mathrm{d}k\,\mathrm{d}\cos\theta\frac{p^2k^2}{p^2-pk\cos\theta+k^2+m_\pi^2-q_0^2}\\ &\times(\Theta^p_{\boldsymbol{p}}\Theta^p_{\boldsymbol{k}} - \Theta^n_{\boldsymbol{p}}\Theta^n_{\boldsymbol{k}})\mathrm{i}\epsilon^{ab3}\\ &+\frac{c_4q_0^2}{16\pi^4f^4m_N}\int \mathrm{d}p\,\mathrm{d}k\,\mathrm{d}\cos\theta\frac{p^2k^2(p^2-2pk\cos\theta+k^2)}{p^2-pk\cos\theta+k^2+m_\pi^2-q_0^2}\\ &\times\begin{cases}-(\Theta^p_{\boldsymbol{p}}+\Theta^n_{\boldsymbol{p}})(\Theta^p_{\boldsymbol{k}}+\Theta^n_{\boldsymbol{k}})\delta^{ab}\\ (\Theta^p_{\boldsymbol{p}}\Theta^n_{\boldsymbol{k}} - \Theta^n_{\boldsymbol{p}}\Theta^p_{\boldsymbol{k}})\mathrm{i}\epsilon^{ab3}\\ (\Theta^p_{\boldsymbol{p}}-\Theta^n_{\boldsymbol{p}})(\Theta^p_{\boldsymbol{k}}-\Theta^n_{\boldsymbol{k}})\delta^{a3}_{b3}\end{cases}.\end{aligned} \tag{5.72}$$

If we use $q_0 = m_\pi$ and $B_0m = m_\pi^2/2$:

$$\begin{aligned}\Sigma^{ab}_{4,21} = {}& \frac{3m_\pi^3(2c_1+c_2+c_3)}{8\pi^4f^4}\int \mathrm{d}p\,\mathrm{d}k\,\mathrm{d}\cos\theta\frac{p^2k^2}{p^2-pk\cos\theta+k^2}\\ &\times(\Theta^p_{\boldsymbol{p}}\Theta^p_{\boldsymbol{k}} - \Theta^n_{\boldsymbol{p}}\Theta^n_{\boldsymbol{k}})\mathrm{i}\epsilon^{ab3}\\ &+\frac{c_4m_\pi^2}{16\pi^4f^4m_N}\int \mathrm{d}p\,\mathrm{d}k\,\mathrm{d}\cos\theta p^2k^2\\ &\times\begin{cases}-(\Theta^p_{\boldsymbol{p}}+\Theta^n_{\boldsymbol{p}})(\Theta^p_{\boldsymbol{k}}+\Theta^n_{\boldsymbol{k}})\delta^{ab}\\ (\Theta^p_{\boldsymbol{p}}\Theta^n_{\boldsymbol{k}} - \Theta^n_{\boldsymbol{p}}\Theta^p_{\boldsymbol{k}})\mathrm{i}\epsilon^{ab3}\\ (\Theta^p_{\boldsymbol{p}}-\Theta^n_{\boldsymbol{p}})(\Theta^p_{\boldsymbol{k}}-\Theta^n_{\boldsymbol{k}})\delta^{a3}_{b3}\end{cases}\end{aligned} \tag{5.73}$$

So in those limits, $\Sigma^{ab}_{4,12} = \Sigma^{ab}_{4,21}$, which means this diagram gives us a $\mathcal{O}(\rho^2)$ dependence.

Fourth diagram: (22)

The last type-4 self-energy diagram is:

$$-\mathrm{i}\Sigma^{ab}_{4,22}(q) = $$

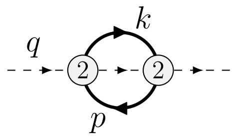

$$= (-1)\frac{(-1)^2}{2!}\int\frac{\mathrm{d}^3\boldsymbol{p}}{(2\pi)^3}\frac{\mathrm{d}^3\boldsymbol{k}}{(2\pi)^3}\frac{1}{4p_0k_0}\frac{\mathrm{i}}{(q+p-k)^2-m_\pi^2}$$
$$\times\,\mathrm{Tr}\left\{[-\mathrm{i}A^{(2)}_{\pi\pi}]^{ac}(\not{p}+m_N)n(\boldsymbol{p})[-\mathrm{i}A^{(2)}_{\pi\pi}]^{cb}(\not{k}+m_N)n(\boldsymbol{k})\right\}. \tag{5.74}$$

The vertex factors are:

$$[-\mathrm{i}A^{(2)}_{\pi\pi}]^{ac} = -\frac{\mathrm{i}}{f^2}\Big[C_L\delta^{ac}+c_4\mathrm{i}\epsilon^{cak}\tau^k[\not{p}-\not{k},\not{q}]\Big], \tag{5.75a}$$
$$C_L \equiv 8c_1B_0m+\frac{2c_2}{m_N^2}q_0p_0(q_0p_0-p_0k_0+\boldsymbol{p}\cdot\boldsymbol{k}+p_0^2-\boldsymbol{p}^2)+2c_3q_0(q_0+p_0-k_0),$$
$$[-\mathrm{i}A^{(2)}_{\pi\pi}]^{cb} = -\frac{\mathrm{i}}{f^2}\Big[C_R\delta^{bc}+c_4\mathrm{i}\epsilon^{cbl}\tau^l[\not{p}-\not{k},\not{q}]\Big], \tag{5.75b}$$
$$C_R \equiv 8c_1B_0m+\frac{2c_2}{m_N^2}q_0k_0(q_0k_0+p_0k_0-\boldsymbol{p}\cdot\boldsymbol{k}-k_0^2+\boldsymbol{k}^2)+2c_3q_0(q_0+p_0-k_0).$$

The result of the traces is:

$$\mathrm{Tr}\{\dots\} = -\frac{1}{f^4}\Big[4C_LC_R(p_0k_0-\boldsymbol{p}\cdot\boldsymbol{k}+m_N^2)(\Theta^p_{\boldsymbol{p}}\Theta^p_{\boldsymbol{k}}+\Theta^n_{\boldsymbol{p}}\Theta^n_{\boldsymbol{k}})\delta^{ab}$$
$$+8c_4(C_L+C_R)q_0(p_0+k_0)(m_N^2-p_0k_0+\boldsymbol{pk})(\Theta^p_{\boldsymbol{p}}\Theta^p_{\boldsymbol{k}}-\Theta^n_{\boldsymbol{p}}\Theta^n_{\boldsymbol{k}})\mathrm{i}\epsilon^{ab3}$$
$$+16c_4q_0^2\Big\{\Big[(p_0+k_0)^2-4m_N^2\Big][p_0k_0-\boldsymbol{pk}]+m_N^2[2p_0k_0-3p_0^2-3k_0^2+4m_N^2]\Big\}$$
$$\times\,[(\Theta^p_{\boldsymbol{p}}+\Theta^n_{\boldsymbol{p}})(\Theta^p_{\boldsymbol{k}}+\Theta^n_{\boldsymbol{k}})\delta^{ab}+(\Theta^n_{\boldsymbol{p}}\Theta^p_{\boldsymbol{k}}-\Theta^p_{\boldsymbol{p}}\Theta^n_{\boldsymbol{k}})\mathrm{i}\epsilon^{ab3}-(\Theta^p_{\boldsymbol{p}}-\Theta^n_{\boldsymbol{p}})(\Theta^p_{\boldsymbol{k}}-\Theta^n_{\boldsymbol{k}})\delta^{a3}_{b3}]\Big]. \tag{5.76}$$

In the large-m_N expansion to leading order, the integrand is:

$$\frac{\mathrm{Tr}\{\dots\}}{p_0k_0((q+p-k)^2-m_\pi^2)} = \frac{32(4c_1B_0m+c_2q_0^2+c_3q_0^2)^2}{f^4(p^2-2pk\cos\theta+k^2+m_\pi^2-q_0^2)}(\Theta^p_{\boldsymbol{p}}\Theta^p_{\boldsymbol{k}}+\Theta^n_{\boldsymbol{p}}\Theta^n_{\boldsymbol{k}})\delta^{ab}+\mathcal{O}(1/m_N), \tag{5.77}$$

so the self-energy is:

$$\Sigma^{ab}_{4,22}(q) = \frac{(4c_1B_0m+c_2q_0^2+c_3q_0^2)^2}{2\pi^4f^4}\int\mathrm{d}p\,\mathrm{d}k\,\mathrm{d}\cos\theta\, p^2k^2\frac{(\Theta^p_{\boldsymbol{p}}\Theta^p_{\boldsymbol{k}}+\Theta^n_{\boldsymbol{p}}\Theta^n_{\boldsymbol{k}})\delta^{ab}}{(p^2-2pk\cos\theta+k^2+m_\pi^2-q_0^2)} \tag{5.78}$$

Now we use $B_0m = m_\pi^2/2$ and $q_0 = m_\pi$:

$$\Sigma^{ab}_{4,22}(q) = \delta^{ab}\frac{m_\pi^2(2c_1+c_2+c_3)^2}{2\pi^4f^4}\int\mathrm{d}p\,\mathrm{d}k\,\mathrm{d}\cos\theta\, p^2k^2\frac{(\Theta^p_{\boldsymbol{p}}\Theta^p_{\boldsymbol{k}}+\Theta^n_{\boldsymbol{p}}\Theta^n_{\boldsymbol{k}})}{(p^2-2pk\cos\theta+k^2)}, \tag{5.79}$$

which means this diagrams yields a $\mathcal{O}(\rho^2)$ dependence as well.

5.2.5. Two-loop diagrams of type 5

The next self energy diagram is:

$$-\mathrm{i}\Sigma_5^{ab}(q^0) = \tag{5.80a}$$

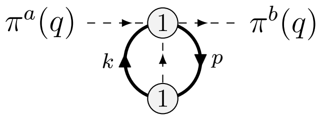

$$= (-1)^L \frac{(-1)^n}{n} \int \frac{\mathrm{d}^3\boldsymbol{p}}{(2\pi)^3} \frac{\mathrm{d}^3\boldsymbol{k}}{(2\pi)^3} \frac{1}{4p_0k_0} \frac{\mathrm{i}}{(p-k)^2 - m_\pi^2}$$
$$\times \operatorname{Tr}\left\{[-\mathrm{i}A_{\pi^3}^{(1)}]^{abc}(\not{k} + m_N)n(\boldsymbol{k})[-\mathrm{i}A_\pi^{(1)}]^c(\not{p} + m_N)n(\boldsymbol{p})\right\}, \tag{5.80b}$$

where $L = 1$, $n = 2$ and we have to replace $p^0 = \sqrt{\boldsymbol{p}^2 + m_N^2}$ and $k^0 = \sqrt{\boldsymbol{k}^2 + m_N^2}$. The pion momentum is $p^\mu - k^\mu$, going in the upwards direction. The relevant terms in the Lagrangian are:

$$A_\pi^{(1)} = \frac{g_A}{2f}\gamma^\mu\gamma^5\partial_\mu\pi^i\tau^i, \tag{5.81a}$$
$$A_{\pi^3}^{(1)} = \frac{g_A}{20f^3}\gamma^\mu\gamma^5\left[3\pi^i\pi^j\partial_\mu\pi^j - \pi^j\pi^j\partial_\mu\pi^i\right]\tau^i, \tag{5.81b}$$

and the vertices are:

$$[-\mathrm{i}A_{\pi^3}^{(1)}]^{abc} = \frac{g_A}{20f^3}\left[\delta_{bc}^{ia}(5\not{q} - 3\not{p} + 3\not{k}) + \delta_{ac}^{ib}(-5\not{q} - 3\not{p} + 3\not{k}) + \delta_{ab}^{ic}2(\not{p} - \not{k})\right]\gamma^5\tau^i, \tag{5.82a}$$
$$[-\mathrm{i}A_\pi^{(1)}]^c = \frac{g_A}{2f}(\not{p} - \not{k})\gamma^5\tau^c. \tag{5.82b}$$

The results for the traces over gamma matrices are are (we simplify using $p^2 = m_N^2 = k^2$):

$$\operatorname{Tr}_S\left\{(5\not{q} - 3\not{p} + 3\not{k})\gamma^5(\not{k} + m_N)(\not{p} - \not{k})\gamma^5(\not{p} + m_N)\right\}$$
$$= 8m_N^2(6m_N^2 - 5q_0(p_0 - k_0) - 6p_0k_0 + 6\boldsymbol{p}\cdot\boldsymbol{k}), \tag{5.83a}$$
$$\operatorname{Tr}_S\left\{(-5\not{q} - 3\not{p} + 3\not{k})\gamma^5(\not{k} + m_N)(\not{p} - \not{k})\gamma^5(\not{p} + m_N)\right\}$$
$$= 8m_N^2(6m_N^2 + 5q_0(p_0 - k_0) - 6p_0k_0 + 6\boldsymbol{p}\cdot\boldsymbol{k}), \tag{5.83b}$$
$$2\operatorname{Tr}_S\left\{(\not{p} - \not{k})\gamma^5(\not{k} + m_N)(\not{p} - \not{k})\gamma^5(\not{p} + m_N)\right\} = 32m_N^2(p_0k_0 - \boldsymbol{p}\cdot\boldsymbol{k} - m_N^2), \tag{5.83c}$$

and the traces over Pauli matrices are:

$$\delta_{bc}^{ia}\operatorname{Tr}_F\left\{\tau^i n(\boldsymbol{k})\tau^c n(\boldsymbol{p})\right\} = [\Theta_{\boldsymbol{p}}^p\Theta_{\boldsymbol{k}}^n + \Theta_{\boldsymbol{p}}^n\Theta_{\boldsymbol{k}}^p]\delta^{ab} + [\Theta_{\boldsymbol{p}}^p\Theta_{\boldsymbol{k}}^n - \Theta_{\boldsymbol{p}}^n\Theta_{\boldsymbol{k}}^p]\mathrm{i}\epsilon^{ab3}$$
$$+ (\Theta_{\boldsymbol{p}}^p - \Theta_{\boldsymbol{p}}^n)(\Theta_{\boldsymbol{k}}^p - \Theta_{\boldsymbol{k}}^n)\delta_{b3}^{a3}, \tag{5.84a}$$
$$\delta_{ac}^{ib}\operatorname{Tr}_F\left\{\tau^i n(\boldsymbol{k})\tau^c n(\boldsymbol{p})\right\} = [\Theta_{\boldsymbol{p}}^p\Theta_{\boldsymbol{k}}^n + \Theta_{\boldsymbol{p}}^n\Theta_{\boldsymbol{k}}^p]\delta^{ab} - [\Theta_{\boldsymbol{p}}^p\Theta_{\boldsymbol{k}}^n - \Theta_{\boldsymbol{p}}^n\Theta_{\boldsymbol{k}}^p]\mathrm{i}\epsilon^{ab3}$$
$$+ (\Theta_{\boldsymbol{p}}^p - \Theta_{\boldsymbol{p}}^n)(\Theta_{\boldsymbol{k}}^p - \Theta_{\boldsymbol{k}}^n)\delta_{b3}^{a3}, \tag{5.84b}$$
$$\delta_{ab}^{ic}\operatorname{Tr}_F\left\{\tau^i n(\boldsymbol{k})\tau^c n(\boldsymbol{p})\right\} = [\Theta_{\boldsymbol{p}}^p\Theta_{\boldsymbol{k}}^p + 2\Theta_{\boldsymbol{p}}^p\Theta_{\boldsymbol{k}}^n + 2\Theta_{\boldsymbol{p}}^n\Theta_{\boldsymbol{k}}^p + \Theta_{\boldsymbol{p}}^n\Theta_{\boldsymbol{k}}^n]\delta^{ab}. \tag{5.84c}$$

		$m^*_{\pi^-}/m_\pi$	$m^*_{\pi^0}/m_\pi$	$m^*_{\pi^+}/m_\pi$	$m^*_\pi/m_\pi(r=1)$
This work	LEC set 1	1.05	0.94	0.81	0.94
	LEC set 2	1.10	0.99	0.87	0.99
	LEC set 3	1.10	0.98	0.86	0.98
Theoretical	Ref. [97]	1.10	1.04	0.99	—
	Refs. [95, 98]	1.06	—	—	—
	Ref. [34]	1.13	—	—	—
	Ref. [99]	—	—	—	0.95
	Ref. [100]	—	—	—	1.03
Experimental	Ref. [101]	$1.17 \sim 1.20$	—	—	—
	Ref. [37]	1.22	—	—	—

Table 5.2.: Comparing the results for the in-medium pion mass at $r = 1.5$ (first three values) and at $r = 1$ (last column). The LEC sets refer to the values given in Table 3.1. All values correspond to densities at normal nuclear density: $\rho = \rho_0$.

Finally, the self-energy is given by:

$$\Sigma_5(q) = \frac{g_A^2 m_N^2}{10(2\pi f)^4} \int \mathrm{d}p\, \mathrm{d}k\, \mathrm{d}\cos\theta \, \frac{p^2 k^2}{p_0 k_0} \frac{1}{2m_N^2 - m_\pi^2 - 2p_0 k_0 + 2pk\cos\theta}$$
$$\begin{cases} 2(k_0 p_0 - pk\cos\theta - m_N^2)(\Theta^p_{\boldsymbol{p}}\Theta^p_{\boldsymbol{k}} - \Theta^p_{\boldsymbol{p}}\Theta^n_{\boldsymbol{k}} - \Theta^n_{\boldsymbol{p}}\Theta^p_{\boldsymbol{k}} + \Theta^n_{\boldsymbol{p}}\Theta^n_{\boldsymbol{k}})\delta^{ab} \\ 5q_0(k_0 - p_0)(\Theta^p_{\boldsymbol{p}}\Theta^n_{\boldsymbol{k}} - \Theta^n_{\boldsymbol{p}}\Theta^p_{\boldsymbol{k}})\mathrm{i}\epsilon^{ab3} \\ -6(k_0 p_0 - pk\cos\theta - m_N^2)(\Theta^p_{\boldsymbol{p}}\Theta^p_{\boldsymbol{k}} - \Theta^p_{\boldsymbol{p}}\Theta^n_{\boldsymbol{k}} - \Theta^n_{\boldsymbol{p}}\Theta^p_{\boldsymbol{k}} + \Theta^n_{\boldsymbol{p}}\Theta^n_{\boldsymbol{k}})\delta^{a3}_{b3}. \end{cases} \tag{5.85}$$

Note that for symmetrical nuclear matter (i.e. $\Theta^p_{\boldsymbol{p}} = \Theta^n_{\boldsymbol{p}}$), this diagram completely vanishes.

5.3. Results: Mass

We show the density dependence of the in-medium pion masses and their dependence on the nucleon ratios in Fig. 5.1, using the three sets of low-energy constants given in Table 3.1, and also in Table 5.2. The left column of Fig. 5.1 shows the three pion masses and their dependence on the nucleon density at a fixed ratio $\rho_n/\rho_p = 1.5$. The right column of Fig. 5.1 shows the same pion masses and how they depend on different nucleon ratios at a fixed nucleon density of $\rho = \rho_0$. The behavior of $m^*_\pi(r)$ is symmetric around $r = \rho_n/\rho_p = 1$, such that the π^0 mass is invariant under the exchange $r \leftrightarrow 1/r$, while $\pi^\pm \to \pi^\mp$.

The mass of the negatively charged pion increases at normal nuclear density and for a nucleon ratio of $r = 1.5$ by 5–10%, depending on the choice of the LECs. This is in quite good agreement

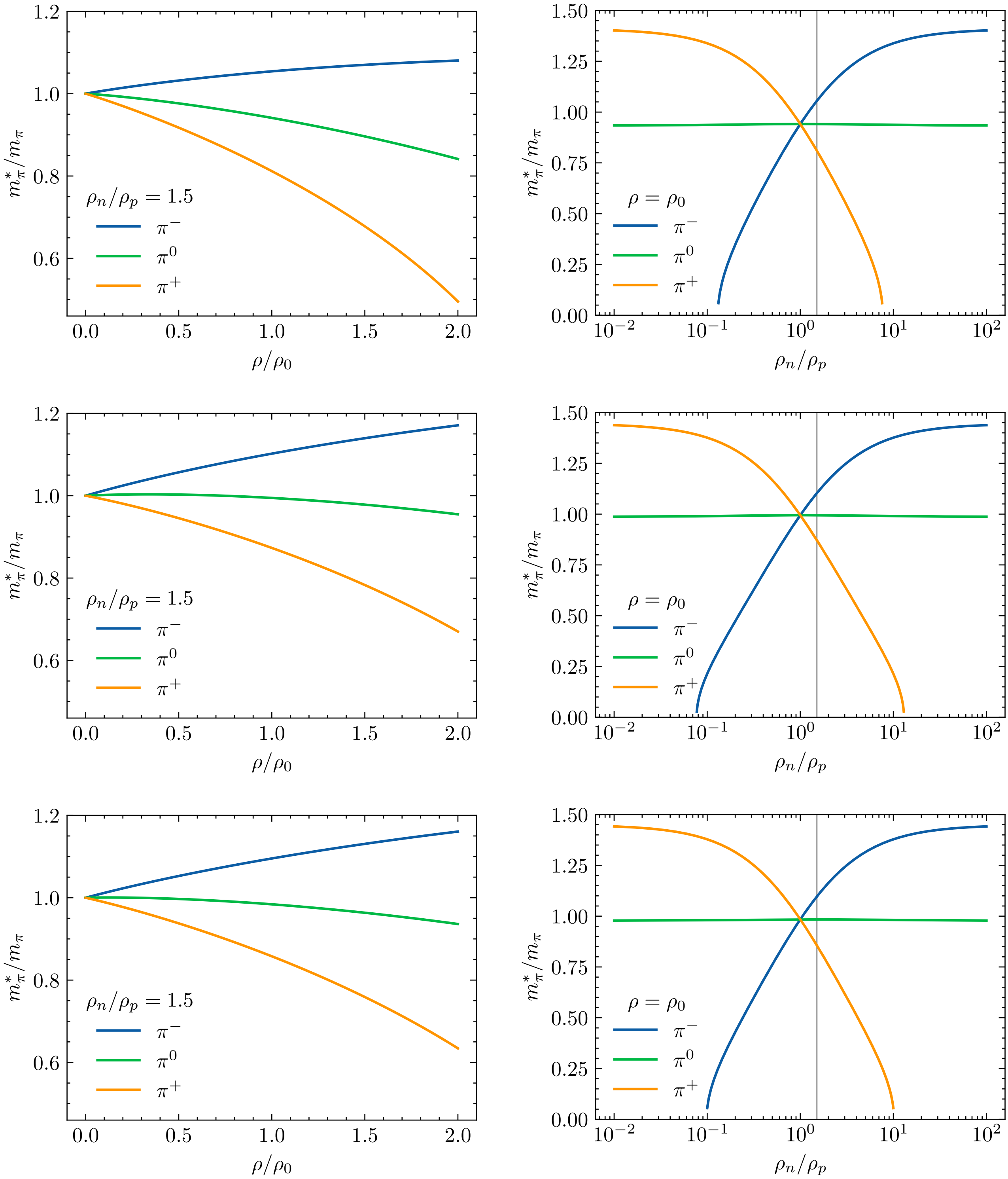

Figure 5.1.: Top to bottom: LEC sets 1, 2, and 3 from Table 3.1. Left: The isospin-asymmetric nuclear matter splits the pion triplet masses. Right: The plots are symmetric around the point $r = \rho_n/\rho_p = 1$, such that under the exchange $r \leftrightarrow 1/r$, the π^0 mass stays the same, but the $\pi^\pm$ masses get exchanged. This behavior is also present in the results for Z and f_π. The vertical grey line marks the ratio $\rho_n/\rho_p = 1.5$.

with other works who computed the same in-medium mass at $\rho = \rho_0$ and $r = 1.5$: Ref. [97] uses a two-loop chiral perturbation theory and reports an increase of 10%. Refs. [95, 98] use functional renormalization group methods and arrive at an increase of 6%. Finally, Ref. [34] uses one-loop in-medium chiral perturbation theory and reports an increase of 13%. The mass of the neutral pion changes only slightly and we found a decrease of 1–5%, and the mass of the positively charged pion decreases by 14–19%. We can compare these values to Ref. [97] which reports an increase of 4% and a decrease of 1%, respectively.

Using experimental data for the optical potential and extrapolating to normal nuclear density, Ref. [101] found an increase of 17–20%. This was obtained by fitting the b_0 parameter in the optical potential to data from ^{207}Pb pionic atoms. A later study performed by Suzuki et al. [37] additionally considered the in-medium change of b_1 in pionic ^{115,119,123}Sn atoms and reported the following values:

$$b_0 = -0.0233/m_\pi, \qquad b_1 = -0.1149/m_\pi, \qquad \mathrm{Re}(B_0) = -0.019/m_\pi^4. \tag{5.86}$$

Using these values in the πN optical potential,

$$V(r) = -\frac{2\pi}{\mu}\left[\epsilon_1\left\{b_0\rho(r) + b_1\rho(r)\frac{r-1}{r+1}\right\} + \epsilon_2\mathrm{Re}(B_0)\rho^2(r)\right], \tag{5.87}$$

leads to a similar increase of around 22% at normal nuclear density. In contrast, a different (Ericson–Weise) parametrization of the optical potential [102],

$$V(r) = -\frac{2\pi}{\mu}\rho(r)\left[b_0 - m_\pi(b_0^2 + 2b_1^2)\right], \tag{5.88}$$

leads to a 11% mass increase of the π^-. We note that this parametrization treats single scattering and double scattering separately, hence we should use an in-vacuum value of $b_0 = -0.01/m_\pi$, as it appears in πN scattering.

In summary, for a neutron-rich nuclear matter, the π^- mass is increased while the π^+ mass gets decreased. For a proton-rich nuclear matter, the opposite is the case. This can be observed in the right column of Fig. 5.1, and can be explained via the Weinberg–Tomozawa theorem [17, 103, 104] of low-energy scattering. Using Clebsch–Gordan coefficients [53], one can show that a neutron-π^- pair couples to a total isospin-3/2 state, whereas a neutron-π^+ pair mostly couples to a total isospin-1/2 state:

$$|n\pi^-\rangle = |\tfrac{1}{2}, -\tfrac{1}{2}, 1, -1\rangle = |\tfrac{3}{2}, -\tfrac{3}{2}\rangle, \tag{5.89a}$$

$$|n\pi^+\rangle = |\tfrac{1}{2}, -\tfrac{1}{2}, 1, 1\rangle = \frac{1}{\sqrt{3}}|\tfrac{3}{2}, \tfrac{1}{2}\rangle + \sqrt{\frac{2}{3}}|\tfrac{1}{2}, \tfrac{1}{2}\rangle. \tag{5.89b}$$

By using the Weinberg–Tomozawa theorem where I denotes the total isospin of the pion-nucleon system,

$$a_I = -\frac{g_V^2 m_\pi}{2\pi f_\pi^2}\left[1 + \frac{m_\pi}{m_N}\right]^{-1}\Big[I(I+1) - \underbrace{I_N(I_N+1)}_{3/4} - \underbrace{I_\pi(I_\pi+1)}_{2}\Big], \tag{5.90}$$

or comparing to experimental data [17, 105], we find that the scattering length of the total isospin-1/2 system is positive (i.e. repulsive interaction), and the scattering length of the total isospin-3/2 system is negative (i.e. attractive interaction):

$$a^{\text{th.}}_{1/2} m_\pi = 0.20, \qquad a^{\text{exp.}}_{1/2} m_\pi = 0.171(5), \tag{5.91}$$

$$a^{\text{th.}}_{3/2} m_\pi = -0.10, \qquad a^{\text{exp.}}_{3/2} m_\pi = -0.088(4). \tag{5.92}$$

One can show that the pion's self-energy in nuclear matter is proportional to the negative T-matrix element of the interaction process (see e.g. Ref. [102], chapter 5.7). And since the T-matrix element is proportional to the scattering length, we conclude that negative scattering length for the $I = 3/2$ system leads to a positive contribution of the π^- self-energy, i.e. a mass increase. The opposite holds for a proton-rich nuclear matter, where $|p\rangle = |\frac{1}{2}\frac{1}{2}\rangle$.

For isospin-symmetric nuclear matter, the masses of all pions decrease equally by 1–6% at normal nuclear density. This is compatible with the results in Ref. [99], which uses an NJL model and reports a decrease of 5%. Ref. [100] uses chiral perturbation theory and reports an increase of 3%.

Around 50 years ago, Migdal [106], Sawyer [107, 108] and Scalapino [109] proposed the idea that pions might undergo a condensation process at high densities due to a p-wave coupling between pions and nucleons (summarized in Ref. [110]). Our calculations suggest that the positively charged pion might condense at $r = 8$–12 at normal nuclear density, see Fig. 5.1. Consequently, the negatively charged pion condensates at the corresponding inverse ratios $1/r$.

One important difference to Ref. [72] is that this work does not employ the large-m_N limit in order to arrive at analytical solutions. This is important e.g. for the symmetric part of Σ_{2b} (i.e. the terms proportional to δ^{ab}):

$$\Sigma^{ab}_{2b}(q) = \frac{2m_N q_0^2}{f^2\pi^2} \int \mathrm{d}p \, \frac{p^2}{\sqrt{p^2 + m_N^2}} \left(\frac{2c_1 m_\pi^2}{q_0^2} - \frac{c_2(p^2 + m_N^2)}{m_N^2} - c_3 \right) [\Theta^p_{\boldsymbol{p}} + \Theta^n_{\boldsymbol{p}}]\delta^{ab}. \tag{5.93}$$

In Ref. [72], the authors assumed a pion at rest $q_0 = m_\pi$ and expanded the integrand in the large-m_N expansion:

$$\Sigma^{ab}_{2b}(q) = \frac{2m_\pi^2}{f^2\pi^2} \int \mathrm{d}p \, p^2 (2c_1 - c_2 - c_3)[\Theta^p_{\boldsymbol{p}} + \Theta^n_{\boldsymbol{p}}]\delta^{ab} + \mathcal{O}(1/m_N^2). \tag{5.94}$$

However, since the combination of LECs $2c_1 - c_2 - c_3$ is proportional to the isoscalar πN scattering length b^+, which is especially small for pions, this term in the large-m_N expansion is small compared to the next one, which is parametrized by $2c_1 + c_2 - c_3$. Hence, by only considering the first term in the large-m_N expansion, one neglects the comparatively large effects of the second leading term. Consequently, our results of the self-energy (and thus the in-medium pion mass) does not agree with Ref. [72].

Before we discuss the next in-medium pion quantities, let us briefly mention other related works that deal with isospin-asymmetric nuclear matter and related hadronic effects. Refs. [111–114] and related works investigated isospin-asymmetric nuclear matter and the possibility of pion condensation in the NJL model. Further meson condensation processes were investigated by Refs. [115, 116], who considered both isospin-asymmetric nuclear matter and strange nuclear matter. In Ref. [36], the authors calculate the s-wave optical potential in isospin-asymmetric nuclear matter. Ref. [117] investigated Δ formation in isospin-asymmetric nuclear matter and Ref. [118] investigated isospin-asymmetric nuclear matter in the holographic Witten–Sakai–Sugimoto model.

5.4. Results: Wave function renormalization

Since the wave function renormalization Z is related to the self-energy by a derivative with respect to q_0^2 as in Eq. (5.18),

$$Z = \left[1 - \left.\frac{\partial\Sigma(p^2)}{\partial p_0^2}\right|_{p=(m_\pi^{*2},\mathbf{0})}\right]^{-1}, \tag{5.95}$$

we will perform this derivative for each self-energy diagram separately.

The type-1 self-energy diagrams yield:

$$\begin{aligned}
\Sigma_1^{ab}(q) &= -\frac{g_A^2 q_0^2}{4\pi^2 f^2}\int \mathrm{d}p\frac{p^2}{p_0}\begin{cases} -\frac{4m_N^2}{4E(p)^2-q_0^2}\left(\Theta_p^p+\Theta_p^n\right)\delta^{ab} \\ \frac{2E(p)}{q_0}\frac{-4p^2+q_0^2}{4E(p)^2-q_0^2}\left(\Theta_p^p-\Theta_p^n\right)\mathrm{i}\epsilon^{ab3}\end{cases}, \\
\frac{\partial\Sigma_1^{ab}}{\partial q_0^2} &= -\frac{g_A^2}{4\pi^2 f^2}\int \mathrm{d}p\frac{p^2}{p_0}\begin{cases} -\frac{16m_N^2p_0^2}{(q_0^2-4p_0^2)^2}\left(\Theta_p^p+\Theta_p^n\right)\delta^{ab} \\ -\frac{p_0(q_0^2(q_0^2-12p_0^2)+4p^2(q_0^2+4p_0^2))}{q_0(q_0^2-4p_0^2)^2}\left(\Theta_p^p-\Theta_p^n\right)\mathrm{i}\epsilon^{ab3}\end{cases},
\end{aligned} \tag{5.96}$$

the first type-2 diagram gives the following contribution:

$$\Sigma_{2a}^{ab}(q) = \frac{q_0\,\rho}{2f^2}\frac{1-r}{1+r}\mathrm{i}\epsilon^{ab3}, \qquad \frac{\partial\Sigma_{2a}^{ab}}{\partial q_0^2} = \frac{\rho}{4q_0 f^2}\frac{1-r}{1+r}\mathrm{i}\epsilon^{ab3}, \tag{5.97}$$

and the second type-2 diagram yields:

$$\begin{aligned}
\Sigma_{2b}^{ab}(q) &= \frac{2m_N q_0^2}{f^2\pi^2}\int \mathrm{d}p\frac{p^2}{E(p)}\begin{cases}\left(\frac{4c_1B_0m}{q_0^2}-\frac{c_2(p^2+m_N^2)}{m_N^2}-c_3\right)[\Theta_{\boldsymbol{p}}^p+\Theta_{\boldsymbol{p}}^n]\delta^{ab} \\ c_4[\Theta_{\boldsymbol{p}}^p-\Theta_{\boldsymbol{p}}^n]\mathrm{i}\epsilon^{ab3}\end{cases}, \\
\frac{\partial\Sigma_{2b}^{ab}}{\partial q_0^2} &= \frac{2m_N}{f^2\pi^2}\int \mathrm{d}p\frac{p^2}{E(p)}\begin{cases}\left(-\frac{c_2(p^2+m_N^2)}{m_N^2}-c_3\right)[\Theta_{\boldsymbol{p}}^p+\Theta_{\boldsymbol{p}}^n]\delta^{ab} \\ c_4[\Theta_{\boldsymbol{p}}^p-\Theta_{\boldsymbol{p}}^n]\mathrm{i}\epsilon^{ab3}\end{cases}.
\end{aligned} \tag{5.98}$$

The type-3 diagram is as follows:

$$\Sigma_3^{ab}(q) = -\frac{g_A^2 m_N^2}{10(2\pi f)^4}\int \mathrm{d}p\,\mathrm{d}k\,\mathrm{d}\cos\theta \frac{p^2k^2}{p_0k_0}\frac{p_0k_0 - pk\cos\theta - m_N^2}{(2m_N^2 - m_\pi^2 - 2p_0k_0 + 2pk\cos\theta)^2}$$
$$\times\begin{cases} v_1(\Theta^p_{\boldsymbol{p}}\Theta^p_{\boldsymbol{k}} + \Theta^n_{\boldsymbol{p}}\Theta^n_{\boldsymbol{k}})\delta^{ab} + (2v_1+v_2+v_3)(\Theta^p_{\boldsymbol{p}}\Theta^n_{\boldsymbol{k}} + \Theta^n_{\boldsymbol{p}}\Theta^p_{\boldsymbol{k}})\delta^{ab} \\ (v_2 - v_3)(\Theta^p_{\boldsymbol{p}}\Theta^n_{\boldsymbol{k}} - \Theta^n_{\boldsymbol{p}}\Theta^p_{\boldsymbol{k}})\mathrm{i}\epsilon^{ab3} \\ (v_2+v_3)(\Theta^p_{\boldsymbol{p}}\Theta^p_{\boldsymbol{k}} - \Theta^p_{\boldsymbol{p}}\Theta^n_{\boldsymbol{k}} - \Theta^n_{\boldsymbol{p}}\Theta^p_{\boldsymbol{k}} + \Theta^n_{\boldsymbol{p}}\Theta^n_{\boldsymbol{k}})\delta^{a3}_{b3} \end{cases},$$

$$\frac{\partial\Sigma_3^{ab}}{\partial q_0^2} = -\frac{g_A^2 m_N^2}{10(2\pi f)^4}\int \mathrm{d}p\,\mathrm{d}k\,\mathrm{d}\cos\theta \frac{p^2k^2}{p_0k_0}\frac{p_0k_0 - pk\cos\theta - m_N^2}{(2m_N^2 - m_\pi^2 - 2p_0k_0 + 2pk\cos\theta)^2}$$
$$\times\begin{cases} 2(\Theta^p_{\boldsymbol{p}}\Theta^p_{\boldsymbol{k}} + \Theta^n_{\boldsymbol{p}}\Theta^n_{\boldsymbol{k}})\delta^{ab} \\ \frac{10}{q_0}(p_0 - k_0)(\Theta^p_{\boldsymbol{p}}\Theta^n_{\boldsymbol{k}} - \Theta^n_{\boldsymbol{p}}\Theta^p_{\boldsymbol{k}})\mathrm{i}\epsilon^{ab3} \\ -6(\Theta^p_{\boldsymbol{p}}\Theta^p_{\boldsymbol{k}} - \Theta^p_{\boldsymbol{p}}\Theta^n_{\boldsymbol{k}} - \Theta^n_{\boldsymbol{p}}\Theta^p_{\boldsymbol{k}} + \Theta^n_{\boldsymbol{p}}\Theta^n_{\boldsymbol{k}})\delta^{a3}_{b3} \end{cases}, \tag{5.99}$$

with:

$$v_1 = 2(p-k)^2 + 2q_0^2 + 2B_0 m, \tag{5.100a}$$
$$2v_1 + v_2 + v_3 = -2(p-k)^2 + 8B_0 m, \tag{5.100b}$$
$$v_2 + v_3 = -6(p-k)^2 - 6q_0^2 + 4B_0 m, \tag{5.100c}$$
$$v_2 - v_3 = 20(p_0 - k_0)q_0, \tag{5.100d}$$

where $(p-k)^2 = 2m_N^2 - 2p_0k_0 + 2pk\cos\theta$. We skip the type-4 diagrams since they are out of the scope of this thesis, and the final diagram is:

$$\Sigma_5(q) = \frac{g_A^2 m_N^2}{10(2\pi f)^4}\int \mathrm{d}p\,\mathrm{d}k\,\mathrm{d}\cos\theta\,\frac{p^2k^2}{p_0k_0}\frac{1}{2m_N^2 - m_\pi^2 - 2p_0k_0 + 2pk\cos\theta}$$
$$\begin{cases} 2(k_0p_0 - pk\cos\theta - m_N^2)(\Theta^p_{\boldsymbol{p}}\Theta^p_{\boldsymbol{k}} - \Theta^p_{\boldsymbol{p}}\Theta^n_{\boldsymbol{k}} - \Theta^n_{\boldsymbol{p}}\Theta^p_{\boldsymbol{k}} + \Theta^n_{\boldsymbol{p}}\Theta^n_{\boldsymbol{k}})\delta^{ab} \\ 5q_0(k_0 - p_0)(\Theta^p_{\boldsymbol{p}}\Theta^n_{\boldsymbol{k}} - \Theta^n_{\boldsymbol{p}}\Theta^p_{\boldsymbol{k}})\epsilon^{ab3} \\ -6(k_0p_0 - pk\cos\theta - m_N^2)(\Theta^p_{\boldsymbol{p}}\Theta^p_{\boldsymbol{k}} - \Theta^p_{\boldsymbol{p}}\Theta^n_{\boldsymbol{k}} - \Theta^n_{\boldsymbol{p}}\Theta^p_{\boldsymbol{k}} + \Theta^n_{\boldsymbol{p}}\Theta^n_{\boldsymbol{k}})\delta^{a3}_{b3} \end{cases},$$

$$\frac{\partial\Sigma_5^{ab}}{\partial q_0^2} = \frac{g_A^2 m_N^2}{10(2\pi f)^4}\int \mathrm{d}p\,\mathrm{d}k\,\mathrm{d}\cos\theta\,\frac{p^2k^2}{p_0k_0}\frac{1}{2m_N^2 - m_\pi^2 - 2p_0k_0 + 2pk\cos\theta}$$
$$\begin{cases} 0 \\ \frac{5}{2q_0}(k_0 - p_0)(\Theta^p_{\boldsymbol{p}}\Theta^n_{\boldsymbol{k}} - \Theta^n_{\boldsymbol{p}}\Theta^p_{\boldsymbol{k}})\epsilon^{ab3} \\ 0 \end{cases}. \tag{5.101}$$

		Z_{π^-}	Z_{π^0}	Z_{π^+}	$Z_\pi(r=1)$
This work	LEC set 1	1.59	1.42	1.26	1.43
	LEC set 2	1.51	1.35	1.18	1.35
	LEC set 3	1.51	1.34	1.17	1.34
Theoretical	Ref. [119]	—	—	—	$1.51 \sim 1.53$
	Ref. [36]	—	—	—	1.57
	Ref. [72]	—	—	—	1.40

Table 5.3.: Comparing the results for the in-medium pion wave function renormalization at $r = 1.5$ (first three values) and at $r = 1$ (last column). The LEC sets refer to the values given in Table 3.1. All values correspond to densities at normal nuclear density: $\rho = \rho_0$.

Another method to calculate the wave function renormalization is to perform a numerical derivative of the self-energy:

$$\frac{\partial \Sigma(q^2)}{\partial q_0^2} \approx \frac{\Sigma(q^2+\delta) - \Sigma(q^2)}{\delta}, \tag{5.102}$$

by calculating the self-energy twice at different values of q_0 and a small enough difference δ.

The density dependence of the in-medium pion wave functions renormalizations is shown in Fig. 5.2, where we use the three sets of low-energy constants given in Table 3.1, and also in Table 5.3. Similar to the in-medium masses, under $r \leftrightarrow 1/r$ the wave function renormalization of π^0 stays the same, whereas $\pi^\pm \leftrightarrow \pi^\mp$.

The in-medium wave function renormalization of the negatively charged pion increases at normal nuclear density by 51–59%, for the neutral pion it increases by 34–42% and for the positively charged pion, the wave function renormalization increases by 17–26%.

In the case of isospin-symmetric nuclear matter, the wave function renormalization of all pions increases by around 34–43% at normal nuclear density. We can compare this to other works, for instance Ref. [119], who used a chiral perturbation theory approach and connected those results to a linear sigma model calculation, and reported an increase of 51–53%. Furthermore, Ref. [36] reports a 57% increase at normal nuclear density using two-loop chiral perturbation theory in order to calculate the pion-nuclear s-wave optical potential.

5.5. Pion decay constant

The pion's decay constant is defined in terms of a matrix element of the axial-vector current between a one-pion state and the vacuum. We will first consider the decay constant in vacuum, in order to show that when using chiral perturbation theory to calculate this matrix element,

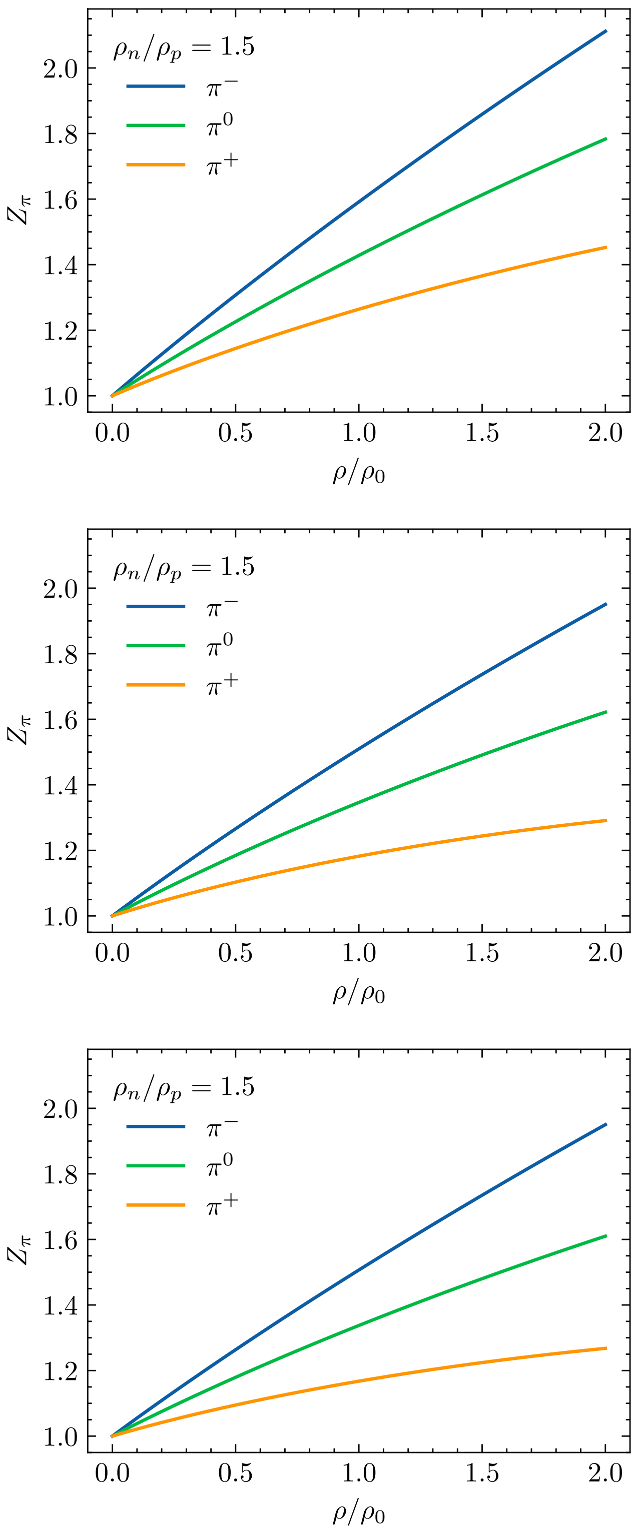

Figure 5.2.: Top to bottom: LEC sets 1, 2, and 3 from Table 3.1. In all cases, the in-medium pion wave function renormalization increases in nuclear matter. For ratios $r < 1$, i.e. more protons than neutrons, the order of the three lines is reversed.

we need an additional factor of $(-\mathrm{i})$, as mentioned in the list of Feynman rules. Afterwards we discuss the in-medium case in more detail and calculate the density dependence of the in-medium pion decay constant.

5.5.1. Decay constant in vacuum

In vacuum, the pion's decay constant is defined by:

$$\langle 0|A_\mu^a(x)|\pi^b(p)\rangle = \mathrm{i} f p_\mu \mathrm{e}^{-\mathrm{i}p\cdot x}\delta^{ab}. \tag{5.103}$$

In chiral perturbation theory, this $A_\mu^a(x)$ is no dynamical field by itself (it has no bilinear term in the Lagrangian), instead it is a function of the pion fields. It is the axial-vector Noether current corresponding to an axial $\mathrm{SU}(2)_L \times \mathrm{SU}(2)_R$ rotation. We can calculate the exact expression for A_μ^a either by using Noether's theorem [58, 59] for an axial-vector rotation, or by investigating the Lagrangian and identifying all terms that couple to the external source a_μ^a:

$$\mathcal{L}_\pi^{(2)} \supset A_\mu^a\, a_a^\mu. \tag{5.104}$$

Either way, this Noether current A_μ^a can be written in terms of the chiral field U as [9, 10]:

$$A_\mu^a = -\mathrm{i}\frac{f^2}{4}\,\mathrm{Tr}\left\{\tau^a\{U, \partial_\mu U^\dagger\}\right\}, \tag{5.105}$$

and by using the relations of U in terms of the pion fields (see Eqs. (2.54) and (2.60b)), we can write this current as:

$$A_\mu^a = -f\partial_\mu \pi^a + \mathcal{O}(\pi^3). \tag{5.106}$$

Defining the decay constant. With the expression of A_μ^a in terms of the pion fields, the following matrix element,

$$\langle 0|A_\mu^a(x)|\pi^b(p)\rangle = \langle 0|-f\partial_\mu \pi^a(x)|\pi^b\rangle, \tag{5.107}$$

actually describes one pion, interacting with another pion[1]. Treating each $\pi^a(x)$ as a separate scalar field, we can write them in the following way [85]:

$$\pi^a(x) = \int \frac{\mathrm{d}^3\boldsymbol{k}}{(2\pi)^3}\frac{1}{\sqrt{2\omega_k}}\left[a_{\boldsymbol{k}}^a \mathrm{e}^{-\mathrm{i}k\cdot x} + a_{\boldsymbol{k}}^{a\dagger}\mathrm{e}^{\mathrm{i}k\cdot x}\right]. \tag{5.108}$$

Thus, the derivative of $\pi^a(x)$, as it appears in Eq. (5.107), can be written as:

$$\partial_\mu \pi^a(x) = \int \frac{\mathrm{d}^3\boldsymbol{k}}{(2\pi)^3}\frac{1}{\sqrt{2\omega_k}}\left[-\mathrm{i}k_\mu a_{\boldsymbol{k}}^a \mathrm{e}^{-\mathrm{i}k\cdot x} + \mathrm{i}k_\mu a_{\boldsymbol{k}}^{a\dagger}\mathrm{e}^{\mathrm{i}k\cdot x}\right]. \tag{5.109}$$

[1] Actually, there are higher terms, cf. Eq. (5.106), but we ignore them for now.

Regarding Eq. (5.107), we can ignore the term with $a^\dagger$, since it will vanish anyway. So we continue only with the first term inside the square brackets, which yields:

$$\langle 0|A^a_\mu(x)|\pi^b(p)\rangle = -f\int \frac{\mathrm{d}^3\boldsymbol{k}}{(2\pi)^3}\frac{1}{\sqrt{2\omega_k}}(-\mathrm{i}k_\mu)\mathrm{e}^{-\mathrm{i}k\cdot x}\langle 0|a^a_{\boldsymbol{k}}|\pi^b(p)\rangle. \tag{5.110}$$

Next we note that, since the creation operator creates a one-particle state out of the vacuum [85] as follows:

$$a^{a\dagger}_{\boldsymbol{p}}|0\rangle = \frac{1}{\sqrt{2\omega_p}}|\pi^a(p)\rangle, \tag{5.111}$$

an annihilation operator will act to a left vacuum as follows:

$$\langle 0|a^a_{\boldsymbol{p}} = \frac{1}{\sqrt{2\omega_p}}\langle\pi^a(p)|. \tag{5.112}$$

This yields the following expression:

$$\langle 0|A^a_\mu(x)|\pi^b(p)\rangle = \mathrm{i}f\int \frac{\mathrm{d}^3\boldsymbol{k}}{(2\pi)^3}\frac{1}{2\omega_k}k_\mu\mathrm{e}^{-\mathrm{i}k\cdot x}\langle\pi^a(k)|\pi^b(p)\rangle. \tag{5.113}$$

Here we use the usual covariant normalization of one-particle states in a quantum field theory [85]:

$$\langle\pi^a(k)|\pi^b(p)\rangle = (2\pi)^3 2\omega_p\delta^{(3)}(\boldsymbol{p}-\boldsymbol{k}), \tag{5.114}$$

to simplify Eq. (5.113):

$$\langle 0|A^a_\mu(x)|\pi^b(p)\rangle = \mathrm{i}f\int \frac{\mathrm{d}^3\boldsymbol{k}}{(2\pi)^3}\frac{1}{2\omega_k}k_\mu\mathrm{e}^{-\mathrm{i}k\cdot x}(2\pi)^3 2\omega_p\delta^{(3)}(\boldsymbol{p}-\boldsymbol{k}) = \mathrm{i}fp_\mu\mathrm{e}^{-\mathrm{i}p\cdot x}, \tag{5.115a}$$

which defines the pion decay constant f. In the last step, even though the delta distribution was only three-dimensional, we were able to replace k_μ with p_μ, since for $\boldsymbol{p}=\boldsymbol{k}$, the following relation holds:

$$p^0 = \omega_p = \sqrt{\boldsymbol{p}^2+m_\pi^2} = \sqrt{\boldsymbol{k}^2+m_\pi^2} = \omega_k = k^0. \tag{5.116}$$

Using chiral perturbation theory. When we want to calculate the decay constant using Eq. (5.103) in-medium, we should calculate Feynman diagrams with one external leg for the pion, coupling to the external axial-vector source. In practice, we treat the external source a^a_μ like a dynamical field when calculating vertices using the Feynman rules laid out in Section 3.4. This leads to the following question: how exactly do we treat a diagram with an external current? For one incoming pion, the S-matrix element can be written using the LSZ formula:

$$\langle f|S|i\rangle = \langle 0_{\text{out}}|\pi^b_{\text{in}}(p)\rangle, \tag{5.117}$$

and this S-matrix element is what we usually calculate using Feynman rules. So let us ignore the axial-vector current for now, and investigate the result of Eq. (5.117). In order to calculate S-matrix elements from vacuum expectation values, we usually make use of a reduction formula, like the Lehmann–Symanzik–Zimmermann (LSZ) formula [85, 120]. For every external line corresponding to a dynamical field, we get a factor which cancels the on-shell propagators of the external lines in a given diagram:

$$\langle f|S|i\rangle = \langle 0_{\mathrm{out}}|\pi^b_{\mathrm{in}}(p)\rangle = \left[\mathrm{i}\int \mathrm{d}^4x\, \mathrm{e}^{-\mathrm{i}p\cdot x}(\Box_x + m_\pi^2)\right]\langle 0|\pi^b(x)|0\rangle. \tag{5.118}$$

Now we use perturbation theory and write this in terms of non-interacting fields:

$$\langle f|S|i\rangle = \mathrm{i}\int \mathrm{d}^4x\, \mathrm{e}^{-\mathrm{i}p\cdot x}(\Box_x + m_\pi^2)\langle 0|\pi^b(x)\mathrm{e}^{\mathrm{i}\int \mathrm{d}z\mathcal{L}_{\mathrm{int}}}|0\rangle. \tag{5.119}$$

The relevant interaction we want to consider is the one given in Eq. (5.104),

$$\mathcal{L}_\pi^{(2)} \supset A^a_\mu\, a^\mu_a, \tag{5.120}$$

therefore by expanding the exponential and only considering the term linear in the axial-vector field, we have:

$$\langle f|S|i\rangle = \mathrm{i}\int \mathrm{d}^4x\, \mathrm{e}^{-\mathrm{i}p\cdot x}(\Box_x + m_\pi^2)\langle 0|\pi^b(x)\mathrm{i}\int \mathrm{d}^4z A^a_\mu(z)a^\mu_a(z)|0\rangle. \tag{5.121}$$

Using Eq. (5.106), we can write the axial-vector Noether current in terms of the pion field:

$$\langle f|S|i\rangle = -f\int \mathrm{d}^4x\, \mathrm{d}^4z\, \mathrm{e}^{-\mathrm{i}p\cdot x}(-\Box_x - m_\pi^2)a^\mu_a(z)\langle 0|\pi^b(x)\partial^z_\mu\pi^a(z)|0\rangle. \tag{5.122}$$

Next we write the partial derivative with respect to z outside of the vacuum expectation value, which we recognize as the pion Feynman propagator,

$$\langle 0|\pi^b(x)\pi^a(z)|0\rangle = \int \frac{\mathrm{d}^4k}{(2\pi)^4}\frac{\mathrm{i}}{k^2 - m_\pi^2 + \mathrm{i}\epsilon}\mathrm{e}^{\mathrm{i}k(x-z)}\delta^{ab}, \tag{5.123}$$

so that the S-matrix element reads:

$$\langle f|S|i\rangle = -f\int \mathrm{d}^4x\, \mathrm{d}^4z\frac{\mathrm{d}^4k}{(2\pi)^4}\,\mathrm{e}^{-\mathrm{i}p\cdot x}(k^2 - m_\pi^2)a^\mu_a(z)(-\mathrm{i}k_\mu)\frac{\mathrm{i}}{k^2 - m_\pi^2 + \mathrm{i}\epsilon}\mathrm{e}^{\mathrm{i}k(x-z)}\delta^{ab}, \tag{5.124}$$

where we let $\Box_x = \partial^x_\mu\partial^\mu_x$ and ∂^z_μ act on the exponential from the Feynman propagator. The LSZ factor precisely cancels the pion propagator and we are left with:

$$\langle f|S|i\rangle = -f\delta^{ab}\int \mathrm{d}^4x\, \mathrm{d}^4z\,\frac{\mathrm{d}^4k}{(2\pi)^4}\,\mathrm{e}^{\mathrm{i}(k-p)\cdot x - \mathrm{i}k\cdot z}a^\mu_a(z)k_\mu. \tag{5.125}$$

We perform the integration over x, yielding a delta distribution,

$$\langle f|S|i\rangle = -f\delta^{ab}\int \mathrm{d}^4z\ \mathrm{d}^4k\,\delta^{(4)}(k-p)\mathrm{e}^{-\mathrm{i}k\cdot z}a^\mu_a(z)k_\mu, \tag{5.126}$$

which renders the k-integration trivial:

$$\langle f|S|i\rangle = -fp_\mu\delta^{ab}\int \mathrm{d}^4z\,\mathrm{e}^{-\mathrm{i}p\cdot z}a_a^\mu(z). \tag{5.127}$$

Now we will focus on the external source again. The way to include the axial-vector current $A_\mu^a(x)$ inside a vacuum expectation value is to perform a functional derivative with respect to $-\mathrm{i}\delta/\delta a_\mu^a(x)$:

$$\langle 0|A_\mu^a(x)|\pi^b(p)\rangle = \frac{\delta}{\mathrm{i}\delta a_\mu^a(x)}\langle 0|\pi^b(p)\rangle. \tag{5.128}$$

In the following we show that by treating the axial-vector current as a dynamical field, we are actually calculating the right-hand side of Eq. (5.128) times i. Therefore, when there is an axial-vector current in the diagram, we have to include an additional factor of $(-\mathrm{i})$ to account for the $1/\mathrm{i}$ in Eq. (5.128).

If we apply this to Eq. (5.127), we get:

$$\frac{\delta}{\mathrm{i}\delta a_\mu^a(x)}\langle f|S|i\rangle = -fp_\mu\delta^{ab}\frac{\delta}{\mathrm{i}\delta a_\mu^a(x)}\int \mathrm{d}^4z\,\mathrm{e}^{-\mathrm{i}p\cdot z}a_a^\mu(z) \tag{5.129a}$$

$$= \mathrm{i}fp_\mu\delta^{ab}\int \mathrm{d}^4z\,\mathrm{e}^{-\mathrm{i}p\cdot z}\delta^{(4)}(z-x) \tag{5.129b}$$

$$= \mathrm{i}fp_\mu\delta^{ab}\mathrm{e}^{-\mathrm{i}p\cdot x}, \tag{5.129c}$$

which is exactly the result we would expect from Eq. (5.115a).

An example in the vacuum. To give an example of why this additional factor of $(-\mathrm{i})$ is necessary, let us consider the vacuum case. In order to calculate f, we consider the following diagram:

$\mathrm{i}\mathcal{M} =$ a_μ^a  $\pi^b(p)$ (5.130)

Using the Feynman rules as described in Section 3.4, this diagram is simply given by i times the pion-axial vertex. The interaction Lagrangian reads to first order,

$$\mathcal{L}_\pi^{(2)} \supset A_\mu^i a_i^\mu = -f\partial_\mu\pi^i a_i^\mu, \tag{5.131}$$

therefore the vertex factor is given after functional differentiation with respect to π^b and a_μ^a (for an incoming pion, the derivative becomes $-\mathrm{i}p_\mu$):

$$\mathcal{L}_{\pi a} = \mathrm{i}fp_\mu\delta^{ab} \tag{5.132}$$

Including the $(-\mathrm{i})$ from Eq. (5.128), the diagram is thus given by:

$$\mathrm{i}\mathcal{M} = (-\mathrm{i})\times\mathrm{i}^2fp_\mu\delta^{ab} = \mathrm{i}fp_\mu\delta^{ab}, \tag{5.133}$$

which is the expected result.

5.5.2. Decay constant in nuclear matter

In nuclear matter, the decay constant is defined as matrix element of the axial-vector current A^a_μ [72] between a one-pion in-medium state and the vacuum:

$$\langle\Omega|A^a_\mu(0)|\pi^{*b}(p)\rangle = \mathrm{i}\Big[p_\mu F^*(p) + n_\mu(p\cdot n)N^*(p)\Big]\delta^{ab}, \tag{5.134}$$

where n_μ is a four-vector that specifies the in-medium rest frame and has $n_\mu n^\mu = 1$. The two form factors F^* and N^* can be functions of $p_\mu p^\mu$ and $p_\mu n^\mu$, in accordance with Lorentz covariance. By taking $n_\mu = (1, \mathbf{0})_\mu$, one can define the temporal and spatial components of the in-medium pion decay constant:

$$\langle\Omega|A^a_0(0)|\pi^{*b}(p)\rangle = \mathrm{i}f_t p_0, \tag{5.135a}$$

$$\langle\Omega|A^a_i(0)|\pi^{*b}(p)\rangle = \mathrm{i}f_s p_i. \tag{5.135b}$$

These in-medium pion decay constants can be obtained for a on-shell pion with $p^0 = m^*_\pi$ and $\boldsymbol{p} = \mathbf{0}$. They are related to the form factors via:

$$f_t = F^*(m^*_\pi, \mathbf{0}) + N^*(m^*_\pi, \mathbf{0}), \tag{5.136a}$$

$$f_s = F^*(m^*_\pi, \mathbf{0}). \tag{5.136b}$$

In order to know which diagrams to calculate in order to determine the in-medium decay constant, let us recall some important in-medium pion relations (see Section 5.1 for more details). The pseudoscalar current and the pion operator are related via $P = \hat{G}_\pi\pi$ and the pion propagator can be written as:

$$\langle\Omega|\pi\pi|\Omega\rangle = \frac{\mathrm{i}Z}{p_0^2 - v_\pi^2\boldsymbol{p}^2 - m^{*2}_\pi + \mathrm{i}\epsilon}.$$

With this, we can use the LSZ reduction formula again and write it as:

$$\langle\Omega|A^a_0(0)|\pi^{*b}(p)\rangle = \left[\frac{\mathrm{i}\sqrt{Z}}{p_0^2 - v_\pi^2\boldsymbol{p}^2 - m^{*2}_\pi + \mathrm{i}\epsilon}\right]^{-1}\langle\Omega|A^a_0(0)\pi|\Omega\rangle. \tag{5.137}$$

Next, we use $\pi = P/\hat{G}_\pi$:

$$\langle\Omega|A^a_0(0)|\pi^{*b}(p)\rangle = \left[\frac{\mathrm{i}\sqrt{Z}}{p_0^2 - v_\pi^2\boldsymbol{p}^2 - m^{*2}_\pi + \mathrm{i}\epsilon}\right]^{-1}\frac{1}{\hat{G}_\pi}\langle\Omega|A^a_0(0)P|\Omega\rangle. \tag{5.138}$$

We now insert a completeness relation between the two currents, but only focus on the pion states:

$$\langle\Omega|A^a_0(0)|\pi^{*b}(p)\rangle = \lim_{p^2\to m^{*2}_\pi}\left[\frac{\mathrm{i}\sqrt{Z}}{p_0^2 - v_\pi^2\boldsymbol{p}^2 - m^{*2}_\pi + \mathrm{i}\epsilon}\right]^{-1}\frac{1}{\hat{G}_\pi}\langle\Omega|A^a_0(0)|\pi\rangle\langle\pi|P|\Omega\rangle. \tag{5.139}$$

The first matrix element on the right-hand side gives us the vertex correction $\hat{f}$ and the second one is proportional to a pion propagator:

$$\langle\Omega|A_0^a(0)|\pi^{*b}(p)\rangle = \lim_{p^2\to m_\pi^{*2}} \left[\frac{\mathrm{i}\sqrt{Z}}{p_0^2 - v_\pi^2\boldsymbol{p}^2 - m_\pi^{*2} + \mathrm{i}\epsilon}\right]^{-1} \frac{1}{\hat{G}_\pi}\mathrm{i}\hat{f}_t p_0 \langle\Omega|\pi\pi|\Omega\rangle\hat{G}_\pi. \tag{5.140}$$

The inverse pion propagator and the pion propagator cancel, which yields:

$$\langle\Omega|A_0^a(0)|\pi^{*b}(p)\rangle = \mathrm{i}\hat{f}_t p_0\sqrt{Z}. \tag{5.141}$$

Finally, since this should be equal to $\mathrm{i}f_t p_0$ due to Eq. (5.135a), we get the relation:

$$f_t = \sqrt{Z}\hat{f}_t. \tag{5.142}$$

This means, we have to calculate 1PI diagrams with an incoming pion and an external axial-vector current A_0 to get $\hat{f}_t$ (the decay constant vertex correction), and then multiply this with the square root of the wave function renormalization $\sqrt{Z}$.

5.6. Calculation of the in-medium pion decay constant

The in-medium pion decay constant is given by $f_t = \hat{f}_t\sqrt{Z}$, where $\hat{f}_t$ is the one-particle irreducible vertex correction to the decay constant and Z is the in-medium pion wave function renormalization. $\hat{f}_t$ can be calculated using the following in-medium correlation function,

$$\langle\Omega|A_0^a|\pi^b(q)\rangle_{1\mathrm{PI}} = \mathrm{i}\delta^{ab}q_0\hat{f}_t \tag{5.143}$$

We discuss in detail how we chose the relevant diagrams in Section 4.2 and list them in Tables 5.4 to 5.8. These tables are organized as follows. For each type of diagram, there can be an interaction from $A^{(1)}$ or $A^{(2)}$. Hence, for each diagram we investigate all possible cases of interactions, $i \in \{1,2\}$ for one vertex or $(i,j) \in \{11,12,21,22\}$ for two vertices. If such a vertex does not exist (because there is no corresponding term in the Lagrangian) we disregard the whole diagram. Still, some diagrams might vanish in the course of the calculation, which will be shown later on. In summary, we will calculate one type-1 diagram, two type-2 diagrams, one type-3 diagrams, four type-4 diagrams and one type-5 diagram:

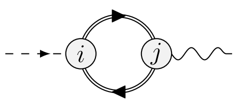

i	1	1	$\cancel{2}^{(1)}$	$\cancel{2}^{(1)}$
j	1	$\cancel{2}^{(2)}$	1	$\cancel{2}^{(2)}$

Table 5.4.: Type 1 $\hat{f}_t$ diagrams. The superscript (1) denotes that the corresponding diagram vanishes because of $A_\pi^{(2)} = 0$, and (2) because of $A_a^{(2)} = 0$. In total, one diagram remains.

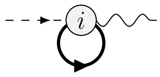

i	1	2

Table 5.5.: Type 2 $\hat{f}_t$ diagrams. Since we cannot exclude any diagram based on the interactions in the Lagrangian, both diagrams remain.

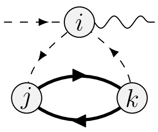

i	$\cancel{1}^{(1)}$	$\cancel{1}^{(1)}$	$\cancel{1}^{(1)}$	$\cancel{1}^{(1)}$	2	2	2	2
j	1	1	$\cancel{2}^{(2)}$	$\cancel{2}^{(2)}$	1	1	$\cancel{2}^{(2)}$	$\cancel{2}^{(2)}$
k	1	$\cancel{2}^{(2)}$	1	$\cancel{2}^{(2)}$	1	$\cancel{2}^{(2)}$	1	$\cancel{2}^{(2)}$

Table 5.6.: Type 3 $\hat{f}_t$ diagrams. The superscript (1) denotes that the corresponding diagram vanishes because of $\mathcal{L}^{(1)} = 0$, and (2) because of $A_\pi^{(2)} = 0$. In total, one diagram remains.

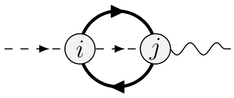

i	1	1	2	2
j	1	2	1	2

Table 5.7.: Type 4 $\hat{f}_t$ diagrams. In total, four diagrams would remain, however as discussed for the self-energy diagrams, those are $\mathcal{O}(\rho^2)$ and therefore out of our scope.

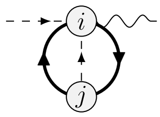

i	1	1	$\cancel{2}^{(1)}$	$\cancel{2}^{(1)}$
j	1	$\cancel{2}^{(2)}$	1	$\cancel{2}^{(2)}$

Table 5.8.: Type 5 $\hat{f}_t$ diagrams. The superscript (1) denotes that the corresponding diagram vanishes because of $A_{a\pi^2}^{(2)} = 0$, and (2) because of $A_\pi^{(2)} = 0$. In total, one diagram remains.

The wavy lines represent axial-vector currents, dashed lines are pions, double lines are Pauli-blocked nucleons and thick lines are in-medium nucleons. We will consider a pion at rest with momentum $q^\mu = (q_0, \mathbf{0})^\mu$.

5.6.1. One-loop diagrams of type 1

The first diagram to calculate the decay constant is given by:

$\hat{f}_{t,1}: \quad \pi^b(q)$ 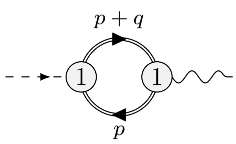 a_0^a (5.144)

This actually corresponds to four diagrams, one where there are two vacuum propagators, two with one vacuum- and one in-medium propagator, and one with two in-medium propagators.

We discard the first one with only vacuum propagators, since we assume that the values for our LECs are already fixed in vacuum. We can also ignore the last one, since if both nucleons are on the mass-shell, this means $p^2 = m_N^2$ and $(p+q)^2 = m_N^2$, while also $p_0 > 0$ and $p_0 + q_0 > 0$. Using the first two equations, we get $2p_0q_0 + q_0^2 = 0$, which we can solve for $p_0 = -q_0/2$. But since $q_0 > 0$, this contradicts the requirement $p_0 > 0$. Thus, the Heaviside function will give zero and the whole diagram vanishes.

The two remaining diagrams are:

$\hat{f}_{t,1a}$: $\pi^b(q)$ 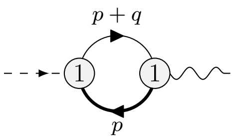 a_0^a , $\hat{f}_{t,1b}$: $\pi^b(q)$ 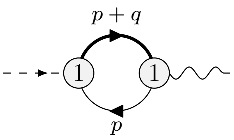 a_0^a . (5.145)

The thin line represents an in-vacuum propagator and the thick line represents the in-medium propagator. These diagrams are now given by the following expressions:

$$\mathrm{i}q_0\hat{f}^{ab}_{t,1a} = (-1)^L\frac{(-1)^n}{n}(-\mathrm{i})\int\frac{\mathrm{d}^3\boldsymbol{p}}{(2\pi)^3}\frac{1}{2E(\boldsymbol{p})}\frac{\mathrm{i}}{(p+q)^2-m_N^2} \times \mathrm{Tr}\left\{[-\mathrm{i}A_\pi^{(1)}]^b(\not{p}+m_N)n(\boldsymbol{p})[-\mathrm{i}A_a^{(1)}]^a(\not{p}+\not{q}+m_N)\right\}\Big|_{p^0\to E(\boldsymbol{p})}, \tag{5.146a}$$

$$\mathrm{i}q_0\hat{f}^{ab}_{t,1b} = (-1)^L\frac{(-1)^n}{n}(-\mathrm{i})\int\frac{\mathrm{d}^3\boldsymbol{p}}{(2\pi)^3}\frac{1}{2E(\boldsymbol{p}+\boldsymbol{q})}\frac{\mathrm{i}}{p^2-m_N^2} \times \mathrm{Tr}\left\{[-\mathrm{i}A_\pi^{(1)}]^b(\not{p}+m_N)[-\mathrm{i}A_a^{(1)}]^a(\not{p}+\not{q}+m_N)n(\boldsymbol{p}+\boldsymbol{q})\right\}\Big|_{p^0\to E(\boldsymbol{p})-q_0}. \tag{5.146b}$$

The relevant terms in the Lagrangian are:

$$A_a^{(1)} = -g_A\gamma^\mu\gamma^5 a_\mu^i\frac{\tau^i}{2}, \tag{5.147a}$$

$$A_\pi^{(1)} = \frac{g_A}{2f}\gamma^\mu\gamma^5\partial_\mu\pi^i\tau^i, \tag{5.147b}$$

and the vertex factors are for both diagrams:

$$[-\mathrm{i}A_\pi^{(1)}]^b = -\frac{g_A}{2f}\not{q}\gamma^5\tau^b, \tag{5.148a}$$

$$[-\mathrm{i}A_a^{(1)}]^a = \mathrm{i}\frac{g_A}{2}\gamma^0\gamma^5\tau^a. \tag{5.148b}$$

The trace in spinor space is the same for both diagrams:

$$\mathrm{Tr}_S\{\cdots\} = -4q_0(m_N^2 + p^2 - p_0q_0 - 2p_0^2), \tag{5.149}$$

however, p_0 is to be replaced by different terms for the two diagrams. Since we assume a pion at rest, $\boldsymbol{q} = \boldsymbol{0}$, the traces in isospin space are similar:

$$\mathrm{Tr}_F\left\{\tau^b n(\boldsymbol{p})\tau^a\right\} = (\Theta_p^p + \Theta_p^n)\delta^{ab} + (\Theta_p^p - \Theta_p^n)\mathrm{i}\epsilon^{ab3}, \tag{5.150a}$$

$$\mathrm{Tr}_{F}\Big\{\tau^b\tau^a n(\boldsymbol{p})\Big\} = (\Theta_p^p + \Theta_p^n)\delta^{ab} - (\Theta_p^p - \Theta_p^n)\mathrm{i}\epsilon^{ab3}. \tag{5.150b}$$

Collecting all coefficients, we can write the sum of the two diagrams as:

$$\hat{f}_{t,1}^{ab} = \frac{g_A^2}{4\pi^2 f}\int \mathrm{d}p\frac{p^2}{E(p)}\begin{cases}\left[\left.\frac{\mathrm{Tr}_S\{\cdots\}}{p_0^2-p^2+2p_0q_0+q_0^2-m_N^2}\right|_{p^0\to E(\boldsymbol{p})} + \left.\frac{\mathrm{Tr}_S\{\cdots\}}{p_0^2-p^2-m_N^2}\right|_{p^0\to E(\boldsymbol{p})-q_0}\right](\Theta_p^p + \Theta_p^n)\,\delta^{ab}, \\ \left[\left.\frac{\mathrm{Tr}_S\{\cdots\}}{p_0^2-p^2+2p_0q_0+q_0^2-m_N^2}\right|_{p^0\to E(\boldsymbol{p})} - \left.\frac{\mathrm{Tr}_S\{\cdots\}}{p_0^2-p^2-m_N^2}\right|_{p^0\to E(\boldsymbol{p})-q_0}\right](\Theta_p^p - \Theta_p^n)\,\mathrm{i}\epsilon^{ab3}.\end{cases} \tag{5.151}$$

The terms inside the integral can be simplified:

$$\left.\frac{\mathrm{Tr}_S\{\cdots\}}{p_0^2-p^2+2p_0q_0+q_0^2-m_N^2}\right|_{p^0\to E(\boldsymbol{p})} + \left.\frac{\mathrm{Tr}_S\{\cdots\}}{p_0^2-p^2-m_N^2}\right|_{p^0\to E(\boldsymbol{p})-q_0} = -\frac{4m_N^2}{4E(p)^2-q_0^2}, \tag{5.152a}$$

$$\left.\frac{\mathrm{Tr}_S\{\cdots\}}{p_0^2-p^2+2p_0q_0+q_0^2-m_N^2}\right|_{p^0\to E(\boldsymbol{p})} - \left.\frac{\mathrm{Tr}_S\{\cdots\}}{p_0^2-p^2-m_N^2}\right|_{p^0\to E(\boldsymbol{p})-q_0} = \frac{2E(p)}{q_0}\frac{-4p^2+q_0^2}{4p^2+4m_N^2-q_0^2}. \tag{5.152b}$$

Therefore we get the following result:

$$\hat{f}_{t,1}^{ab} = \frac{g_A^2}{4\pi^2 f}\int \mathrm{d}p\frac{p^2}{E(p)}\begin{cases}\left[-\frac{4m_N^2}{4E(p)^2-q_0^2}\right](\Theta_p^p + \Theta_p^n)\,\delta^{ab} \\ \left[\frac{2E(p)}{q_0}\frac{-4p^2+q_0^2}{4p^2+4m_N^2-q_0^2}\right](\Theta_p^p - \Theta_p^n)\,\mathrm{i}\epsilon^{ab3}\end{cases}. \tag{5.153}$$

After evaluating the first integral analytically, we can write down the diagonal part of the diagram as follows:

$$\hat{f}_1^{\mathrm{diag}} = -\frac{g_A^2 m_N \rho}{f(4m_N^2-q_0^2)} + (\rho^{4/3}). \tag{5.154}$$

5.6.2. One-loop diagrams of type 2

Leading-order interactions

The next diagram to calculate the decay constant is given by:

$\hat{f}_{t,2a}:$ 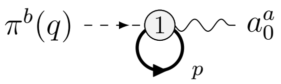

(5.155)

This can be written as an integral:

$$\mathrm{i}q_0\hat{f}_{t,2a}^{ab} = (-1)^L\frac{(-1)^n}{n}(-\mathrm{i})\int\frac{\mathrm{d}^3\boldsymbol{p}}{(2\pi)^3}\frac{1}{2E(\boldsymbol{p})}\,\mathrm{Tr}\Big\{[-\mathrm{i}A_{\pi a}^{(1)}]^{ab}(\not{p}+m_N)n(\boldsymbol{p})\Big\}, \tag{5.156}$$

where $(-1)^L$ accounts for $L=1$ fermionic loop, $\frac{(-1)^n}{n}$ must be included for $n=1$ Fermi-sea insertions and $(-\mathrm{i})$ comes from the fact that we have one external current in our correlation function. Also, since the nucleon is on its mass shell, p^0 must be replaced with $E(\boldsymbol{p})$. The relevant term in the Lagrangian reads:

$$A_{\pi a}^{(1)} = -\frac{1}{2f}\gamma^\mu \pi^i a_\mu^j \epsilon^{ijk}\tau^k, \tag{5.157}$$

so the vertex factor is:

$$[-\mathrm{i}A_{\pi a}^{(1)}]^{ab} = \frac{\mathrm{i}}{2f}\gamma^0\epsilon^{bak}\tau^k. \tag{5.158}$$

The traces are:

$$\mathrm{Tr}_S\left\{\gamma^0(\not{p} + m_N)\right\} = 4p^0, \tag{5.159a}$$
$$\mathrm{Tr}_F\left\{\tau^k n(\boldsymbol{p})\right\} = (\Theta^p_{\boldsymbol{p}} - \Theta^n_{\boldsymbol{p}})\delta^{k3}. \tag{5.159b}$$

Using the relation of the nucleon densities and the Fermi momenta,

$$\int \frac{\mathrm{d}^3\boldsymbol{p}}{(2\pi)^3}\Theta^i_{\boldsymbol{p}} = \frac{\rho_i}{2} \qquad (i = p, n), \tag{5.160}$$

we can write down the solution analytically:

$$\hat{f}_{t,2a} = \frac{\rho}{2q_0 f}\frac{1-r}{1+r}\mathrm{i}\epsilon^{ab3}. \tag{5.161}$$

Next-to-leading order interactions

The next diagram to calculate the decay constant is given by:

$\hat{f}_{t,2b}:$

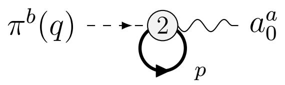

(5.162)

This can be written as an integral:

$$\mathrm{i}q_0\hat{f}^{ab}_{t,2b} = (-1)^L\frac{(-1)^n}{n}(-\mathrm{i})\int\frac{\mathrm{d}^3\boldsymbol{p}}{(2\pi)^3}\frac{1}{2E(\boldsymbol{p})}\,\mathrm{Tr}\left\{[-\mathrm{i}A^{(2)}_{\pi a}]^{ab}(\not{p} + m_N)n(\boldsymbol{p})\right\}, \tag{5.163}$$

where $(-1)^L$ accounts for $L = 1$ fermionic loop, $\frac{(-1)^n}{n}$ must be included for $n = 1$ Fermi-sea insertions and $(-\mathrm{i})$ comes from the fact that we have one external current in our correlation function. Also, since the nucleon is on its mass shell, p^0 must be replaced with $E(\boldsymbol{p})$. The relevant term in the Lagrangian reads:

$$A^{(2)}_{\pi a} = -\frac{2c_2}{fm_N^2}\partial_\mu\pi^i a^i_\nu\partial^\mu\partial^\nu + \frac{2c_3}{f}\partial_\mu\pi^i a^{\mu i} - \frac{\mathrm{i}c_4}{f}\epsilon^{ijk}\tau^k\partial_\mu\pi^i a^j_\nu[\gamma^\mu,\gamma^\nu], \tag{5.164}$$

so the vertex factor is:

$$[-\mathrm{i}A^{(2)}_{\pi a}]^{ab} = -\frac{2c_2}{fm_N^2}p_0^2 q_0\delta^{ab} - \frac{2c_3}{f}q_0\delta^{ab}, \tag{5.165}$$

and since it is diagonal in both spinor and isospin space, the traces can be evaluated easily:

$$\mathrm{Tr}_S\left\{\not{p} + m_N\right\} = 4m_N, \qquad \mathrm{Tr}_F\{n(\boldsymbol{p})\} = \Theta^p_{\boldsymbol{p}} + \Theta^n_{\boldsymbol{p}}. \tag{5.166}$$

Putting everything together, the vertex correction is given by:

$$\hat{f}^{ab}_{t,2b} = \delta^{ab}\frac{2m_N}{f\pi^2}\int \mathrm{d}p \frac{p^2}{E(p)}\left(c_2\frac{p^2+m_N^2}{m_N^2} + c_3\right)(\Theta^p_{\boldsymbol{p}} + \Theta^n_{\boldsymbol{p}}). \tag{5.167}$$

We can perform this integral analytically and get the result:

$$\hat{f}^{\mathrm{diag}}_2 = \frac{2\rho(c_2+c_3)}{f} + \mathcal{O}(\rho^{4/3}) \tag{5.168}$$

5.6.3. Two-loop diagrams of type 3

The third diagram to calculate the decay constant is given by:

$\hat{f}^{ab}_{t,3}$:

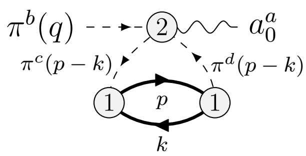

(5.169)

This can be written as

$$\begin{aligned} \mathrm{i}q^0\hat{f}^{ab}_{t,3} = (-1)^L\frac{(-1)^n}{n}(-\mathrm{i})\frac{1}{2}\int\frac{\mathrm{d}^3\boldsymbol{k}}{(2\pi)^3}\frac{1}{2k_0}\int\frac{\mathrm{d}^3\boldsymbol{p}}{(2\pi)^3}\frac{1}{2p_0}[\mathrm{i}\mathcal{L}_{\pi^3a}]^{abcd}\left(\frac{\mathrm{i}}{(p-k)^2-m_\pi^2}\right)^2 \\ \times\,\mathrm{Tr}\left\{[-\mathrm{i}A^{(1)}_\pi]^c(\not{k}+m_N)n(\boldsymbol{k})[-\mathrm{i}A^{(1)}_\pi]^d(\not{p}+m_N)n(\boldsymbol{p})\right\}, \end{aligned} \tag{5.170}$$

where we include a factor $(-1)^L$ for one fermionic loop, $(-1)^2/2$ for two Fermi-sea insertions, $(-\mathrm{i})$ since we have one source in the correlation function and $1/2$ is a symmetry factor for this diagram. The relevant terms in the Lagrangian are:

$$\mathcal{L}^{(2)}_{\pi^3a} = \frac{1}{5f}a^i_\mu\partial^\mu\pi^j\pi^k\pi^l(3\delta^{ij}\delta^{kl} - 4\delta^{ik}\delta^{jl}), \tag{5.171a}$$

$$A^{(1)}_\pi = \frac{g_A}{2f}\gamma^\mu\gamma^5\partial_\mu\pi^i\tau^i, \tag{5.171b}$$

and the corresponding vertex factors are:

$$[\mathrm{i}\mathcal{L}_{\pi^3a}]^{abcd} = \frac{1}{5f}\left[(-6q^0)\delta^{ab}_{cd} + (4q^0 - 10p^0 + 10k^0)\delta^{ac}_{bd} + (4q^0 + 10p^0 - 10k^0)\delta^{ad}_{bc}\right], \tag{5.172a}$$

$$[-\mathrm{i}A^{(1)}_\pi]^c = -\frac{g_A}{2f}(\not{p} - \not{k})\gamma^5\tau^c, \tag{5.172b}$$

$$[-\mathrm{i}A^{(1)}_\pi]^d = \frac{g_A}{2f}(\not{p} - \not{k})\gamma^5\tau^d. \tag{5.172c}$$

The trace in spinor space can be evaluated using the fact that both nucleons are on-shell, i.e. $p^2 = m_N^2$ as well as $k^2 = m_N^2$:

$$\mathrm{Tr}_S\left\{\not{k}\gamma^5(\not{p} + m_N)\not{k}\gamma^5(\not{p} + \not{k} + m_N)\right\} = 16m_N^2(p_0k_0 - \boldsymbol{p}\cdot\boldsymbol{k} - m_N^2). \tag{5.173}$$

The trace over Pauli matrices is:

$$[\mathrm{i}\mathcal{L}_{\pi^3 a}]^{abcd}\,\mathrm{Tr}_F\left\{\tau^c n(\boldsymbol{k})\tau^d n(\boldsymbol{p})\right\} = \frac{1}{5f}\begin{cases} -2q_0(3\Theta^p_{\boldsymbol{p}}\Theta^p_{\boldsymbol{k}} + 2\Theta^p_{\boldsymbol{p}}\Theta^n_{\boldsymbol{k}} + 2\Theta^n_{\boldsymbol{p}}\Theta^p_{\boldsymbol{k}} + 3\Theta^n_{\boldsymbol{p}}\Theta^n_{\boldsymbol{k}})\delta^{ab} \\ 20(k_0 - p_0)(\Theta^p_{\boldsymbol{p}}\Theta^n_{\boldsymbol{k}} - \Theta^n_{\boldsymbol{p}}\Theta^p_{\boldsymbol{k}})\mathrm{i}\epsilon^{ab3} \\ 8q_0(\Theta^p_{\boldsymbol{p}}\Theta^p_{\boldsymbol{k}} - \Theta^p_{\boldsymbol{p}}\Theta^n_{\boldsymbol{k}} - \Theta^n_{\boldsymbol{p}}\Theta^p_{\boldsymbol{k}} + \Theta^n_{\boldsymbol{p}}\Theta^n_{\boldsymbol{k}})\delta^{a3}_{b3} \end{cases} \tag{5.174}$$

where $\Theta^x_{\boldsymbol{y}}$ is an abbreviation for $\Theta(k_F^x - |\boldsymbol{y}|)$, the Heaviside step function that ensures that the nucleon's momentum stays below the Fermi momentum. Finally, $\hat{f}_3$ is given by:

$$\begin{aligned}\hat{f}^{ab}_{t,3} = \frac{m_N^2 g_A^2}{(2\pi)^5 f^3 q_0}\int \mathrm{d}p\,\mathrm{d}k\,\mathrm{d}(\cos\theta)\,\frac{p^2k^2}{p_0k_0}\frac{p_0k_0 - pk\cos\theta - m_N^2}{(2m_N^2 - 2p_0k_0 + 2pk\cos\theta - m_\pi^2)^2} \\ \times\begin{cases} -2q_0(3\Theta^p_{\boldsymbol{p}}\Theta^p_{\boldsymbol{k}} + 2\Theta^p_{\boldsymbol{p}}\Theta^n_{\boldsymbol{k}} + 2\Theta^n_{\boldsymbol{p}}\Theta^p_{\boldsymbol{k}} + 3\Theta^n_{\boldsymbol{p}}\Theta^n_{\boldsymbol{k}})\delta^{ab} \\ 20(k_0 - p_0)(\Theta^p_{\boldsymbol{p}}\Theta^n_{\boldsymbol{k}} - \Theta^n_{\boldsymbol{p}}\Theta^p_{\boldsymbol{k}})\mathrm{i}\epsilon^{ab3} \\ 8q_0(\Theta^p_{\boldsymbol{p}}\Theta^p_{\boldsymbol{k}} - \Theta^p_{\boldsymbol{p}}\Theta^n_{\boldsymbol{k}} - \Theta^n_{\boldsymbol{p}}\Theta^p_{\boldsymbol{k}} + \Theta^n_{\boldsymbol{p}}\Theta^n_{\boldsymbol{k}})\delta^{a3}_{b3} \end{cases}.\end{aligned} \tag{5.175}$$

5.6.4. Two-loop diagrams of type 4

First diagram

The first diagram to calculate the decay constant is given by:

$\hat{f}^{ab}_{t,4a}: \quad \pi^b(q)$ 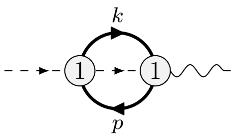 a_0^a (5.176)

where the intermediate pion has momentum $q^\mu + p^\mu - k^\mu$. This can be written as:

$$\begin{aligned}\mathrm{i}\hat{f}^{ab}_{t,4a}q^0 = (-1)^L\frac{(-1)^n}{n}(-\mathrm{i})\int\frac{\mathrm{d}^3\boldsymbol{p}}{(2\pi)^3}\frac{\mathrm{d}^3\boldsymbol{k}}{(2\pi)^3}\frac{1}{4E_pE_k}\frac{\mathrm{i}}{(q+p-k)^2 - m_\pi^2} \\ \times\,\mathrm{Tr}\left\{[-\mathrm{i}A^{(1)}_{\pi^2}]^{bc}(\not{p} + m_N)n(\boldsymbol{p})[-\mathrm{i}A^{(1)}_{\pi a}]^{ca}(\not{k} + m_N)n(\boldsymbol{k})\right\}.\end{aligned} \tag{5.177}$$

The terms in the Lagrangian are:

$$A^{(1)}_{\pi\pi} = \frac{1}{4f^2}\gamma^\mu\pi^i\partial_\mu\pi^j\epsilon^{ijk}\tau^k, \tag{5.178a}$$

$$A^{(1)}_{\pi a} = -\frac{1}{2f}\gamma^\mu\pi^i a^j_\mu\epsilon^{ijk}\tau^k, \tag{5.178b}$$

and the vertex factors are:

$$[-\mathrm{i}A^{(1)}_{\pi^2}]^{bc} = \frac{1}{4f^2}(2\not{q} + \not{p} - \not{k})\epsilon^{bck}\tau^k, \tag{5.179a}$$

$$[-\mathrm{i}A^{(1)}_{\pi a}]^{ca} = \frac{\mathrm{i}}{2f}\gamma^0\epsilon^{cal}\tau^l. \tag{5.179b}$$

The trace yields:

$$\begin{aligned}&\mathrm{Tr}\left\{[-\mathrm{i}A^{(1)}_{\pi^2}]^{bc}(\not{p} + m_N)n(\boldsymbol{p})[-\mathrm{i}A^{(1)}_{\pi a}]^{ca}(\not{k} + m_N)n(\boldsymbol{k})\right\}\\ &= \frac{8\mathrm{i}q_0}{(2f)^3}(E_pE_k + \boldsymbol{p}\cdot\boldsymbol{k} + m_N^2)\begin{cases}-(\Theta^p_{\boldsymbol{p}} + \Theta^n_{\boldsymbol{p}})(\Theta^p_{\boldsymbol{k}} + \Theta^n_{\boldsymbol{k}})\,\delta^{ab}\\ -(\Theta^p_{\boldsymbol{p}}\Theta^n_{\boldsymbol{k}} - \Theta^n_{\boldsymbol{p}}\Theta^p_{\boldsymbol{k}})\,\mathrm{i}\epsilon^{ab3}\\ (\Theta^p_{\boldsymbol{p}} - \Theta^n_{\boldsymbol{p}})(\Theta^p_{\boldsymbol{k}} - \Theta^n_{\boldsymbol{k}})\,\delta^{a3}_{b3}\end{cases},\end{aligned} \tag{5.180}$$

with this, the diagram is given by:

$$\begin{aligned}\hat{f}^{ab}_{t,4a} &= -\frac{1}{(2f)^3}\int\frac{\mathrm{d}^3\boldsymbol{p}}{(2\pi)^3}\frac{\mathrm{d}^3\boldsymbol{k}}{(2\pi)^3}\frac{1}{E_pE_k}\frac{E_pE_k + \boldsymbol{p}\cdot\boldsymbol{k} + m_N^2}{(q+p-k)^2 - m_\pi^2}\\ &\times\begin{cases}-(\Theta^p_{\boldsymbol{p}} + \Theta^n_{\boldsymbol{p}})(\Theta^p_{\boldsymbol{k}} + \Theta^n_{\boldsymbol{k}})\,\delta^{ab}\\ -(\Theta^p_{\boldsymbol{p}}\Theta^n_{\boldsymbol{k}} - \Theta^n_{\boldsymbol{p}}\Theta^p_{\boldsymbol{k}})\,\mathrm{i}\epsilon^{ab3}\\ (\Theta^p_{\boldsymbol{p}} - \Theta^n_{\boldsymbol{p}})(\Theta^p_{\boldsymbol{k}} - \Theta^n_{\boldsymbol{k}})\,\delta^{a3}_{b3}\end{cases}.\end{aligned} \tag{5.181}$$

This is the same integrand we encountered in the type-4 self-energy diagrams, i.e. also this type-4 decay constant diagram is of order $\mathcal{O}(\rho^2)$. And in fact, the other type-4 diagrams are as well.

5.6.5. Two-loop diagrams of type 5

The final diagram to calculate the decay constant is given by:

$\hat{f}^{ab}_{t,5}$: 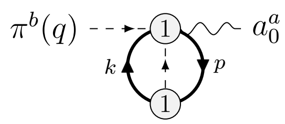

(5.182)

where the pion momentum is $p^\mu - k^\mu$ in the upwards direction. This can be written as:

$$\begin{aligned}\mathrm{i}q_0\hat{f}^{ab}_{t,5} &= (-1)^L\frac{(-1)^n}{n}(-\mathrm{i})\int\frac{\mathrm{d}^3\boldsymbol{p}}{(2\pi)^3}\frac{\mathrm{d}^3\boldsymbol{k}}{(2\pi)^3}\frac{1}{4p_0k_0}\frac{\mathrm{i}}{(p-k)^2 - m_\pi^2}\\ &\times\mathrm{Tr}\left\{[-\mathrm{i}A^{(1)}_{\pi^2 a}]^{abc}(\not{k} + m_N)n(\boldsymbol{k})[-\mathrm{i}A^{(1)}_{\pi}]^c(\not{p} + m_N)n(\boldsymbol{p})\right\}.\end{aligned} \tag{5.183}$$

The relevant terms in the Lagrangian are:

$$A^{(1)}_{\pi^2 a} = \frac{g_A}{4f^2}\gamma^\mu\gamma^5\pi^i\pi^j a^k_\mu\tau^l(\delta^{ij}_{kl} - \delta^{ik}_{jl}), \tag{5.184a}$$

$$A_{\pi}^{(1)} = \frac{g_A}{2f}\gamma^{\mu}\gamma^5\partial_{\mu}\pi^i\tau^i, \tag{5.184b}$$

and the vertices are:

$$[-\mathrm{i}A_{\pi^2 a}^{(1)}]^{abc} = \mathrm{i}\frac{g_A}{4f^2}\gamma^0\gamma^5(\delta^{ab}\tau^c + \delta^{ac}\tau^b - 2\delta^{bc}\tau^a), \tag{5.185a}$$

$$[-\mathrm{i}A_{\pi}^{(1)}]^{c} = \frac{g_A}{2f}(\not{p} - \not{k})\gamma^5\tau^c. \tag{5.185b}$$

The traces are calculated to be:

$$\mathrm{Tr}_{S}\Big\{\gamma^0\gamma^5(\not{k} + m_N)(\not{p} - \not{k})\gamma^5(\not{p} + m_N)\Big\} = 8m_N^2(k_0 - p_0), \tag{5.186a}$$

$$\mathrm{Tr}_{F}\Big\{(\delta^{ab}\tau^c + \delta^{ac}\tau^b - 2\delta^{bc}\tau^a)n(\boldsymbol{k})\tau^c n(\boldsymbol{p})\Big\} = \begin{cases} (\Theta_{\boldsymbol{p}}^p\Theta_{\boldsymbol{k}}^p + \Theta_{\boldsymbol{p}}^p\Theta_{\boldsymbol{k}}^n + \Theta_{\boldsymbol{p}}^n\Theta_{\boldsymbol{k}}^p + \Theta_{\boldsymbol{p}}^n\Theta_{\boldsymbol{k}}^n)\delta^{ab} \\ -3(\Theta_{\boldsymbol{p}}^p\Theta_{\boldsymbol{k}}^n - \Theta_{\boldsymbol{p}}^n\Theta_{\boldsymbol{k}}^p)\mathrm{i}\epsilon^{ab3} \\ -(\Theta_{\boldsymbol{p}}^p\Theta_{\boldsymbol{k}}^p - \Theta_{\boldsymbol{p}}^p\Theta_{\boldsymbol{k}}^n - \Theta_{\boldsymbol{p}}^n\Theta_{\boldsymbol{k}}^p + \Theta_{\boldsymbol{p}}^n\Theta_{\boldsymbol{k}}^n)\delta_{b3}^{a3} \end{cases}. \tag{5.186b}$$

Finally, this diagram is given by:

$$\hat{f}_{t,5} = -\frac{g_A^2 m_N^2}{2^6\pi^4 f^3 q_0}\int \mathrm{d}p\,\mathrm{d}k\,\mathrm{d}\cos\theta\,\frac{p^2k^2}{p_0k_0}\frac{k_0 - p_0}{2m_N^2 - m_\pi^2 - 2p_0k_0 + 2pk\cos\theta} \times \begin{cases} (\Theta_{\boldsymbol{p}}^p\Theta_{\boldsymbol{k}}^p + \Theta_{\boldsymbol{p}}^p\Theta_{\boldsymbol{k}}^n + \Theta_{\boldsymbol{p}}^n\Theta_{\boldsymbol{k}}^p + \Theta_{\boldsymbol{p}}^n\Theta_{\boldsymbol{k}}^n)\delta^{ab} \\ -3(\Theta_{\boldsymbol{p}}^p\Theta_{\boldsymbol{k}}^n - \Theta_{\boldsymbol{p}}^n\Theta_{\boldsymbol{k}}^p)\mathrm{i}\epsilon^{ab3} \\ -(\Theta_{\boldsymbol{p}}^p\Theta_{\boldsymbol{k}}^p - \Theta_{\boldsymbol{p}}^p\Theta_{\boldsymbol{k}}^n - \Theta_{\boldsymbol{p}}^n\Theta_{\boldsymbol{k}}^p + \Theta_{\boldsymbol{p}}^n\Theta_{\boldsymbol{k}}^n)\delta_{b3}^{a3} \end{cases}. \tag{5.187}$$

5.7. Results: Decay constant

In this section, we discuss the in-medium pion decay constants. We show their density dependence in Fig. 5.3, using the three sets of low-energy constants given in Table 3.1, and also in Table 5.9.

The in-medium decay constant for the negatively charged pion decreases by around 9–18% at normal nuclear density. This is consistent with the results reported in Ref. [35], which reports a decrease of 12% at normal nuclear density. The authors were able to determine the parameter b_1^*, which is used to parametrize the isovector part of the s-wave pion-nucleus optical potential. The numerical value of b_1^* was obtained from pionic atom and π^--nucleus scattering data. The authors found the following relation between $b_1^{(*)}$ and $f^{(*)}$: $b_1/b_1^* = (f^*/f)^2$, and since the in-medium quantity b_1^* was found to be enhanced in nuclear matter, the authors concluded that the in-medium pion decay constant would be reduced in nuclear matter. Furthermore, our calculations show that the decay constants for the neutral pion decrease by around 25–34% and for the positively charged pion by around 41–48%, depending on the choice of the LECs.

		$f^*_{\pi^-}/f_\pi$	$f^*_{\pi^0}/f_\pi$	$f^*_{\pi^+}/f_\pi$	$f^*_\pi/f_\pi(r=1)$
This work	LEC set 1	0.82	0.66	0.52	0.66
	LEC set 2	0.90	0.74	0.59	0.74
	LEC set 3	0.91	0.75	0.59	0.75
Theoretical	Ref. [35]	0.88	—	—	—
	Ref. [72]	—	—	—	0.75
	Refs. [34, 94]	—	—	—	0.74
	Ref. [99]	—	—	—	0.87
Experimental	Ref. [121]	0.80	—	—	—

Table 5.9.: Comparing the results for the in-medium pion decay constant at $r = 1.5$ (first three values) and at $r = 1$ (last column). The LEC sets refer to the values given in Table 3.1. All values correspond to densities at normal nuclear density: $\rho = \rho_0$.

For isospin-symmetric nuclear matter, all three decay constants behave the same and decrease by around 25–34% at normal nuclear density. This agrees well with other works (in the following all values are given at $\rho = \rho_0$), e.g. Ref. [72], which reported a 25% decrease and Refs. [34, 94], who used a one-loop in-medium chiral perturbation theory to arrive at a 26% decrease. Furthermore, Ref. [99] used a NJL model and reports a decrease of 13% and Ref. [121] reports a decrease of 20% by deriving s-wave pion nucleus potential parameters.

5.7.1. In-Medium Gell-Mann–Oakes–Renner Relation

The GMOR relation [122] connects the quark condensate $\langle\bar{q}q\rangle = \langle\bar{u}u + \bar{d}d\rangle$ to hadronic (i.e. pion) quantities:

$$m_\pi^2 f_\pi^2 = -\frac{m_u + m_d}{2}\langle\bar{q}q\rangle. \tag{5.188}$$

In order to derive an in-medium version of the Gell-Mann–Oakes–Renner (GOR) relation, we follow Ref. [35], but generalize their discussion to isospin-asymmetric nuclear matter. We start with the following correlation function,

$$\begin{aligned}
\Pi_5^{ab}(q) &= \int \mathrm{d}^4x\, \mathrm{e}^{\mathrm{i}q\cdot x}\partial^\mu\langle\Omega|\mathsf{T}A_\mu^a(x)P^b(0)|\Omega\rangle && (5.189\text{a})\\
&= \int \mathrm{d}^4x\,(-\partial^\mu\mathrm{e}^{\mathrm{i}q\cdot x})\langle\Omega|\mathsf{T}A_\mu^a(x)P^b(0)|\Omega\rangle && (5.189\text{b})\\
&= -\mathrm{i}q^\mu\int \mathrm{d}^4x\, \mathrm{e}^{\mathrm{i}q\cdot x}\langle\Omega|\mathsf{T}A_\mu^a(x)P^b(0)|\Omega\rangle, && (5.189\text{c})
\end{aligned}$$

such that in the soft limit:

$$\Pi_5^{ab}(0) = -\mathrm{i}\delta^{ab}\langle\bar{q}q\rangle^*. \tag{5.190}$$

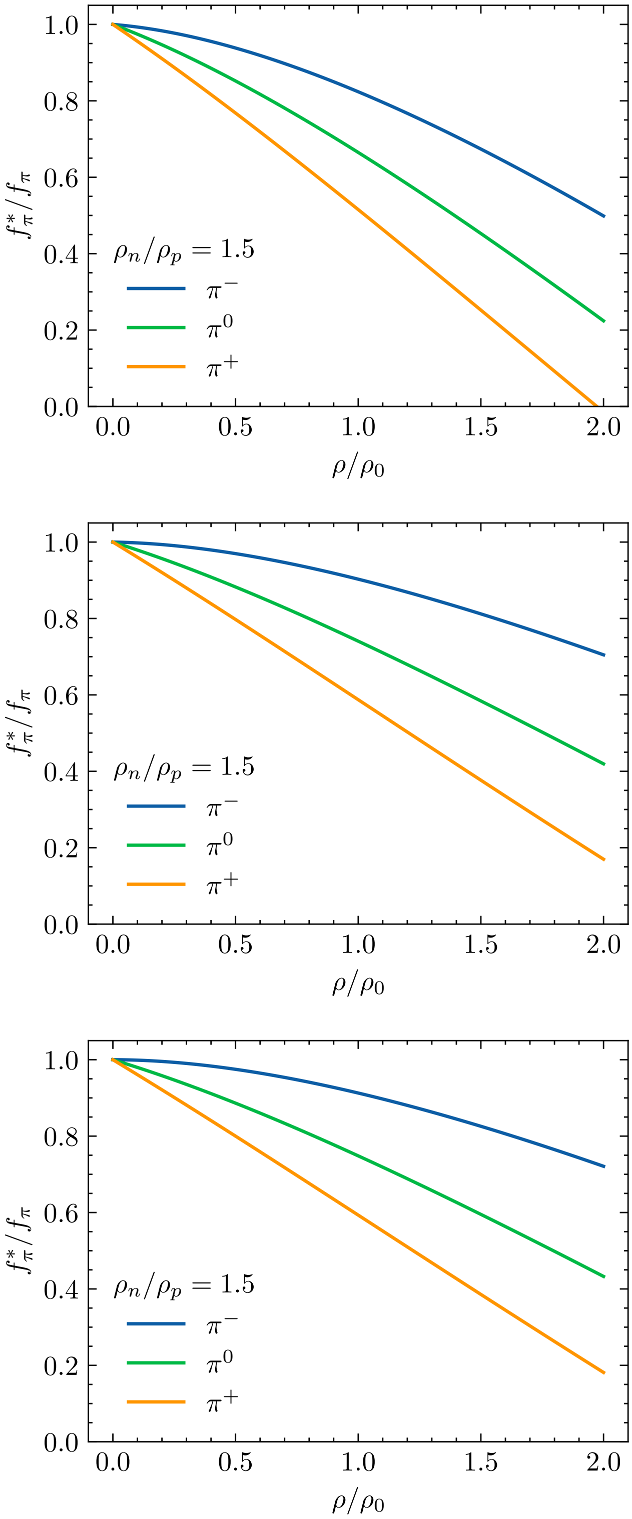

Figure 5.3.: Top to bottom: LEC sets 1, 2, and 3 from Table 3.1. The in-medium pion decay constant decreases in nuclear matter compared to its vacuum value. For $\rho_n > \rho_p$, the decay constant of the positively charged pion decreases the most rapidly, for $\rho_n < \rho_p$, the order of the three lines is reversed.

We insert a complete set of hadronic states,

$$\mathbb{1} = \sum_n \int \frac{\mathrm{d}^3\boldsymbol{p}_n}{(2\pi)^3 2E_n} |n(p_n)\rangle\langle n(p_n)|, \tag{5.191}$$

where $p_n^\mu = (E_n, \boldsymbol{p}_n)$ into the matrix element in Eq. (5.189):

$$\begin{aligned}\langle\Omega|\mathsf{T}A_\mu^a(x)P^b(0)|\Omega\rangle = \sum_n \int \frac{\mathrm{d}^3\boldsymbol{p}_n}{(2\pi)^3 2E_n} \Bigg[&\Theta(x^0)\langle\Omega|A_\mu^a(x)|n(p_n)\rangle\langle n(p_n)|P^b(0)|\Omega\rangle \\ &+ \Theta(-x^0)\langle\Omega|P^b(0)|n(p_n)\rangle\langle n(p_n)|A_\mu^a(x)|\Omega\rangle\Bigg].\end{aligned} \tag{5.192}$$

The states we are interested in are the pions $|\pi^{*a}(p)\rangle$. We use these matrix elements:

$$\langle\Omega|A_\mu^a(x)|\pi^{*b}(p)\rangle = \mathrm{i}[f_d\delta^{ab} + f_o\mathrm{i}\epsilon^{ab3} + f_3\delta^{a3}\delta^{b3}]p_\mu \mathrm{e}^{-\mathrm{i}p\cdot x} \equiv \mathrm{i}f_{ab}p_\mu\mathrm{e}^{-\mathrm{i}p\cdot x}, \tag{5.193a}$$

$$\langle\Omega|P^a(x)|\pi^{*b}(p)\rangle = [G_d\delta^{ab} + G_o\mathrm{i}\epsilon^{ab3} + G_3\delta^{a3}\delta^{b3}]\mathrm{e}^{-\mathrm{i}p\cdot x} \equiv G_{ab}\mathrm{e}^{-\mathrm{i}p\cdot x}, \tag{5.193b}$$

where $f_{\pi^\pm} = f_d \pm f_o$ and $f_{\pi^0} = f_d + f_3$, as discussed in Appendix B.3. Note that, for isospin-symmetric nuclear matter, these matrix elements would only be proportional to δ^{ab}. We obtain:

$$\begin{aligned}\langle\Omega|\mathsf{T}A_\mu^a(x)P^b(0)|\Omega\rangle = \mathrm{i}\sum_n \int &\frac{\mathrm{d}^3\boldsymbol{p}_n}{(2\pi)^3}\frac{(p_n)_\mu}{2E_n} \\ &\times\left[\Theta(x^0)f_{an}\bar{G}_{bn}\mathrm{e}^{-\mathrm{i}p_n\cdot x} - \Theta(-x^0)\bar{f}_{an}G_{bn}\mathrm{e}^{\mathrm{i}p_n\cdot x}\right],\end{aligned} \tag{5.194}$$

where a bar denotes a complex conjugate (since a star usually denotes an in-medium quantity in this thesis). We can now use the following mathematical identity:

$$\Theta(\pm x^0)\mathrm{e}^{\mp\mathrm{i}E_n x^0} = \pm\frac{1}{2\pi\mathrm{i}}\int_{-\infty}^{\infty}\mathrm{d}\omega\,\frac{\mathrm{e}^{\mathrm{i}\omega x^0}}{\omega \pm E_n \mp \mathrm{i}\epsilon}. \tag{5.195}$$

By using this, we can write the integral as a four-dimensional momentum integral:

$$\langle\Omega|\mathsf{T}A_\mu^a(x)P^b(0)|\Omega\rangle = \sum_n \int \frac{\mathrm{d}^4p_n}{(2\pi)^4}\frac{(p_n)_\mu}{2E_n}\left[\frac{f_{an}\bar{G}_{bn}\mathrm{e}^{\mathrm{i}(p_n^0 t + \boldsymbol{p}_n\cdot x)}}{p^0 + E_n - \mathrm{i}\epsilon} + \frac{\bar{f}_{an}G_{bn}\mathrm{e}^{\mathrm{i}(p_n^0 t - \boldsymbol{p}_n\cdot x)}}{p^0 - E_n + \mathrm{i}\epsilon}\right]. \tag{5.196}$$

We use this expression in the correlation function Eq. (5.189):

$$\Pi_5^{ab}(q) = -\mathrm{i}\sum_n \int \mathrm{d}^4x\,\frac{\mathrm{d}^4p_n}{(2\pi)^4}\frac{q\cdot p_n}{2E_n}\mathrm{e}^{\mathrm{i}q\cdot x}\left[\frac{f_{an}\bar{G}_{bn}\mathrm{e}^{\mathrm{i}(p_n^0 t + \boldsymbol{p}_n\cdot x)}}{p^0 + E_n - \mathrm{i}\epsilon} + \frac{\bar{f}_{an}G_{bn}\mathrm{e}^{\mathrm{i}(p_n^0 t - \boldsymbol{p}_n\cdot x)}}{p^0 - E_n + \mathrm{i}\epsilon}\right], \tag{5.197}$$

so that we can perform the integration over d^4x:

$$\Pi_5^{ab}(q) = -\mathrm{i}\sum_n \int \mathrm{d}^4p_n\,\frac{q\cdot p_n}{2E_n}\left[\frac{f_{an}\bar{G}_{bn}\delta^{(3)}(\boldsymbol{p}_n - \boldsymbol{q})}{p^0 + E_n - \mathrm{i}\epsilon} + \frac{\bar{f}_{an}G_{bn}\delta^{(3)}(\boldsymbol{p}_n + \boldsymbol{q})}{p^0 - E_n + \mathrm{i}\epsilon}\right]\delta(p_n^0 + q^0). \tag{5.198}$$

Also the integration over d^4p_n is now trivial and we obtain:

$$\Pi_5^{ab}(q) = \mathrm{i}\sum_n \frac{1}{2E_n}\left[\frac{q^2 f_{an}\bar{G}_{bn}}{q^0 - E_n + \mathrm{i}\epsilon} + \frac{(q_0^2 + \boldsymbol{q}^2)\bar{f}_{an}G_{bn}}{q^0 + E_n - \mathrm{i}\epsilon}\right]. \tag{5.199}$$

If we have zero-modes in the system, we get the following expression in the soft limit:

$$\lim_{q^\mu \to 0} \Pi_5^{ab}(q) = \sum_n \mathrm{Re}\left[\bar{f}_{an}G_{bn}\right] = -\delta^{ab}\langle\bar{q}q\rangle^*, \tag{5.200}$$

which is a generalized Glashow–Weinberg relation. For different values for a and b, we get:

$$\mathrm{Re}\begin{pmatrix} \bar{f}_{11}G_{11} + \bar{f}_{12}G_{12} & \bar{f}_{11}G_{21} + \bar{f}_{12}G_{22} & 0 \\ \bar{f}_{21}G_{11} + \bar{f}_{22}G_{12} & \bar{f}_{21}G_{21} + \bar{f}_{22}G_{22} & 0 \\ 0 & 0 & \bar{f}_{33}G_{33} \end{pmatrix} = -\begin{pmatrix} \langle\bar{q}q\rangle^* & 0 & 0 \\ 0 & \langle\bar{q}q\rangle^* & 0 \\ 0 & 0 & \langle\bar{q}q\rangle^* \end{pmatrix}, \tag{5.201}$$

which we can rewrite as:

$$\mathrm{Re}\begin{pmatrix} \bar{f}_dG_d + \bar{f}_oG_o & -\mathrm{i}(\bar{f}_dG_o + \bar{f}_oG_d) & 0 \\ \mathrm{i}(\bar{f}_dG_o + \bar{f}_oG_d) & \bar{f}_dG_d + \bar{f}_oG_o & 0 \\ 0 & 0 & (\bar{f}_d + \bar{f}_3)(G_d + G_3) \end{pmatrix} = -\langle\bar{q}q\rangle^*\mathbb{1}_3. \tag{5.202}$$

Using $f_{\pi^\pm} = f_d \pm f_o$ and $f_{\pi^0} = f_d + f_3$, we rewrite the equations along the diagonal to:

$$\frac{1}{2}\mathrm{Re}\left[\bar{f}_{\pi^+}G_{\pi^+} + \bar{f}_{\pi^-}G_{\pi^-}\right] = -\langle\bar{q}q\rangle^*, \tag{5.203a}$$

$$\mathrm{Re}\left[\bar{f}_{\pi^0}G_{\pi^0}\right] = -\langle\bar{q}q\rangle^*. \tag{5.203b}$$

These generalized Glashow–Weinberg relations are valid in the chiral limit.

Next, we use the PCAC relation $\partial^\mu A_\mu^a(x) = mP^a(x)$ and evaluate it between the vacuum and a pion state:

$$\langle\Omega|\partial^\mu A_\mu^\pm(x)|\pi^{*\pm}(p)\rangle = \sqrt{2}f_{\pi^\pm}m_{\pi^\pm}^{*2}\mathrm{e}^{-\mathrm{i}p\cdot x}, \qquad \langle\Omega|\partial^\mu A_\mu^0(x)|\pi^{*0}(p)\rangle = f_{\pi^0}m_{\pi^0}^{*2}\mathrm{e}^{-\mathrm{i}p\cdot x}, \tag{5.204a}$$

$$m\langle\Omega|P^\pm(x)|\pi^{*\pm}(p)\rangle = m\sqrt{2}G_{\pi^\pm}\mathrm{e}^{-\mathrm{i}p\cdot x}, \qquad m\langle\Omega|P^0(x)|\pi^{*0}(p)\rangle = mG_{\pi^0}\mathrm{e}^{-\mathrm{i}p\cdot x}. \tag{5.204b}$$

such that: $f_{\pi^{\pm,0}}m_{\pi^{\pm,0}}^{*2} = mG_{\pi^{\pm,0}}$. We can use this to substitute for $G_{\pi^{\pm,0}}$, in order to arrive at generalized GOR relations:

$$\frac{|f_{\pi^+}|^2m_{\pi^+}^{*2} + |f_{\pi^-}|^2m_{\pi^-}^{*2}}{2} = -m\langle\bar{q}q\rangle^*, \tag{5.205a}$$

$$|f_{\pi^0}|^2m_{\pi^0}^2 = -m\langle\bar{q}q\rangle^*. \tag{5.205b}$$

Using the values from the LEC set 3, we get the following result:

$$\frac{|f_{\pi^+}|^2m_{\pi^+}^{*2} + |f_{\pi^-}|^2m_{\pi^-}^{*2}}{2}\Big/[-m\langle\bar{q}q\rangle^*] \approx 1.13, \tag{5.206a}$$

$$|f_{\pi^0}|^2m_{\pi^0}^2\Big/[-m\langle\bar{q}q\rangle^*] \approx 0.97. \tag{5.206b}$$

Here we used the following in-vacuum quantities: $m \equiv (m_u + m_d)/2 \approx 3.4$ MeV, $m_\pi = 138$ MeV, $f_\pi = 92.4$ MeV, and $\frac{1}{2}\langle\bar{u}u + \bar{d}d\rangle_0 \approx -[272(5)\text{ MeV}]^3$ [93]. Since the GOR relation is valid up to $\mathcal{O}(m) = \mathcal{O}(m_\pi^2)$ where m is the quark mass, the deviation occurring in Eq. (5.206) can be understood due to higher-order contributions.

6. Summary

In the scope of this thesis we thoroughly discussed the effect that isospin breaking of the surrounding nuclear matter has on the in-medium quark condensate, as well as in-medium pion properties. To this end, we devised in-medium chiral perturbation theory to calculate the density dependence of those quantities.

We have computed the density dependence of the $\langle \bar{u}u + \bar{d}d \rangle^*$ quark condensate in isospin-asymmetric nuclear matter using an SU(2) in-medium chiral perturbation theory up to second order in the chiral counting. Our results show that the reduction of the magnitude of the quark condensate in an isospin asymmetric nuclear matter with $\rho_n/\rho_p = 1.5$ agrees with the phenomenological result obtained using experimental observations, and also confirm previous theoretical estimates. Furthermore, our results show that the effect of the isospin-asymmetric nuclear matter is weak, yet non-zero. This is because contributions beyond the linear density are rather small due to smaller Fermi motion in low densities. Nucleon-nucleon correlations, which play a role at $\mathcal{O}(\rho^2)$, could contribute to the deviation of the $\langle \bar{u}u + \bar{d}d \rangle^*$ quark condensate in the asymmetric nuclear matter from that in the symmetric nuclear matter. We have extended our formalism to SU(3), which allowed us to perform a linear-density approximation of the density dependence of the condensate difference $\langle \bar{u}u - \bar{d}d \rangle^*$, as well as the strange condensate $\langle \bar{s}s \rangle^*$. For the condensate difference $\langle \bar{u}u - \bar{d}d \rangle^*$ in particular, we investigated explicit isospin breaking via non-equal light quark masses in the Lagrangian, which had a quantitatively similar effect as the isospin breaking via the surrounding nuclear matter. Nevertheless, we have found that the magnitude of the splitting is not so large in comparison with the in-medium reduction of the quark condensate $\langle \bar{q}q \rangle^*$. It would be interesting to obtain the low-energy constants of the SU(3) chiral Lagrangian by experimental scattering data. While this work used values obtained from a fit to octet baryon masses via Gell-Mann–Okubo relations, a determination via scattering data is currently in preparation[1].

In order to investigate the in-medium pion properties, we started by precisely defining the in-medium pion wave function and related quantities. We then used in-medium chiral perturbation theory to calculate the density dependence of the pion self-energy, which was composed of three components, corresponding to the three pions in the pion triplet. By diagonalizing the self-energy in the physical pion basis, we were able to compute the in-medium mass and wave function renormalization for the charged $\pi^\pm$ and neutral π^0 pions separately. This splitting

[1] Y. Iizawa, D. Jido, S. Hübsch (in preparation).

of the isospin triplet quantities is due to the isospin-asymmetry we introduced in the nuclear matter. At a neutron-to-proton ratio of around 1.5, the π^- mass increased, whereas the $\pi^{0,+}$ masses decreased. By plotting the pion masses at normal nuclear density over varying nucleon ratios, we saw that the positively charged pion might undergo a condensation process at a neutron-to-proton ratio of around 8 to 12. Since these plots are logarithmically symmetric around isospin-symmetric nuclear matter, the negatively charged pion might undergo such a condensation at corresponding inverse ratios.

The in-medium wave function renormalization increased in nuclear matter for all three pions. And by using our results for the in-medium wave function renormalization, we also calculated the 1PI vertex correction to the in-medium pion decay constant, which decreases in nuclear matter and also shows a similar splitting of triplet pion quantities.

Future works might include nucleon-nucleon interaction terms in the Lagrangian. This would lead to new effects beyond the linear density and a new scale for the density expansion, while also enabling to reach higher densities. It should be certainly intriguing to perform dynamical calculations in the SU(3) in-medium chiral perturbation theory beyond the linear density approximation, where meson loop amplitudes become reachable.

A. Physical background

A.1. Details on the SU(3) extension

In Appendix A.1.1, we present a relation between commutators of currents and various combinations of quark fields. In Appendix A.1.2, we use the chiral Ward identity to show which diagrams need to be considered in order to calculate the desired quark condensates. In the following sections, we quickly discuss the SU(3) Lagrangian that we will use in Appendix A.1.3 and show the diagrams that we compute in Appendix A.1.4.

A.1.1. Current algebra commutator relation

Based on the QCD current algebra (see for instance chapter 1.4.3 in Ref. [10]), we have the following equal-time commutator relation between the zero-component of an axial-vector current $A_\mu^a = \bar{q}\gamma_\mu\gamma^5\frac{\lambda^a}{2}q$ and a pseudoscalar current $P^a = \bar{q}\mathrm{i}\gamma^5\lambda^a q$:

$$[A_0^a(x), P^b(y)]_{x^0=y^0} = -\mathrm{i}\delta^{(3)}(\boldsymbol{x}-\boldsymbol{y})\left[\sqrt{\frac{2}{3}}\delta^{ab}S^0(x) + d^{abc}S^c(x)\right], \tag{A.1}$$

where the scalar current is $S^a = \bar{q}\lambda^a q$. Since the Noether charge is defined as the spatial integral over the zero-component of the axial-vector current, $Q_5^a = \int \mathrm{d}^3\boldsymbol{x}A_0^a(x)$, we can integrate and write the commutator relation as:

$$[Q_5^a, P^b(0)] = -\mathrm{i}\left[\sqrt{\frac{2}{3}}\delta^{ab}S^0(0) + d^{abc}S^c(0)\right]. \tag{A.2}$$

If we choose certain values of a and b, we get specific combinations of scalar quark field combinations. For $a = 3$ and $b = 8$, we get the difference of up and down currents:

$$[Q_5^3, P^8(0)] = -\frac{\mathrm{i}}{\sqrt{3}}S^3(0) = -\frac{\mathrm{i}}{\sqrt{3}}[\bar{u}u - \bar{d}d], \tag{A.3}$$

the values $a = 3$ and $b = 3$ lead to the sum of up and down currents:

$$\begin{aligned}
[Q_5^3, P^3(0)] &= -\mathrm{i}\left[\sqrt{\frac{2}{3}}S^0(0) + d^{338}S^8(0)\right] \\
&= -\mathrm{i}\left[\sqrt{\frac{2}{3}}\sqrt{\frac{2}{3}}(\bar{u}u + \bar{d}d + \bar{s}s) + \frac{1}{\sqrt{3}}\frac{1}{\sqrt{3}}(\bar{u}u + \bar{d}d - 2\bar{s}s)\right] \\
&= -\mathrm{i}\left[\bar{u}u + \bar{d}d\right],
\end{aligned} \tag{A.4}$$

and for $a = b = \{4, 5, 6, 7\}$, we can involve the strange currents:

$$\begin{aligned}
[Q_5^4, P^4(0)] &= -\mathrm{i}\left[\sqrt{\frac{2}{3}}S^0(0) + d^{443}S^3(0) + d^{448}S^8(0)\right] \\
&= -\mathrm{i}\left[\sqrt{\frac{2}{3}}\sqrt{\frac{2}{3}}(\bar{u}u + \bar{d}d + \bar{s}s) + \frac{1}{2}(\bar{u}u - \bar{d}d) + (-\frac{1}{2\sqrt{3}})\frac{1}{\sqrt{3}}(\bar{u}u + \bar{d}d - 2\bar{s}s)\right] \\
&= -\mathrm{i}\left[\frac{2}{3}(\bar{u}u + \bar{d}d + \bar{s}s) + \frac{1}{2}(\bar{u}u - \bar{d}d) - \frac{1}{6}(\bar{u}u + \bar{d}d - 2\bar{s}s)\right] \\
&= -\mathrm{i}\left[\bar{u}u + \bar{s}s\right],
\end{aligned} \tag{A.5a}$$

$$[Q_5^5, P^5(0)] = (\ldots) = -\mathrm{i}\left[\bar{u}u + \bar{s}s\right], \tag{A.5b}$$

$$[Q_5^6, P^6(0)] = (\ldots) = -\mathrm{i}\left[\bar{d}d + \bar{s}s\right], \tag{A.5c}$$

$$[Q_5^7, P^7(0)] = (\ldots) = -\mathrm{i}\left[\bar{d}d + \bar{s}s\right]. \tag{A.5d}$$

Note that we define $\lambda^0 = \sqrt{2/3}\mathbb{1}$, in order to be consistent with the normalization condition $\mathrm{Tr}\left\{\lambda^a\lambda^b\right\} = 2\delta^{ab}$. The SU(3) structure constants are listed in Appendix B.4.3. In the next section, we will use these commutators and show how to compute the in-medium condensates.

A.1.2. Chiral Ward identity in the SU(3) case

We start with the divergence of the following time-ordered product:

$$\partial^\mu[\mathsf{T}A_\mu^a(x)P^b(0)] = \mathsf{T}[\partial^\mu A_\mu^a(x)P^b(0)] + \delta(x^0)[A_0^a(x), P^b(0)]. \tag{A.6}$$

We can use the partially-conserved axial current (PCAC) relation:

$$\partial^\mu A_\mu^a(x) = \mathrm{i}\bar{q}\left\{M, \frac{\lambda_a}{2}\right\}\gamma^5 q, \tag{A.7}$$

with $M = \mathrm{diag}\,(m, m, m_s)$ the quark mass matrix. We need the following values of a:

$$\partial^\mu A_\mu^3(x) = \mathrm{i}\bar{q}\{M, \frac{\lambda_3}{2}\}\gamma^5 q = \mathrm{i}m\bar{q}\lambda_3\gamma^5 q = mP^3, \tag{A.8a}$$

$$\partial^\mu A_\mu^4(x) = \mathrm{i}\bar{q}\{M, \frac{\lambda_4}{2}\}\gamma^5 q = \mathrm{i}\frac{m + m_s}{2}\bar{q}\lambda_4\gamma^5 q = \frac{m + m_s}{2}P^4, \tag{A.8b}$$

$$\partial^\mu A_\mu^5(x) = \mathrm{i}\bar{q}\{M, \frac{\lambda_5}{2}\}\gamma^5 q = \mathrm{i}\frac{m+m_s}{2}\bar{q}\lambda_5\gamma^5 q = \frac{m+m_s}{2}P^5, \tag{A.8c}$$

$$\partial^\mu A_\mu^6(x) = \mathrm{i}\bar{q}\{M, \frac{\lambda_6}{2}\}\gamma^5 q = \mathrm{i}\frac{m+m_s}{2}\bar{q}\lambda_6\gamma^5 q = \frac{m+m_s}{2}P^6, \tag{A.8d}$$

$$\partial^\mu A_\mu^7(x) = \mathrm{i}\bar{q}\{M, \frac{\lambda_7}{2}\}\gamma^5 q = \mathrm{i}\frac{m+m_s}{2}\bar{q}\lambda_7\gamma^5 q = \frac{m+m_s}{2}P^7. \tag{A.8e}$$

Now we evaluate the whole equation Eq. (A.6) between the in-medium vacuum $|\Omega\rangle$,

$$\partial^\mu \Pi_{5\mu}^{38}(x,0) = m\Pi^{38}(x,0) + \delta(x^0)\langle\Omega|[A_0^3(x), P^8(0)]|\Omega\rangle, \tag{A.9a}$$

$$\partial^\mu \Pi_{5\mu}^{33}(x,0) = m\Pi^{33}(x,0) + \delta(x^0)\langle\Omega|[A_0^3(x), P^3(0)]|\Omega\rangle, \tag{A.9b}$$

$$\partial^\mu \Pi_{5\mu}^{44}(x,0) = \frac{m+m_s}{2}\Pi^{44}(x,0) + \delta(x^0)\langle\Omega|[A_0^4(x), P^4(0)]|\Omega\rangle, \tag{A.9c}$$

$$\partial^\mu \Pi_{5\mu}^{55}(x,0) = \frac{m+m_s}{2}\Pi^{55}(x,0) + \delta(x^0)\langle\Omega|[A_0^5(x), P^5(0)]|\Omega\rangle, \tag{A.9d}$$

$$\partial^\mu \Pi_{5\mu}^{66}(x,0) = \frac{m+m_s}{2}\Pi^{66}(x,0) + \delta(x^0)\langle\Omega|[A_0^6(x), P^6(0)]|\Omega\rangle, \tag{A.9e}$$

$$\partial^\mu \Pi_{5\mu}^{77}(x,0) = \frac{m+m_s}{2}\Pi^{77}(x,0) + \delta(x^0)\langle\Omega|[A_0^7(x), P^7(0)]|\Omega\rangle, \tag{A.9f}$$

where we abbreviated:

$$\Pi_{5\mu}^{ab}(x,0) = \langle\Omega|\mathsf{T}A_\mu^a(x)P^b(0)|\Omega\rangle, \qquad \Pi^{ab}(x,0) = \langle\Omega|\mathsf{T}P^a(x)P^b(0)|\Omega\rangle. \tag{A.10}$$

We perform a Fourier transformation to momentum space,

$$-\mathrm{i}q^\mu \Pi_{5\mu}^{38}(q) = m\Pi^{38}(q) + \int \mathrm{d}^3\boldsymbol{x}\, \mathrm{e}^{-\mathrm{i}\boldsymbol{q}\cdot\boldsymbol{x}}\langle\Omega|[A_0^a(x), P^b(0)]|\Omega\rangle, \tag{A.11a}$$

$$-\mathrm{i}q^\mu \Pi_{5\mu}^{33}(q) = m\Pi^{33}(q) + \int \mathrm{d}^3\boldsymbol{x}\, \mathrm{e}^{-\mathrm{i}\boldsymbol{q}\cdot\boldsymbol{x}}\langle\Omega|[A_0^3(x), P^3(0)]|\Omega\rangle, \tag{A.11b}$$

$$-\mathrm{i}q^\mu \Pi_{5\mu}^{44}(q) = \frac{m+m_s}{2}\Pi^{44}(q) + \int \mathrm{d}^3\boldsymbol{x}\, \mathrm{e}^{-\mathrm{i}\boldsymbol{q}\cdot\boldsymbol{x}}\langle\Omega|[A_0^4(x), P^4(0)]|\Omega\rangle, \tag{A.11c}$$

$$-\mathrm{i}q^\mu \Pi_{5\mu}^{55}(q) = \frac{m+m_s}{2}\Pi^{55}(q) + \int \mathrm{d}^3\boldsymbol{x}\, \mathrm{e}^{-\mathrm{i}\boldsymbol{q}\cdot\boldsymbol{x}}\langle\Omega|[A_0^5(x), P^5(0)]|\Omega\rangle, \tag{A.11d}$$

$$-\mathrm{i}q^\mu \Pi_{5\mu}^{66}(q) = \frac{m+m_s}{2}\Pi^{66}(q) + \int \mathrm{d}^3\boldsymbol{x}\, \mathrm{e}^{-\mathrm{i}\boldsymbol{q}\cdot\boldsymbol{x}}\langle\Omega|[A_0^6(x), P^6(0)]|\Omega\rangle, \tag{A.11e}$$

$$-\mathrm{i}q^\mu \Pi_{5\mu}^{77}(q) = \frac{m+m_s}{2}\Pi^{77}(q) + \int \mathrm{d}^3\boldsymbol{x}\, \mathrm{e}^{-\mathrm{i}\boldsymbol{q}\cdot\boldsymbol{x}}\langle\Omega|[A_0^7(x), P^7(0)]|\Omega\rangle, \tag{A.11f}$$

and take the soft limit $q^\mu \to 0$. This allows us to integrate over the last term, which gives the corresponding conserved Noether charge according to $Q_5^a = \int \mathrm{d}^3\boldsymbol{x}\, A_0^a(x)$:

$$-\mathrm{i}\lim_{q\to 0} q^\mu \Pi_{5\mu}^{38}(q) = m\Pi^{38}(0) + \langle\Omega|[Q_5^3, P^8(0)]|\Omega\rangle, \tag{A.12a}$$

$$-\mathrm{i}\lim_{q\to 0} q^\mu \Pi_{5\mu}^{33}(q) = m\Pi^{33}(0) + \langle\Omega|[Q_5^3, P^3(0)]|\Omega\rangle, \tag{A.12b}$$

$$-\mathrm{i}\lim_{q\to 0} q^\mu \Pi_{5\mu}^{44}(q) = \frac{m+m_s}{2}\Pi^{44}(0) + \langle\Omega|[Q_5^4, P^4(0)]|\Omega\rangle, \tag{A.12c}$$

$$-\mathrm{i}\lim_{q\to 0} q^\mu \Pi_{5\mu}^{55}(q) = \frac{m+m_s}{2}\Pi^{55}(0) + \langle\Omega|[Q_5^5, P^5(0)]|\Omega\rangle, \tag{A.12d}$$

$$-\mathrm{i}\lim_{q\to 0} q^\mu \Pi^{66}_{5\mu}(q) = \frac{m+m_s}{2}\Pi^{66}(0) + \langle\Omega|[Q^6_5, P^6(0)]|\Omega\rangle, \tag{A.12e}$$

$$-\mathrm{i}\lim_{q\to 0} q^\mu \Pi^{77}_{5\mu}(q) = \frac{m+m_s}{2}\Pi^{77}(0) + \langle\Omega|[Q^7_5, P^7(0)]|\Omega\rangle. \tag{A.12f}$$

In order to continue, we employ the SU(3) chiral transformation behavior of the pseudoscalar current, Eq. (A.3) (and subsequent relations), to write the equation like this:

$$m\Pi^{38}(0) + \mathrm{i}\lim_{q\to 0} q^\mu \Pi^{38}_{5\mu}(q) = \frac{\mathrm{i}}{\sqrt{3}}\langle\bar{u}u - \bar{d}d\rangle^*, \tag{A.13a}$$

$$m\Pi^{33}(0) + \mathrm{i}\lim_{q\to 0} q^\mu \Pi^{33}_{5\mu}(q) = \mathrm{i}\langle\bar{u}u + \bar{d}d\rangle^*, \tag{A.13b}$$

$$\frac{m+m_s}{2}\Pi^{44}(0) + \mathrm{i}\lim_{q\to 0} q^\mu \Pi^{44}_{5\mu}(q) = \mathrm{i}\langle\bar{u}u + \bar{s}s\rangle^*, \tag{A.13c}$$

$$\frac{m+m_s}{2}\Pi^{55}(0) + \mathrm{i}\lim_{q\to 0} q^\mu \Pi^{55}_{5\mu}(q) = \mathrm{i}\langle\bar{u}u + \bar{s}s\rangle^*, \tag{A.13d}$$

$$\frac{m+m_s}{2}\Pi^{66}(0) + \mathrm{i}\lim_{q\to 0} q^\mu \Pi^{66}_{5\mu}(q) = \mathrm{i}\langle\bar{d}d + \bar{s}s\rangle^*, \tag{A.13e}$$

$$\frac{m+m_s}{2}\Pi^{77}(0) + \mathrm{i}\lim_{q\to 0} q^\mu \Pi^{77}_{5\mu}(q) = \mathrm{i}\langle\bar{d}d + \bar{s}s\rangle^*. \tag{A.13f}$$

In the soft limit, the second term on the left-hand side vanishes, since we don't have zero modes, so by calculating Π^{ab} in chiral perturbation theory, we can infer the density dependence of the condensates:

$$\langle\bar{u}u - \bar{d}d\rangle^* = -\mathrm{i}\sqrt{3}m\Pi^{38}(0), \tag{A.14a}$$

$$\langle\bar{u}u + \bar{d}d\rangle^* = -\mathrm{i}m\Pi^{33}(0), \tag{A.14b}$$

$$\langle\bar{u}u + \bar{s}s\rangle^* = -\mathrm{i}\frac{m+m_s}{2}\Pi^{44}(0), \tag{A.14c}$$

$$\langle\bar{u}u + \bar{s}s\rangle^* = -\mathrm{i}\frac{m+m_s}{2}\Pi^{55}(0), \tag{A.14d}$$

$$\langle\bar{d}d + \bar{s}s\rangle^* = -\mathrm{i}\frac{m+m_s}{2}\Pi^{66}(0), \tag{A.14e}$$

$$\langle\bar{d}d + \bar{s}s\rangle^* = -\mathrm{i}\frac{m+m_s}{2}\Pi^{77}(0). \tag{A.14f}$$

For the strange condensates, we actually calculate them like this, using a linear combination of correlation functions:

$$\langle\bar{u}u + \bar{s}s\rangle^* = -\mathrm{i}\frac{m+m_s}{4}\left[\Pi^{44}(0) + \Pi^{55}(0)\right], \tag{A.15a}$$

$$\langle\bar{d}d + \bar{s}s\rangle^* = -\mathrm{i}\frac{m+m_s}{4}\left[\Pi^{66}(0) + \Pi^{77}(0)\right], \tag{A.15b}$$

and use the following relations:

$$\langle(P_4 + \mathrm{i}P_5)(P_4 - \mathrm{i}P_5)\rangle^* = \langle P_4P_4 + P_5P_5\rangle^* = \left[\Pi^{44}(0) + \Pi^{55}(0)\right], \tag{A.16a}$$

$$\langle(P_6 + \mathrm{i}P_7)(P_6 - \mathrm{i}P_7)\rangle^* = \langle P_6P_6 + P_7P_7\rangle^* = \left[\Pi^{66}(0) + \Pi^{77}(0)\right], \tag{A.16b}$$

so that we finally have:

$$\langle \bar{u}u - \bar{d}d\rangle^* = -\mathrm{i}m\langle\Omega|P^3P^8|\Omega\rangle^*, \tag{A.17a}$$

$$\langle \bar{u}u + \bar{d}d\rangle^* = -\mathrm{i}m\langle\Omega|P^3P^3|\Omega\rangle^*, \tag{A.17b}$$

$$\langle \bar{u}u + \bar{s}s\rangle^* = -\mathrm{i}\frac{m+m_s}{2}\left\langle\left(\frac{P_4+\mathrm{i}P_5}{\sqrt{2}}\right)\left(\frac{P_4-\mathrm{i}P_5}{\sqrt{2}}\right)\right\rangle^*, \tag{A.17c}$$

$$\langle \bar{d}d + \bar{s}s\rangle^* = -\mathrm{i}\frac{m+m_s}{2}\left\langle\left(\frac{P_6+\mathrm{i}P_7}{\sqrt{2}}\right)\left(\frac{P_6-\mathrm{i}P_7}{\sqrt{2}}\right)\right\rangle^*. \tag{A.17d}$$

These combinations of pseudoscalar currents in Eqs. (A.17c) and (A.17d) makes it convenient to perform calculations using kaons.

A.1.3. SU(3) chiral perturbation theory

We use the following SU(3) chiral Lagrangian [78, 123] with a meson-only part and meson-baryon interactions:

$$\mathcal{L} = \mathcal{L}_\Phi^{(2)} + \mathcal{L}_{MB}^{(1)} + \mathcal{L}_{MB}^{(2)}, \tag{A.18}$$

where:

$$\mathcal{L}_\Phi^{(2)} = \frac{f^2}{4}\operatorname{Tr}\left\{D_\mu U^\dagger D^\mu U + \chi^\dagger U + \chi U^\dagger\right\}, \tag{A.19a}$$

$$\mathcal{L}_{MB}^{(1)} = \operatorname{Tr}\left\{\bar{B}(\mathrm{i}\not{D} - M_0)B)\right\} - \frac{D}{2}\operatorname{Tr}\left\{\bar{B}\gamma^\mu\gamma^5\{u_\mu, B\}\right\} - \frac{F}{2}\operatorname{Tr}\left\{\bar{B}\gamma^\mu\gamma^5[u_\mu, B]\right\}, \tag{A.19b}$$

$$\mathcal{L}_{MB}^{(2)} = b_D\operatorname{Tr}\left\{\bar{B}\{\chi_+, B\}\right\} + b_F\operatorname{Tr}\left\{\bar{B}[\chi_+, B]\right\} + b_0\operatorname{Tr}\left\{\bar{B}B\right\}\operatorname{Tr}\left\{\chi_+\right\} + \dots \tag{A.19c}$$

There are many more terms that would be allowed by chiral symmetry to enter $\mathcal{L}_{MB}^{(2)}$, however those are not relevant to the present calculations.

The meson octet $\Phi = \Phi^a\lambda^a/\sqrt{2}$ is given in terms of the chiral field $U = \exp\left(\mathrm{i}\sqrt{2}\Phi/f\right)$:

$$U = \mathbb{1} + \frac{\mathrm{i}\sqrt{2}}{f}\Phi - \frac{1}{f^2}\Phi^2 + \dots, \qquad U^\dagger = \mathbb{1} - \frac{\mathrm{i}\sqrt{2}}{f}\Phi - \frac{1}{f^2}\Phi^2 + \dots, \tag{A.20}$$

where we identify the physical fields as follows:

$$\Phi = \begin{pmatrix} \frac{\Phi_3}{\sqrt{2}} + \frac{\Phi_8}{\sqrt{6}} & \frac{\Phi_1 - \mathrm{i}\Phi_2}{\sqrt{2}} & \frac{\Phi_4 - \mathrm{i}\Phi_5}{\sqrt{2}} \\ \frac{\Phi_1 + \mathrm{i}\Phi_2}{\sqrt{2}} & -\frac{\Phi_3}{\sqrt{2}} + \frac{\Phi_8}{\sqrt{6}} & \frac{\Phi_6 - \mathrm{i}\Phi_7}{\sqrt{2}} \\ \frac{\Phi_4 + \mathrm{i}\Phi_5}{\sqrt{2}} & \frac{\Phi_6 + \mathrm{i}\Phi_7}{\sqrt{2}} & -\frac{2}{\sqrt{6}}\Phi_8 \end{pmatrix} = \begin{pmatrix} \frac{\pi^0}{\sqrt{2}} + \frac{\eta}{\sqrt{6}} & \pi^+ & K^+ \\ \pi^- & -\frac{\pi^0}{\sqrt{2}} + \frac{\eta}{\sqrt{6}} & K^0 \\ K^- & \bar{K}^0 & -\frac{2}{\sqrt{6}}\eta \end{pmatrix}. \tag{A.21}$$

These fields are related by:

$$\Phi_1 = \frac{1}{\sqrt{2}}(\pi^+ + \pi^-), \qquad \pi^+ = \frac{1}{\sqrt{2}}(\Phi_1 - \mathrm{i}\Phi_2), \tag{A.22a}$$

$$\Phi_2 = \frac{\mathrm{i}}{\sqrt{2}}(\pi^+ - \pi^-), \qquad \pi^- = \frac{1}{\sqrt{2}}(\Phi_1 + \mathrm{i}\Phi_2), \tag{A.22b}$$

$$\Phi_3 = \pi^0, \qquad \pi^0 = \Phi_3, \tag{A.22c}$$

$$\Phi_4 = \frac{1}{\sqrt{2}}(K^+ + K^-), \qquad K^+ = \frac{1}{\sqrt{2}}(\Phi_4 - \mathrm{i}\Phi_5), \tag{A.22d}$$

$$\Phi_5 = \frac{\mathrm{i}}{\sqrt{2}}(K^+ - K^-), \qquad K^- = \frac{1}{\sqrt{2}}(\Phi_4 + \mathrm{i}\Phi_5), \tag{A.22e}$$

$$\Phi_6 = \frac{1}{\sqrt{2}}(K^0 + \bar{K}^0), \qquad K^0 = \frac{1}{\sqrt{2}}(\Phi_6 - \mathrm{i}\Phi_7), \tag{A.22f}$$

$$\Phi_7 = \frac{\mathrm{i}}{\sqrt{2}}(K^0 - \bar{K}^0), \qquad \bar{K}^0 = \frac{1}{\sqrt{2}}(\Phi_6 + \mathrm{i}\Phi_7), \tag{A.22g}$$

$$\Phi_8 = \eta, \qquad \eta = \Phi_8. \tag{A.22h}$$

Since we will only perform a linear density (first order, i.e. no loop diagrams) calculation, this simple parametrization of the chiral field is more convenient than the parametrization we used in the SU(2) case.

The scalar ($s = s^a\lambda^a$) and pseudoscalar fields ($p = p^a\lambda^a$) are contained in χ:

$$\chi = 2B_0(s + \mathrm{i}p), \qquad \chi^\dagger = 2B_0(s - \mathrm{i}p), \tag{A.23}$$

where we set $s = M = \mathrm{diag}\,(m, m, m_s) = \frac{2m+m_s}{3}\mathbb{1} + \frac{m-m_s}{\sqrt{3}}\lambda_8$ in the case that $m_u = m_d = m$, or

$$s = \begin{pmatrix} m_u & 0 & 0 \\ 0 & m_d & 0 \\ 0 & 0 & m_s \end{pmatrix} = \underbrace{\frac{m_u + m_d + m_s}{3}}_{\frac{2m+m_s}{3}}\mathbb{1} + \underbrace{\frac{m_u - m_d}{2}}_{\delta m}\lambda^3 + \underbrace{\frac{m_u + m_d - 2m_s}{2\sqrt{3}}}_{\frac{m-m_s}{\sqrt{3}}}\lambda^8 \tag{A.24}$$

where $m = (m_u + m_d)/2$ and $\delta m = (m_u - m_d)/2$, if we want to include explicit isospin breaking in the Lagrangian. Note that the notation $\lambda^0 = \sqrt{2/3}\mathbb{1}$ is also common, which ensures that the normalization of Gell-Mann matrices $\mathrm{Tr}\left\{\lambda^a\lambda^b\right\} = 2\delta^{ab}$ holds also for $a = 0$.

The baryon octet $B = B^a\lambda^a/\sqrt{2}$ is given by:

$$B = \begin{pmatrix} \frac{B_3}{\sqrt{2}} + \frac{B_8}{\sqrt{6}} & \frac{B_1 - \mathrm{i}B_2}{\sqrt{2}} & \frac{B_4 - \mathrm{i}B_5}{\sqrt{2}} \\ \frac{B_1 + \mathrm{i}B_2}{\sqrt{2}} & -\frac{B_3}{\sqrt{2}} + \frac{B_8}{\sqrt{6}} & \frac{B_6 - \mathrm{i}B_7}{\sqrt{2}} \\ \frac{B_4 + \mathrm{i}B_5}{\sqrt{2}} & \frac{B_6 + \mathrm{i}B_7}{\sqrt{2}} & -\frac{2}{\sqrt{6}}B_8 \end{pmatrix} \equiv \begin{pmatrix} \frac{\Sigma^0}{\sqrt{2}} + \frac{\Lambda}{\sqrt{6}} & \Sigma^+ & p \\ \Sigma^- & -\frac{\Sigma^0}{\sqrt{2}} + \frac{\Lambda}{\sqrt{6}} & n \\ \Xi^- & \Xi^0 & -\frac{2}{\sqrt{6}}\Lambda \end{pmatrix}, \tag{A.25}$$

and their adjoints $\bar{B} = \bar{B}^a\lambda^a/\sqrt{2}$ by:

$$\bar{B} = \begin{pmatrix} \frac{\bar{B}_3}{\sqrt{2}} + \frac{\bar{B}_8}{\sqrt{6}} & \frac{\bar{B}_1 - \mathrm{i}\bar{B}_2}{\sqrt{2}} & \frac{\bar{B}_4 - \mathrm{i}\bar{B}_5}{\sqrt{2}} \\ \frac{\bar{B}_1 + \mathrm{i}\bar{B}_2}{\sqrt{2}} & -\frac{\bar{B}_3}{\sqrt{2}} + \frac{\bar{B}_8}{\sqrt{6}} & \frac{\bar{B}_6 - \mathrm{i}\bar{B}_7}{\sqrt{2}} \\ \frac{\bar{B}_4 + \mathrm{i}\bar{B}_5}{\sqrt{2}} & \frac{\bar{B}_6 + \mathrm{i}\bar{B}_7}{\sqrt{2}} & -\frac{2}{\sqrt{6}}\bar{B}_8 \end{pmatrix} \equiv \begin{pmatrix} \frac{\bar{\Sigma}^0}{\sqrt{2}} + \frac{\bar{\Lambda}}{\sqrt{6}} & \bar{\Sigma}^- & \bar{\Xi}^- \\ \bar{\Sigma}^+ & -\frac{\bar{\Sigma}^0}{\sqrt{2}} + \frac{\bar{\Lambda}}{\sqrt{6}} & \bar{\Xi}^0 \\ \bar{p} & \bar{n} & -\frac{2}{\sqrt{6}}\bar{\Lambda} \end{pmatrix}. \tag{A.26}$$

The baryon fields B^a are given in terms of the physical fields as:

$$B_1 = \frac{1}{\sqrt{2}}(\Sigma^+ + \Sigma^-), \qquad \bar{B}_1 = \frac{1}{\sqrt{2}}(\bar{\Sigma}^+ + \bar{\Sigma}^-), \tag{A.27a}$$

$$B_2 = \frac{\mathrm{i}}{\sqrt{2}}(\Sigma^+ - \Sigma^-), \qquad \bar{B}_2 = \frac{\mathrm{i}}{\sqrt{2}}(\bar{\Sigma}^- - \bar{\Sigma}^+), \tag{A.27b}$$

$$B_3 = \Sigma^0, \qquad \bar{B}_3 = \bar{\Sigma}^0, \tag{A.27c}$$

$$B_4 = \frac{1}{\sqrt{2}}(p + \Xi^-), \qquad \bar{B}_4 = \frac{1}{\sqrt{2}}(\bar{p} + \bar{\Xi}^-), \tag{A.27d}$$

$$B_5 = \frac{\mathrm{i}}{\sqrt{2}}(p - \Xi^-), \qquad \bar{B}_5 = \frac{\mathrm{i}}{\sqrt{2}}(\bar{\Xi}^- - \bar{p}), \tag{A.27e}$$

$$B_6 = \frac{1}{\sqrt{2}}(n + \Xi^0), \qquad \bar{B}_6 = \frac{1}{\sqrt{2}}(\bar{n} + \bar{\Xi}^0), \tag{A.27f}$$

$$B_7 = \frac{\mathrm{i}}{\sqrt{2}}(n - \Xi^0), \qquad \bar{B}_7 = \frac{\mathrm{i}}{\sqrt{2}}(\bar{\Xi}^0 - \bar{n}), \tag{A.27g}$$

$$B_8 = \Lambda, \qquad \bar{B}_8 = \bar{\Lambda}, \tag{A.27h}$$

and the physical fields are given in terms of the B^a baryon fields as:

$$\Sigma^+ = \frac{1}{\sqrt{2}}(B_1 - \mathrm{i}B_2), \qquad \bar{\Sigma}^+ = \frac{1}{\sqrt{2}}(\bar{B}_1 + \mathrm{i}\bar{B}_2), \tag{A.28a}$$

$$\Sigma^- = \frac{1}{\sqrt{2}}(B_1 + \mathrm{i}B_2), \qquad \bar{\Sigma}^- = \frac{1}{\sqrt{2}}(\bar{B}_1 - \mathrm{i}\bar{B}_2), \tag{A.28b}$$

$$\Sigma^0 = B_3, \qquad \bar{\Sigma}^0 = \bar{B}_3, \tag{A.28c}$$

$$p = \frac{1}{\sqrt{2}}(B_4 - \mathrm{i}B_5), \qquad \bar{p} = \frac{1}{\sqrt{2}}(\bar{B}_4 + \mathrm{i}\bar{B}_5), \tag{A.28d}$$

$$n = \frac{1}{\sqrt{2}}(B_6 - \mathrm{i}B_7), \qquad \bar{n} = \frac{1}{\sqrt{2}}(\bar{B}_6 + \mathrm{i}\bar{B}_7), \tag{A.28e}$$

$$\Xi^- = \frac{1}{\sqrt{2}}(B_4 + \mathrm{i}B_5), \qquad \bar{\Xi}^- = \frac{1}{\sqrt{2}}(\bar{B}_4 - \mathrm{i}\bar{B}_5), \tag{A.28f}$$

$$\Xi^0 = \frac{1}{\sqrt{2}}(B_6 + \mathrm{i}B_7), \qquad \bar{\Xi}^0 = \frac{1}{\sqrt{2}}(\bar{B}_6 - \mathrm{i}\bar{B}_7), \tag{A.28g}$$

$$\Lambda = B_8, \qquad \bar{\Lambda} = \bar{B}_8. \tag{A.28h}$$

The field χ_+ is defined as:

$$\chi_+ = u\chi^\dagger u + u^\dagger \chi u^\dagger, \tag{A.29}$$

where $u^2 = U$, as in the SU(2) case:

$$u = \mathbb{1} + \frac{\mathrm{i}}{\sqrt{2}f}\Phi - \frac{1}{4f^2}\Phi^2 + \ldots, \qquad u^\dagger = \mathbb{1} - \frac{\mathrm{i}}{\sqrt{2}f}\Phi - \frac{1}{4f^2}\Phi^2 + \ldots \tag{A.30}$$

A.1.4. Kaon interaction Lagrangian

We want to calculate the following correlation functions:

$$\Pi^{38} = \langle \Omega | P^3 P^8 | \Omega \rangle^*, \tag{A.31a}$$

$$\Pi^{33} = \langle \Omega | P^3 P^3 | \Omega \rangle^*, \tag{A.31b}$$

$$\Pi^{4+i5,4-i5} = \left\langle \left(\frac{P_4 + \mathrm{i}P_5}{\sqrt{2}} \right) \left(\frac{P_4 - \mathrm{i}P_5}{\sqrt{2}} \right) \right\rangle^*, \tag{A.31c}$$

$$\Pi^{6+i7,6-i7} = \left\langle \left(\frac{P_6 + \mathrm{i}P_7}{\sqrt{2}} \right) \left(\frac{P_6 - \mathrm{i}P_7}{\sqrt{2}} \right) \right\rangle^*, \tag{A.31d}$$

in order to compute $\langle \bar{u}u - \bar{d}d \rangle^*$, $\langle \bar{u}u + \bar{d}d \rangle^*$, $\langle \bar{u}u + \bar{s}s \rangle^*$ and $\langle \bar{d}d + \bar{s}s \rangle^*$, respectively, as derived in Eq. (A.17). We will show the specific diagrams later when we actually calculate the in-medium condensates.

It is easy to show that the interaction between a mesonic field and a pseudoscalar current is given by:

$$[\mathrm{i}\mathcal{L}_{\Phi^a p^b}] = 2\mathrm{i}B_0 f \delta^{ab}, \tag{A.32}$$

however for further interactions involving the kaons, we need to take a closer look at the interaction terms of the Lagrangian[1].

This is the interaction Lagrangian in terms of Φ^a:

$$\begin{aligned}\mathcal{L}_{\bar{N}N\Phi p} &= \frac{8B_0(b_0 + b_D)}{f} \Big[\bar{p}p\Phi_4 p_4 + \bar{p}p\Phi_5 p_5 + \bar{n}n\Phi_6 p_6 + \bar{n}n\Phi_7 p_7 \Big] \\ &\quad + \frac{4B_0(2b_0 + b_D - b_F)}{f} \Big[\bar{n}n\Phi_4 p_4 + \bar{n}n\Phi_5 p_5 + \bar{p}p\Phi_6 p_6 + \bar{p}p\Phi_7 p_7 \Big],\end{aligned} \tag{A.33a}$$

$$\begin{aligned}\mathcal{L}_{\bar{N}N\Phi^2} &= -\frac{2B_0(m + m_s)(b_0 + b_D)}{f^2} \Big[\bar{p}p\Phi_4^2 + \bar{p}p\Phi_5^2 + \bar{n}n\Phi_6^2 + \bar{n}n\Phi_7^2 \Big] \\ &\quad - \frac{B_0(m + m_s)(2b_0 + b_D - b_F)}{f^2} \Big[\bar{n}n\Phi_4^2 + \bar{n}n\Phi_5^2 + \bar{p}p\Phi_6^2 + \bar{p}p\Phi_7^2 \Big].\end{aligned} \tag{A.33b}$$

We do not have a mixing between $\Phi_{4,5,6,7}$. Since the kaons are given by:

$$\begin{aligned}
\Phi_4 &= \frac{1}{\sqrt{2}}(K^+ + K^-), & K^+ &= \frac{1}{\sqrt{2}}(\Phi_4 - \mathrm{i}\Phi_5), \\
\Phi_5 &= \frac{\mathrm{i}}{\sqrt{2}}(K^+ - K^-), & K^- &= \frac{1}{\sqrt{2}}(\Phi_4 + \mathrm{i}\Phi_5), \\
\Phi_6 &= \frac{1}{\sqrt{2}}(K^0 + \bar{K}^0), & K^0 &= \frac{1}{\sqrt{2}}(\Phi_6 - \mathrm{i}\Phi_7), \\
\Phi_7 &= \frac{\mathrm{i}}{\sqrt{2}}(K^0 - \bar{K}^0), & \bar{K}^0 &= \frac{1}{\sqrt{2}}(\Phi_6 + \mathrm{i}\Phi_7),
\end{aligned}$$

[1]Since the kaons are given as a superposition of mesonic fields, we derive their interaction vertices more carefully.

we can substitute Φ^a for the physical kaon fields:

$$\begin{aligned}\mathcal{L}_{\bar{N}N\Phi p} =& \frac{8B_0(b_0+b_D)}{\sqrt{2}f}\\&\times\Big[\bar{p}p(K^+ + K^-)p_4 + \bar{p}p\mathrm{i}(K^+ - K^-)p_5 + \bar{n}n(K^0+\bar{K}^0)p_6 + \bar{n}n\mathrm{i}(K^0-\bar{K}^0)p_7\Big]\\&+\frac{4B_0(2b_0+b_D-b_F)}{\sqrt{2}f}\\&\times\Big[\bar{n}n(K^+ + K^-)p_4 + \bar{n}n\mathrm{i}(K^+ - K^-)p_5 + \bar{p}p(K^0+\bar{K}^0)p_6 + \bar{p}p\mathrm{i}(K^0-\bar{K}^0)p_7\Big],\end{aligned} \tag{A.34a}$$

$$\begin{aligned}\mathcal{L}_{\bar{N}N\Phi^2} =& -\frac{2B_0(m+m_s)(b_0+b_D)}{2f^2}\\&\times\Big[\bar{p}p(K^+ + K^-)^2 - \bar{p}p(K^+ - K^-)^2 + \bar{n}n(K^0+\bar{K}^0)^2 - \bar{n}n(K^0-\bar{K}^0)^2\Big]\\&-\frac{B_0(m+m_s)(2b_0+b_D-b_F)}{2f^2}\\&\times\Big[\bar{n}n(K^+ + K^-)^2 - \bar{n}n(K^+ - K^-)^2 + \bar{p}p(K^0+\bar{K}^0)^2 - \bar{p}p(K^0-\bar{K}^0)^2\Big].\end{aligned} \tag{A.34b}$$

After simplifying these expressions, we get:

$$\begin{aligned}\mathcal{L}_{\bar{N}N\Phi p} =& \frac{8B_0(b_0+b_D)}{\sqrt{2}f}\\&\times\Bigg[\bar{p}p\Big[K^+(p_4+\mathrm{i}p_5) + K^-(p_4-\mathrm{i}p_5)\Big] + \bar{n}n\Big[K^0(p_6+\mathrm{i}p_7)+\bar{K}^0(p_6-\mathrm{i}p_7)\Big]\Bigg]\\&+\frac{4B_0(2b_0+b_D-b_F)}{\sqrt{2}f}\\&\times\Bigg[\bar{n}n\Big[K^+(p_4+\mathrm{i}p_5) + K^-(p_4-\mathrm{i}p_5)\Big] + \bar{p}p\Big[K^0(p_6+\mathrm{i}p_7)+\bar{K}^0(p_6-\mathrm{i}p_7)\Big]\Bigg],\end{aligned} \tag{A.35a}$$

$$\begin{aligned}\mathcal{L}_{\bar{N}N\Phi^2} =& -\frac{4B_0(m+m_s)(b_0+b_D)}{f^2}\Big[\bar{p}pK^+K^- + \bar{n}nK^0\bar{K}^0\Big]\\&-\frac{2B_0(m+m_s)(2b_0+b_D-b_F)}{f^2}\Big[\bar{n}nK^+K^- + \bar{p}pK^0\bar{K}^0\Big].\end{aligned} \tag{A.35b}$$

Now we can read off the following interaction terms for the charged kaons:

$$[\mathrm{i}\mathcal{L}_{\bar{p}p\frac{P^4+\mathrm{i}P^5}{\sqrt{2}}K^+}] = \frac{8\mathrm{i}B_0(b_0+b_D)}{f}, \tag{A.36a}$$

$$[\mathrm{i}\mathcal{L}_{\bar{n}n\frac{P^4+\mathrm{i}P^5}{\sqrt{2}}K^+}] = \frac{4\mathrm{i}B_0(2b_0+b_D-b_F)}{f}, \tag{A.36b}$$

$$[\mathrm{i}\mathcal{L}_{\bar{p}p\frac{P^4-\mathrm{i}P^5}{\sqrt{2}}K^-}] = \frac{8\mathrm{i}B_0(b_0+b_D)}{f}, \tag{A.36c}$$

$$[\mathrm{i}\mathcal{L}_{\bar{n}n\frac{P^4-\mathrm{i}P^5}{\sqrt{2}}K^-}] = \frac{4\mathrm{i}B_0(2b_0+b_D-b_F)}{f}, \tag{A.36d}$$

$$[\mathrm{i}\mathcal{L}_{\bar{p}pK^+K^-}] = -\frac{4\mathrm{i}B_0(m+m_s)(b_0+b_D)}{f^2}, \tag{A.36e}$$

$$[\mathrm{i}\mathcal{L}_{\bar{n}nK^+K^-}] = -\frac{2\mathrm{i}B_0(m+m_s)(2b_0+b_D-b_F)}{f^2}, \tag{A.36f}$$

and similarly for the electrically neutral kaons:

$$[\mathrm{i}\mathcal{L}_{\bar{p}p\frac{P^6+\mathrm{i}P^7}{\sqrt{2}}K^0}] = \frac{4\mathrm{i}B_0(2b_0+b_D-b_F)}{f}, \tag{A.37a}$$

$$[\mathrm{i}\mathcal{L}_{\bar{n}n\frac{P^6+\mathrm{i}P^7}{\sqrt{2}}K^0}] = \frac{8\mathrm{i}B_0(b_0+b_D)}{f}, \tag{A.37b}$$

$$[\mathrm{i}\mathcal{L}_{\bar{p}p\frac{P^6-\mathrm{i}P^7}{\sqrt{2}}\bar{K}^0}] = \frac{4\mathrm{i}B_0(2b_0+b_D-b_F)}{f}, \tag{A.37c}$$

$$[\mathrm{i}\mathcal{L}_{\bar{n}n\frac{P^6-\mathrm{i}P^7}{\sqrt{2}}\bar{K}^0}] = \frac{8\mathrm{i}B_0(b_0+b_D)}{f}, \tag{A.37d}$$

$$[\mathrm{i}\mathcal{L}_{\bar{p}pK^0\bar{K}^0}] = -\frac{2\mathrm{i}B_0(m+m_s)(2b_0+b_D-b_F)}{f^2}, \tag{A.37e}$$

$$[\mathrm{i}\mathcal{L}_{\bar{n}nK^0\bar{K}^0}] = -\frac{4\mathrm{i}B_0(m+m_s)(b_0+b_D)}{f^2}. \tag{A.37f}$$

A.2. Interactions in the Lagrangian

In this section, we list all the interactions in the Lagrangian that we use in this thesis. First, these are the interactions coming from the chiral Lagrangian, involving only the pion field and external sources,

$$\mathcal{L}^{(2)}_{\pi} = \frac{f^2}{4}\,\mathrm{Tr}\left\{D_\mu U^\dagger D^\mu U + \chi^\dagger U + \chi U^\dagger\right\}$$

- The π-p vertex:

$$\mathcal{L}^{(2)}_{\pi p} = 2fB_0\pi^i p^i. \tag{A.38}$$

- The π-a vertex:

$$\mathcal{L}^{(2)}_{\pi a} = -f\partial_\mu\pi^i\frac{a^\mu_i}{2}. \tag{A.39}$$

- The $\pi\pi\pi$-p vertex:

$$\mathcal{L}^{(2)}_{\pi^3 p} = -\frac{B_0}{5f}p^i\pi^i\pi^j\pi^j. \tag{A.40}$$

- The π^4 vertex:

$$\mathcal{L}^{(2)}_{\pi^4} = \frac{1}{10f^2}\partial_\mu \pi^i \partial^\mu \pi^j \pi^k \pi^l (3\delta^{ik}\delta^{jl} - \delta^{ij}\delta^{kl}) - \frac{mB_0}{20f^2}\pi^i\pi^i\pi^j\pi^j. \tag{A.41}$$

- The π^3-a_μ vertex:

$$\mathcal{L}^{(2)}_{\pi^3 a} = \frac{1}{5f} a^i_\mu \partial^\mu \pi^j \pi^k \pi^l (3\delta^{ij}\delta^{kl} - 4\delta^{ik}\delta^{jl}). \tag{A.42}$$

Using the first term in the expansion of the pion-nucleon interaction operator A,

$$A^{(1)} = -\mathrm{i}\gamma^\mu \Gamma_\mu - \mathrm{i} g_A \gamma^\mu \gamma^5 \Delta_\mu,$$

we find the following interactions relevant for this thesis (note that the only parameter is g_A),

- The NN-a_μ vertex:

$$A^{(1)}_a = -g_A \gamma^\mu \gamma^5 a^i_\mu \frac{\tau^i}{2}. \tag{A.43}$$

- The NN-πa_μ vertex:

$$A^{(1)}_{\pi a} = -\frac{1}{2f}\gamma^\mu \pi^i a^j_\mu \epsilon^{ijk}\tau^k. \tag{A.44}$$

- The NN-$\pi\pi a_\mu$ vertex:

$$A^{(1)}_{\pi^2 a} = \frac{g_A}{4f^2}\gamma^\mu\gamma^5 \pi^a \pi^b a^c_\mu \tau^d (\delta^{ab}_{cd} - \delta^{ac}_{bd}). \tag{A.45}$$

- The NN-π vertex:

$$A^{(1)}_{\pi} = \frac{g_A}{2f}\gamma^\mu\gamma^5 \partial_\mu \pi^i \tau^i. \tag{A.46}$$

- The NN-$\pi\pi$ vertex:

$$A^{(1)}_{\pi\pi} = \frac{1}{4f^2}\gamma^\mu \pi^i \partial_\mu \pi^j \epsilon^{ijk}\tau^k. \tag{A.47}$$

- The NN-$\pi\pi\pi$ vertex:

$$A^{(1)}_{\pi^3} = \frac{g_A}{20f^3}\gamma^\mu\gamma^5 \left[3\pi^i\pi^j\partial_\mu\pi^j - \pi^j\pi^j\partial_\mu\pi^i\right]\tau^i. \tag{A.48}$$

The second term, $A^{(2)}$ is given by:

$$\begin{aligned} A^{(2)} = &-c_1 \,\mathrm{Tr}_F\{\chi_+\} + \frac{c_2}{2m_N^2}\,\mathrm{Tr}_F\{u_\mu u_\nu\}\, D^\mu D^\nu - \frac{c_3}{2}\,\mathrm{Tr}_F\{u_\mu u^\mu\} + \frac{c_4}{2}\gamma^\mu\gamma^\nu[u_\mu, u_\nu] \\ &- c_5 \hat{\chi}_+ - \frac{\mathrm{i}c_6}{8m_N}\gamma^\mu\gamma^\nu F^+_{\mu\nu} - \frac{\mathrm{i}c_7}{8m_N}\gamma^\mu\gamma^\nu\,\mathrm{Tr}_F\left\{F^+_{\mu\nu}\right\}, \end{aligned}$$

and leads to these interactions:

- The NN-π vertex:

$$A^{(2)}_{\pi} = 0. \tag{A.49}$$

- The NN-$\pi\pi\pi$ vertex:

$$A^{(2)}_{\pi^3} = 0. \tag{A.50}$$

- The NN-a_μ vertex:

$$A^{(2)}_{a} = 0. \tag{A.51}$$

- The NN-πa_μ vertex:

$$A^{(2)}_{\pi a} = -\frac{2c_2}{f m_N^2}\partial_\mu \pi^i a^i_\nu \partial^\mu \partial^\nu + \frac{2c_3}{f}\partial^\mu \pi^i a^i_\mu - \frac{\mathrm{i}c_4}{f}\epsilon^{ijk}\tau^k \partial_\mu \pi^i a^j_\nu [\gamma^\mu, \gamma^\nu]. \tag{A.52}$$

- The NN-πp vertex:

$$A^{(2)}_{\pi p} = -\frac{8c_1 B_0}{f} p^i \pi^i. \tag{A.53}$$

- The NN-$\pi\pi$ vertex:

$$A^{(2)}_{\pi\pi} = \frac{4B_0 c_1 m}{f^2}\pi^i\pi^i + \frac{c_2}{f^2 m_N^2}\partial_\mu \pi^i \partial_\nu \pi^i \partial^\mu \partial^\nu - \frac{c_3}{f^2}\partial_\mu \pi^i \partial^\mu \pi^i + \frac{\mathrm{i}c_4}{f^2}\epsilon^{ijk}\tau^k \gamma^\mu\gamma^\nu \partial_\mu \pi^i \partial_\nu \pi^j. \tag{A.54}$$

A.2.1. Interactions in the SU(3) Lagrangian

From the SU(3) Lagrangian Eq. (A.18):

$$\mathcal{L} = \mathcal{L}^{(2)}_{\Phi} + \mathcal{L}^{(1)}_{MB} + \mathcal{L}^{(2)}_{MB}, \tag{A.55}$$

where:

$$\mathcal{L}^{(2)}_{\Phi} = \frac{f^2}{4}\operatorname{Tr}\left\{ D_\mu U^\dagger D^\mu U + \chi^\dagger U + \chi U^\dagger \right\}, \tag{A.56a}$$

$$\mathcal{L}^{(1)}_{MB} = \operatorname{Tr}\left\{ \bar{B}(\mathrm{i}\not{D} - M_0)B) \right\} - \frac{D}{2}\operatorname{Tr}\left\{ \bar{B}\gamma^\mu\gamma^5\{u_\mu, B\} \right\} - \frac{F}{2}\operatorname{Tr}\left\{ \bar{B}\gamma^\mu\gamma^5[u_\mu, B] \right\}, \tag{A.56b}$$

$$\mathcal{L}^{(2)}_{MB} = b_D \operatorname{Tr}\left\{ \bar{B}\{\chi_+, B\} \right\} + b_F \operatorname{Tr}\left\{ \bar{B}[\chi_+, B] \right\} + b_0 \operatorname{Tr}\left\{ \bar{B}B \right\} \operatorname{Tr}\{\chi_+\} + \dots, \tag{A.56c}$$

we get the following interactions. First, the interactions with external currents are:

$$\mathcal{L}_{\Phi p} = 2B_0 f \Phi^a p^a \quad (a = 1, .., 8), \tag{A.57a}$$

$$\mathcal{L}_{\bar{N}Np^0\eta_8} = -\frac{4\sqrt{2}B_0(b_D - 3b_F)}{3f}(\bar{p}p + \bar{n}n)p^0\eta_8, \tag{A.57b}$$

$$\mathcal{L}_{\bar{N}Np^0\pi^0} = \frac{4\sqrt{\frac{2}{3}}B_0(b_D + b_F)}{f}(\bar{p}p - \bar{n}n)p^0\pi^0, \tag{A.57c}$$

$$\mathcal{L}_{\bar{N}Np^8\pi^0} = \frac{4B_0(b_D + b_F)}{\sqrt{3}f}(\bar{p}p - \bar{n}n)p^8\pi^0, \tag{A.57d}$$

$$\mathcal{L}_{\bar{N}Np^3\eta_8} = \frac{4B_0(b_D + b_F)}{\sqrt{3}f}(\bar{p}p - \bar{n}n)p^3\eta_8, \tag{A.57e}$$

$$\mathcal{L}_{\bar{N}Np^3\pi^0} = \frac{4B_0(2b_0 + b_D + b_F)}{f}(\bar{p}p + \bar{n}n)p^3\pi^0, \tag{A.57f}$$

$$\mathcal{L}_{\bar{N}Np^8\eta_8} = \frac{4B_0(6b_0 + 5b_D - 3b_F)}{3f}(\bar{p}p + \bar{n}n)p^8\eta_8, \tag{A.57g}$$

and these interactions do not exist: $\mathcal{L}_{p^0\pi^0} = \mathcal{L}_{p^0\eta} = 0$.

Interactions without external currents:

$$\mathcal{L}_{\pi^0\eta_8} = -\frac{2B_0\,\delta m}{\sqrt{3}}\pi^0\eta_8, \tag{A.58a}$$

$$\begin{aligned}\mathcal{L}_{\bar{N}N\pi^0\eta_8} = &-\frac{4B_0\delta m(2b_0 + b_D + b_F)}{\sqrt{3}f^2}(\bar{p}p + \bar{n}n)\pi^0\eta_8 \\ &- \frac{4B_0 m(b_D + b_F)}{\sqrt{3}f^2}(\bar{p}p - \bar{n}n)\pi^0\eta_8,\end{aligned} \tag{A.58b}$$

$$\begin{aligned}\mathcal{L}_{\bar{N}N\eta_8\eta_8} = &-\frac{2B_0[m(2b_0 + b_D + b_F) + 4m_s(b_0 + b_D - b_F))}{3f^2}(\bar{p}p + \bar{n}n)\eta_8\eta_8 \\ &- \frac{2B_0\delta m(b_D + b_F)}{3f^2}(\bar{p}p - \bar{n}n)\eta_8\eta_8,\end{aligned} \tag{A.58c}$$

$$\mathcal{L}_{\bar{N}N\pi^0\pi^0} = -\frac{4B_0 m(2b_0 + b_D + b_F)}{f^2}(\bar{p}p + \bar{n}n)\pi^0\pi^0. \tag{A.58d}$$

Interactions involving electrically charged kaons:

$$\mathcal{L}_{\bar{p}p\frac{P^4+\mathrm{i}P^5}{\sqrt{2}}K^+} = \frac{8B_0(b_0 + b_D)}{f}\bar{p}p\frac{P^4 + \mathrm{i}P^5}{\sqrt{2}}K^+, \tag{A.59a}$$

$$\mathcal{L}_{\bar{n}n\frac{P^4+\mathrm{i}P^5}{\sqrt{2}}K^+} = \frac{4B_0(2b_0 + b_D - b_F)}{f}\bar{n}n\frac{P^4 + \mathrm{i}P^5}{\sqrt{2}}K^+, \tag{A.59b}$$

$$\mathcal{L}_{\bar{p}p\frac{P^4-\mathrm{i}P^5}{\sqrt{2}}K^-} = \frac{8B_0(b_0 + b_D)}{f}\bar{p}p\frac{P^4 - \mathrm{i}P^5}{\sqrt{2}}K^-, \tag{A.59c}$$

$$\mathcal{L}_{\bar{n}n\frac{P^4-\mathrm{i}P^5}{\sqrt{2}}K^-} = \frac{4B_0(2b_0 + b_D - b_F)}{f}\bar{n}n\frac{P^4 - \mathrm{i}P^5}{\sqrt{2}}K^-, \tag{A.59d}$$

$$\mathcal{L}_{\bar{p}pK^+K^-} = -\frac{4B_0(m + m_s)(b_0 + b_D)}{f^2}\bar{p}pK^+K^-, \tag{A.59e}$$

$$\mathcal{L}_{\bar{n}nK^+K^-} = -\frac{2B_0(m + m_s)(2b_0 + b_D - b_F)}{f^2}\bar{n}nK^+K^-, \tag{A.59f}$$

and similarly for the electrically neutral kaons:

$$\mathcal{L}_{\bar{p}p\frac{P^6+\mathrm{i}P^7}{\sqrt{2}}K^0} = \frac{4B_0(2b_0 + b_D - b_F)}{f}\bar{p}p\frac{P^6 + \mathrm{i}P^7}{\sqrt{2}}K^0, \tag{A.60a}$$

$$\mathcal{L}_{\bar{n}n\frac{P^6+\mathrm{i}P^7}{\sqrt{2}}K^0} = \frac{8B_0(b_0+b_D)}{f}\bar{n}n\frac{P^6+\mathrm{i}P^7}{\sqrt{2}}K^0, \tag{A.60b}$$

$$\mathcal{L}_{\bar{p}p\frac{P^6-\mathrm{i}P^7}{\sqrt{2}}\bar{K}^0} = \frac{4B_0(2b_0+b_D-b_F)}{f}\bar{p}p\frac{P^6-\mathrm{i}P^7}{\sqrt{2}}\bar{K}^0, \tag{A.60c}$$

$$\mathcal{L}_{\bar{n}n\frac{P^6-\mathrm{i}P^7}{\sqrt{2}}\bar{K}^0} = \frac{8B_0(b_0+b_D)}{f}\bar{n}n\frac{P^6-\mathrm{i}P^7}{\sqrt{2}}\bar{K}^0, \tag{A.60d}$$

$$\mathcal{L}_{\bar{p}pK^0\bar{K}^0} = -\frac{2B_0(m+m_s)(2b_0+b_D-b_F)}{f^2}\bar{p}pK^0\bar{K}^0, \tag{A.60e}$$

$$\mathcal{L}_{\bar{n}nK^0\bar{K}^0} = -\frac{4B_0(m+m_s)(b_0+b_D)}{f^2}\bar{n}nK^0\bar{K}^0. \tag{A.60f}$$

A.3. Spinor conventions

In this section, we summarize our conventions for quantized fermionic fields, following Ref. [85]. The nucleon and its conjugate can be expanded as:

$$N(x) = \sum_{s=1}^{2}\int\frac{\mathrm{d}^3\boldsymbol{p}}{(2\pi)^3}\frac{1}{\sqrt{2\omega_p}}\left(a^s_{\boldsymbol{p}}u^s_{\boldsymbol{p}}\mathrm{e}^{-\mathrm{i}p\cdot x}+b^{s\dagger}_{\boldsymbol{p}}v^s_{\boldsymbol{p}}\mathrm{e}^{\mathrm{i}p\cdot x}\right), \tag{A.61a}$$

$$\bar{N}(x) = \sum_{s=1}^{2}\int\frac{\mathrm{d}^3\boldsymbol{p}}{(2\pi)^3}\frac{1}{\sqrt{2\omega_p}}\left(a^{s\dagger}_{\boldsymbol{p}}\bar{u}^s_{\boldsymbol{p}}\mathrm{e}^{\mathrm{i}p\cdot x}+b^{s}_{\boldsymbol{p}}\bar{v}^s_{\boldsymbol{p}}\mathrm{e}^{-\mathrm{i}p\cdot x}\right), \tag{A.61b}$$

where $a^{s(\dagger)}_{\boldsymbol{p}}$ the annihilation (creation) operator for a nucleon of momentum $\boldsymbol{p}$ and spin s, and $b^{s(\dagger)}_{\boldsymbol{p}}$ the annihilation (creation) operator for an anti-nucleon of momentum $\boldsymbol{p}$ and spin s. They fulfill the following anticommutator relations:

$$\{a^s_{\boldsymbol{p}}, a^{s'\dagger}_{\boldsymbol{p}'}\} = (2\pi)^3\delta^{(3)}(\boldsymbol{p}-\boldsymbol{p}')\delta_{ss'} = \{b^s_{\boldsymbol{p}}, b^{s'\dagger}_{\boldsymbol{p}'}\}. \tag{A.62}$$

Next, $u^s_{\boldsymbol{p}}$ and $v^s_{\boldsymbol{p}}$ are four-component spinors that can be written in terms of two two-component (Weyl) spinors,

$$u^s_{\boldsymbol{p}} = \begin{pmatrix}\sqrt{p\cdot\sigma}\,\xi_s\\ \sqrt{p\cdot\bar{\sigma}}\,\xi_s\end{pmatrix}, \qquad v^s_{\boldsymbol{p}} = \begin{pmatrix}\sqrt{p\cdot\sigma}\,\eta_s\\ -\sqrt{p\cdot\bar{\sigma}}\,\eta_s\end{pmatrix}, \tag{A.63}$$

where we can choose a basis for the spinors as the eigenvectors of the third Pauli matrix, σ^3,

$$\xi_1 = \eta_1 = \begin{pmatrix}1\\0\end{pmatrix}, \qquad \xi_2 = \eta_2 = \begin{pmatrix}0\\1\end{pmatrix}, \qquad \sigma^\mu = \begin{pmatrix}1\\ \boldsymbol{\sigma}\end{pmatrix}, \qquad \bar{\sigma}^\mu = \begin{pmatrix}1\\ -\boldsymbol{\sigma}\end{pmatrix}. \tag{A.64}$$

Here, ξ_1 and ξ_2 represent spin-up and spin-down along the z-axis, respectively, whereas we have to flip these assignments for the antiparticle spinors η, where η_1 and η_2 stand for spin-down and spin-up, respectively. The square root over $\sqrt{p\cdot\sigma}$ is to be treated by taking the positive square root of the operator's eigenvalue, that is for a nucleon propagating in z-direction with $p^\mu = (E, 0, 0, p_z)^\mu$:

$$\sqrt{p \cdot \sigma} \begin{pmatrix} 1 \\ 0 \end{pmatrix} = \begin{pmatrix} \sqrt{E - p_z} \\ \sqrt{E + p_z} \end{pmatrix}. \tag{A.65}$$

Finally, the spinors are normalized according to[2]:

$$\bar{u}^s_{\boldsymbol{p}} u^{s'}_{\boldsymbol{p}} = 2m\delta_{ss'}, \qquad \bar{v}^s_{\boldsymbol{p}} v^{s'}_{\boldsymbol{p}} = -2m\delta_{ss'}, \tag{A.66a}$$

$$u^{s\dagger}_{\boldsymbol{p}} u^{s'}_{\boldsymbol{p}} = 2E(\boldsymbol{p})\delta_{ss'}, \qquad v^{s\dagger}_{\boldsymbol{p}} v^{s'}_{\boldsymbol{p}} = 2E(\boldsymbol{p})\delta_{ss'}, \tag{A.66b}$$

where—independent of the choice of the normalization—the equalities $\bar{u}u = \frac{m}{E(\boldsymbol{p})} u^\dagger u$ and $\bar{v}v = -\frac{m}{E(\boldsymbol{p})} v^\dagger v$ hold. For two spinors with three-momenta in opposite directions, we have:

$$u^{s\dagger}_{\boldsymbol{p}} v^{s'}_{-\boldsymbol{p}} = 0, \qquad v^{s\dagger}_{\boldsymbol{p}} u^{s'}_{-\boldsymbol{p}} = 0. \tag{A.67}$$

The spinors u and v are orthogonal to each other with respect to their Dirac adjoint, but not with respect to their Hermitian adjoint:

$$\bar{u}^s_{\boldsymbol{p}} v^{s'}_{\boldsymbol{p}} = 0, \qquad \bar{v}^s_{\boldsymbol{p}} u^{s'}_{\boldsymbol{p}} = 0, \tag{A.68a}$$

$$u^{s\dagger}_{\boldsymbol{p}} v^{s'}_{\boldsymbol{p}} \neq 0, \qquad v^{s\dagger}_{\boldsymbol{p}} u^{s'}_{\boldsymbol{p}} \neq 0. \tag{A.68b}$$

Lastly, their outer product yields:

$$\sum_s u^s_{\boldsymbol{p}} \bar{u}^s_{\boldsymbol{p}} = \not{p} + m_N, \qquad \sum_s v^s_{\boldsymbol{p}} \bar{v}^s_{\boldsymbol{p}} = \not{p} - m_N. \tag{A.69}$$

[2]The spinors can be normalized arbitrarily, as long as $u^\dagger u$ and $v^\dagger v$ transform under Lorentz transformations like the zero-component of a four vector in order to have a Lorentz invariant probability $\mathrm{d}P \sim \mathrm{d}^3\boldsymbol{x}\, \bar{\psi}\gamma^0\psi \sim \mathrm{d}^3\boldsymbol{x}\psi^\dagger\psi$. Refs. [85, 124–128] choose the same normalization as this thesis, where $\bar{u}u = 2m = -\bar{v}v$. On the other hand, Refs. [55, 56, 129, 130] choose a normalization where $\bar{u}u = 1 = -\bar{v}v$.

B. Mathematical Background

B.1. How to expand the chiral field

We choose the following parametrization of the chiral field U:

$$U(\pi) = \exp\left[\mathrm{i}\boldsymbol{\pi}\frac{y(\pi^2)}{2\sqrt{\pi^2}}\right] = \cos\left(\frac{y(\pi^2)}{2}\right) + \mathrm{i}\frac{\boldsymbol{\pi}}{\sqrt{\pi^2}}\sin\left(\frac{y(\pi^2)}{2}\right), \tag{B.1}$$

where $\boldsymbol{\pi} = \pi^a\tau^a$ and $\boldsymbol{\pi}^2 = \pi^a\tau^a\pi^b\tau^b = \pi^a\pi^a\mathbb{1} = \pi^2\mathbb{1}$. We will now discuss how this expansion into sine and cosine functions work, as well as how to deal with the function $y(\pi^2)$. To start, we define the matrix M as:

$$M = \boldsymbol{\pi}\frac{y(\pi^2)}{2\sqrt{\pi^2}} = \frac{y(\pi^2)}{2\sqrt{\pi^2}}\begin{pmatrix} \pi^3 & \pi^1 - \mathrm{i}\pi^2 \\ \pi^1 + \mathrm{i}\pi^2 & \pi^3 \end{pmatrix}. \tag{B.2}$$

Since $\boldsymbol{\pi}^2 = \pi^2\mathbb{1}$, the square of this matrix M, and in fact all even powers of M are easily obtained:

$$M^2 = \pi^2\mathbb{1}\frac{y(\pi^2)^2}{4\pi^2} = \left(\frac{y(\pi^2)}{2}\right)^2\mathbb{1}, \qquad M^{2n} = \left(\frac{y(\pi^2)}{2}\right)^{2n}\mathbb{1}. \tag{B.3}$$

In contrast, the odd powers are:

$$M^{2n+1} = \left(\frac{y(\pi^2)}{2}\right)^{2n+1}\frac{\boldsymbol{\pi}}{\sqrt{\pi^2}}. \tag{B.4}$$

Using these results, the exponential of M can be separated into a part proportional to the identity matrix, and a part proportional to the pion fields:

$$\exp\left[\mathrm{i}M\right] = \mathbb{1} + \mathrm{i}M - \frac{1}{2}M^2 - \frac{\mathrm{i}}{3!}M^3 + \dots \tag{B.5a}$$

$$= \left[1 + \left(\frac{y(\pi^2)}{2}\right)^2 + \dots\right]\mathbb{1} + \mathrm{i}\left[\frac{y(\pi^2)}{2} - \frac{1}{3!}\left(\frac{y(\pi^2)}{2}\right)^3 + \dots\right]\frac{\boldsymbol{\pi}}{\sqrt{\pi^2}}. \tag{B.5b}$$

The terms in brackets are exactly the Taylor expanded terms of a cosine and a sine function, which directly yields Eq. (B.1).

The function $y(\pi^2)$ is defined to satisfy:

$$y(\pi^2) - \sin\Big(y(\pi^2)\Big) = \frac{4}{3}\left(\frac{\pi^2}{f^2}\right)^{3/2}. \tag{B.6}$$

a_1	a_3	a_5	a_7	a_9	a_{11}	a_{13}	a_{15}	a_{17}	$\dots$	a_{2n}
2	$\frac{2}{15}$	$\frac{4}{175}$	$\frac{8}{1\,575}$	$\frac{86}{67\,375}$	$\frac{9\,704}{28\,153\,125}$	$\frac{1\,211\,512}{12\,415\,528\,125}$	$\frac{265\,816}{9\,306\,171\,875}$	$\frac{66\,170\,151\,332}{7\,719\,664\,999\,921\,875}$		0

Table B.1.: The first nine nonvanishing coefficients in the series expansion of $y(\pi^2)$. All coefficients a_n with n an even integer vanish.

In order to solve this, we set $\eta \equiv (\pi^2/f^2)^{1/2}$ for brevity and make a power series ansatz,

$$y(\pi^2) = \sum_{n=0}^{\infty} a_n \eta^n, \quad \eta = \sqrt{\frac{\pi^2}{f^2}}. \tag{B.7}$$

The terms corresponding to $n < 0$ would produce inverse pion fields in the Lagrangian, so we ignore those, and the term corresponding to $n = 0$ has to vanish, since for $\eta = 0$, the equation simplifies to $y = \sin(y)$, which is only solved by $y = 0$. By using this ansatz iteratively in Eq. (B.6), we can compare coefficients of various powers of η. The first few of these equations are

$$n = 1 \qquad 0 = 0 \tag{B.8a}$$

$$n = 2 \qquad 0 = 0 \tag{B.8b}$$

$$n = 3 \qquad \frac{a_1^3}{6} = \frac{4}{3} \tag{B.8c}$$

$$n = 4 \qquad \frac{1}{2} a_1^2 a_2 = 0 \tag{B.8d}$$

$$n = 5 \qquad -\frac{a_1^5}{120} + \frac{1}{2} a_3 a_1^2 + \frac{1}{2} a_2^2 a_1 = 0 \tag{B.8e}$$

$$\vdots \qquad \vdots$$

At any given order of η^n, there are only terms involving a_m with $m \leq n$. And since with each step in increasing order, only one new term enters the equation, one can calculate the values for a_n step by step. More precisely, comparing coefficients at order n enables us to calculate a_{n-2}. The result for $y(\pi^2)$ reads:

$$y(\pi^2) = 2\eta + \frac{2}{15}\eta^3 + \frac{4}{175}\eta^5 + \frac{8}{1\,575}\eta^7 + \frac{86}{67\,375}\eta^9 \cdots, \quad \eta = \sqrt{\frac{\pi^2}{f^2}}. \tag{B.9}$$

However, in order to evaluate the chiral field U, we need the sine and cosine of this function. By using their respective series expansion, those terms are given by:

$$\cos\left(\frac{y(\pi^2)}{2}\right) = 1 - \frac{1}{2}\eta^2 - \frac{1}{40}\eta^4 - \frac{11}{2\,800}\eta^6 - \frac{823}{1\,008\,000}\eta^8 + \cdots, \tag{B.10a}$$

$$\sin\left(\frac{y(\pi^2)}{2}\right) = \eta - \frac{1}{10}\eta^3 - \frac{19}{1\,400}\eta^5 - \frac{71}{25\,200}\eta^7 - \frac{17\,753}{25\,872\,000}\eta^9 + \cdots \tag{B.10b}$$

With this, the chiral field is given as

$$U(\pi) = \mathbb{1} + \mathrm{i}\frac{\boldsymbol{\pi}}{f} - \frac{1}{2}\frac{\pi^2}{f^2} - \frac{\mathrm{i}}{10}\frac{\boldsymbol{\pi}\pi^2}{f^3} - \frac{1}{40}\frac{(\pi^2)^2}{f^4} - \frac{19\mathrm{i}}{1\,400}\frac{\boldsymbol{\pi}(\pi^2)^2}{f^5} + \cdots \tag{B.11}$$

If one takes a derivative of Eq. (B.6), we get an equation for y', which we need in order to deal with $\partial_\mu U$:

$$y'(\pi^2) - \cos(y)y'(\pi^2) = \frac{2}{f^2}\sqrt{\frac{\pi^2}{f^2}}. \tag{B.12}$$

If we rearrange this equation, we get an expression for y' in terms of the sine function of y. Therefore we can do a series expansion, similar to Eqs. (B.10a) and (B.10b):

$$y'(\pi^2) = \frac{1}{f^2\sin^2(y/2)}\sqrt{\frac{\pi^2}{f^2}} \tag{B.13a}$$

$$= \frac{1}{f^2}\sqrt{\frac{f^2}{\pi^2}}\left(1 + \frac{1}{5}\frac{\pi^2}{f^2} + \frac{2}{35}\left(\frac{\pi^2}{f^2}\right)^2 + \frac{4}{225}\left(\frac{\pi^2}{f^2}\right)^3 + \frac{387}{67\,375}\left(\frac{\pi^2}{f^2}\right)^4 + \cdots\right). \tag{B.13b}$$

The following Mathematica code can be used to quickly calculate the function $y(\pi^2)$ to any odd-number order (the order should be chosen odd, since coefficients a_n with n even are zero anyway):

```
order = 51;
Subscript[a, 1] = 2;
y = Sum[Subscript[a, i] x^i, {i, 1, order, 2}];
If[OddQ[order] && Positive[order],
  For[i = 5, i < order + 4, i += 2,
    rule = Solve[
      Normal[Series[y - Sin[y] - 4/3 x^3, {x, 0, i}]]/x^i == 0][[1]];
    y = y /. rule
   ]
]
```

where the variable `order` has to be an odd number, greater than zero. Furthermore, we use `x` to abbreviate $x = \sqrt{\pi^2/f^2}$. In order to check whether the code ran successfully, the following code should simply evaluate to `True`, since it is the defining equation of $y(\pi^2)$ up to the designated order:

```
Series[y - Sin[y] == 4/3 x^3, {x, 0, order}]
```

Functions of $y(\pi^2)$ can then be expanded like this:

```
Series[1/x Sin[y/4], {x, 0, 6}]
```

which results in:

$$\sqrt{\frac{f^2}{\pi^2}}\sin(y/4) = \frac{1}{2} + \frac{1}{80}\frac{\pi^2}{f^2} + \frac{81}{44\,800}\left(\frac{\pi^2}{f^2}\right)^2 + \frac{1\,171}{3\,225\,600}\left(\frac{\pi^2}{f^2}\right)^3 + O\left((\pi^2/f^2)^{7/2}\right). \tag{B.14}$$

Another possibility is to use the open-source Python library `SymPy` [131]:

```
import sympy

order = 10
x, i = sympy.symbols('x i')
y = sympy.Sum(sympy.Indexed('a',i) * x**i,(i,1,order)).doit()

for i in range(0, order+1, 2):
    y = y.subs(sympy.Indexed('a',i), 0) # set a_2n = 0
y = y.subs(sympy.Indexed('a',1), 2)     # set  a_1 = 2

for i in range(3, order, 2):
    print("Order x^{0} done.    ".format(i), end="\r", flush=True)
    eq = y - sympy.sin(y) - 4*x**3/3
    eq_expanded = eq.series(x, 0, i+4).removeO() / x**(i+2)
    sol = sympy.solve(eq_expanded, sympy.Indexed('a',i))
    y = y.subs(sympy.Indexed('a',i), sol[0])

# The following line should return 0
test = (y - sympy.sin(y) - 4*x**3/3).series(x, 0, order).removeO()
if not test:
    print("Coefficients determined successfully.")
```

After a successful determination of the coefficients a_n, one can evaluate functions of $y(\pi^2)$ as follows:

```
(1/x * sympy.sin(y/4)).series(x, 0, 6)
```

which returns the same expansion as seen in Eq. (B.14).

B.2. Changing the basis of the self-energy

In our calculations, we calculated the in-medium pion self-energy in the so-called mathematical pion basis: $\{\pi^1, \pi^2, \pi^3\}$. However, the physical states are the charged pions: $\{\pi^+, \pi^-, \pi^0\}$.

These states are related via the following system of linear equations:

$$\pi^+ = \frac{1}{\sqrt{2}}(\pi^1 - \mathrm{i}\pi^2), \qquad \pi^1 = \frac{1}{\sqrt{2}}(\pi^+ + \pi^-), \tag{B.15a}$$

$$\pi^- = \frac{1}{\sqrt{2}}(\pi^1 + \mathrm{i}\pi^2), \qquad \pi^2 = \frac{\mathrm{i}}{\sqrt{2}}(\pi^+ - \pi^-), \tag{B.15b}$$

$$\pi^0 = \pi^3, \qquad \pi^3 = \pi^0. \tag{B.15c}$$

For a matrix given in the mathematical basis, $\mathcal{O}_{\text{math}}$, we can calculate the same matrix in the physical basis, $\mathcal{O}_{\text{phys}}$, via the following calculation:

$$\mathcal{O}_{\text{phys}} = T^{-1}\,\mathcal{O}_{\text{math}}\,T, \tag{B.16}$$

where the transformation matrix T is a matrix whose columns are the coordinates of the vectors in the new (physical) basis with respect to the old (mathematical) one. Thus, T is given by

$$T = \begin{pmatrix} \frac{1}{\sqrt{2}} & \frac{1}{\sqrt{2}} & 0 \\ -\frac{\mathrm{i}}{\sqrt{2}} & \frac{\mathrm{i}}{\sqrt{2}} & 0 \\ 0 & 0 & 1 \end{pmatrix}. \tag{B.17}$$

The pion properties are calculated in the mathematical basis and typically contain the following flavor structures: $\mathcal{O}^{ab}_{\text{math}} \sim \mathcal{O}_1\delta^{ab} + \mathcal{O}_2\mathrm{i}\epsilon^{ab3} + \mathcal{O}_3\delta^{a3}\delta^{b3}$. This leads to the following general form of $\mathcal{O}_{\text{math}}$:

$$\mathcal{O}_{\text{math}} = \begin{pmatrix} \mathcal{O}_1 & \mathrm{i}\mathcal{O}_2 & 0 \\ -\mathrm{i}\mathcal{O}_2 & \mathcal{O}_1 & 0 \\ 0 & 0 & \mathcal{O}_1 + \mathcal{O}_3 \end{pmatrix}. \tag{B.18}$$

If we now apply Eq. (B.16), we get

$$\mathcal{O}_{\text{phys}} = \begin{pmatrix} \mathcal{O}_1 + \mathcal{O}_2 & 0 & 0 \\ 0 & \mathcal{O}_1 - \mathcal{O}_2 & 0 \\ 0 & 0 & \mathcal{O}_1 + \mathcal{O}_3 \end{pmatrix}, \tag{B.19}$$

and confirm that in the physical basis, the various pion properties are diagonal.

B.3. Changing the basis of the decay constant

While the charged pions are defined like this:

$$\pi^\pm = \frac{1}{\sqrt{2}}(\pi^1 \mp \mathrm{i}\pi^2), \qquad \pi^0 = \pi^3, \tag{B.20}$$

the charged currents are defined without this factor of $\sqrt{2}$:

$$J^\pm = J^1 \pm \mathrm{i}J^2, \qquad J^0 = J^3, \tag{B.21}$$

since the ladder operators for the SU(2) algebra are defined as $\mathsf{t}^{\pm} = \mathsf{t}^1 \pm \mathrm{i}\mathsf{t}^2$.

A given diagram for the decay constant can contain the following terms, $f^{ab} = f_1\delta^{ab} + f_2\mathrm{i}\epsilon^{ab3} + f_3\delta^{a3}\delta^{b3}$. Therefore the possible results for f^{ab} are

$$\begin{pmatrix} f_1 & \mathrm{i}f_2 & 0 \\ -\mathrm{i}f_2 & f_1 & 0 \\ 0 & 0 & f_1 + f_3 \end{pmatrix} \tag{B.22}$$

Lastly, if $f = 92$ MeV, then we have to include a factor of $\sqrt{2}$ when dealing with charged states:

$$\langle\Omega|J^a|\pi^b\rangle \propto f^{ab} \qquad\qquad \langle\Omega|J^{\pm}|\pi^{\pm}\rangle \propto \sqrt{2}f_{\pm} \tag{B.23}$$

Now since the currents and the pions transform differently, how do we calculate the charged decay constants? It turns out that the same relation holds as for the self-energy which we derived in the previous section. To see this, we write

$$\langle\Omega|J^+|\pi^+\rangle = \langle\Omega|\Big[J^1 + \mathrm{i}J^2\Big]\frac{1}{\sqrt{2}}\Big[|\pi^1\rangle - \mathrm{i}|\pi^2\rangle\Big] \tag{B.24a}$$

$$= \frac{1}{\sqrt{2}}\langle\Omega|J^1|\pi^1\rangle + \frac{1}{\sqrt{2}}\langle\Omega|J^2|\pi^2\rangle + \frac{\mathrm{i}}{\sqrt{2}}\langle\Omega|J^2|\pi^1\rangle - \frac{\mathrm{i}}{\sqrt{2}}\langle\Omega|J^1|\pi^2\rangle \tag{B.24b}$$

$$\propto \frac{1}{\sqrt{2}}f^{11} + \frac{1}{\sqrt{2}}f^{22} + \frac{\mathrm{i}}{\sqrt{2}}f^{21} - \frac{\mathrm{i}}{\sqrt{2}}f^{12} \tag{B.24c}$$

$$= \sqrt{2}\Big[\frac{1}{2}f^{11} + \frac{1}{2}f^{22} + \frac{\mathrm{i}}{2}f^{21} - \frac{\mathrm{i}}{2}f^{12}\Big] \tag{B.24d}$$

$$= \sqrt{2}\Big[\frac{1}{2}f_1 + \frac{1}{2}f_1 + \frac{1}{2}f_2 + \frac{1}{2}f_2\Big] \tag{B.24e}$$

$$= \sqrt{2}\Big[f_1 + f_2\Big] \tag{B.24f}$$

$$\stackrel{!}{=} \sqrt{2}f_+ \tag{B.24g}$$

In a similar way, one can calculate

$$\langle\Omega|J^+|\pi^-\rangle = 0 \tag{B.25a}$$

$$\langle\Omega|J^+|\pi^0\rangle = 0 \tag{B.25b}$$

$$\langle\Omega|J^-|\pi^+\rangle = 0 \tag{B.25c}$$

$$\langle\Omega|J^-|\pi^-\rangle = \sqrt{2}\Big[f_1 - f_2\Big] \tag{B.25d}$$

$$\langle\Omega|J^-|\pi^0\rangle = 0 \tag{B.25e}$$

$$\langle\Omega|J^0|\pi^+\rangle = 0 \tag{B.25f}$$

$$\langle\Omega|J^0|\pi^-\rangle = 0 \tag{B.25g}$$

$$\langle\Omega|J^0|\pi^0\rangle = \Big[f_1 + f_3\Big] \tag{B.25h}$$

The charged decay constants can be calculated exactly like the charged self-energies, viz. $\Sigma^{\pm} = \Sigma_1 \pm \Sigma_2$ and $\Sigma^0 = \Sigma_1 + \Sigma_3$, since the "missing" factor of $\sqrt{2}$ is present in Eq. (B.23). In summary:

$$f_{\pm} = f_1 \pm f_2, \qquad\qquad f_0 = f_1 + f_3. \tag{B.26}$$

B.4. Useful identities

This section lists useful mathematical identities involving the Pauli matrices, and the Dirac gamma matrices. These relations are very useful to calculate the traces that result from applying the Feynman rules to our diagrams.

B.4.1. Pauli matrices

The Pauli matrices are a set of three 2×2-matrices, which are Hermitian and unitary:

$$\tau^1 = \begin{pmatrix} 0 & 1 \\ 1 & 0 \end{pmatrix}, \quad \tau^2 = \begin{pmatrix} 0 & -\mathrm{i} \\ \mathrm{i} & 0 \end{pmatrix}, \quad \tau^3 = \begin{pmatrix} 1 & 0 \\ 0 & -1 \end{pmatrix}. \tag{B.27}$$

The commutator of two Pauli matrices is:

$$[\tau^a, \tau^b] = 2\mathrm{i}\epsilon^{abc}\tau^c, \tag{B.28}$$

and the anticommutator reads:

$$\{\tau^a, \tau^b\} = 2\delta^{ab}\mathbb{1}. \tag{B.29}$$

From the commutator and the anticommutator, one can derive this general expression for the product of two Pauli matrices:

$$\tau^a\tau^b = \delta^{ab}\mathbb{1} + \mathrm{i}\epsilon^{abc}\tau^c. \tag{B.30}$$

Finally, we often evaluate the trace over a certain number of Pauli matrices:

$$\mathrm{Tr}\left\{\tau^a\right\} = 0, \tag{B.31a}$$
$$\mathrm{Tr}\left\{\tau^a\tau^b\right\} = 2\delta^{ab}, \tag{B.31b}$$
$$\mathrm{Tr}\left\{\tau^a\tau^b\tau^c\right\} = 2\mathrm{i}\epsilon^{abc}, \tag{B.31c}$$
$$\mathrm{Tr}\left\{\tau^a\tau^b\tau^c\tau^d\right\} = 2(\delta^{ab}\delta^{cd} - \delta^{ac}\delta^{bd} + \delta^{ad}\delta^{bc}). \tag{B.31d}$$

B.4.2. Traces over Pauli matrices

We often have to evaluate traces over Pauli matrices, especially involving the matrix $n(\boldsymbol{p})$,

$$\begin{aligned} n(\boldsymbol{p}) &= \begin{pmatrix} \Theta(k_F^p - |\boldsymbol{p}|) & 0 \\ 0 & \Theta(k_F^n - |\boldsymbol{p}|) \end{pmatrix} \\ &= \frac{1}{2}\Big[\Theta(k_F^p - |\boldsymbol{p}|) + \Theta(k_F^n - |\boldsymbol{p}|)\Big]\mathbb{1} + \frac{1}{2}\Big[\Theta(k_F^p - |\boldsymbol{p}|) - \Theta(k_F^n - |\boldsymbol{p}|)\Big]\tau^3, \end{aligned} \tag{B.32}$$

where we usually abbreviate $\Theta(k_F^i - |\boldsymbol{p}|) \equiv \Theta_{\boldsymbol{p}}^i$. The following traces are often used:

$$\mathrm{Tr}_F\{n(\boldsymbol{p})n(\boldsymbol{q})\} = \Theta_{\boldsymbol{p}}^p\Theta_{\boldsymbol{q}}^p + \Theta_{\boldsymbol{p}}^n\Theta_{\boldsymbol{q}}^n, \tag{B.33a}$$

$$\mathrm{Tr}_F\{\tau^a n(\boldsymbol{p})n(\boldsymbol{q})\} = [\Theta_{\boldsymbol{p}}^p\Theta_{\boldsymbol{q}}^p - \Theta_{\boldsymbol{p}}^n\Theta_{\boldsymbol{q}}^n]\delta^{a3}, \tag{B.33b}$$

$$\mathrm{Tr}_F\{n(\boldsymbol{p})\tau^a n(\boldsymbol{q})\} = [\Theta_{\boldsymbol{p}}^p\Theta_{\boldsymbol{q}}^p - \Theta_{\boldsymbol{p}}^n\Theta_{\boldsymbol{q}}^n]\delta^{a3}, \tag{B.33c}$$

$$\begin{aligned} \mathrm{Tr}_F\Big\{\tau^a n(\boldsymbol{p})\tau^b n(\boldsymbol{q})\Big\} &= [\Theta_{\boldsymbol{p}}^p\Theta_{\boldsymbol{q}}^n + \Theta_{\boldsymbol{p}}^n\Theta_{\boldsymbol{q}}^p]\delta^{ab} + [\Theta_{\boldsymbol{p}}^p\Theta_{\boldsymbol{q}}^n - \Theta_{\boldsymbol{p}}^n\Theta_{\boldsymbol{q}}^p]\mathrm{i}\epsilon^{a3b} \\ &\quad + [\Theta_{\boldsymbol{p}}^p\Theta_{\boldsymbol{q}}^p - \Theta_{\boldsymbol{p}}^p\Theta_{\boldsymbol{q}}^n - \Theta_{\boldsymbol{p}}^n\Theta_{\boldsymbol{q}}^p + \Theta_{\boldsymbol{p}}^n\Theta_{\boldsymbol{q}}^n]\delta^{a3}\delta^{b3}. \end{aligned} \tag{B.33d}$$

B.4.3. Gell-Mann matrices and SU(3) structure constants

The eight Gell-Mann matrices λ^a are a basis of linearly independent 3×3 Hermitian matrices with vanishing trace. They are conventionally normalized by the following equation:

$$\mathrm{Tr}\Big\{\lambda^a\lambda^b\Big\} = 2\delta^{ab}. \tag{B.34a}$$

The product of two Gell-Mann matrices can be evaluated by using the following relations:

$$[\lambda^a, \lambda^b] = 2\mathrm{i}f^{abc}\lambda^c, \tag{B.35a}$$

$$\{\lambda^a, \lambda^b\} = \frac{4}{3}\delta^{ab}\mathbb{1} + 2d^{abc}\lambda^c, \tag{B.35b}$$

$$\lambda^a\lambda^b = \frac{2}{3}\delta^{ab}\mathbb{1} + (d^{abc} + \mathrm{i}f^{abc})\lambda^c. \tag{B.35c}$$

Here, the totally antisymmetric and totally symmetric structure constants can be defined like this:

$$\mathrm{Tr}\Big\{\lambda^a[\lambda^b, \lambda^c]\Big\} = 4\mathrm{i}f^{abc}, \tag{B.36a}$$

$$\mathrm{Tr}\Big\{\lambda^a\{\lambda^b, \lambda^c\}\Big\} = 4d^{abc}. \tag{B.36b}$$

Their numeric values are as follows. Any combination of indices that is not listed vanishes:

$$f^{123} = 1, \tag{B.37a}$$

$$f^{147} = -f^{156} = f^{246} = f^{257} = f^{345} = -f^{367} = \frac{1}{2}, \tag{B.37b}$$

$$f^{458} = f^{678} = \frac{\sqrt{3}}{2}. \tag{B.37c}$$

Similarly, the totally symmetric structure constants are:

$$d^{118} = d^{228} = d^{338} = -d^{888} = \frac{1}{\sqrt{3}}, \tag{B.38a}$$

$$d^{448} = d^{558} = d^{668} = d^{778} = -\frac{1}{2\sqrt{3}}, \tag{B.38b}$$

$$d^{344} = d^{355} = -d^{366} = -d^{377} = -d^{247} = d^{146} = d^{157} = d^{256} = \frac{1}{2}. \tag{B.38c}$$

We will also make use of one additional Gell-Mann matrix, $\lambda^0 = \sqrt{2/3}\mathbb{1}$, where the normalization is chosen such that it agrees with Eq. (B.34a).

B.4.4. Dirac gamma matrices

In d space-time dimensions, there are $2^{\lfloor d/2 \rfloor}$ gamma matrices. The defining property of the gamma matrices is their anticommutation relation, expressed by the Clifford algebra,

$$\{\gamma^\mu, \gamma^\nu\} = \gamma^\mu\gamma^\nu + \gamma^\nu\gamma^\mu = 2\eta^{\mu\nu}\mathbb{1}, \tag{B.39}$$

where $\eta^{\mu\nu}$ is the inverse of the mostly-minus Minkowski metric $\eta_{\mu\nu} = \operatorname{diag}(1, -1, -1, -1)_{\mu\nu}$. When a four-vector contracts with a gamma matrix, we use the Feynman-slash notation,

$$\not{p} \equiv p_\mu\gamma^\mu = p^\mu\gamma_\mu. \tag{B.40}$$

Additionally to the four gamma matrices, one can define a fifth matrix,

$$\gamma^5 = \mathrm{i}\gamma^0\gamma^1\gamma^2\gamma^3 = \pm\frac{\mathrm{i}}{4!}\epsilon_{\mu\nu\alpha\beta}\gamma^\mu\gamma^\nu\gamma^\alpha\gamma^\beta, \qquad \text{for } \epsilon_{0123} = \pm 1, \tag{B.41}$$

where the choice of the sign corresponding to the definition of ϵ_{0123}. The following traces over gamma matrices are often used in this work:

$$\operatorname{Tr}\{\gamma^\mu\} = \operatorname{Tr}\{\gamma^\mu\gamma^\nu\gamma^\sigma\} = \operatorname{Tr}\{\gamma^{\mu_1}\cdots\gamma^{\mu_{2n+1}}\} = 0 \quad \forall n \in \mathbb{N}, \tag{B.42a}$$

$$\operatorname{Tr}\left\{\gamma^5\gamma^\mu\right\} = \operatorname{Tr}\left\{\gamma^5\gamma^\mu\gamma^\nu\gamma^\sigma\right\} = \operatorname{Tr}\left\{\gamma^5\gamma^{\mu_1}\cdots\gamma^{\mu_{2n+1}}\right\} = 0 \quad \forall n \in \mathbb{N}, \tag{B.42b}$$

$$\operatorname{Tr}\left\{\gamma^5\right\} = \operatorname{Tr}\left\{\gamma^5\gamma^\mu\gamma^\nu\right\} = 0, \tag{B.42c}$$

$$\operatorname{Tr}\{\gamma^\mu\gamma^\nu\} = 4\eta^{\mu\nu}, \tag{B.42d}$$

$$\operatorname{Tr}\{\gamma^\mu\gamma^\nu\gamma^\sigma\gamma^\rho\} = 4(\eta^{\mu\nu}\eta^{\sigma\rho} - \eta^{\mu\sigma}\eta^{\nu\rho} + \eta^{\mu\rho}\eta^{\nu\sigma}), \tag{B.42e}$$

$$\operatorname{Tr}\left\{\gamma^5\gamma^\mu\gamma^\nu\gamma^\sigma\gamma^\rho\right\} = \pm 4\mathrm{i}\epsilon^{\mu\nu\sigma\rho} \qquad \text{for } \epsilon_{0123} = \pm 1. \tag{B.42f}$$

B.4.5. Employing the large nucleon mass limit

We can use this limit to evaluate the following integrals:

$$\begin{aligned}\frac{m_N}{\pi^2}\int_0^\infty \mathrm{d}p\,\frac{p^2}{\sqrt{p^2+m_N^2}}\Theta^p_{\boldsymbol{p}} &= \rho_p + \mathcal{O}(1/m_N^2) \\ &= \frac{\rho}{1+r} + \mathcal{O}(1/m_N^2),\end{aligned} \tag{B.43a}$$

$$
\begin{aligned}
\frac{m_N}{\pi^2}\int_0^\infty \mathrm{d}p\,\frac{p^2}{\sqrt{p^2+m_N^2}}\Theta^n_{\boldsymbol{p}} &= \rho_n + \mathcal{O}(1/m_N^2) \\
&= \frac{\rho\, r}{1+r} + \mathcal{O}(1/m_N^2), \qquad \text{(B.43b)}
\end{aligned}
$$

$$
\frac{m_N}{\pi^2}\int_0^\infty \mathrm{d}p\,\frac{p^2}{\sqrt{p^2+m_N^2}}(\Theta^p_{\boldsymbol{p}}+\Theta^n_{\boldsymbol{p}}) = \rho + \mathcal{O}(1/m_N^2), \qquad \text{(B.43c)}
$$

$$
\frac{m_N}{\pi^2}\int_0^\infty \mathrm{d}p\,\frac{p^2}{\sqrt{p^2+m_N^2}}(\Theta^p_{\boldsymbol{p}}-\Theta^n_{\boldsymbol{p}}) = \rho\frac{1-r}{1+r} + \mathcal{O}(1/m_N^2), \qquad \text{(B.43d)}
$$

where $\rho = \rho_p + \rho_n$ and $r = \rho_n/\rho_p$.

Bibliography

[1] S. Hübsch and D. Jido, *Density dependence of the quark condensate in isospin-asymmetric nuclear matter*, Phys. Rev. C **104**, 015202 (2021), `arXiv:2103.08823 [nucl-th]`.

[2] S. Hübsch and D. Jido, *Pion mass, wave function renormalization and decay constant in isospin-asymmetric nuclear matter*, (in preparation) (2021).

[3] D. J. Gross and F. Wilczek, *Ultraviolet behavior of non-abelian gauge theories*, Phys. Rev. Lett. **30**, 1343 (1973).

[4] H. D. Politzer, *Reliable perturbative results for strong interactions?*, Phys. Rev. Lett. **30**, 1346 (1973).

[5] G. Ecker, *Chiral perturbation theory*, Progress in Particle and Nuclear Physics **35**, 1 (1995).

[6] V. Bernard, N. Kaiser, and U.-G. Meißner, *Chiral dynamics in nucleons and nuclei*, International Journal of Modern Physics E **4**, 193 (1995), `arXiv:hep-ph/9501384`.

[7] A. Pich, *Effective field theory* (1998), `arXiv:hep-ph/9806303`.

[8] T. R. Hemmert, B. R. Holstein, and J. Kambor, *Chiral Lagrangians and δ(1232) interactions*, J. Phys. G **24**, 1831 (1998), `arXiv:hep-ph/9712496`.

[9] S. Scherer and M. R. Schindler, *A chiral perturbation theory primer* (2005), `arXiv:hep-ph/0505265`.

[10] S. Scherer and M. R. Schindler, *A primer for chiral perturbation theory*, Lecture Notes in Physics No. 830 (Springer, 2012).

[11] M. L. Goldberger and S. B. Treiman, *Decay of the pi meson*, Phys. Rev. **110**, 1178 (1958).

[12] H. Pagels and A. Zepeda, *Where are the corrections to the Goldberger–Treiman relation?*, Phys. Rev. D **5**, 3262 (1972).

[13] Y. Nambu, *Axial vector current conservation in weak interactions*, Phys. Rev. Lett. **4**, 380 (1960).

[14] Y. Nambu and G. Jona-Lasinio, *Dynamical model of elementary particles based on an analogy with superconductivity. I*, Phys. Rev. **122**, 345 (1961).

[15] Y. Nambu and G. Jona-Lasinio, *Dynamical model of elementary particles based on an analogy with superconductivity. II*, Phys. Rev. **124**, 246 (1961).

[16] M. Gell-Mann and M. Lévy, *The axial vector current in beta decay*, Il Nuovo Cimento (1955-1965) **16**, 705 (1960).

[17] S. Weinberg, *Pion scattering lengths*, Phys. Rev. Lett. **17**, 616 (1966).

[18] S. Weinberg, *Dynamical approach to current algebra*, Phys. Rev. Lett. **18**, 188 (1967).

[19] R. Dashen and M. Weinstein, *Soft pions, chiral symmetry, and phenomenological Lagrangians*, Phys. Rev. **183**, 1261 (1969).

[20] S. Coleman, J. Wess, and B. Zumino, *Structure of phenomenological Lagrangians. I*, Physical Review **177**, 2239 (1969).

[21] C. G. Callan Jr, S. Coleman, J. Wess, and B. Zumino, *Structure of phenomenological Lagrangians. II*, Physical Review **177**, 2247 (1969).

[22] J. M. Charap, *Closed-loop calculations using a chiral-invariant Lagrangian*, Phys. Rev. D **2**, 1554 (1970).

[23] J. M. Charap, *Closed-loop calculations using a chiral-invariant Lagrangian: An addendum*, Phys. Rev. D **3**, 1998 (1971).

[24] L.-F. Li and H. Pagels, *Perturbation theory about a Goldstone symmetry*, Phys. Rev. Lett. **26**, 1204 (1971).

[25] P. Langacker and H. Pagels, *Chiral perturbation theory*, Phys. Rev. D **8**, 4595 (1973).

[26] H. Lehmann, *Chiral invariance and effective range expansion for pion-pion scattering*, Physics Letters B **41**, 529 (1972).

[27] H. Lehmann and H. Trute, *Second-order effects in chiral-invariant pion Lagrangians and the use of superpropagators*, Nuclear Physics B **52**, 280 (1973).

[28] G. Ecker and J. Honerkamp, *Covariant perturbation theory and chiral superpropagators*, Physics Letters B **42**, 253 (1972).

[29] G. Ecker and J. Honerkamp, *Pion-pion scattering from an SU(3) × SU(3) invariant Lagrangian*, Nuclear Physics B **62**, 509 (1973).

[30] J. Gasser and H. Leutwyler, *Chiral perturbation theory to one loop*, Annals of Physics **158**, 142 (1984).

[31] J. Gasser and H. Leutwyler, *Chiral perturbation theory: Expansions in the mass of the strange quark*, Nuclear Physics B **250**, 465 (1985).

[32] J. Bijnens, G. Colangelo, and G. Ecker, *The mesonic chiral lagrangean of order* p^6, Journal of High Energy Physics **1999**, 020 (1999).

[33] J. A. Oller, *Chiral Lagrangians at finite density*, Phys. Rev. C **65**, 025204 (2002), `arXiv:hep-ph/0101204`.

[34] U.-G. Meißner, J. A. Oller, and A. Wirzba, *In-medium chiral perturbation theory beyond the mean-field approximation*, Annals of Physics **297**, 27 (2002), `arXiv:nucl-th/0109026`.

[35] D. Jido, T. Hatsuda, and T. Kunihiro, *In-medium pion and partial restoration of chiral symmetry*, Phys. Lett. B **670**, 109 (2008), `arXiv:0805.4453 [nucl-th]`.

[36] E. E. Kolomeitsev, N. Kaiser, and W. Weise, *Chiral dynamics of deeply bound pionic atoms*, Phys. Rev. Lett. **90**, 092501 (2003), `arXiv:nucl-th/0207090`.

[37] K. Suzuki, M. Fujita, H. Geissel, H. Gilg, A. Gillitzer, R. S. Hayano, S. Hirenzaki, K. Itahashi, M. Iwasaki, P. Kienle, M. Matos, G. Münzenberg, T. Ohtsubo, M. Sato, M. Shindo, T. Suzuki, H. Weick, M. Winkler, T. Yamazaki, and T. Yoneyama, *Precision spectroscopy of pionic* 1*s states of Sn nuclei and evidence for partial restoration of chiral symmetry in the nuclear medium*, Phys. Rev. Lett. **92**, 072302 (2004), `arXiv:nucl-ex/0211023`.

[38] E. Friedman, M. Bauer, J. Breitschopf, H. Clement, H. Denz, E. Doroshkevich, A. Erhardt, G. J. Hofman, R. Meier, G. J. Wagner, and G. Yaari, *In-medium isovector* πN *amplitude from low-energy pion scattering*, Phys. Rev. Lett. **93**, 122302 (2004), `arXiv:nucl-ex/0404031`.

[39] E. Friedman, M. Bauer, J. Breitschopf, H. Clement, H. Denz, E. Doroshkevich, A. Erhardt, G. J. Hofman, S. Kritchman, R. Meier, G. J. Wagner, and G. Yaari, *Elastic scattering of low energy pions by nuclei and the in-medium isovector* πN *amplitude*, Phys. Rev. C **72**, 034609 (2005), `arXiv:nucl-ex/0507008`.

[40] J. I. Kapusta and E. V. Shuryak, *Weinberg-type sum rules at zero and finite temperature*, Phys. Rev. D **49**, 4694 (1994).

[41] C. DeTar and T. Kunihiro, *Linear sigma model with parity doubling*, Phys. Rev. D **39**, 2805 (1989).

[42] H. Kim, D. Jido, and M. Oka, *Properties of $N^*(1535)$ at finite density in the extended parity-doublet models*, Nuclear Physics A **640**, 77 (1998).

[43] D. Jido, Y. Nemoto, M. Oka, and A. Hosaka, *Chiral symmetry for positive and negative parity nucleons*, Nuclear Physics A **671**, 471 (2000).

[44] D. Jido, M. Oka, and A. Hosaka, *Chiral symmetry of baryons*, Progress of Theoretical Physics **106**, 873 (2001).

[45] T. Hatsuda, T. Kunihiro, and H. Shimizu, *Precursor of chiral symmetry restoration in the nuclear medium*, Phys. Rev. Lett. **82**, 2840 (1999).

[46] D. Jido, T. Hatsuda, and T. Kunihiro, *In-medium $\pi\pi$ correlation induced by partial restoration of chiral symmetry*, Phys. Rev. D **63**, 011901 (2000), `arXiv:hep-ph/0008076`.

[47] T. Hyodo, D. Jido, and T. Kunihiro, *Nature of the σ meson as revealed by its softening process*, Nuclear Physics A **848**, 341 (2010).

[48] H. Hellmann, *Einführung in die Quantenchemie* (Leipzig: Franz Deuticke, 1937).

[49] R. P. Feynman, *Forces in molecules*, Phys. Rev. **56**, 340 (1939).

[50] T. D. Cohen, R. J. Furnstahl, and D. K. Griegel, *Quark and gluon condensates in nuclear matter*, Phys. Rev. C **45**, 1881 (1992).

[51] G. Chanfray and M. Ericson, *Quark condensate in the nuclear medium*, Nuclear Physics A **556**, 427 (1993).

[52] G. Li and C. Ko, *Quark condensate in nuclear matter*, Physics Letters B **338**, 118 (1994).

[53] P. A. Zyla *et al.* (Particle Data Group), *Review of particle physics*, Progress of Theoretical and Experimental Physics **2020**, 083C01 (2020).

[54] K. Fujikawa, H. Suzuki, *et al.*, *Path integrals and quantum anomalies*, 122 (Oxford University Press on Demand, 2004).

[55] C. Itzykson and J.-B. Zuber, *Quantum field theory* (Courier Corporation, 2012).

[56] L. H. Ryder, *Quantum field theory*, 2nd ed. (Cambridge University Press, 2001).

[57] S. Weinberg, *The quantum theory of fields*, Vol. 2 (Cambridge University Press, 1996).

[58] E. Noether, *Invariante Variationsprobleme*, Nachrichten von der Gesellschaft der Wissenschaften zu Göttingen, Mathematisch-Physikalische Klasse **1918**, 235 (1918).

[59] E. Noether, *Invariant variation problems (English translation)*, Transport Theory and Statistical Physics **1**, 186 (1971).

[60] V. A. Miransky, *Dynamical symmetry breaking in quantum field theories* (World Scientific, 1993).

[61] E. Fabri and L. E. Picasso, *Quantum field theory and approximate symmetries*, Phys. Rev. Lett. **16**, 408 (1966).

[62] Y. Nambu, *Quasi-particles and gauge invariance in the theory of superconductivity*, Physical Review **117**, 648 (1960).

[63] J. Goldstone, *Field theories with superconductor solutions*, Il Nuovo Cimento (1955-1965) **19**, 154 (1961).

[64] J. Goldstone, A. Salam, and S. Weinberg, *Broken symmetries*, Physical Review **127**, 965 (1962).

[65] S. Weinberg, *Phenomenological Lagrangians*, Physica A: Statistical Mechanics and its Applications **96**, 327 (1979).

[66] S. Weinberg, *Nonlinear realizations of chiral symmetry*, Physical Review **166**, 1568 (1968).

[67] M. Bando, T. Kugo, and K. Yamawaki, *Nonlinear realization and hidden local symmetries*, Physics Reports **164**, 217 (1988).

[68] S. Goda and D. Jido, *Chiral condensate at finite density using chiral Ward identity*, Phys. Rev. C **88**, 065204 (2013), `arXiv:1308.2660 [nucl-th]`.

[69] I. S. Gerstein, R. Jackiw, B. W. Lee, and S. Weinberg, *Chiral loops*, Phys. Rev. D **3**, 2486 (1971).

[70] S. L. Adler, *Consistency conditions on the strong interactions implied by a partially conserved axial-vector current*, Physical Review **137**, B1022 (1965).

[71] R. Akhoury and A. Alfakih, *Invariant background field method for chiral Lagrangians including Wess–Zumino terms*, Annals of Physics **210**, 81 (1991).

[72] S. Goda and D. Jido, *Pion properties at finite nuclear density based on in-medium chiral perturbation theory*, Prog. Theor. Exp. Phys. **2014**, 033D03 (2014), `arXiv:1312.0832 [nucl-th]`.

[73] N. Hasan, J. Green, S. Meinel, M. Engelhardt, S. Krieg, J. Negele, A. Pochinsky, and S. Syritsyn, *Nucleon axial, scalar, and tensor charges using lattice QCD at the physical pion mass*, Phys. Rev. D **99**, 114505 (2019), `arXiv:1903.06487 [hep-lat]`.

[74] U.-G. Meißner, *Quark mass dependence of baryon properties*, PoS LAT2005 **009** (2005), arXiv:hep-lat/0509029 [hep-lat].

[75] V. Bernard, N. Kaiser, and U.-G. Meißner, *Aspects of chiral pion-nucleon physics*, Nuclear Physics A **615**, 483 (1997), arXiv:hep-ph/9611253 [hep-ph].

[76] H. Denz, P. Amaudruz, J. Brack, J. Breitschopf, P. Camerini, J. Clark, H. Clement, L. Felawka, E. Fragiacomo, E. Gibson, N. Grion, G. Hofman, B. Jamieson, E. Mathie, R. Meier, G. Moloney, D. Ottewell, O. Patarakin, J. Patterson, M. Pavan, S. Piano, K. Raywood, R. Ristinen, R. Rui, M. Sevior, G. Smith, J. Stahov, R. Tacik, G. Wagner, F. von Wrochem, and D. Yeomans, *$\pi^{\pm}p$ differential cross sections at low energies*, Physics Letters B **633**, 209 (2006).

[77] K. Aoki, *In-medium modification of Nambu–Goldstone boson properties induced by wave-function renormalization under partial restoration of chiral symmetry*, Ph.D. thesis, Tokyo Metropolitan University (2019).

[78] L.-S. Geng, *Recent development in SU(3) covariant baryon chiral perturbation theory*, Frontiers of Physics **8**, 328 (2013), arXiv:1301.6815 [nucl-th].

[79] B. Kubis and U. G. Meißner, *Baryon form factors in chiral perturbation theory*, The European Physical Journal C - Particles and Fields **18**, 747 (2001), arXiv:hep-ph/0010283.

[80] M. Holmberg and S. Leupold, *The relativistic chiral Lagrangian for decuplet and octet baryons at next-to-leading order*, The European Physical Journal A **54**, 103 (2018), arXiv:1802.05168 [hep-ph].

[81] K. Aoki and D. Jido, *K^+–nucleus elastic scattering revisited from the perspective of partial restoration of chiral symmetry*, Progress of Theoretical and Experimental Physics **2017**, 103D01 (2017), arXiv:1705.07548 [nucl-th].

[82] W. Cameron, A. Hirata, R. Jennings, W. Morton, E. Cazzoli, G. Giacomelli, P. Lugaresi-Serra, G. Mandrioli, A. Minguzzi-Ranzi, E. Castelli, M. Furlan, P. Poropat, C. Omero, and M. Sessa, *K^+p elastic scattering from 130 to 755 MeV/c*, Nuclear Physics B **78**, 93 (1974).

[83] P. Haensel, A. Y. Potekhin, and D. G. Yakovlev, *Neutron stars 1: Equation of state and structure*, Vol. 326 (Springer Science & Business Media, 2007).

[84] E. Chabanat, P. Bonche, P. Haensel, J. Meyer, and R. Schaeffer, *A Skyrme parametrization from subnuclear to neutron star densities*, Nuclear Physics A **627**, 710 (1997).

[85] M. D. Schwartz, *Quantum field theory and the standard model* (Cambridge University Press, 2014).

[86] V. Shtabovenko, R. Mertig, and F. Orellana, *FeynCalc 9.3: New features and improvements* (2020), `arXiv:2001.04407 [hep-ph]`.

[87] V. Shtabovenko, R. Mertig, and F. Orellana, *New developments in FeynCalc 9.0*, Computer Physics Communications **207**, 432 (2016), `arXiv:1601.01167 [hep-ph]`.

[88] R. Mertig, M. Böhm, and A. Denner, *Feyn Calc - computer-algebraic calculation of Feynman amplitudes*, Computer Physics Communications **64**, 345 (1991).

[89] P. Virtanen, R. Gommers, T. E. Oliphant, M. Haberland, T. Reddy, D. Cournapeau, E. Burovski, P. Peterson, W. Weckesser, J. Bright, S. J. van der Walt, M. Brett, J. Wilson, K. J. Millman, N. Mayorov, A. R. J. Nelson, E. Jones, R. Kern, E. Larson, C. J. Carey, İ. Polat, Y. Feng, E. W. Moore, J. VanderPlas, D. Laxalde, J. Perktold, R. Cimrman, I. Henriksen, E. A. Quintero, C. R. Harris, A. M. Archibald, A. H. Ribeiro, F. Pedregosa, P. van Mulbregt, and SciPy 1.0 Contributors, *SciPy 1.0: Fundamental algorithms for scientific computing in Python*, Nature Methods **17**, 261 (2020).

[90] C. R. Harris, K. J. Millman, S. J. van der Walt, R. Gommers, P. Virtanen, D. Cournapeau, E. Wieser, J. Taylor, S. Berg, N. J. Smith, R. Kern, M. Picus, S. Hoyer, M. H. van Kerkwijk, M. Brett, A. Haldane, J. F. del Río, M. Wiebe, P. Peterson, P. Gérard-Marchant, K. Sheppard, T. Reddy, W. Weckesser, H. Abbasi, C. Gohlke, and T. E. Oliphant, *Array programming with NumPy*, Nature **585**, 357 (2020).

[91] J. D. Hunter, *Matplotlib: A 2D graphics environment*, Computing in Science & Engineering **9**, 90 (2007).

[92] N. Kaiser, P. d. Homont, and W. Weise, *In-medium chiral condensate beyond linear density approximation*, Phys. Rev. C **77**, 025204 (2008), `arXiv:0711.3154`.

[93] P. Gubler and D. Satow, *Recent progress in QCD condensate evaluations and sum rules*, Progress in Particle and Nuclear Physics **106**, 1 (2019), `arXiv:1812.00385`.

[94] A. Lacour, J. A. Oller, and U.-G. Meißner, *The chiral quark condensate and pion decay constant in nuclear matter at next-to-leading order*, Journal of Physics G: Nuclear and Particle Physics **37**, 125002 (2010), `arXiv:1007.2574 [nucl-th]`.

[95] M. Drews and W. Weise, *From asymmetric nuclear matter to neutron stars: A functional renormalization group study*, Phys. Rev. C **91**, 035802 (2015), `arXiv:1412.7655 [nucl-th]`.

[96] C. Vafa and E. Witten, *Restrictions on symmetry breaking in vector-like gauge theories*, Nucl. Phys. B **234**, 173 (1984).

[97] N. Kaiser and W. Weise, *Systematic calculation of s-wave pion and kaon self-energies in asymmetric nuclear matter*, Physics Letters B **512**, 283 (2001), `arXiv:nucl-th/0102062`.

[98] M. Drews and W. Weise, *Functional renormalization group studies of nuclear and neutron matter*, Progress in Particle and Nuclear Physics **93**, 69 (2017), `arXiv:1610.07568 [nucl-th]`.

[99] P. T. P. Hutauruk, Y. Oh, and K. Tsushima, *Electroweak properties of pions in a nuclear medium*, Phys. Rev. C **99**, 015202 (2019), `arXiv:1810.08874 [nucl-th]`.

[100] A. Wirzba and V. Thorsson, *In-medium effective chiral Lagrangians and the pion mass in nuclear matter*, Preprint (1995), `arXiv:hep-ph/9502314`.

[101] K. Itahashi, K. Oyama, R. S. Hayano, H. Gilg, A. Gillitzer, M. Knülle, M. Münch, W. Schott, P. Kienle, H. Geissel, N. Iwasa, G. Münzenberg, S. Hirenzaki, H. Toki, and T. Yamazaki, *Deeply bound π^- states in ^{207}Pb formed in the $^{208}Pb(d,^3He)$ reaction. II. deduced binding energies and widths and the pion-nucleus interaction*, Phys. Rev. C **62**, 025202 (2000).

[102] W. Weise and T. Ericson, *Pions and nuclei* (Clarendon, 1988).

[103] Y. Tomozawa, *Axial-vector coupling constant renormalization and the meson-baryon scattering lenghts*, Il Nuovo Cimento A (1971-1996) **46**, 707 (1966).

[104] A. W. Thomas and W. Weise, *The structure of the nucleon* (Wiley-VCH, 2001).

[105] J. Hamilton and W. Woolcock, *Determination of pion-nucleon parameters and phase shifts by dispersion relations*, Reviews of Modern Physics **35**, 737 (1963).

[106] A. Migdal, *ZhETF 61 (1971) 2210*, JETP (Sov. Phys.) **34**, 1184 (1972).

[107] R. F. Sawyer, *Condensed π^- phase in neutron-star matter*, Phys. Rev. Lett. **29**, 382 (1972).

[108] R. F. Sawyer, *Condensed π^- phase in neutron-star matter (errata)*, Phys. Rev. Lett. **29**, 823 (1972).

[109] D. J. Scalapino, *π^- condensate in dense nuclear matter*, Phys. Rev. Lett. **29**, 386 (1972).

[110] G. Brown and W. Weise, *Pion condensates*, Physics Reports **27**, 1 (1976).

[111] T. Khunjua, K. Klimenko, and R. Zhokhov, *Dense quark matter with chiral and isospin imbalance: Njl-model consideration*, EPJ Web of Conferences **191**, 05015 (2018), arXiv:1901.03049 [hep-ph].

[112] T. G. Khunjua, K. Klimenko, and R. N. Zhokhov-Larionov, *Affinity of NJL_2 and NJL_4 model results on duality and pion condensation in chiral asymmetric dense quark matter*, EPJ Web of Conferences **191**, 05016 (2018), arXiv:1812.01860 [hep-ph].

[113] T. G. Khunjua, V. C. Zhukovsky, K. G. Klimenko, and R. N. Zhokhov, *Duality and charged pion condensation in chirally asymmetric dense quark matter in the framework of an NJL_2 model*, International Journal of Modern Physics: Conference Series **47**, 1860093 (2018), arXiv:1808.05162 [hep-ph].

[114] T. G. Khunjua, K. G. Klimenko, and R. N. Zhokhov, *Charged pion condensation and duality in dense and hot chirally and isospin asymmetric quark matter in the framework of the NJL_2 model*, Physical Review D **100**, 10.1103/physrevd.100.034009 (2019), arXiv:1907.04151 [hep-ph].

[115] A. Mammarella, *Aspects of meson condensation*, EPJ Web of Conferences **126**, 04029 (2016), arXiv:1509.06887 [hep-ph].

[116] A. Mammarella and M. Mannarelli, *Meson physics in asymmetric matter*, Journal of Physics: Conference Series **861**, 012017 (2017), arXiv:1705.02169 [hep-ph].

[117] Q. Li and Z. Li, *The density- and isospin- dependent Δ-formation cross section and its decay width* (2017), arXiv:1712.02062 [nucl-th].

[118] N. Kovensky and A. Schmitt, *Isospin asymmetry in holographic baryonic matter* (2021), arXiv:2105.03218 [hep-ph].

[119] G. Chanfray, M. Ericson, and M. Oertel, *In-medium modification of the isovector pion–nucleon amplitude*, Physics Letters B **563**, 61 (2003), arXiv:nucl-th/0211035.

[120] H. Lehmann, K. Symanzik, and W. Zimmermann, *Zur Formulierung quantisierter Feldtheorien*, Il Nuovo Cimento (1955-1965) **1**, 205 (1955).

[121] P. Kienle and T. Yamazaki, *Pions in nuclei, a probe of chiral symmetry restoration*, Progress in Particle and Nuclear Physics **52**, 85 (2004).

[122] M. Gell-Mann, R. J. Oakes, and B. Renner, *Behavior of current divergences under $SU_3 \times SU_3$*, Phys. Rev. **175**, 2195 (1968).

[123] X. L. Ren, L. S. Geng, J. M. Camalich, J. Meng, and H. Toki, *Octet baryon masses in next-to-next-to-next-to-leading order covariant baryon chiral perturbation theory*, Journal of High Energy Physics **2012**, 73 (2012), `arXiv:1209.3641 [nucl-th]`.

[124] M. Srednicki, *Quantum field theory* (Cambridge University Press, 2010).

[125] T. Lancaster and S. J. Blundell, *Quantum field theory for the gifted amateur* (OUP Oxford, 2014).

[126] L. D. Landau and E. Lifshitz, *Quantum electrodynamics* (Pergamon Press, 1983).

[127] M. Thomson, *Modern particle physics* (Cambridge University Press, 2013).

[128] M. E. Peskin and D. V. Schroeder, *An introduction to quantum field theory* (CRC Press, 2018).

[129] F. Mandl and G. Shaw, *Quantum field theory* (John Wiley & Sons, 2010).

[130] T. Ohlsson, *Relativistic quantum physics: From advanced quantum mechanics to introductory quantum field theory* (Cambridge University Press, 2011).

[131] A. Meurer, C. P. Smith, M. Paprocki, O. Čertík, S. B. Kirpichev, M. Rocklin, A. Kumar, S. Ivanov, J. K. Moore, S. Singh, T. Rathnayake, S. Vig, B. E. Granger, R. P. Muller, F. Bonazzi, H. Gupta, S. Vats, F. Johansson, F. Pedregosa, M. J. Curry, A. R. Terrel, v. Roučka, A. Saboo, I. Fernando, S. Kulal, R. Cimrman, and A. Scopatz, *SymPy: symbolic computing in Python*, PeerJ Computer Science **3**, e103 (2017).